united nations
educational, scientific
and cultural
organization

international atomic
energy agency

the
abdus salam
international centre for theoretical physics

H4.SMR/1150 - 7

Fifth Workshop on Non-Linear Dynamics
and Earthquake Prediction

4 - 22 October 1999

Experiments with CN in Italy and Seismic Hazard

Part I

G. F. Panza

Department of Earth Sciences
Trieste, Italy

PAGEOPH, Vol. 134, No. 1 (1990)

0033-4553/90/010079-14$1.50 + 0.20/0

On Intermediate-Term Earthquake Prediction in Central Italy

V. I. KEILIS-BOROK[1,3], I. V. KUZNETSOV[1,3], G. F. PANZA[2], I. M. ROTWAIN[1,3], and G. COSTA[2]

Abstract—The Time of Increased Probability (TIP) for the occurrence of a strong earthquake is determined in Central Italy. This is done with an algorithm that has been successfully applied in other regions of the world (algorithm CN, from the initials of California and Nevada, where the first diagnoses of TIPs were made). The use of normalized functions allows direct application of the orginal algorithm to the new region being studied, without any *ad hoc* adjustment of the parameters.

Retrospective analysis carried on until 1986 shows that TIPs occupy 26 percent of the total time considered and precede four out of five strong earthquakes. Forward monitoring indicates the possible existence of a TIP started in May 1988.

Several tests indicate that the results obtained are quite stable, even when using catalogues from different agencies. Apart from obvious practical interest, this research is essential for the worldwide investigation of self-similarity in the origin of strong earthquakes.

Key words: Seismology, earthquake prediction, self-similarity, algorithm CN, Central Italy.

1. Introduction

The algorithm is described in full detail by GABRIELOV *et al.* (1986) and KEILIS-BOROK *et al.* (1988) and has been applied for the first time to the California-Nevada (CN) region by ALLEN *et al.* (1983). Here, we consider the specific version described by KEILIS-BOROK *et al.* (1988). The algorithm CN is designed to diagnose the Time of Increased Probability of strong earthquake (TIP) from a set of traits of the earthquake's flow. The traits considered are the level of seismic activity (intensity of earthquakes flow), its variation in time, clustering of earthquakes in space and time and their concentration in space.

[1] International Institute of Earthquake Prediction Theory and Mathematical Geophysics, Academy of Sciences of the U.S.S.R., Warshavskoye, 79, K.2, 113556 Moscow, U.S.S.R.

[2] Universita degli Studi di Trieste, Istituto di Geodesia e Geofisica, Via dell'Universita, 7, 34123 Trieste, Italy.

[3] International Center for Earth and Environmental Sciences (ICS), 34100 Trieste Miramar.

Table 1

Function	Definition
SIGMA (t)	SIGMA $(t) = \Sigma\, 10^{\beta(M_i - \alpha)}$ The main shocks with $m_i \le M_i \le M_0 - 0.1$ and origin time $(t - 3$ years$) \le t_i \le t$ are included in summation; $\alpha = 4.5$, $\beta = 1.00$.
$S_{\max}(t)$	$S_{\max}(t) = \max\left\{\frac{S_1}{N_1}, \frac{S_2}{N_2}, \frac{S_3}{N_3}\right\}$, where S_j is calculated as SIGMA(t) for the events with the origin time $(t - j$ years$) \le t_i \le (t - (j-1)$ years$)$, and N_j is the number of earthquakes in the sum.
$Z_{\max}(t)$	$Z_{\max}(t) = \max\left\{\frac{Z_1}{N_1^{2/3}}, \frac{Z_2}{N_2^{2/3}}, \frac{Z_3}{N_3^{2/3}}\right\}$, where Z_j is calculated as S_j with $\beta = 0.5$, and N_j is the same as in the definition of $S_{\max}(t)$.
$N_2(t)$	The number of main shocks with $M \ge m_3$, which occurred in the time interval $(t - 3$ years, $t)$.
$N_3(t)$	The number of main shocks with $M \ge m_2$, which occurred in the time interval $(t - 10$ years, $t - 7$ years$)$.
$K(t)$	$K(t) = K_1 - K_2$, where K_1 is the number of main shocks with $M_1 \ge m_2$ and origin time $(t - 2 \cdot j$ years$) \le t_i \le (t - 2 \cdot (j-1)$ years$)$.
$B_{\max}(t)$	The largest number of aftershocks for the main shocks with $M_i \ge m_0 - 1.9$ and origin time within $((t - 3$ years$), t)$. Aftershocks are counted within a radius of 50 km for the first 2 days after the main shock and for $M > M_0 - 3.6$.
$G(t)$	$G(t) = 1 - P$, where P is the ratio of the number of the main shocks with $M_j \ge m_2$ to the number of the main shocks with $M_j \ge m_1$. Only main shocks with origin time $(t - 1$ year$) \le t_j \le t$ are considered.
$q(t)$	$q(t) = \sum_{j=1}^{6} \max\{0, 6a_2 - n_j\}$, where a_2 is the average annual number of main shocks with $M_1 \ge m_2$, n_j is the number of main shocks with $M_1 \ge m_2$ and origin time $(t - (8+j)$ years$) \le t_1 \le (t - (2+j)$ years$)$

For a given territory the traits are represented by certain functions of time defined in Table 1; these are computed, within a sliding time window, using the earthquakes contained in the catalogues. In the computations the aftershocks are not considered, but the number of aftershocks is included as one of the parameters ($B_{\max}$) characterizing a main shock. All functions depend upon magnitude (see Table 1). The first three functions are evaluated counting each earthquake with a weight proportional to the magnitude, while for the remaining six functions the earthquakes are counted with equal weight, independently of their individual magnitude.

The functions representing the traits are normalized so that these functions can be applied uniformly to territories with different sizes and seismicities. The introduction of normalization is also of obvious interest in connection with the possibility

of identifying self-similarity in the flow of earthquakes. The normalization is obtained by choosing three mangitude ranges, m_1, m_2, m_3. These ranges are defined by the condition that, in the territory analysed, the average annual number of earthquakes with $M \geq m_1$ (or m_2, or m_3) is equal to a constant, a_1 (or a_2, or a_3), common to all territories. In this way the intensities of flows of earthquakes are equalized. The values $a_1 = 3$, $a_2 = 1.4$ and $a_3 = 0.36$ were determined empirically for the California-Nevada territory, and will be used in this paper also.

At each time, within the territory being considered, the flow of the earthquakes is represented by the vector formed with the values of the different functions.

The problem of earthquake prediction can be formulated as follows: given the values of the functions at a given time t, determine whether the time interval $(t, t + \tau)$ belongs to a TIP of a main shock, or of a foreshock with magnitude M greater than a selected magnitude threshold M_0. For each territory the value of M_0 is chosen very close to the magnitude of the event with average return period of 5–7 years. The values of M_0 that have thus far been determined by GABRIELOV *et al.* (1986), DMITRIEVA *et al.* (1990), and KEILIS-BOROK *et al.* (1989) are in the range 4.5–7.5.

In our analysis of the flow of earthquakes, the time axis has been divided into intervals termed D, N and X. Intervals D extend for two years before each strong earthquake ($M \geq M_0$). Intervals X extend for three years after each strong earthquake; intervals of type X can become intervals of type D if a strong earthquake occurs within the three years. The remaining time intervals are termed N.

For a given region, the functions are discretized by defining the thresholds small, medium and large, on the basis of the quantiles levels 1/3 and 2/3. For all discretized functions, we estimate which combinations of the different functions are more typical for intervals D, and which for intervals N. These combinations, named characteristic features, were defined for the first time for California and Nevada by the method of pattern recognition (GELFAND *et al.*, 1976) with the purpose of predicting earthquakes having local magnitude $M_1 \geq 6.4$.

Table 1 shows the list of the selected functions, which are evaluated in the region under consideration. Following the procedure of pattern recognition, features D are defined by the condition that, in general, they occur during time intervals D, and not, during time intervals N. Features N are defined by the opposite condition. Each feature corresponds to a discretized value of the function, or to a combination of such values, for 2 or 3 functions.

The following rule was determined empirically by Keilis-Borók *et al.* (1989): a TIP is declared for one year at the time t if

$$n_D(t) - n_N(t) \geq V = 5 \tag{1}$$

$$\sigma(t) = 10^{-\beta(M_0-\alpha)}\Sigma 10^{\beta(M_i-\alpha)} < E = 4.9, \tag{2}$$

where

$$\beta = 1; \quad \alpha = 5; \quad M_i \geq M_0 - 1.4.$$

Here $n_D(t)$ is the number of characteristic features D that the flow of earthquakes has at the time t, and $n_N(t)$ is the number of the features of opposite kind N. The function $\sigma(t)$ is proportional to the total seismic energy released in the whole region within a period of 3 years before time t, and normalized by the seismic energy of an earthquake of magnitude M_0. The TIP during which a strong earthquake does not occur is defined, in this context, a false alarm. Consecutive TIPs may overlap and therefore give rise to alarm periods longer than one year. TIPs are interrupted if $\sigma(t) > E$, therefore false-alarm durations may be shorter than one year. A strong earthquake that occurs outside the TIPs is termed a "failure to predict".

The algorithm is formulated in a normalized manner; therefore, it can be transferred from one territory to another without additional retrofitting of parameters. In each territory only boundaries and the value of M_0 are defined with some degree of freedom.

The algorithm has been successfully applied to several regions: Central Asia, Caucasus, Western Turkmenia, Kamchatka and Kuril Islands, Eastern-Carpathians, Belgium, Cocos plate, Gulf of California, and Northern-Appalachians (GABRIELOV *et al.*, 1986; DMITRIEVA *et al.*, 1990; KEILIS-BOROK *et al.*, 1989). The results can be summarized as follows: on a worldwide scale, TIPs precede 27 out of 34 strong earthquakes and, in different regions, occupy, on the average, about 24 percent of the time interval analyzed.

For the Italian territory, clustering has been analysed by BOTTARI and NERI (1983). Only earthquake prediction based on clustering has been considered by CAPUTO *et al.* (1983) and CAPUTO (1983). Here we apply the CN algorithm for intermediate-term earthquake prediction in Central Italy.

2. Earthquake Statistics

The algorithm CN has been applied to the catalogues ENEL, CSEM, ING and PFG. In a first step we used the data until 1986, taken from ENEL, CSEM and ING. Events contained in CSEM but not present in ENEL or ING were included in the list of events used in this paper. Furthermore as far as magnitude is concerned M_l (local magnitude) has been used whenever available. If M_l is not available M_s (surface waves magnitude) from CSEM is used; if even M_s is not available we used M_b (body waves magnitude) from CSEM; for the events for which even M_b is not available we used M_d (coda magnitude) from ING. Initially we analysed the whole Italian territory. Tables 2–4 are constructed from ENEL, CSEM and ING and show the distribution of earthquakes versus magnitude and time, for different parts: Northern (lat. 48–45 N), Central (lat. 45–39.5 N) and Southern (lat. 39.5–35 N). The completeness of the catalogue we have constructed for these parts is quite different. For Central Italy it is reasonable to assume that our catalogue is sufficiently complete for magnitude greater than 4.0, after 1950.

Table 2

Distribution of earthquakes in magnitude and time (Northern Italy)

Year	0	Magnitude ≥ 3.0	3.1	3.2	3.3	3.4	3.5	4.0	4.5	5.0	5.5	6.0
1940	10	·	·	·	·	·	·	·	·	·	·	·
1941	1	·	·	·	·	·	·	·	·	·	·	·
1942	8	1	1	1	1	1	1	·	·	·	·	·
1943	21	4	4	4	4	4	4	4	3	·	·	·
1944	2	·	·	·	·	·	·	·	·	·	·	·
1945	3	1	1	1	1	1	1	1	1	·	·	·
1946	3	·	·	·	·	·	·	·	·	·	·	·
1947	10	1	1	1	1	1	1	1	·	·	·	·
1948	15	·	·	·	·	·	·	·	·	·	·	·
1949	29	2	2	2	2	2	2	2	1	·	·	·
1950	6	·	·	·	·	·	·	·	·	·	·	·
1951	8	3	3	3	3	3	3	3	1	·	·	·
1952	8	1	1	1	1	1	1	1	·	·	·	·
1953	2	1	1	1	1	1	1	·	·	·	·	·
1954	11	2	2	2	2	2	2	1	1	·	·	·
1955	15	1	1	1	1	1	1	1	·	·	·	·
1956	7	1	1	1	1	1	1	1	1	·	·	·
1957	10	·	·	·	·	·	·	·	·	·	·	·
1958	9	·	·	·	·	·	·	·	·	·	·	·
1959	17	3	3	3	3	3	3	3	2	·	·	·
1960	41	4	4	4	4	4	4	4	2	·	·	·
1961	17	·	·	·	·	·	·	·	·	·	·	·
1962	7	·	·	·	·	·	·	·	·	·	·	·
1963	16	1	1	1	1	1	1	·	·	·	·	·
1964	30	·	·	·	·	·	·	·	·	·	·	·
1965	18	·	·	·	·	·	·	·	·	·	·	·
1966	30	1	1	1	1	1	1	·	·	·	·	·
1967	25	2	2	2	2	2	1	1	1	·	·	·
1968	30	3	3	3	3	3	3	2	2	·	·	·
1969	17	2	2	2	2	2	2	1	·	·	·	·
1970	13	4	4	4	4	4	4	1	·	·	·	·
1971	29	8	8	8	8	8	7	2	·	·	·	·
1972	18	1	1	1	1	1	1	·	·	·	·	·
1973	14	4	4	4	4	4	3	2	·	·	·	·
1974	14	3	3	3	3	3	3	1	·	·	·	·
1975	7	5	5	5	5	5	4	3	1	·	·	·
1976	628	174	174	174	174	174	154	61	21	11	5	3
1977	117	30	30	30	30	30	18	8	2	1	1	·
1978	56	26	26	26	26	23	19	6	1	·	·	·
1979	62	20	20	20	20	19	17	6	3	·	·	·
1980	62	12	12	12	12	9	8	4	1	1	·	·
1981	45	17	17	17	17	12	10	3	1	·	·	·
1982	54	15	15	15	15	12	10	2	·	·	·	·
1983	67	19	19	19	19	17	12	7	3	·	·	·
1984	59	18	18	18	18	17	15	3	1	·	·	·
1985	61	11	11	11	11	9	6	1	·	·	·	·
1986	151	34	29	24	20	16	12	4	2	·	·	·
1987	155	29	18	11	9	4	4	2	·	·	·	·
1988	182	23	20	15	9	7	6	3	2	1	·	·
1989	109	7	6	3	3	3	3	·	·	·	·	·

Table 3

Distribution of earthquakes in magnitude and time (Central Italy)

Year	Magnitude ≥ 0	0.3	3.1	3.2	3.3	3.4	3.5	4.0	4.5	5.0	5.5	6.0
1940	107	6	6	6	6	6	6	6	2	·	·	·
1941	191	4	4	4	4	4	4	4	2	1	·	·
1942	59	·	·	·	·	·	·	·	·	·	·	·
1943	52	5	5	5	5	5	5	4	2	·	·	·
1944	2	2	2	2	·	·	·	·	·	·	·	·
1945	7	4	4	4	4	4	4	4	2	1	·	·
1946	9	2	2	2	2	2	2	2	·	·	·	·
1947	40	6	6	6	5	5	5	5	3	1	·	·
1948	45	7	7	7	6	6	6	6	5	1	·	·
1949	54	4	4	4	3	3	3	2	·	·	·	·
1950	52	5	5	5	5	5	5	4	3	1	·	·
1951	34	10	10	10	10	10	10	10	4	1	·	·
1952	17	8	8	8	8	8	8	6	·	·	·	·
1953	26	9	9	9	9	9	7	4	·	·	·	·
1954	17	4	4	4	4	4	4	2	2	·	·	·
1955	49	12	12	12	10	10	10	6	2	1	·	·
1956	96	17	17	17	16	16	16	10	4	1	·	·
1957	105	21	21	21	19	19	19	12	5	·	·	·
1958	61	6	6	6	3	3	3	3	1	1	·	·
1959	89	6	6	6	6	6	6	5	3	1	1	·
1960	82	21	21	19	17	13	10	3	·	·	·	·
1961	74	26	26	26	25	25	25	16	9	·	·	·
1962	83	28	28	27	26	25	24	16	6	4	3	1
1963	137	48	48	43	39	35	32	17	6	4	2	·
1964	86	18	18	18	14	14	14	10	4	1	·	·
1965	69	35	35	34	34	32	29	15	4	·	·	·
1966	63	16	16	16	10	9	9	6	·	·	·	·
1967	56	19	19	17	15	15	14	11	5	1	1	·
1968	60	29	29	27	24	21	16	9	1	·	·	·
1969	71	32	32	27	26	24	24	12	3	·	·	·
1970	113	39	39	37	34	32	26	13	1	·	·	·
1971	329	80	74	68	60	57	50	21	6	1	·	·
1972	355	183	144	129	112	76	52	25	5	2	·	·
1973	165	31	30	27	25	22	20	13	1	·	·	·
1974	208	74	67	61	53	50	44	16	3	1	·	·
1975	104	32	29	28	25	18	13	4	2	·	·	·
1976	137	61	49	49	41	39	36	14	5	2	·	·
1977	211	89	56	55	42	39	34	17	3	·	·	·
1978	108	81	66	65	46	45	38	14	5	·	·	·
1979	465	234	142	142	91	88	75	19	5	2	1	·
1980	745	234	213	185	159	141	120	60	24	6	1	1
1981	283	116	86	67	58	54	46	14	4	·	·	·
1982	185	95	83	74	68	57	49	18	5	1	·	·
1983	88	64	56	46	41	31	29	10	4	2	1	·
1984	211	143	134	127	107	98	84	33	8	4	3	·
1985	120	79	71	58	53	43	36	10	2	2	·	·
1986	1247	193	154	120	92	67	57	17	4	·	·	·
1987	879	106	85	64	53	43	34	13	2	·	·	·
1988	971	66	49	44	36	30	22	8	2	1	·	·
1989	634	21	16	15	13	11	7	2	·	·	·	·

Table 4

Distribution of earthquakes in magnitude and time (Southern Italy)

Year	Magnitude ≥ 0	3.0	3.1	3.2	3.3	3.4	3.5	4.0	4.5	5.0	5.5	6.0
1940	7	2	2	2	2	2	2	2	2	·	·	·
1941	20	1	1	1	1	1	1	1	1	1	1	1
1942	5	1	1	1	1	1	1	1	·	·	·	·
1943	3	1	1	1	1	1	1	1	·	·	·	·
1944	·	·	·	·	·	·	·	·	·	·	·	·
1945	1	·	·	·	·	·	·	·	·	·	·	·
1946	6	·	·	·	·	·	·	·	·	·	·	·
1947	67	·	·	·	·	·	·	·	·	·	·	·
1948	7	·	·	·	·	·	·	·	·	·	·	·
1949	41	1	1	1	1	1	1	1	1	1	1	·
1950	41	5	5	5	5	5	5	3	1	1	·	·
1951	4	·	·	·	·	·	·	·	·	·	·	·
1952	22	5	5	5	5	5	4	1	·	·	·	·
1953	8	3	3	3	3	3	3	1	·	·	·	·
1954	26	5	5	5	5	5	5	4	2	1	·	·
1955	38	1	1	1	1	1	1	·	·	·	·	·
1956	4	2	2	2	2	2	2	1	·	·	·	·
1957	18	3	3	3	3	3	3	2	2	2	1	·
1958	7	·	·	·	·	·	·	·	·	·	·	·
1959	17	3	3	3	2	2	2	1	1	1	1	·
1960	12	2	2	2	2	2	2	·	·	·	·	·
1961	7	5	5	4	4	2	1	1	1	1	·	·
1962	6	·	·	·	·	·	·	·	·	·	·	·
1963	9	1	1	1	1	1	1	1	·	·	·	·
1964	2	·	·	·	·	·	·	·	·	·	·	·
1965	7	2	2	2	2	2	2	2	1	·	·	·
1966	5	·	·	·	·	·	·	·	·	·	·	·
1967	7	4	4	4	4	3	3	3	3	1	·	·
1968	177	144	144	137	124	101	94	44	15	6	5	1
1969	22	5	5	5	5	5	5	1	·	·	·	·
1970	16	2	2	2	1	1	1	1	1	·	·	·
1971	21	4	4	4	4	4	4	3	1	·	·	·
1972	23	1	1	1	1	1	1	1	·	·	·	·
1973	10	1	1	1	1	1	1	1	1	·	·	·
1974	40	20	19	19	18	16	15	7	1	·	·	·
1975	12	4	4	4	4	4	3	1	·	·	·	·
1976	29	14	13	13	12	12	12	6	·	·	·	·
1977	28	17	16	16	15	15	15	8	3	1	·	·
1978	153	86	72	72	61	61	55	18	3	2	2	·
1979	107	54	34	34	23	23	21	6	1	1	·	·
1980	82	56	55	52	50	47	39	14	4	3	1	·
1981	36	30	27	27	26	25	21	14	5	1	·	·
1982	37	18	14	14	14	13	11	1	·	·	·	·
1983	13	13	13	13	13	13	13	7	3	1	1	1
1985	17	14	14	13	13	13	11	8	2	·	·	·
1986	288	80	64	47	34	22	14	1	·	·	·	·
1987	208	26	18	15	8	5	4	2	1	·	·	·
1988	375	15	12	11	6	4	3	·	·	·	·	·
1989	302	12	9	7	6	5	4	·	·	·	·	·

For the Northern and Southern parts a sufficient degree of completeness can be seen only after 1976. Our definition of sufficient completeness is justified by the fact that all functions, with the exception of $B_{\max}(t)$, depend upon events with magnitude greater than m_1. This threshold, on the basis of the flow of earthquakes, deduced from catalogues ENEL, CSEM, ING, has been estimated to be equal to 4.4. The function $B_{\max}(t)$ depends on events with magnitude greater than $M_0 - 3.6$. In its definition, therefore, it is also necessary to use events with relatively small magnitudes.

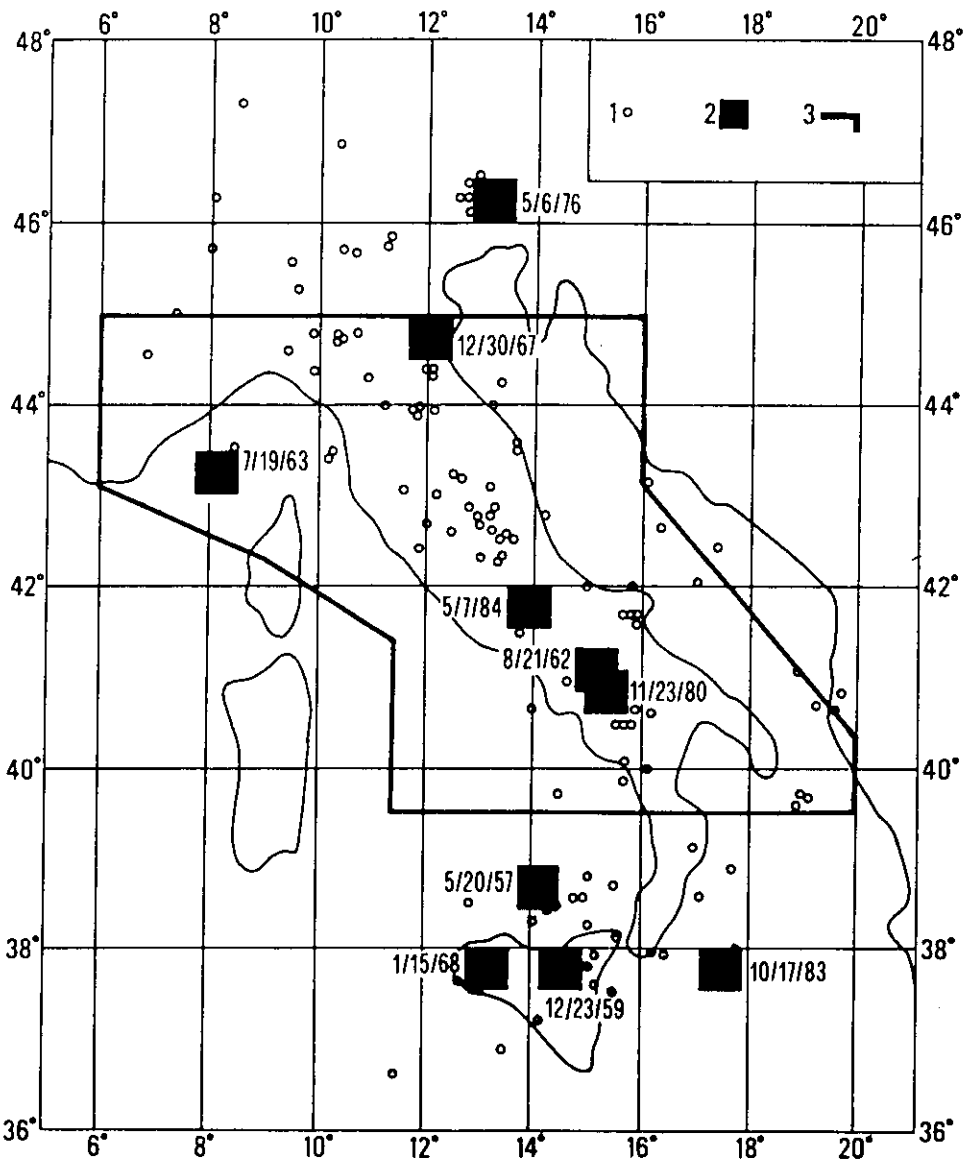

Figure 1
Epicenters of earthquakes recorded in the period 1950–1985 [9, 10, 11]; 1—epicenters of earthquakes with $M \geq 4.5$; 2—epicenters of earthquakes with $M \geq 5.6$ identified by their date of occurrence; 3—boundary of selected region (Central Italy).

On the basis of this preliminary analysis we decided to test the algorithm for Central Italy. The boundaries of the territory considered are shown in Figure 1 as thick solid lines and have been drawn on the basis of the spatial distribution of epicenters, and the scheme of morphostructural zonation (CAPUTO *et al.*, 1980). The region chosen includes the zone along which there is interaction between different lithospheric blocks (Figure 2) as outlined by surface wave dispersion analysis

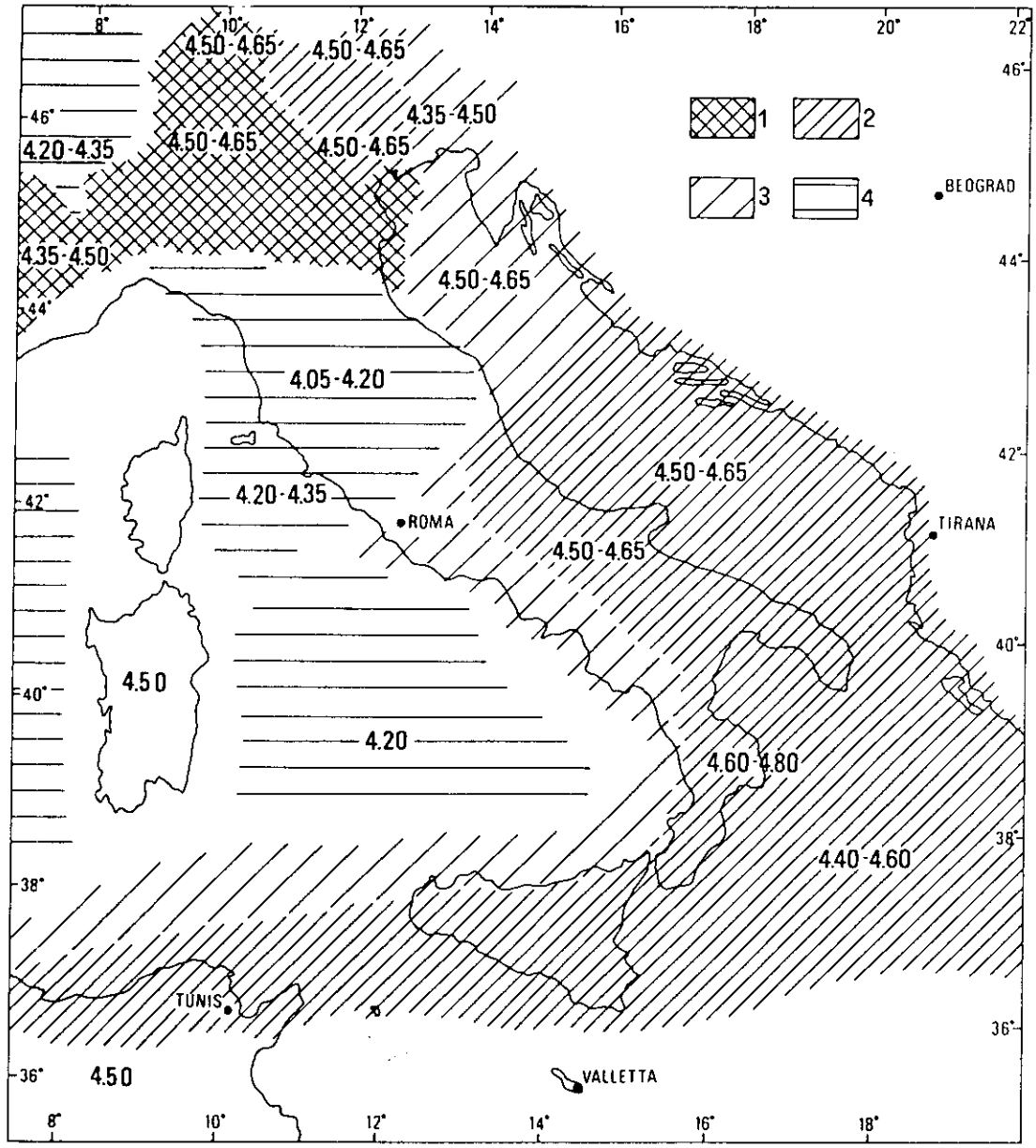

Figure 2

Schematic regionalization of the elastic properties of the lithospheric sub-Moho layer, the 'lid', as deduced from surface waves dispersion analysis (CALCAGNILE and PANZA, 1981): 1—lid thickness not exceeding 105 km; 2—lid thickness not exceeding 75 km; 3—lid thickness not exceeding 45 km; 4—lid thickness not exceeding 15 km. The three digits numbers indicate the average *S*-wave velocity in the lid.

(CALCAGNILE and PANZA, 1981). Catalogues ENEL and ING contain useful information only for longitudes less than 19 E. The extension to 20 E has been made using CSEM for the time interval 1976–1988.

Before 1971, magnitude was determined only for a fraction of the earthquakes with $M < 4$. The approximate number of all earthquakes listed up to 1971 is about the same as for listed earthquakes with $M \geq 3$ after 1971. Accordingly, in this study, we have used all earthquakes that are listed before 1971, and earthquakes with a magnitude greater than or equal to 3 thereafter.

We consider only earthquakes with focal depth $H < 100$ km, and we define as strong earthquakes the events with $M \geq 5.6$. In other words we choose the threshold $M_0 = 5.6$. The list of such events is given in Table 5. This magnitude threshold is chosen because earthquakes with $M \geq 5.6$ have an average return period of about 6 years (see Table 6), as in most of the regions considered in previous studies. Since events n.1 and n.2 of Table 5 have the same coordinates and occurred on the same day they cannot be considered separately in our analysis. Therefore the number of strong earthquakes to be actually predicted reduces to five.

Table 5

Strong earthquakes in Central Italy, $M \geq 5.6$, 1950–1989

No.	Date	$\phi°$, N	$\lambda°$, E	H	Magnitude M_1	M_d	M_b	M_s
1	21. 8.1962	41.13	15.12	40	5.8	—	—	—
2	21. 8.1962	41.13	15.12	40	6.0	—	—	—
3	19. 7.1963	43.15	8.08	29	5.6	—	—	—
4	30.12.1967	44.80	12.05	35	5.8	—	—	—
5	23.11.1980	40.86	15.33	18	6.5	—	6.28	6.7
6	7. 5.1984	41.76	13.89	16	—	5.4	5.43	5.7

Table 6

Average return period of strong earthquakes (Central Italy)

M ≥	5.0	5.1	5.2	5.3	5.4	5.5	5.6	5.7	5.8	5.9	6.0
Years	1.1	2	2	2.3	2.5	3.5	5.7	7	9	9	17

3. Diagnosis of TIPs

As allowed by the normalization, algorithm *CN* is applied without any change in the numerical parameters, with the purpose of testing the general validity of the results obtained in other parts of the world. In fact, a proper change in the parameters can lead to better predictions—actually better data fitting—in each region, but this requires that we assume different physical processes for the

Table 7

Strong earthquakes and TIPs for Central Italy ($V = 5, E = 4.9$)

Start of TIP	Strong earthquake Date	M	End of false alarm	Duration of TIP, months
1. 1.1958			1. 1.1959	12
1.11.1961	21. 8.1962	5.8; 6.0		10
22. 8.1962	19. 7.1963	5.6		11
	30.12.1967	5.8		failure to predict
1. 3.1972			1. 5.1975	38
1.11.1979	23.11.1980	6.5		13
1. 3.1984	7. 5.1984	5.7		2
8. 5.1984			1.11.1986	30
1. 5.1988				>15

occurrence of the earthquakes in different regions.

Aftershocks are identified by the algorithm described by KEILIS-BOROK *et al.* (1980). The choice of $M_0 = 5.6$ and the discretization of functions is made on the basis of the information contained in the catalogues ENEL, CSEM, and ING up to 1986.

TIPs diagnosed in such a way are compared with strong earthquakes ($M \geq M_0$) in Table 7 and in Figure 3a. TIPs occupy 26 percent of the total time interval

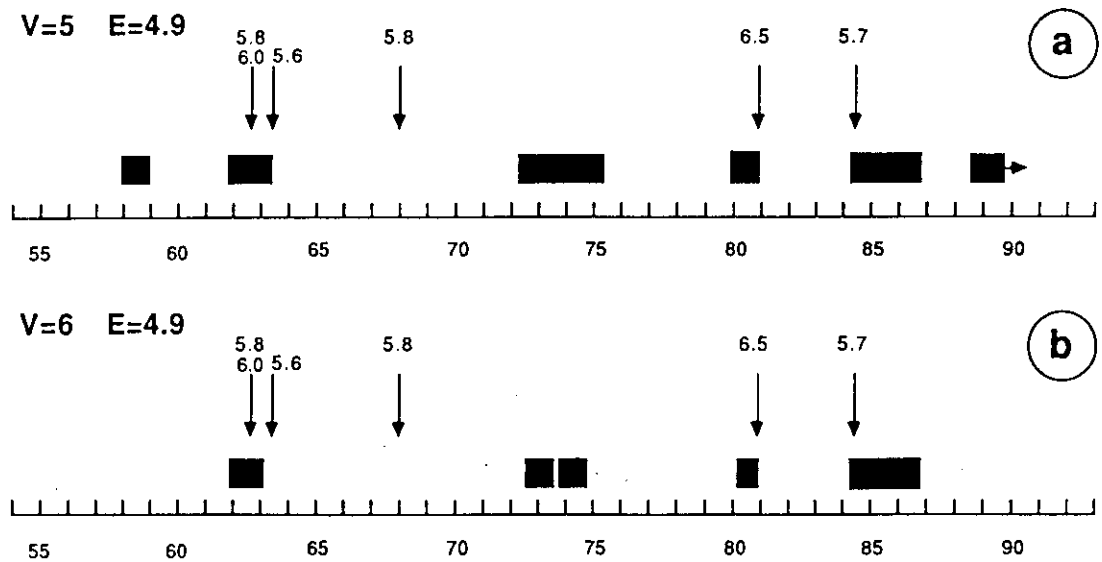

Figure 3

Part a). Results of the diagnosis of TIPs for Central Italy as deduced from catalogues ENEL, ING, CSEM; $M_0 = 5.6$, $E = 4.9$, $V = 5$; Part b). Results of the diagnosis of TIPs for Central Italy as deduced from catalogues ENEL, ING, CSEM; $M_0 = 5.6$, $E = 4.9$, $V = 6$; the time of occurrence of a strong earthquake is indicated by an arrow and a number above giving its magnitude; TIP is indicated by black rectangle.

considered (1954–1986) and precede 4 out of 5 strong earthquakes. The value reached by the function $\sigma(t)$ after the last strong earthquake (May 7, 1984, $M = 5.7$) is not sufficient to interrupt the TIP. This gives rise to a false alarm. If V is increased from 5 to 6 the total duration of TIPs is reduced by about 17 percent with an additional failure to predict (Figure 3b). Even if we observe 3 false alarms, i.e. TIPs not followed by strong earthquakes, the forward monitoring of TIPs may give very useful practical information.

4. Forward Monitoring

Forward monitoring, utilizing the available data which describe the seismic activity until August 1989 (ING and CSEM), shows that TIPs occupy 30 percent of the total time interval (1954–1989) and that there is a current TIP started on May 1988. The current TIP is not identified if the threshold V is increased to 6.

5. Stability

To test the stability of the results shown in Figure 3, the procedure has been repeated using catalogues PFG and ING. In this case there are only four strong earthquakes ($M \geq 5.6$) since in PFG and ING the events of December 30, 1967 and May 7, 1984 have magnitude 5.4. TIPs, shown in Figures 4a and 4b, occupy 32 and

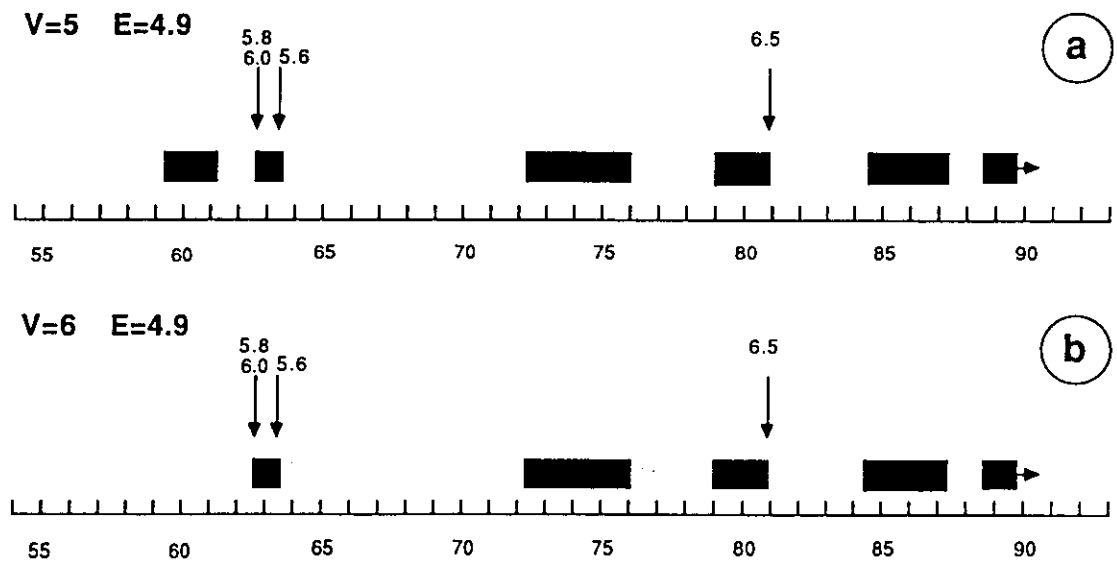

Figure 4

Part a). Results of the diagnosis of TIPs for Central Italy as deduced from catalogues PFG and ING $M_0 = 5.6$, $E = 4.9$, $V = 5$; Part b). Results of the diagnosis of TIPs for Central Italy as deduced from catalogues PFG and ING $M_0 = 5.6$, $E = 4.9$, $V = 6$; the time of occurrence of a strong earthquake is indicated by an arrow and a number above giving its magnitude; TIP is indicated by black rectangle.

27 percent of the total time interval (1954–1989) for $V = 5$ and $V = 6$, respectively. The overall picture shown in Figure 4 is not significantly different from that contained in Figure 3. The main differences are the failure to predict the event of August 21, 1962 when catalog PFG and ING are used, and the absence of a current TIP when catalogs ENEL, CSEM and ING are used with the threshold $V = 6$.

The false alarms in the time intervals 1972–1975 and 1984–1986 have some peculiar aspects. In fact, the first could be associated with the event with magnitude 5.4 which occurred, within the considered area, in October 1974. The assumption for this magnitude value of an underestimate of 0.2 units will lead to the prediction of the event, with a significant reduction of the duration of the subsequent false alarm over the entire period of observation (1954–1989). The second false alarm may be connected with the event of magnitude 5.6 which occurred in Thessaly, Greece, on April 30, 1985. From this it is evident how critical the selection of the area is within which TIPS are sought. Therefore we are now investigating the possibility of using other variants of regionalization based on geological and geophysical interpretations. This is made even more necessary by the existence of a possible current TIP, declared on the basis of traits which are characterizing the seismicity of a zone near the eastern border of the region we have defined as Central Italy. The features are based on B_{max}, whose high value is associated with the 5.4 magnitude earthquake of April 26, 1988 with epicentral coordinates 42.31 N and 16.59 E.

Acknowledgments

This research was partly carried out within the framework of the Pilot Activities of the International Center for Earth and Environmental Sciences (ICS), Trieste Miramar. Partial financial support was given by CNR-Gruppo Nazionale per la Difesa dai Terremoti, contract n.88.01067.54.

We are grateful to Fred Schwab for his comments on revising this manuscript.

REFERENCES

ALLEN, C., HUTTON, K., KEILIS-BOROK, V. I., KNOPOFF, L., KOSOBOKOV, V. G., KUZNETSOV, I. V., and ROTWAIN, I. M. (1983), *Selfsimilar Premonitory Seismicity Patterns*, Abstract, XVIII Congress of IUGG, Hamburg.

BOTTARI, A., and NERI, G. (1983), *Some Statistical Properties of a Sequence of Historical Calabro-Peloration Earthquakes*, J. Geophys. Res. *88*, 1209–1212.

CALCAGNILE, G., and PANZA, G. F. (1981), *The Main Characteristics of the Lithosphere-Asthenosphere System in Italy and Surrounding Regions*, Pure Appl. Geophys. *119*, 865–879.

CAPUTO, M., KEILIS-BOROK, V. I., OFICEROVA, E. N., RANZMAN, E. Ya., ROTWAIN, I. M., and SOLOVIEV, A. A. (1980), *Pattern Recognition of Earthquakes Prone Areas in Italy*, Phys. Earth Planet. Interiors *21*, 305–320.

CAPUTO, M., CONSOLE, R., GABRIELOV, A. M., KEILIS-BOROK, V. I., and SIDORENKO, T. V. (1983), *Long-term Premonitory Seismicity Patterns in Italy*, Geophys. J. R. Astr. Soc. *75*, 71–75.

CAPUTO, M. (1983), *The Occurrence of Large Earthquakes in South Italy*, Tectonophysics *99*, 73–83.

CSEM, *European-Mediterranean Hypocenters Data File 1976–1988* (CSEM, Strasbourg 1989).

DMITRIEVA, O. E., ROTWAIN, I. M., KEILIS-BOROK, V. I., and DE BECKER, M. (1990), *Premonitory Seismicity Patterns in a Platform Region (Ardennes-Rhenish and Brabant Massives, Lower Rhone Graben), 1989*, Computational Seismology *23*, (in press).

ENEL, *Catalogue of Earthquakes of Italy, Years 1000–1980* (Publication ENEL, Roma 1980).

GABRIELOV, A. M., DMITRIEVA, O. E., KEILIS-BOROK, V. I., KOSOBOKOV, V. G., KUZNETSOV, I. V., LEVSHINA, T. A., MIRZOEV, K. M., MOLCHAN, G. M., NEGMATULLAEV, S. Kh., PISARENKO, V. F., PROZOROV, A. G., RINEHART, W., ROTWAIN, I. M., SHEBALIN, P. N., SHNIRMAN, M. G., and SCHREIDER, S. Yu., *Algorithms of Long-Term Earthquakes' Prediction*, International School for Research Oriented to Earthquake Prediction-Algorithms, Software and Data Handling (Lima, Peru, September 1986).

GELFAND, I. M., GUBERMAN, Sh. A., KEILIS-BOROK, V. I., KNOPOFF, L., PRESS, F., RANZMAN, E. Ya., ROTWAIN, I. M., and SADOVSKY, A. M. (1976), *Pattern Recognition Applied to Earthquake Epicenters in California*, Phys. Earth. Planet. Int. *11*, 227–283.

ING, *Seismological Reports 1981–1988* (ING, Rome 1982–1989).

KEILIS-BOROK, V. I., KNOPOFF, L., and ROTWAIN, I. M. (1980), *Bursts of Aftershocks, Long-Term Precursors of Strong Earthquakes*, Nature *283* (5744), 259–263.

KEILIS-BOROK, V. I., KNOPOFF, L., ROTWAIN I. M., and ALLEN, C. R. (1988), *Intermediate-term Prediction of Occurrence Times of Strong Earthquakes*, Nature *335* (6192), 690–694.

KEILIS-BOROK, V. I., and ROTWAIN, I. M. (1989), *Diagnostics of TIPs of Strong Earthquakes in Northern Appalachians*, Computational Seismology *22*, 18–23.

PFG, *Catalogo dei terremoti italiani dall'anno 1000 al 1980* (ed. Postpischl, D.) (CNR-P. F. Geodinamica, 1985).

(Received January 12, 1989, revised September 12, 1989, accepted January 30, 1990)

PAGEOPH, Vol. 145, No. 2 (1995) 0033-4553/95/020259-17$1.50 + 0.20/0

Stability of Premonitory Seismicity Pattern and Intermediate-term Earthquake Prediction in Central Italy

G. COSTA,[1,2] G. F. PANZA[1,2] and I. M. ROTWAIN[3]

Abstract—The algorithm CN makes use of normalized functions. Therefore the original algorithm, developed for the California-Nevada region, can be directly applied, without adjustment of the parameters, to the determination of the Time of Increased Probability (TIP) of strong earthquakes for Central Italy. The prediction is applied to the events with magnitude $M \geq M_0 = 5.6$, which in Central Italy have a return period of about six years. The routinely available digital earthquake bulletins of the Istituto Nazionale di Geofisica (ING), Rome, permits continuous monitoring. Here we extend to November 1994 the first study made by Keilis-Borok *et al.* (1990b). On the basis of the combined analysis of seismicity and seismotectonic, we formulate a new regionalization, which reduces the total alarm time and the failures to predict, and narrows the spatial uncertainty of the prediction with respect to the results of KEILIS-BOROK *et al.* (1990b).

The premonitory pattern is stable when the key parameters of the CN algorithm and the duration of the learning period are changed, and when different earthquake catalogues are used.

The anlysis of the period 1904–1940, for which $M_0 = 6$, allows us to identify self-similar properties between the two periods, in spite of the considerably higher seismicity level of the earlier time interval compared with the recent one.

Key words: Seismicity, earthquake prediction, seismotectonic, regionalization, Italy.

1. Introduction

The algorithm CN, described in full detail by GABRIELOV *et al.* (1986), KEILIS-BOROK *et al.* (1988) and KEILIS-BOROK *et al.* (1990a), has been applied to Central Italy for the first time by KEILIS-BOROK *et al.* (1990b). CN is designed to define the Time of Increased Probability (TIP) of strong earthquakes. For this purpose the traits considered are the level of seismic activity, its variation in time, clustering of the earthquakes in space and time, and their concentration in space.

[1] Istituto di Geodesia e Geofisica, Università degli Studi di Trieste, via dell'Università 7, 34123 Trieste, Italy.

[2] International Center for Theoretical Physics, ICTP, 34100 Trieste Miramar, Italy.

[3] International Institute of Earthquake Prediction Theory and Mathematical Geophysics, Academy of Sciences of Russia, Warshavskoye, 79, K.2, 113556, Moscow, Russia.

Table 1

Functions used in the algorithm CN

$SIGMA(T)$	$SIGMA(t) = \sum 10^{\beta(M_i - \alpha)}$; the main shocks with $m_i \le M_i \le -0.1$ and origin time ($t - 3$ years) $\le t_i \le t$ are included in the summation; $\alpha = 4.5$, $\beta = 100$.
$S_{max}(t)$	$S_{max}(t) = \max\{S_1/N_1, S_2/N_2, S_3/N_3\}$ where S_j is calculated as $SIGMA(t)$ for the events with the origin time ($t - j$ years) $\le t_i \le (t - (j-1)$ years), and N_j is the number of earthquakes in the sum.
$Z_{max}(t)$	$Z_{max}(t) = \max\{Z_1/N_1^{2/3}, Z_2/N_2^{2/3}, Z_3/N_3^{2/3}\}$ where Z_j is calculated as S_j, but with $\beta = 0.5$ and N_j is the number of earthquakes in the sum.
$N_2(t)$	Number of main shocks with $M \ge m_3$, which occurred in the time interval ($t - 3$ years, t).
$N_3(t)$	Number of main shocks with $M \ge m_2$, which occurred in the time interval ($t - 10$ years, $t - 7$ years).
$K(t)$	$K(t) = K_1 - K_2$, where K_j is the number of main shocks with $M_i \ge m_2$ and origin time ($t - 2j$ years) $\le t_i \le (t - 2(j-1)$ years).
$B_{max}(t)$	Maximum number of aftershocks for each main shock, counted within a radius of 50 km for the first 2 days after the main shock and for $M > M_0 - 3.6$.
$G(t)$	$G(t) = 1 - P$, where P is the ratio among the number of the main shocks with $M_j \ge m_2$ ($m_2 > m_1$) and the number of the main shocks with $M_j \ge m_1$. Only main shocks with origin time t_j in the interval ($t - 1$ year) $\le t_j \le t$ are considered.
$q(t)$	$q(t) = \sum_{j=1}^{6} \max\{0, 6a_2 - n_j\}$, where a_2 is the average annual number of main shocks with $M_j \ge m_2$, n_j is the number of main shocks with $M_j \ge m_2$ and origin time ($t - (8+j)$ years) $\le t_i \le (t - (2+j)$ years).

The functions which describe the traits for a given territory are defined in Table 1. These functions are normalized so that they can be applied to different territories, with different seismicity, without *ad hoc* adjustment. The normalization is obtained by choosing the three magnitude thresholds, m_1, m_2 and m_3, satisfying the condition that, in the territory under study, the average annual number of events with $M \ge m_i$ is equal to the constants, a_i, common to all seismically active territories.

The flow of the earthquakes is represented, at each time t, by the vector formed by the values of the different functions at time t. The value of the minimum magnitude of the events to be predicted (strong earthquakes), M_0, satisfies in general two simultaneous conditions: 1) to correspond to events with a return period of about six years; 2) to be as close as possible to a minimum in the histogram Magnitude-Number of events (Fig. 1). Condition 1 is introduced accordingly with the criteria used for the California-Nevada region; and condition 2 is introduced to minimize the effect of the threshold introduced by the choice of M_0. We will refer to those conditions as "CN rule."

In the CN analysis of the flow of earthquakes, the time axis is divided into three intervals: D (dangerous), N (nondangerous) and X (undetermined). The D intervals extend for two years before each strong event ($M \ge M_0$). Intervals X extend for

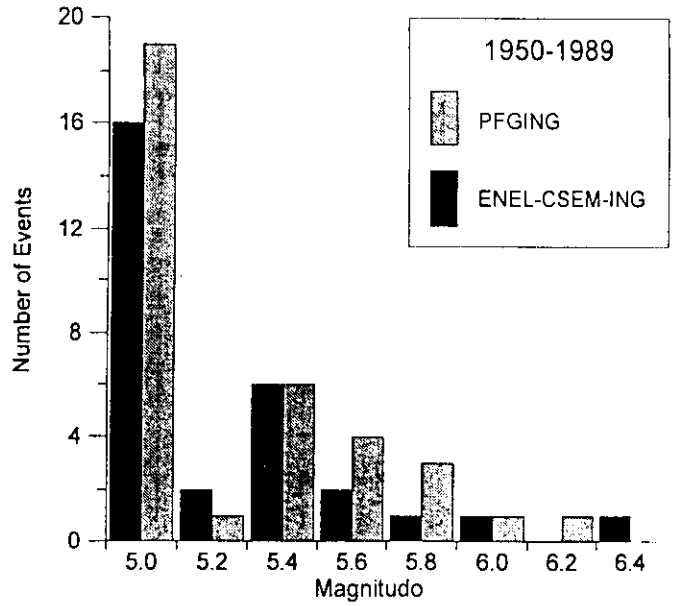

Figure 1
Histogram Magnitude-Number of events, with step 0.2 in magnitude, in the years 1950–1989 for the new regionalization proposed in this paper.

three years after each strong event; if a strong earthquake occurs within three years, the X period becomes a D period. The remaining time intervals are N intervals.

The functions defined in Table 1 are discretized by defining the thresholds as small, medium and large, on the basis of the quantile levels 1/3 and 2/3. We then estimate the combinations of the different discretized functions which are more typical for intervals D, and for intervals N. Following the procedure of pattern recognition, features D are defined by the condition that in general they occur during the intervals D and not during the intervals N. Features N are defined by the reverse condition. Each feature corresponds to a discretized value of the function, or to a combination of such values, for two or three functions.

A TIP is declared at the time t for one year if

$$n_{D(t)} - n_{N(t)} \geq V = 5$$

$$\sigma(t) = 10^{-\beta(M_0 - \alpha)} \sum 10^{\beta(M_i - \alpha)} < E = 4.9 \qquad (1)$$

where

$$\beta = 1; \quad \alpha = 0.5$$

$n_{D(t)}$ is the number of characteristic features D which the flow of earthquakes has at time t; $n_{N(t)}$ is the number of features N; in each main shock's area, $\sigma(t)$ is a function proportional to the total number of earthquakes, with magnitude M_i, occurring within a period of three years before time t.

Consecutive TIPs may overlap and induce an alarm period exceeding one year. The TIP can be interrupted if $\sigma(t) > E$, in which case the TIP can be shorter than one year. If during a TIP we have no strong event we have a "false alarm," if we have a strong event outside the TIP we have a "failure to predict."

All the constants and the definition of D and N features appearing in the algorithm CN are determined from the retrospective analysis of the California-Nevada seismicity (KEILIS-BOROK *et al.*, 1990a).

2. *Tectonics and Regionalization*

Central Italy is characterized by the presence of two arcs, the north-central Apennines and the Calabrian arc, of tectonic shortening. Starting from their present-day structure and analyzing the time-space evolution of the thrust belt-fore-deep-foreland system, PATACCA *et al.* (1990) reached the conclusion that the deformation has been strictly controlled by the dipping of the foreland lithosphere sinking beneath the mountain chain peninsula and not directly by the collision between Europe and Africa. This hypothesis is strongly supported by surface waves dispersion measurements (CALCAGNILE and PANZA, 1981; PANZA *et al.*, 1982; SUHADOLC and PANZA, 1988; DELLA VEDOVA *et al.*, 1991), and more recent investigations which combine different geophysical data sets regarding aeromagnetic and gravity anomalies with the available structural information concerning the lithosphere-asthenosphere system (MARSON *et al.*, 1994).

The arc present in the north-central Apennines can be divided in two main structures parallel to his axis: one is an area of compression, and the second is a zone of extension (Fig. 2). These two main structures are crossed by a few transfer zones.

The passive subduction of the Po-Adriatic-Ionian lithosphere by gravitational sinking appears as a reasonable mechanism to explain contemporaneous geodynamic events such as mountain building in the Apennines and extension in the Tyrrhenian area. The partition of the Apennines into two major arcs may be related to the differential sinking of the foreland lithosphere in the Northern Apennines and in the Calabrian Arc.

The regionalization is a very important factor in producing a useful prediction, minimizing the spatial uncertainty. The area in which a strong earthquake must be predicted must be the smallest possible, but there are some limitations to its minimum dimensions: 1) the borders of the area must not cross continuous seismotectonic zones, at least the ones easily identifiable, and, 2) the annual number of earthquakes must be ≥ 3 for the magnitude for which the catalogue is completed.

The regionalization used by KEILIS-BOROK *et al.* (1990b) (Fig. 3), based only on the boundaries and completeness of ENEL catalogue, covers an area of about 6.3×10^5 km^2 and allows us to obtain overall satisfactory results, but without negligible false alarms and failures to predict (Fig. 4).

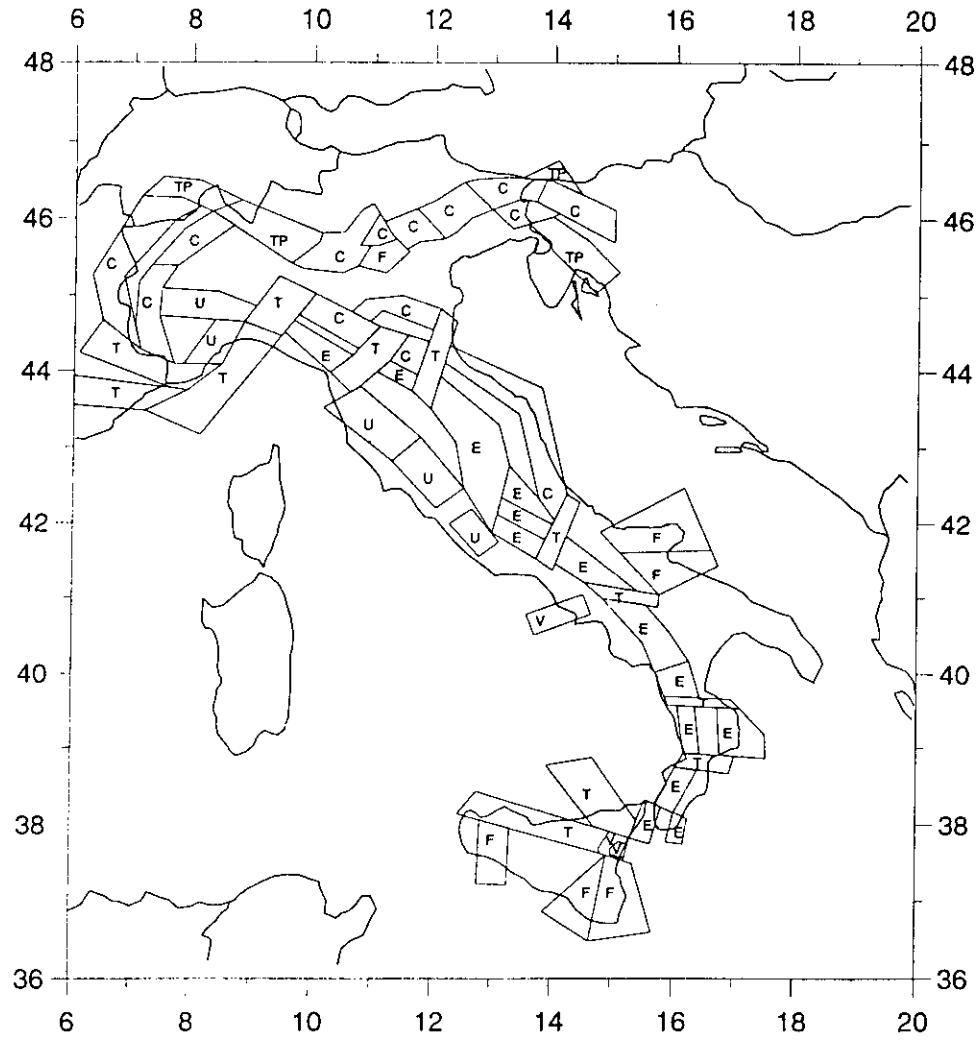

Figure 2
Seismotectonic map of PATACCA *et al.* (1990): *E*) extension areas, *C*) compressional areas, *T*) transition areas, *F*) areas of fracture in foreland zone, *TP*) transpressive areas, *V*) volcanic areas, and *U*) undefined areas.

The analysis of the occurrence, just before the TIPs, of the events with a magnitude greater than the minimum magnitude, m_1, used in the definition of the functions in the CN algorithm, reveals that in all the three-year time intervals which immediately precede the TIPs, it is possible to identify three distinct seismically active areas: the Apennines, the Ancona zone and the Gargano region (compare Fig. 5 with Fig. 6). The seismicity along the Apennines is present during all TIPs, while the events along the eastern border of the Adriatic microplate in the Ancona zone and in the Gargano region, occur only before the false alarms (Figs. 6c,d). This may suggest that the earthquakes along the Apennines are independent from the seismicity of the other two areas (Ancona zone and Gargano region) and that the events in the Ancona zone and in the Gargano region are associated with dynamic processes of the lithospheric blocks, which are different than those

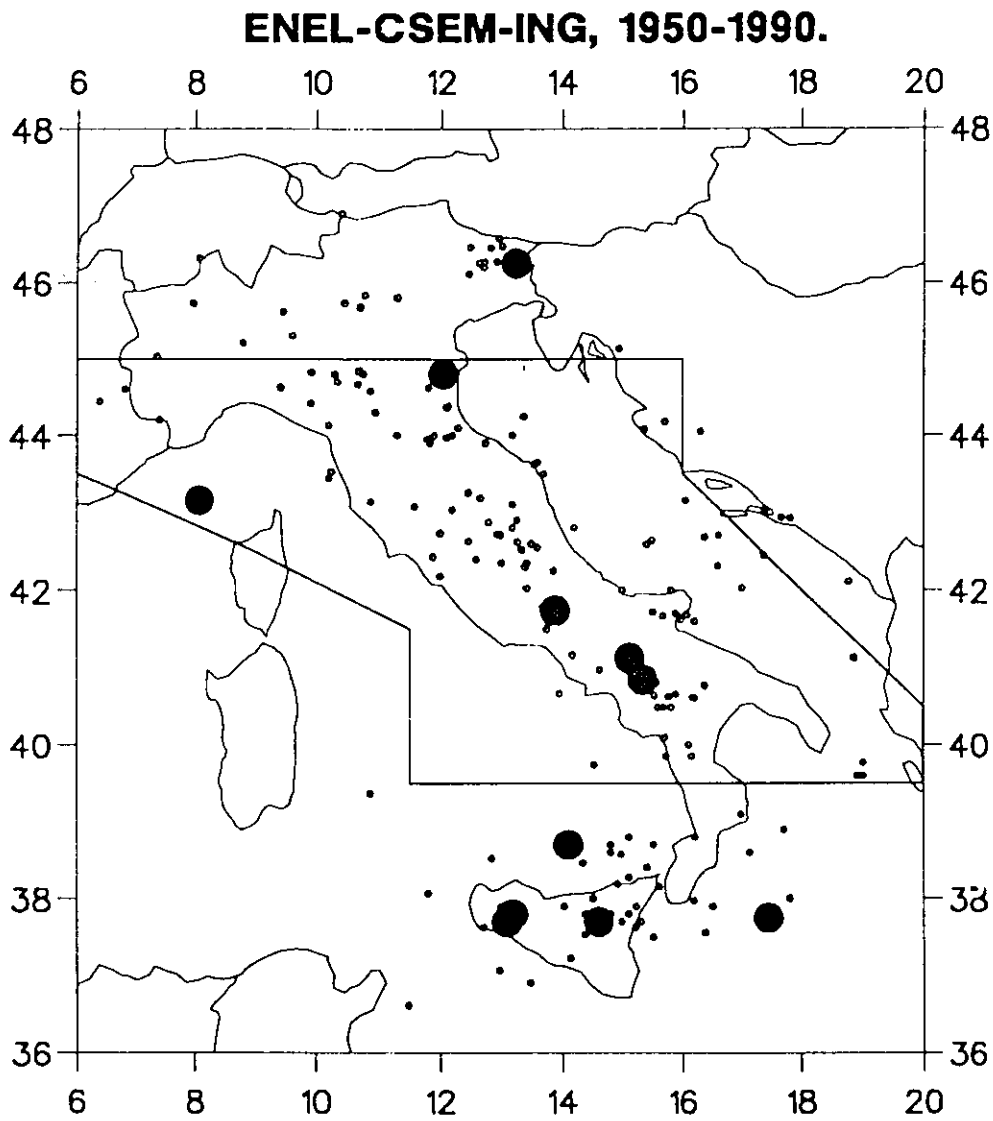

Figure 3
Epicenters recorded in the period 1950–1990; small dots indicate events with magnitude $M \geq 4.4$; large dots indicate events with magnitude $M \geq M_0 = 5.6$; the poligon indicates the boundaries of the regionalization proposed by KEILIS-BOROK *et al.* (1990b).

characterizing the Apennines. The events in the Ancona zone and in the Gargano region can be correlated with the seismicity of the eastern border of the Adriatic microplate (compare Fig. 5 with Fig. 6).

The map of the main shocks in Italy, obtained from the PFG-ING catalogue, shows that there are two maxima in the number of events in the Apennines (Umbria and Lazio) and, in general, a very large number of events along the Apennines from Liguria to Campania (Fig. 7a); this area can be separated from the other seismic regions in Italy. The map of the events with $M \geq m_1 = 4.4$, shown in Fig. 7c, indicates that the earthquakes in the Ancona and Gargano regions can be separated from the events located in the Apennines. The tectonic map by PATACCA

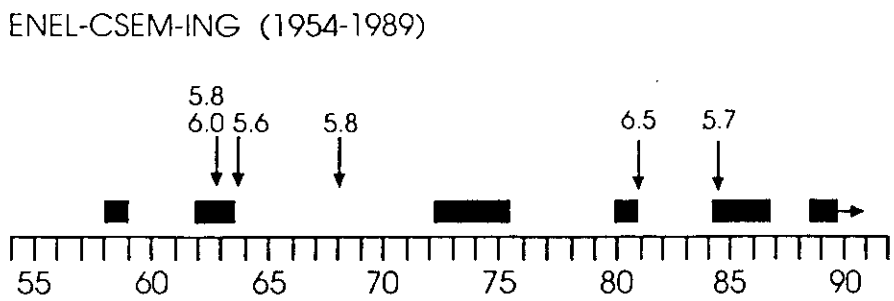

Figure 4
Results of the diagnosis of TIPs, for the regionalization of Figure 2, as deduced from the catalogue ENEL-CSEM-ING; $M_0 = 5.6$. The time of occurence of a strong earthquake is indicated by an arrow and the number above it gives the magnitude; TIPs are indicated by block rectangles (KEILIS-BOROK, *et al.*, 1990b).

et al. (1990) illustrates two nearly parallel NW-SE elongated active areas (Fig. 7b) in the Central Apennines (Toscana, Umbria, Marche). The alignment near the Adriatic Sea is in a compressive state, while the other, more westerly, has an extensional character. The Gargano region has, on the other hand, exhibited a tectonic behavior characterized by the coexistence of mechanisms of dip-slip, oblique-slip, and strike-slip type (PATACCA *et al.*, 1990).

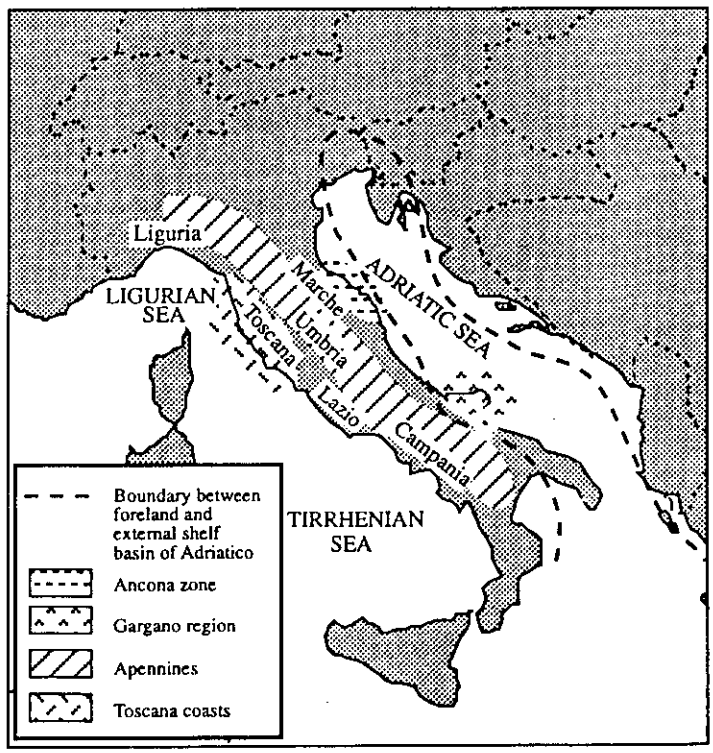

Figure 5
Map showing the boundary between foreland and external shelf basin of Adriatic after HORVARTH and CHANNEL (1976) and other geographical references, mentioned in the text.

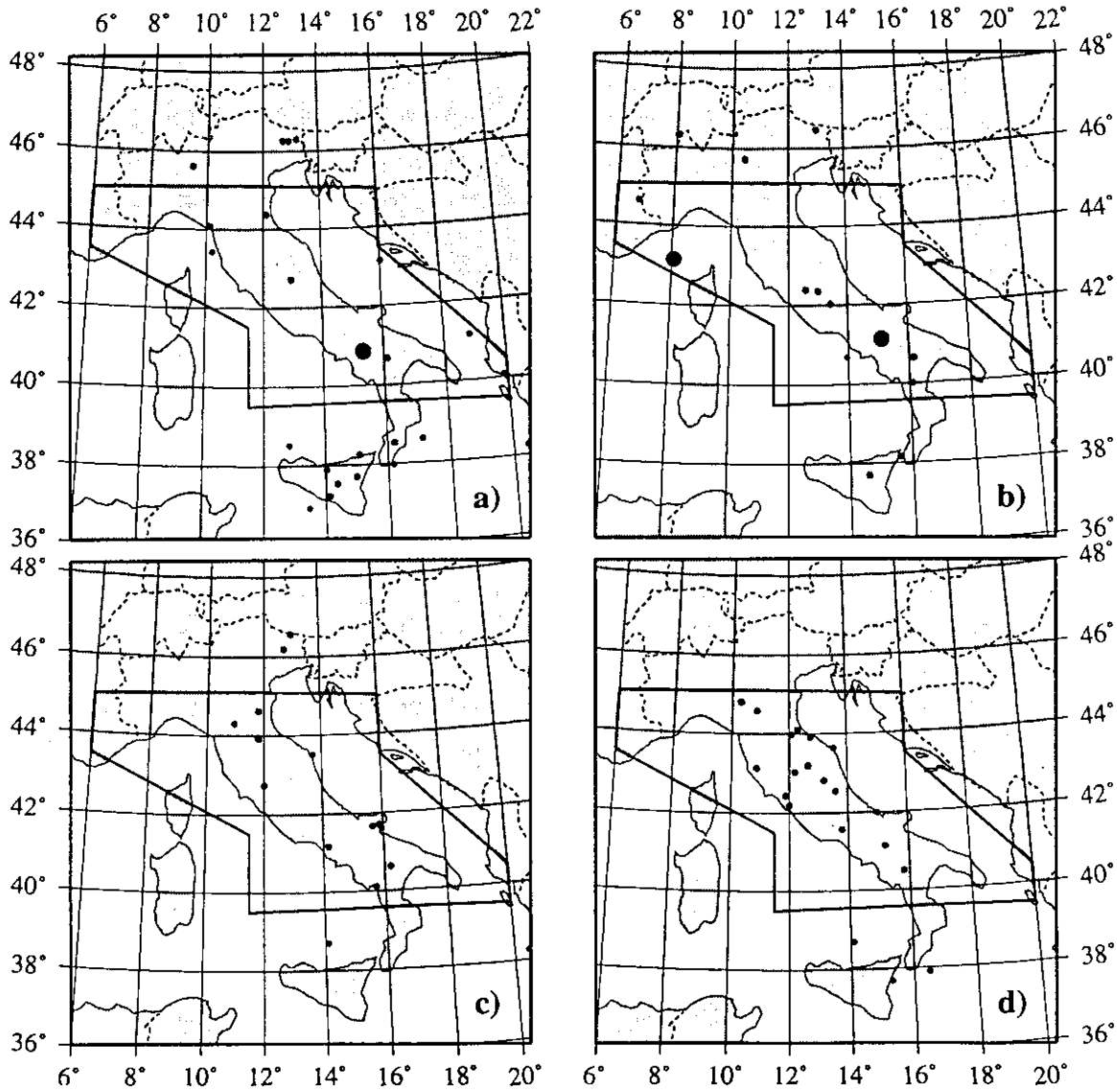

Figure 6
Main shocks (small dots) with $M \geq m_1 = 4.4$ for three years before the TIP, and strong earthquake (large dot). The polygon indicates the boundaries of the regionalization. Only the events inside the PFG polygon are considered; a) the TIP started in 1979; b) the TIP started in 1961; c) the TIP started in 1958; d) the TIP started in 1972.

Taking into account these seismotectonic features, and mainly considering the analysis of the occurrence, just before the TIPs, of the events with a magnitude greater than the minimum magnitude used in the definition of the functions, a new rough regionalization is proposed, which does not cut very active regions and includes the seismicity maxima present in the Apennines and the extensional areas oriented NW-SE, and excludes the Ancona zone and the Gargano region (Fig. 7b). The Ligurian Sea, Tyrrhenian Sea and the coasts of Toscana are excluded, since the very low seismicity in these areas does not occur in the periods just before the TIPs (Fig. 6), and therefore does not influence the functions used by the CN algorithm.

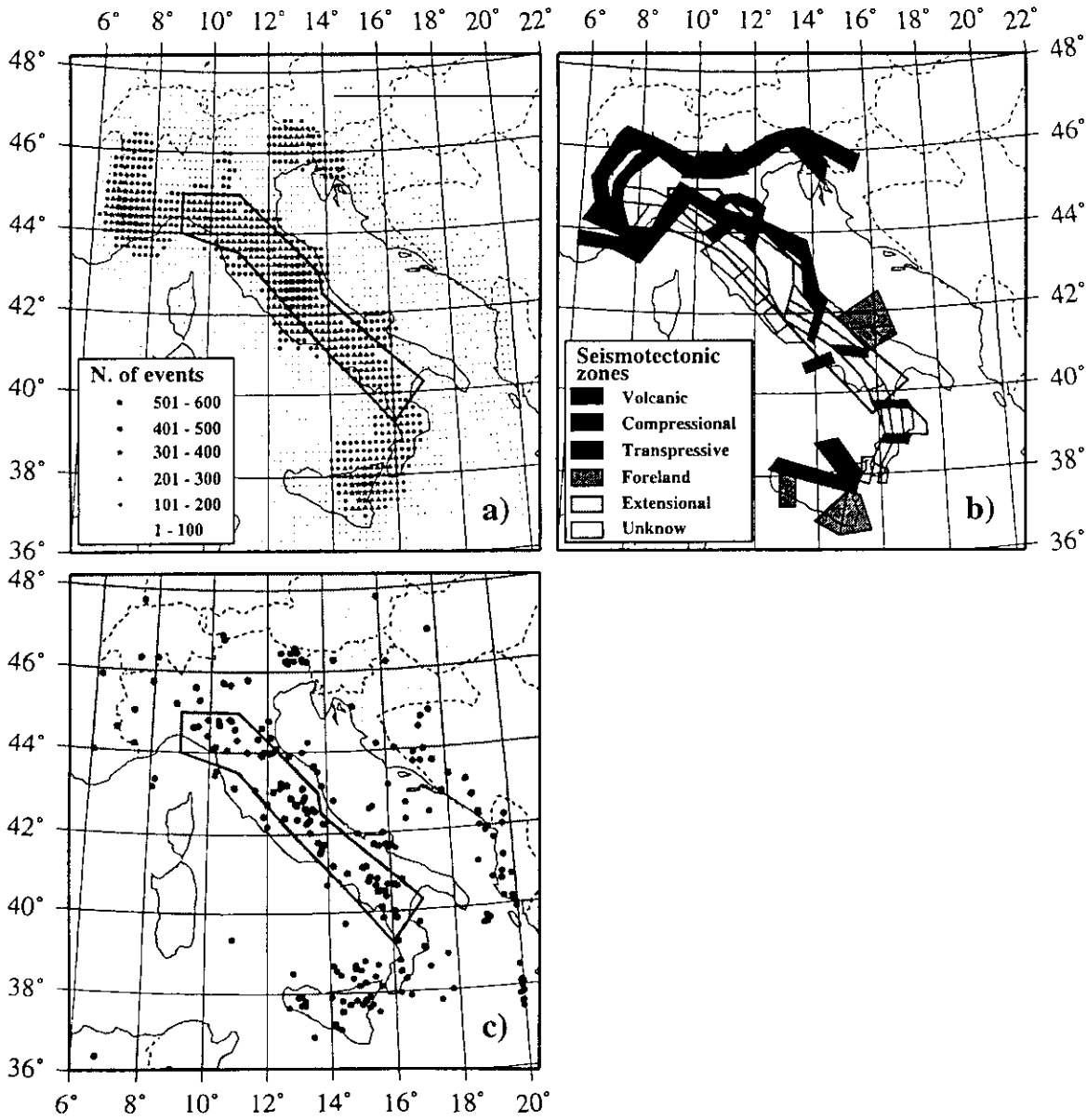

Figure 7

New regionalization for the diagnosis of TIPs superimposed to: a) map of seismicity. In the map it is represented by the total number of earthquakes, smoothed within a 0.6° diameter circle. Each smoothing circle is centered on the knots of a grid of 0.2° × 0.2°. It has been used as the main shocks catalogue from 1000 to 1990 from the PFG-ING catalogue, using the criteria proposed by KEILIS-BOROK *et al.* (1980) for the aftershock identification; b) seismotectonic map of Patacca; c) main events with magnitude $M \geq 4.4$. Catalogue ENEL-CSEM-ING.

The borders deliberately only roughly follow the main seismotectonic features, since we are interested here in describing the results of a first-order refinement of regionalization. A more detailed regionalization, made following the borders of each seismogenetic zone and taking into account their character, will be the subject of a forthcoming paper.

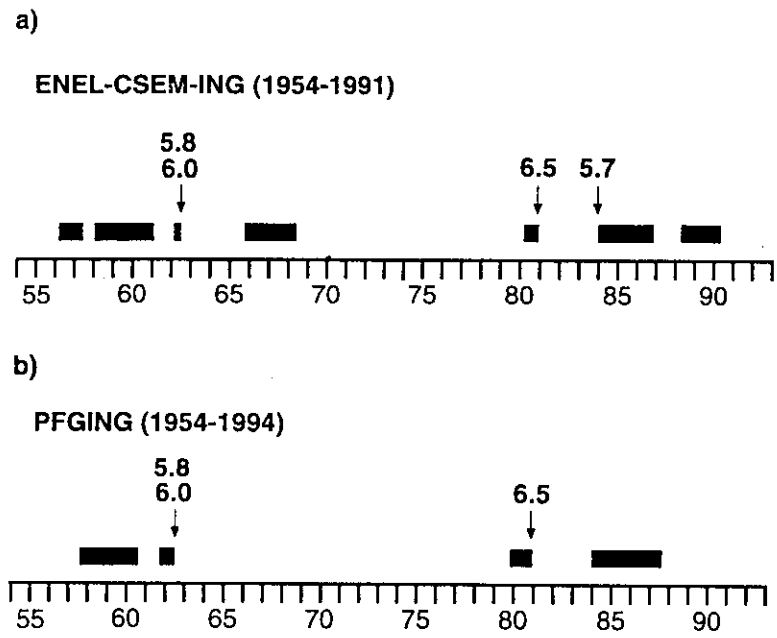

Figure 8

Results of the diagnosis of TIPs for the new regionalization. The time of occurrence of a strong earthquake is indicated by an arrow and the number above it gives the magnitude; TIPs are indicated by block rectangles, a) catalogue ENEL-CSEM-ING, $M_0 = 5.6$; b) catalogue PFG-ING, $M_0 = 5.6$.

The area of the new regionalization is only about the 15% of the one used by KEILIS-BOROK *et al.* (1990b), consequently, the number of earthquakes is significantly reduced. The repetition of the analysis made by KEILIS-BOROK *et al.* (1990b), using the new regionalization and the catalogue ENEL-CSEM-ING, allows us to predict the four strong events with a total alarm period of about 32% of the total time with no failure to predict (Fig. 8a).

In global application, the CN algorithm places about 80% of the strong earthquakes into the alarms occupying 20–40% of the space-time considered (KEILIS-BOROK *et al.*, 1990b). The predictive power of this algorithm is of course stronger than those figures since the expectation time (the volume of alarm until the strong earthquake) is much shorter, around 10 to 20%.

The statistical significance is established strictly to date only for one component of CN algorithm, namely the abnormal clustering used as an independent precursor in different formalizations. The statistical significance of the algorithm CN as a whole is being tested by forward prediction but no final conclusions are reached, and, among others, the forward prediction in Central Italy, performed using the new regionalization proposed in this paper, is a base test for the statistical significance of the algorithm CN.

3. Stability

The test of the stability of the premonitory seismicity pattern and of the feasibility of the prediction has been carried out with respect to changes: 1) in

catalogues, 2) in regionalization, 3) in the length of the learning period, and 4) in the thresholds for the rules to declare a TIP.

A new catalogue (PFG-ING) has been prepared. For the period 1900–1979, the new catalogue is formed by the PFG catalogue, which is the revised version of the ENEL catalogue; from 1980, the ING catalogue has been used. The magnitude M_l (local magnitude) has been considered whenever available; if M_l is not available, the values M_I (magnitude from intensity), in the PFG catalogue, and M_d (duration magnitude), in the ING catalogue, have been applied.

The learning period, which must extend at least twenty years and have a balanced number of N and D periods, is the period in which the catalogue is analyzed in order to define the values of the thresholds m_1, m_2, m_3 and the values of the functions in the periods immediately before a strong earthquake (D periods) and in the periods without strong earthquakes (N periods). The stability of the premonitory pattern has been successfully tested using two different learning periods, 1954–1980 and 1954–1986. Since within the time interval 1980–1986 there is only one D period, the stability of the results is mainly relevant with respect to changes of m_1, m_2, m_3. The properties that must be satisfied by the learning periods do not permit to consider other larger differences in the time interval employed.

The differences which are present in the available catalogues are quite significant, as can be seen from Figure 1; for example, in the catalogue ENEL-CSEM-ING there are four strong earthquakes with $M \geq 5.6$, while in the PFG-ING catalogue there are only three earthquakes with $M \geq 5.6$. Since the histogram Magnitude-Number of events for the PFG-ING catalogue has a minimum slightly less than $M = 5.4$, and the events with a magnitude above this threshold have a return period of about six years, the analysis is made using the value of $M_0 = 5.4$ also. The results of the processing of both catalogues, for the two different regionalizations and for two different values of M_0, are reported in Table 2. The results are satisfactory and stable, mainly when the regionalization which takes into account seismotectonic considerations is used. In particular, using the PFG-ING catalogue all strong events are predicted and the total alarm occupies about 23% of the total time, a percentage significantly less than the one obtained with the analysis performed with the ENEL-CSEM-ING catalogue (Fig. 8b). The results of the stability analysis confirm that the revision of the ENEL catalogue produced a higher quality data file: the PFG catalogue.

In general, the number of predictable failures is zero or one, and the total alarm time is less than 35% of the total time. In only two cases (variants 4 and 5 in Table 2) is there a large number of failures to predict. In these two cases the catalogue used is the PFG-ING and the regionalization is the one based only on catalogue boundaries and completeness.

The thresholds for the rules to declare a TIP are given by equations (1). The value of the parameters E and V obtained empirically in the California-Nevada region, and subsequently used with success in other regions of the world, are

Table 2

Results of the stability tests of the premonitory seismicity pattern. The old regionalization is the one proposed by KEILIS-BOROK et al. (1990b) and the new is the regionalization proposed in this paper. The old catalogue is the ENEL-CSEM-ING and the new catalogue is the PFG-ING. A is the number of events to be predicted, B is the number of failures to predict, C is the percent of total time occupied by alarms, D is the number of false alarms.

	M_0		Regionalization		Learning period		Catalogue used for learning		Catalogue used for analysis		Threshold parameters		Results			
N°	5.4	5.6	old	new	1954 1980	1954 1986	old	new	old	new	*V*	*E*	*A*	*B*	*C*	*D*
1		X	X			X	X		X		5	4.9	6	1	26.0	5
2		X	X			X		X	X		5	4.9	6	1	33.3	4
3		X	X			X	X			X	5	4.9	4	1	29.6	4
4		X	X			X		X		X	5	4.9	4	3	27.4	4
5	X	X	X		X			X		X	5	4.9	8	4	26.9	2
6	X			X	X			X		X	5	4.9	5	1	37.4	3
7	X			X		X		X		X	5	4.9	5	1	31.9	3
8		X		X	X			X		X	5	4.9	3	0	23.7	2
9		X		X		X		X	X		5	4.9	4	0	31.5	5
10		X		X		X		X		X	5	4.9	3	0	23.3	2

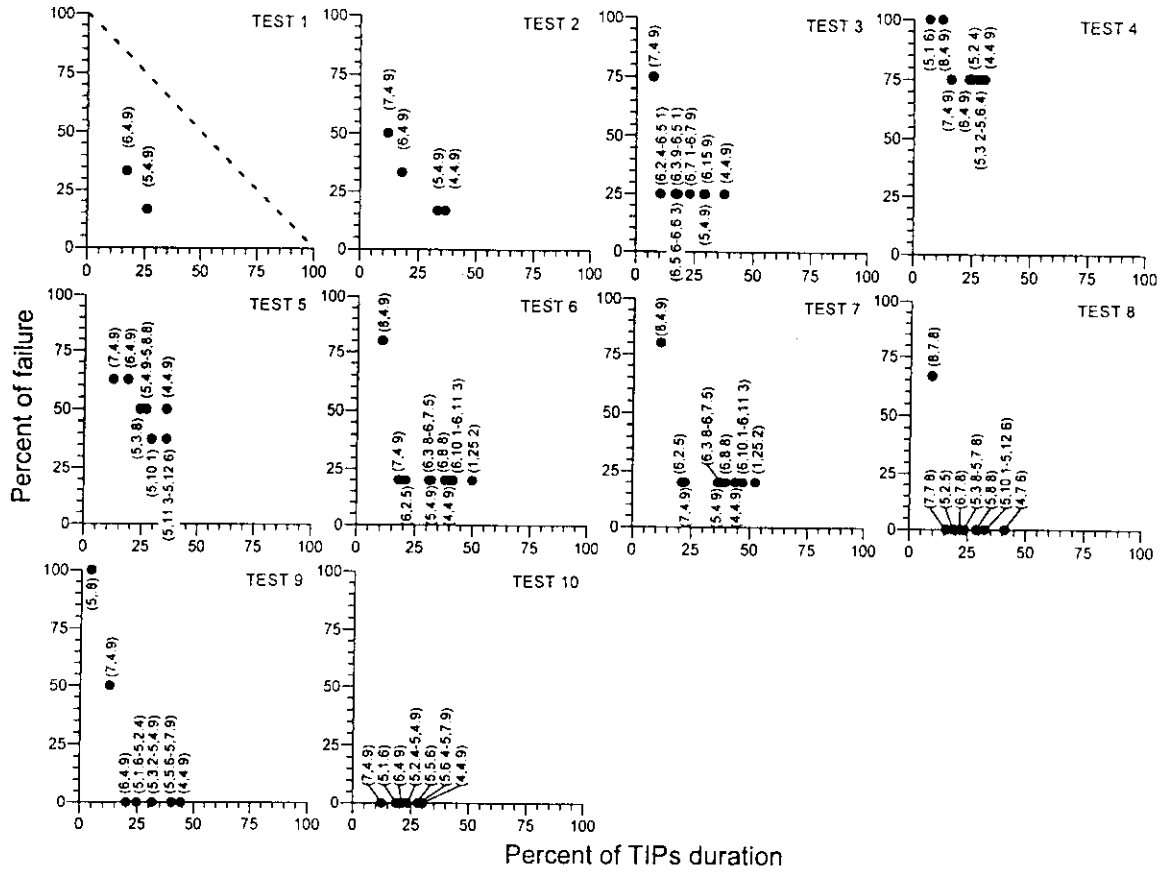

Figure 9
Diagrams [percent of failures to predict] – [percent of TIPs] duration obtained varying the parameters V and E in the tests of Table 5. Between brackets the values of V and E are given in the order. In each test, random results are represented by points outside the triangle (0, 0), (100, 0) (0, 100) shown, for example, in TEST 1 as gray area.

$E = 4.9$ and $V = 5$, as shown in Table 2 (KEILIS-BOROK *et al.*, 1990a). To test the stability of the premonitory pattern, the values of E and V have been changed with respect to the default values. The results obtained changing these two values, for all the variants given in Table 2, are shown in Figure 9. The results are very stable even for variations of E and V in a rather large range. The stability is lost only for extreme values of the two parameters. Figure 9 supplies a measure of the non-randomness of the different predictions: in each test random results are represented by points outside the triangle (0, 0), (100, 0), (0, 100), shown, for example in TEST 1 as gray area. For instance random results are obtained in test 4 with $V = 5$, $E = 1.6$ and with $V = 8$, $E = 4.9$, and test 9 with $V = 5$, $E = 0.8$.

4. Period 1904–1940

The analysis of the PFG catalogue reveals that information, sufficiently complete for the use of the algorithm CN, is contained also in the period 1904–1940,

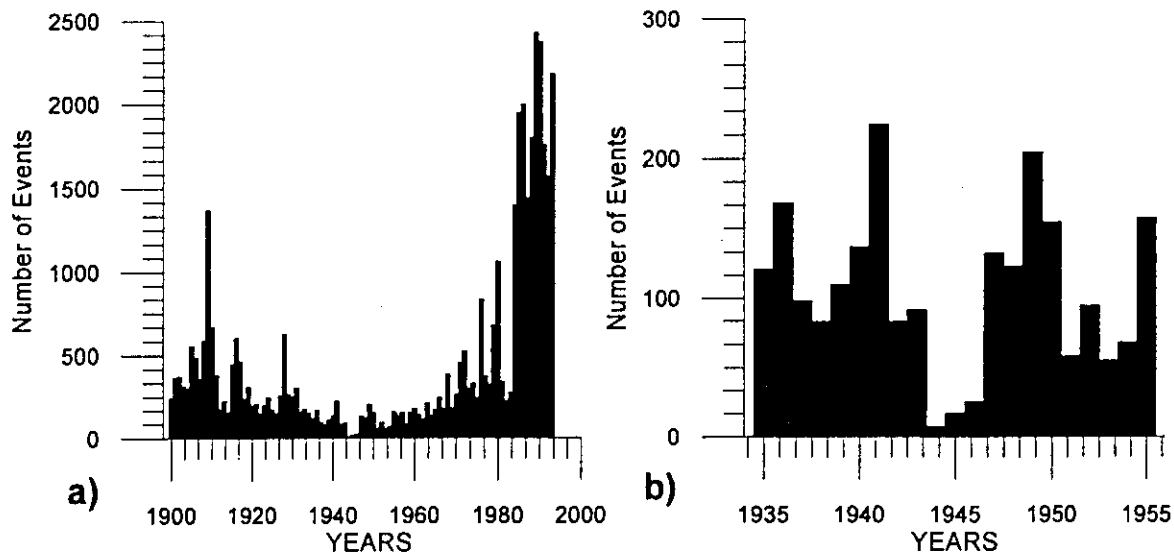

Figure 10
Histogram Magnitude – Number of events in the years: a) 1900–1994; b) 1935–1955.

the incompleteness of the catalogue in the period 1941–1953 being strongly correlated with World War 2 (Fig. 10). Therefore the algorithm CN has been applied to the period 1904–1940, using the same time interval as learning period. The seismicity in this time interval is higher than in the period 1954–1991 and therefore the magnitude, M_0, corresponding to events with a return period of about

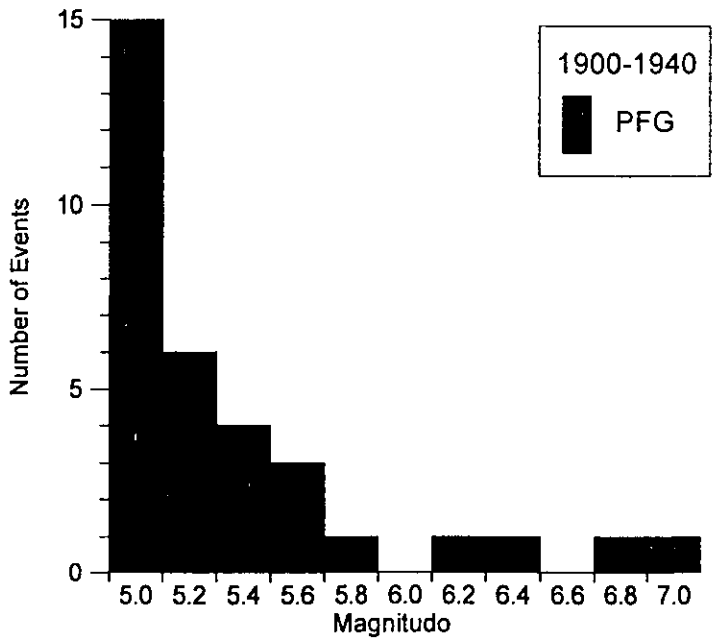

Figure 11
Histogram Magnitude – Number of events, with step of 0.2 in magnitude, in the years 1900 - 1940 for the new regionalization proposed in the paper. Catalogue PFG.

Table 3

Results obtained from the analysis of two different periods, 1904–1940 and 1954–1990, characterized by different seismicity levels. A is the number of events to be predicted, B is the number of failures to predict, C is the percent of total time occupied by alarms, D is the number of false alarms

	M_0		Learning period		Analysis period		Threshold parameters		Results			
			1904	1954	1904	1954						
N°	5.6	6.0	1940	1980	1940	1990	*V*	*E*	*A*	*B*	*C*	*D*
1		X	X		X		5	4.7	3	1	38.0	7
2		X	X			X	5	4.7	2	1	33.6	5
3	X			X		X	5	4.9	3	0	23.7	2
4	X		X		X		5	3.1	7	4	22.3	5
5	X			X	X		5	3.1	7	3	40.0	8
6	X		X			X	5	4.9	3	2	16.1	2

six years and to a minimum in the histogram Number of events – Magnitude, i.e., the M_0 satisfying the CN rule, is around 6.0 (Fig. 11).

The results obtained for $M_0 = 6.0$ are reported in Table 3, variant 1. The number of strong events is three; two of them are predicted, and the alarm occupies about 38.0% of the total time (Fig. 12). If, brooking the CN rule, the value of M_0 is decreased to 5.6, equal to the threshold M_0 used for the period with lower

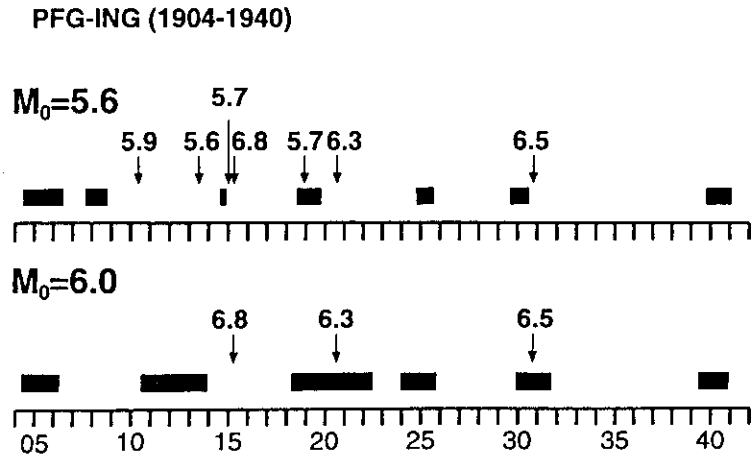

Figure 12

Results, based on catalogues PFG-ING, of the diagnosis of TIPs for the new regionalization; and for two different thresholds M_0. The time of occurrence of a strong earthquake is indicated by an arrow and the number above it gives the magnitude; TIPs are indicated by block rectangles.

seismicity 1950–1994, the number of strong events becomes seven and the performance of the algorithm is very poor: three events are predicted, and the alarm duriation is equal to 22.3% of the total time (variant 4, Table 3).

Even if the level of seismicity in the time interval 1904–1940 is considerably higher than in the period 1954–1994, the good results of the diagnosis of TIPs for each interval separately indicate that self-similarity characterizes the seismicity of the two periods.

5. Conclusion

A significant reduction of the spatial uncertainty in the identification of a TIP has been obtained using a regionalization based not only on catalogue completeness but also on seismotectonic evidences. The use of such regionalization, in general, increases the stability of the premonitory pattern. All the stability tests demonstrate that the CN algorithm in Central Italy produces very stable results.

Our research suggests use of the catalogue PFG-ING, the new regionalization, and the threshold $M_0 = 5.6$, for the routine forward monitoring, which satisfies the condition of having a return period approaching six years.

The analysis of the period 1904–1940 shows that even when the catalogue completeness threshold corresponds to a magnitude as high as 4.0, the CN algorithm still supplies useful information. The comparison of the results obtained during the periods 1904–1940 and 1954–1994 supplies further evidence favoring the existence of self-similarity in the occurrence of earthquakes (e.g., KAGAN and KNOPOFF, 1981).

Acknowledgments

The authors are very grateful to Prof. V. I. Keilis-Borok, Drs. A. Gabrielov and S. Schreider for stimulating discussions. One of the authors, (I. M. Rotwain), thanks ICTP for financial support for her stay in Trieste, during which a large part of this work was undertaken. We acknowledge financial support from MURST (40% and 60%) funds, CNR-Gruppo Nazionale per la difesa dai Terremoti contracts nos. 91.02539.54, 92.02867.54 and NATO linkage grants SA. 12-2-02 (ENVIRLG 931206) and SA. 12-5-02 (CN. SUPPL 94880).

REFERENCES

DELLA VEDOVA, B., MARSON, I., PANZA, G. F., and SUHADOLC, P. (1991), *Upper Mantle Properties of the Tuscan-Tyrrhenian Area: A Key for Understanding the Recent Tectonic Evolution of the Italian Region*, Tectonophys. *195*, 311–318.

CALCAGNILE, G., and PANZA, G. F. (1981), *The Main Characteristics of the Lithosphere-astenosphere System in Italy and Surrounding Regions*, Pure and Appl. Geophys. 119, 865–879.

CSEM, *European-Mediterranean Hypo-centers Data File* 1976–1988 (Csem, Strasbourg 1989).

ENEL, *Catalogue of Earthquake of Italy, Years 1000–1980* (Publication ENEL, Roma 1980).

GABRIELOV, A. M., DMITRIEVA, O. E., KEILIS-BOROK, V. I., KOSOBOKOV, V. G., KUZNETSOV, I. V., LEVSHINA, T. A., MIRZOEV, K. M., MOLCHAN, G. M., NEGMATULLAEV, S. Kh., PISARENKO, V. F., PROZOROV, A. G., RINEHART, W., ROTWAIN, I. M., SHLBALIN, P. N., SHNIRMAN, M. G., and SCHREIDER, S. Yu (1986), *Algorithms of Long-term Earthquakes' Prediction*, International School for Research Oriented to Earthquake Prediction-algorithms, Software and Data Handling (Lima, Peru, 1986).

HORVATH, F., and CHANNEL, J. E. T. (1976), *Further evidence relevant to the African/Adriatic promotory as a paleogeographic premise for Alpine orogency*, International Symposium on the Structural History of the Mediterranean Basins, Split (Yugoslavia) 25–29 October 1976 (eds. Biju-Duval, B. and Montadert, L.) (EDITIONS TECHNIP, Paris 1977), pp. 133–142.

ING, *Seismological Reports 1980–1991* (ING, Roma 1982–1991).

KAGAN, Y. Y., and KNOPOFF, L. (1981), *Stochastic Synthesis of Earthquake Catalogs* Geophys. J. R. Astr. Soc. *86*, 303–320.

KEILIS-BOROK, V. I., KNOPOFF, L., and ROTWAIN, I. M. (1980), *Burst of Aftershocks, Long-term Precursors of Strong Earthquakes*, Nature *283* (5744), 259–263.

KEILIS-BOROK, V. I., KNOPOFF, L., ROTWAIN, I., and ALLEN, C. R. (1988), *Intermediate-term Prediction of Occurence Times of Strong Earthquakes*, Nature *335* (6192), 690–694.

KEILIS-BOROK, V. I., and ROTWAIN, I. (1990a), *Diagnosis of Time of Increased Probability of Strong Earthquakes in Different Regions of the World: Algorithm CN*, Phys. Earth Planet. Inter. *61*, 57–72.

KEILIS-BOROK, V. I., KUZNETSOV, I. V., PANZA, G. F., ROTWAIN, I. M., and COSTA, G. (1990b), *On Intermediate-term Earthquake Prediction in Central Italy*, Pure Appl. Gesphys. *134*, 79–92.

MARSON, I., PANZA, G. F., and SUHADOLC, P. (1994), *Crust and Upper Mantle Models along the Active Tyrrhenian Rim*, Terra Nova, in press.

PANZA, G. F., MUELLER, S., CALCAGNILE, G., and KNOPOFF, L. (1982), *Delineation of the North Central Italian Upper Mantle Anomaly*, Nature *296*, 238–239.

PATACCA, E., SARTORI R., and SCANDONE, P. (1990), *Tyrrhenian Basin and Apenninic Arcs: Kinematic Relation since Late Tortonian Times*, Mem. Soc. Geol. It. *45*, 425–451.

PFG, *Catalogo dei terremoti italiani dall'anno 1000 al 1980* (ed. Postpischl, D.) (CNR-P.F. Geodinamica 1985).

SUHADOLC, P., and PANZA, G. F. (1988), *The European-African Collision and its Effects on the Lithosphere-asthenosphere System*, Tectonophys. *146*, 59–66.

(Received May 16, 1994, accepted January 5, 1995)

PAGEOPH, Vol. 147, No. 1 (1996)

0033-4553/96/010119-12$1.50 + 0.20/0

Seismotectonic Models and CN Algorithm: The Case of Italy

GIOVANNI COSTA,[1,2] IVANKA OROZOVA-STANISHKOVA,[1,2]
GIULIANO FRANCESCO PANZA[1,2] and IRINA M. ROTWAIN[3]

Abstract—The CN algorithm is utilized here both for the intermediate term earthquake prediction and to validate the seismotectonic model of the Italian territory. Using the results of the analysis, made through the CN algorithm and taking into account the seismotectonic model, three main areas, one for Northern Italy, one for Central Italy and one for Southern Italy, are defined. Two transition areas between the three main areas are delineated. The earthquakes which occurred in these two areas contribute to the precursor phenomena identified by the CN algorithm in each main area.

Key words: Earthquakes prediction, seismotectonics, seismicity.

1. Introduction

The analysis of the Time of Increased Probability (TIP) of a strong earthquake with magnitude greater than, or equal to a given threshold M_0, based on the algorithm CN, makes use of normalized functions, which describe the seismicity pattern of the analyzed area. Therefore the original algorithm, developed for the California-Nevada region, can be directly used, without any adjustment, in areas with different size and level of seismicity.

It has been shown by COSTA *et al.* (1995) that a regionalization, supported by seismological and tectonic arguments, leads to the reduction of the alarm duration (TIP) and of the failures to predict, and increases the stability of the algorithm. Therefore, the CN algorithm permits to deal with the development of modern regional geodynamic models, involving relationships between the key structural features which control the seismicity, and the selection of the optimal causative fault system for prediction purposes (RUNDKVIST and ROTWAIN, 1994).

The algorithm CN is described in full detail by GABRIELOV *et al.* (1986) and KEILIS-BOROK and ROTWAIN (1990). An application to Central Italy is given by

[1]Dipartimento Scienze della Terra, Università degli Studi di Trieste, via E. Weiss 4, 34127 Trieste, Italy.

[2]International Center for Theoretical Physics-ICTP, 34100 Trieste Miramar, Italy.

[3]International Institute of Earthquake Prediction Theory and Mathematical Geophysics, Academy of Sciences of the U.S.S.R., Warshavskoye, 79, K.2, 113556, Moscow, U.S.S.R.

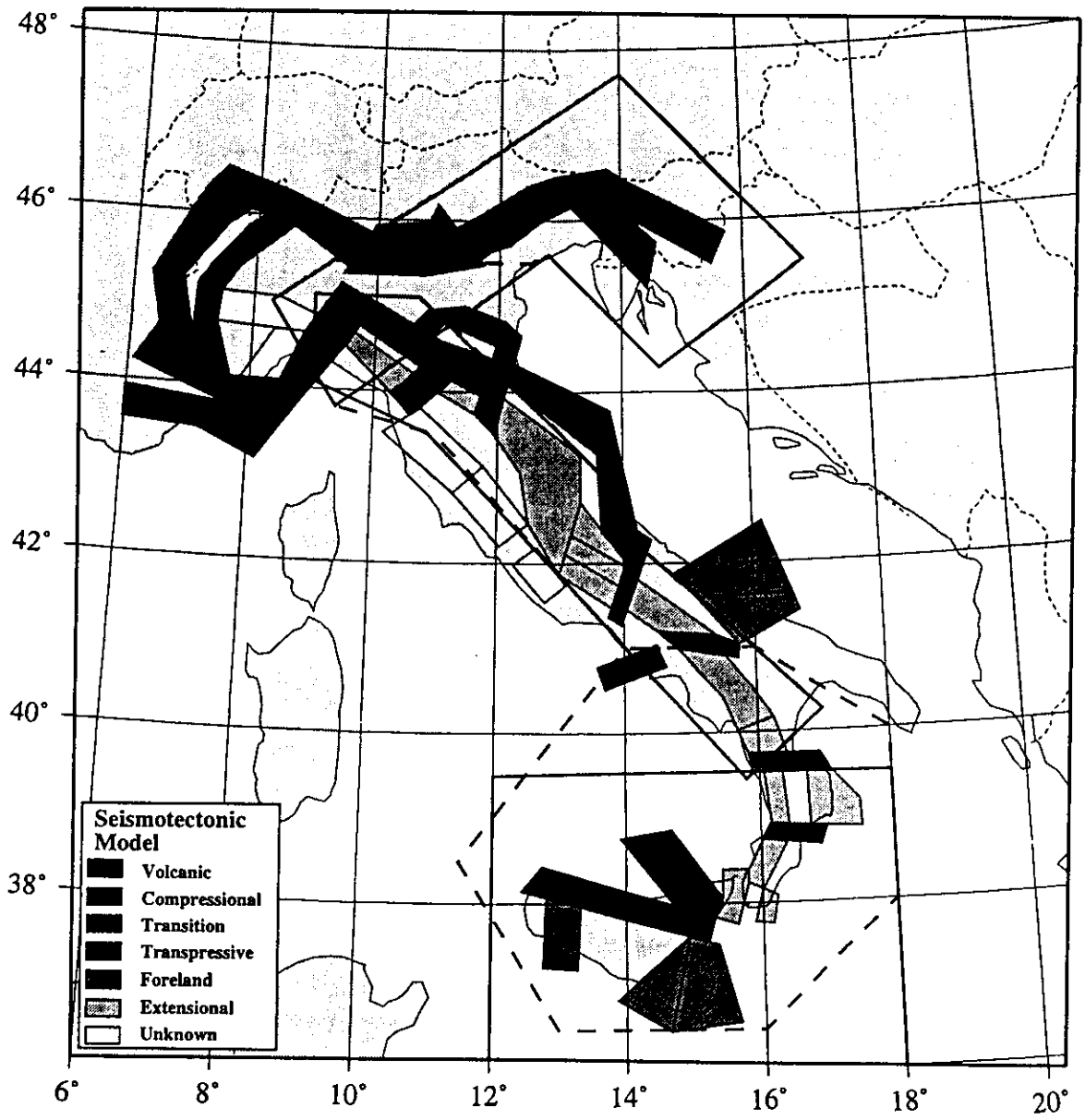

Figure 1
Seismotectonic model of Italy (PATACCA *et al.*, 1990) and regionalization into three main and two transition areas.

KEILIS-BOROK *et al.* (1990), where the borders of the studied area are defined simply according to the completeness of the used catalogue. The analysis of the seismicity and seismotectonic considerations permit the definition of a more detailed regionalization of Central Italy and the testing of the stability of the method (COSTA *et al.*, 1995).

In the present study the analysis is extended to the whole Italian territory. Using the seismotectonic model of Italy (PATACCA *et al.*, 1990) and the spatial distribution of the epicenters (Fig. 1), the country is divided into three main areas (Fig. 2).

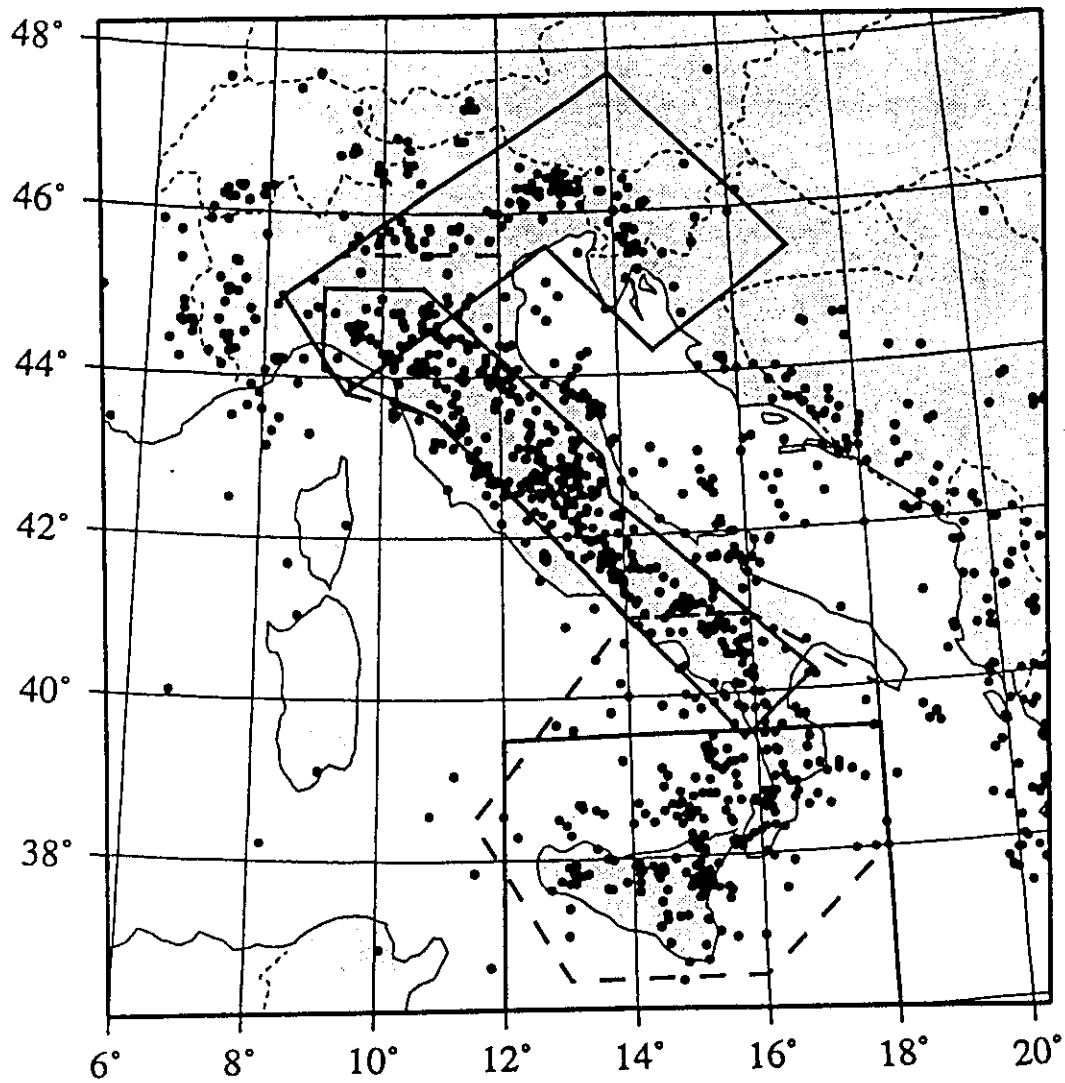

Figure 2
Seismicity map ($M \geq 4.0$) and boundaries of the three main areas in Italy. Dashed line marks variants of the regionalization.

Each of them is characterized by a dominant seismotectonic behavior, with varying seismicity pattern, therefore the appropriate M_0 is used in each area.

The catalogue used routinely for the application of the CN algorithm in Italy has been compiled as follows: for the period 1900–1979 it is taken the PFG (POSTPISCHL, 1985) and since 1980 it is continued with the ING (Istituto Nazionale di Geofisica, 1994) catalogue. This catalogue hereafter is referred as PFGING. M_I (magnitude from intensity), M_d (duration magnitude) and M_L (local magnitude) are available in this catalogue.

2. Geodynamic Outline

The Italian territory can be divided into three main tectonics areas (Northern, Central, and Southern Italy) with different types of recent motion (PATACCA and

SCANDONE, 1989; DAL PIAZ and POLINO, 1989). Each of these main areas is subdivided into several smaller seismogenic zones with different seismotectonic characteristics and behavior (Fig. 1).

The first area, Northern Italy (north of 44°N), is characterized by the presence of the Alpine arc, which is generally uplifting (MUELLER, 1982). The eastern part of the area (Friuli), where one of the branches of the Southern Alps turns to the south along the Adriatic Sea (Dinaric Alps), the western part of the area, and the areas of contact between the Southern Alps and the Northern Apennines are characterized by compression (DAL PIAZ and POLINO, 1989). In the Friuli zone some westerly strike-slip motion is also present (PAVONI *et al.*, 1992). Therefore, in Northern Italy the majority of the seismogenic zones are compressive or transpressive (Fig. 1).

In Central italy two arcs of tectonic shortening, the North-Central Apennines and the Calabrian arc, meet. According to PATACCA and SCANDONE (1989) the deformation in this area has been strictly controlled by the sinking of the foreland lithosphere beneath the mountain chain peninsula and not directly by the collision between Europe and Africa. This hypothesis is strongly supported by surface waves dispersion measurements (CALCAGNILE and PANZA, 1981; PANZA *et al.*, 1982; SUHADOLC and PANZA, 1988), and other more recent investigations (DELLA VEDOVA *et al.*, 1991; MARSON *et al.*, 1995). The North-Central Apennines arc can be divided into two main structures, parallel to its axis: the first one is a zone of compression, and the second one is a zone of extension (Fig. 1). These two main structures are crossed by few transfer zones. Previous studies (COSTA *et al.*, 1991, 1995), have shown that the zones of extension and compression in Central Italy should not be jointly considered in the regionalization.

According to PATACCA *et al.* (1990), the 41°N parallel divides the Apennines chain in two completely different tectonic domains, and this line is proposed to separate Central from Southern Italy. The division of the Apennines into two major arcs may be related to the different sinking of the foreland lithosphere in the Northern Apennines and in the Calibrian arc (MARSON *et al.*, 1995). The passive subduction of the Po-Adriatic-Ionic lithosphere, caused by gravitational sinking, appears as a reasonable mechanism to explain contemporaneous geodynamic events such as mountain building in the Apennines and the extension in the Tyrrhenian area.

Southern Italy is characterized by very complex tectonics and different seismotectonic zones with extensive, transfer, foreland and volcanic character, can be recognized. The complexity here is even increased by the presence of several intermediate and deep focus earthquakes (CAPUTO *et al.*, 1970), related to the Calabrian arc (Eastern Sicily, Calabria). This arc, which is the most important tectonic structure in Southern Italy, is an old subduction zone, where the deep-focus earthquakes are related to the existence of a lithospheric slab which may represent, in its deepest parts, the remnant of the Adriatic lithosphere which subducted

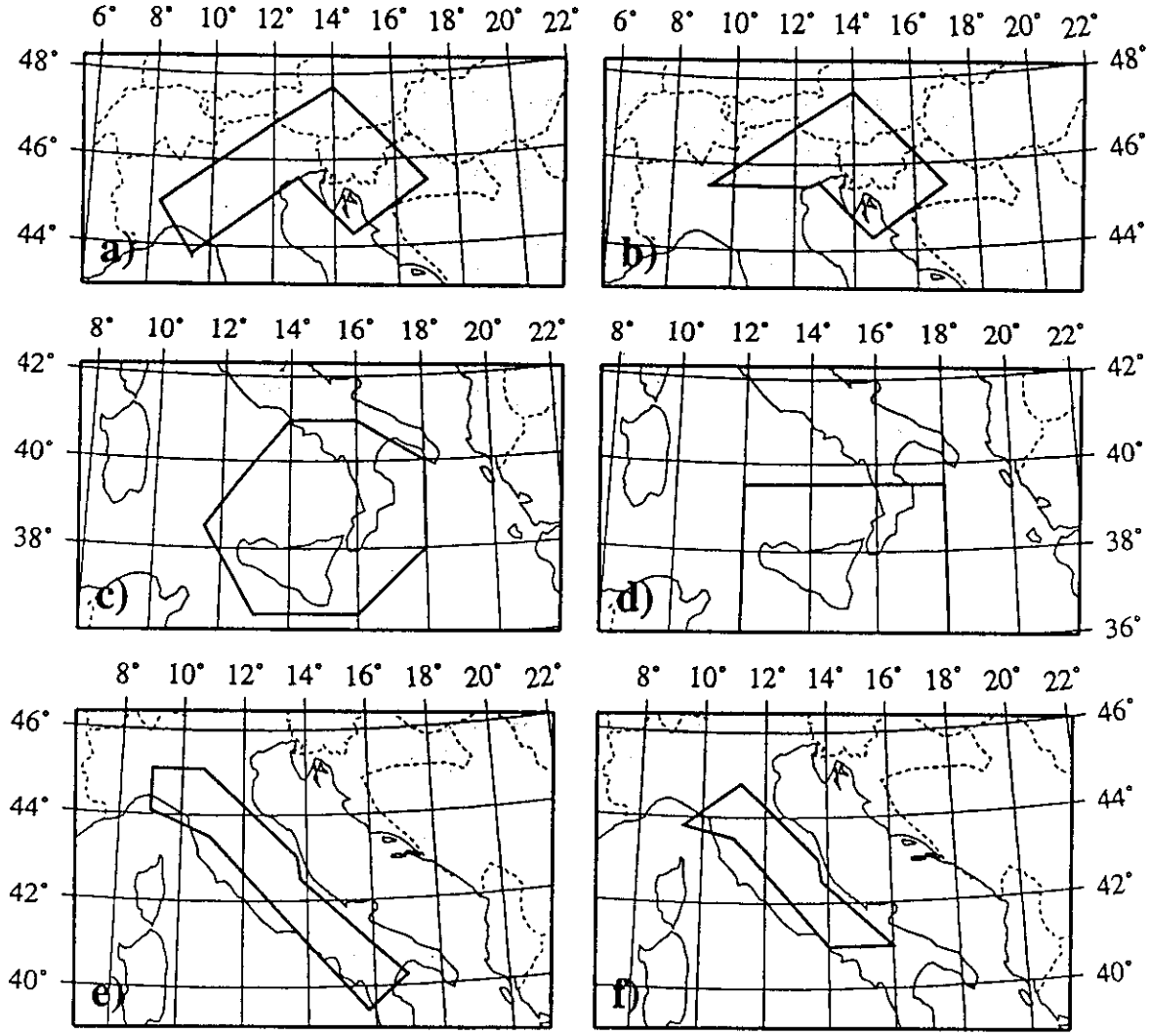

Figure 3
Different regionalizations, considered in the present study: a) first variant considered in Northern Italy (area 1); b) second variant considered in Northern Italy (area 2); c) first variant considered in Southern Italy (area 1); d) second variant considered in Southern Italy (area 2); e) Central Italy regionalization according to COSTA *et al.* (1995) (area 1); f) second regionalization considered in Central Italy (area 2).

Corsica-Sardinia before the opening of the Tyrrhenian Sea (PATACCA and SCANDONE, 1989).

3. Regionalization

To minimize the spatial uncertainty, the area in which a strong earthquake must be predicted, should be as small as possible, but there are two rules that limit its minimum dimensions: 1) the border of the area must be drawn following to the extent possible the minima in seismic activity; 2) the annual number of earthquakes with magnitude greater or equal to the completeness threshold of the catalogue must be greater or equal to 3.

Table 1

Earthquake catalogues used in Northern Italy

Catalog	Period	Magnitude	Priority
PFGING	1000–1992	M_I, M_d, M_L	M_L, M_d, M_I
ALPOR	1000–1985	M_I, M_L	M_L, M_I
NEIC	1900–1992	m_b, M_s, M_L	M_L, M_s, m_b
Final	1900–1992	$M_{(ALPOR)}$, $M_{(PFGING)}$, $M_{(NEIC)}$	MAX

Note:
The priority M_1, M_2, M_3 indicates that the magnitude M_1 has been used whenever available. If M_1 is not available, M_2 has been used, etc. MAX = Max(M_1, M_2, M_3).

The borders between the three main areas: Northern, Central and Southern, described in Section 2, are not sharply defined and they can be better represented by a transition domain. In fact, as we will see, the division of the Italian territory into three main areas, separated by two transition areas, seems to be consistent with the indications given concerning the properties of seismicity by the CN algorithm. A synoptic representation of the different areas is given in Figure 2, while the shapes of the two variants of each main area are given in Figure 3.

3.1. Northern Italy

The Alpine arc, the most important tectonic feature in Northern Italy, is crossed by different political borders and consequently the catalogue PFGING is fairly incomplete for our purposes. To fill in the gap it was necessary to add the information contained in two other catalogues: ALPOR (1987) and NEIC (1992). ALPOR is the catalogue of the Eastern Alps, compiled at the Osservatorio Geofisico Sperimentale, Trieste, Italy. In this catalogue two magnitudes are reported: M_I and M_L. NEIC is the catalogue of the National Earthquake Information Center (NEIC, USGS, Denver, USA). In this catalogue the body wave magnitude, m_b, the surface wave magnitudes, M_S, and M_L are reported.

The catalogue which we used in the application of the CN algorithm to Northern Italy is obtained merging ALPOR, PFGING and NEIC. Taking into account the uncertainties, which are intrinsic in the three different catalogues considered, the events differing in origin time by less than 1 minute and in epicentral location by less than 0.5°, both in latitude and longitude, are considered the same event. The priority in the choice of the magnitude to be used in the further processing is given in Table 1. The aftershocks are eliminated, using the criteria given by KEILIS-BOROK *et al.* (1980), and only the events with magnitude greater than, or equal to 3 have been used.

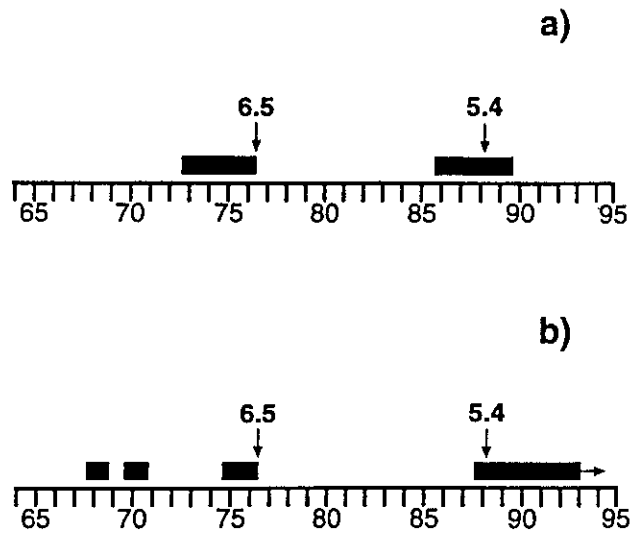

Figure 4
Results of the CN analysis in Northern Italy: a) area 1; b) area 2. The arrows indicate earthquakes with $M \geq M_0$, TIPs are marked by black rectangles.

According to the standards used in the CN algorithm (COSTA *et al.*, 1995), the magnitude threshold for the definition of the strong earthquakes is chosen to be $M_0 = 5.4$. In the present study the period 1960–1992 is analyzed because of the significant incompleteness of the catalogue before 1960. In the region, only two strong earthquakes occurred during the last 30 years ($M = 6.5$, May 6, 1976 and $M = 5.4$, January 2, 1988). The $M = 6.0$ September 15, 1976 event is a strong aftershock, identified as Related Strong Earthquake by VOROBIEVA and PANZA (1993), and therefore it is not a target of the CN algorithm.

There are two important tectonic features in Northern Italy: the intersection of the Alps and the Dinarides in Friuli and the intersection of the Alps and the Apennines in Liguria. Because of the complexity of the region, it is rather difficult to define the appropriate borders of the area to be considered for the purposes of the CN algorithm. To solve this problem, an hypothesis has been formulated that the stress, responsible for earthquake occurrence, "propagates" along a major fault or tectonic structure and "accumulates" at the edges of this structure, and/or in the areas of intersection with other important faults or tectonic structures. Therefore, for the purposes of earthquake prediction, the events concentrated at the edges, or in the areas of intersections with other structures, of a given tectonic structure cannot be considered independent and should be all contained in the same area. In the present study, the Alpine arc is considered as the structure along which the tectonic stress propagates, and the events concentrated on both of its edges, western and eastern, are assumed to be correlated, and therefore included in the same area.

The seismogenic region, thus defined, is shown in Figure 3a. The two strong events are predicted and the TIP duration is 27% of the total time (see Fig. 4a). There is only one false alarm after the strong earthquake of 1988.

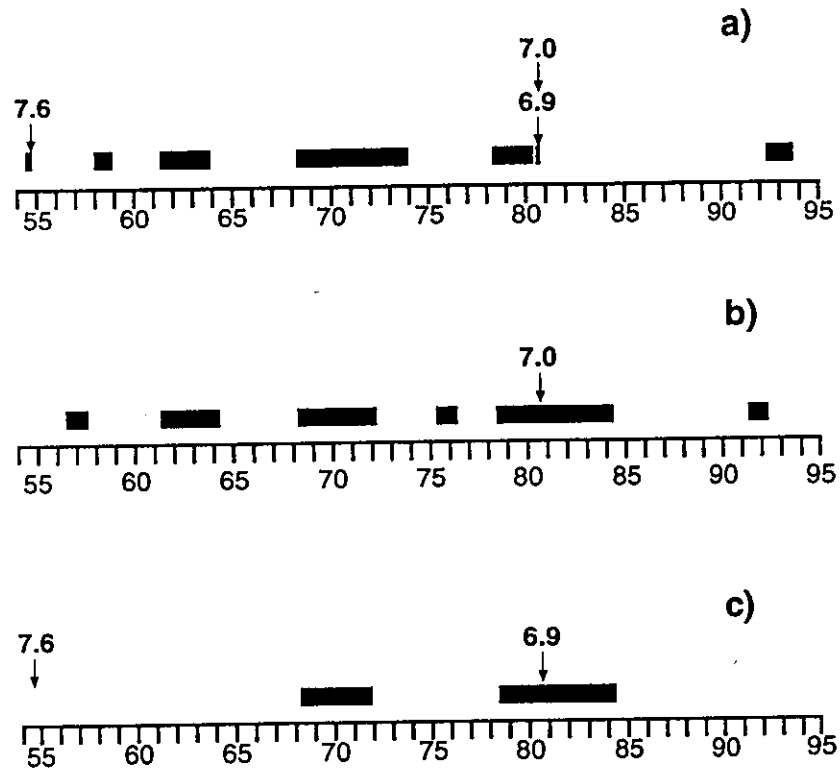

Figure 5

Results of the CN analysis in Southern Italy: a) area 1; b) area 1, considering only the shallow events; c) area 2. The arrows indicate earthquakes with $M \geq M_0$, TIPs are marked by black rectangles. The magnitude 6.9 is referred to an intermediate-depth earthquake in the Tyrrhenian Sea, while the magnitude 7 (taken from the PFGING catalogue) corresponds to the Irpinia, 1980, earthquake.

In order to test the hypothesis that the earthquakes, concentrated on the edges of a tectonic structure or in the areas of intersection with other structures, cannot be neglected for the purposes of earthquake prediction, a second regionalization (Fig. 3b), which includes only the compressive domains in the Eastern Alps (Fig. 1) is considered. The two strong events are predicted (Fig. 4b), but the TIP duration increases to 34% of the total time, and there are three false alarms.

3.2. Southern Italy

If we take the magnitude priority MAX (see note of Table 1) the utilized catalogue, PFGING, can be considered complete in this part of Italy only after 1950, and for magnitudes over three. The magnitude threshold in the definition of the strong earthquakes has been chosen as $M_0 = 6.5$.

Following the idea of PATACCA *et al.* (1990), that the 41°N parallel divides the Apennines into two completely different tectonic domains, for Southern Italy the area shown in Figure 3c has been delineated. The results of the CN algorithm applied to this area are reported in Figure 5a. All three strong earthquakes ($M = 7.6$, November 23, 1954, $M = 7.0$ November 23, and $M = 6.9$, November 24,

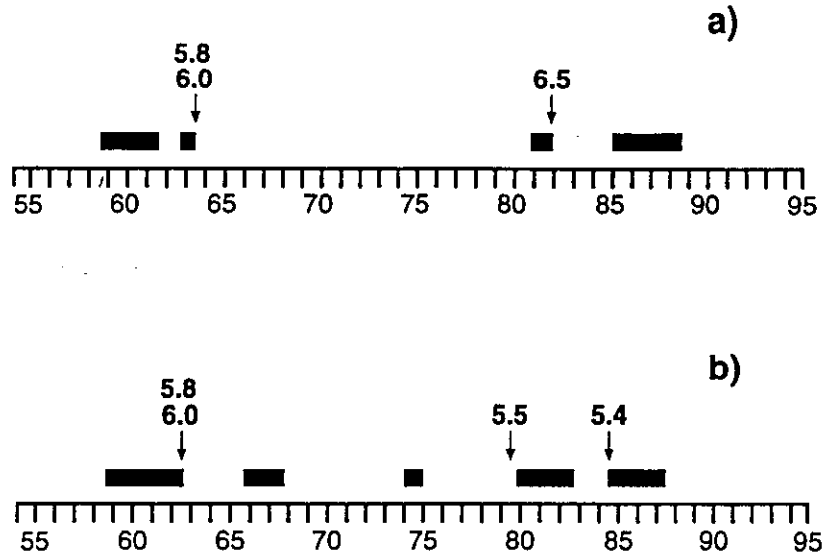

Figure 6
Results of the CN analysis in Central Italy: a) area 1; b) area 2. The arrows indicate earthquakes with $M \geq M_0$, TIPs are marked by black rectangles.

both in 1980) are predicted and the duration of TIP is 33% of the total time. There are five false alarms.

To study the influence of the relevant deep seismicity we consider only the shallow earthquakes and thus the only strong event to be predicted is the $M = 7.0$, November 23, 1980 earthquake. The diagnosis of the CN algorithm is given in Figure 5b. The strong event is predicted, but the duration of TIP increases up to 44% of the total time and there are six false alarms. This result indicates that the shallow and the deep seismicity in this area are not independent, in contrast with observations in other parts of the world (KEILIS-BOROK and ROTWAIN, 1990).

As a second test, according to the regionalization for Central Italy proposed by COSTA *et al.* (1995), the northern border of Southern Italy is traced along the 39.5° parallel (Fig. 3d). In this area the two strong earthquakes to be predicted are the $M = 7.6$, November 23, 1954 and the $M = 6.9$, November 23, 1980 events. The 1980 earthquake is predicted with a TIP duration lasting for 25% of the total time; the 1954, $M = 7.6$, event is a failure to predict and there are two false alarms (Fig. 5c).

3.3. Central Italy

The CN algorithm initially has been applied to Central Italy (KEILIS-BOROK *et al.*, 1990; COSTA *et al.*, 1995), because the catalogue PFGING is rather complete here. In the present study, utilizing the regionalization shown in Figure 3e, given by COSTA *et al.* (1995), we extend the analysis through the end of 1994 (Fig. 6a).

The definition of the areas in Northern and Southern Italy makes necessary a revision of the regionalization of Central Italy. In fact, the regionalizations for

Table 2

Final results

	Northern Italy		Southern Italy			Central Italy	
	Area 1	Area 2	Area 1	Area 1*	Area 2	Area 1	Area 2
Events	2	2	3	1	2	3	4
Predicted	2	2	3	1	1	3	3
False alarms	1	2	5	6	2	2	4
Failures to predict	0	0	0	0	1	0	1
% of TIPs	27	34	33	44	25	23	38

*Only shallow events.

Northern and Southern Italy, proposed in the present study, contain some zones (see Fig. 2), previously included in Central Italy (COSTA *et al.*, 1995). The new regionalization for this area is presented in Figure 3f. Four strong earthquakes occurred in the area: $M = 5.8$ and $M = 6.0$, both on August 21, 1962, $M = 5.5$, September 19, 1979 and $M = 5.4$, May 7, 1984. As can be seen from Figure 6b, three of the four strong earthquakes are predicted by the CN algorithm, while the 1979 event is a failure to predict; there are four false alarms and the TIPs increase, with respect to the previous study (COSTA *et al.*, 1995), from 30% to 38% of the total time.

Only the crustal earthquakes which occurred in Central Italy are used to obtain the results shown in Figure 6. According to the model proposed by MARSON *et al.* (1995), few intermediate and deep earthquakes belong to Central Italy and should be considered when using the CN algorithm. However, their inclusion in the data set does not affect the results, and this is not surprising since the number of these events and their size are small.

4. Conclusions

Three main areas in Italy (Northern, Central and Southern, each having a distinct seismicity pattern) have been analyzed in the present study, utilizing the CN algorithm. The separation among them is not marked by sharp boundaries, and on the basis of different zonations, it is possible to identify intersection areas, which can be assigned to either bordering main areas. The TIPs duration decreases in each main area when the intersection areas are included in it (Table 2). On the basis of these results, one can conclude that the fault systems belonging to the domains of intersection are involved in the generation of strong earthquakes in the bordering main areas and, therefore, for the purpose of earthquake prediction, they must be considered together with the faulting system of the main areas.

In Southern Italy, where numerous, intermediate and deep focus events occur, all the earthquakes (shallow, intermediate and deep focus) should be used for the purposes of intermediate-term earthquake prediction.

HABERMANN and CREAMER (1994) analyzed M8 (KEILIS-BOROK and KOSOBOKOV, 1986), a prediction algorithm similar to CN, and suggested that the algorithm preferentially identifies TIPs during periods of systematically increased magnitudes. The systematic increase of magnitudes has the same effect of changes in the completeness of the catalogue used in the prediction. The analysis of the completeness of the PFGING catalogue, made by MOLCHAN *et al.* (1995), allows us to state that the TIPs, diagnosed by the CN algorithm, cannot be obviously associated with the changes in the completeness level of the catalogue.

Acknowledgments

The authors are very grateful to Professor V. I. Keilis-Borok for stimulating discussions. One of the authors (I. Rotwain) thanks ICTP for financial support for her stay in Trieste during which a large part of this work has been done. We acknowledge financial support from MURST (40% and 60%) funds, CNR-Gruppo Nazionale per la difesa dai Terremoti contracts nos. 92.02867.54 and 93.02492.54 and INTAS 94-232 contract.

REFERENCES

ALPOR. (1987), *Catalogue of the Eastern Alps*, Osservatorio Geofisico Sperimentale, Trieste, Italy (computer file).

CALCAGNILE, G., and PANZA, G. F. (1981), *The Main Characteristics of the Lithosphere-astenosphere System in Italy and Surroundings Regions*, Pure and Appl. Geophys. *119*, 865–879.

CAPUTO, M. G., PANZA, G. F., and POSTPISCHL, D. (1970), *Deep Structure of the Mediterranian Basin*, J. Geophys. Res. *75*, 4919–4923.

COSTA, G., PANZA, G. F., and ROTWAIN, I. M. (1991), *Time of increased probability for earthquakes with $M > 5.6$ in Central Italy*. Proceedings of International Conference on Earthquake Predictions: State-of-the Art. Strasbourg, France, 15–18 October.

COSTA, G., PANZA, G. F., and ROTWAIN, I. M. (1995), *Stability of Premonitory Seismicity Pattern and Intermediate-term Earthquake Prediction in Central Italy*, Pure and Appl. Geophys. *145*, 259–275.

DAL PIAZ, G. V., and POLINO, R., *Evolution of the Alpine Tethys*. In *The Lithosphere in Italy* (eds. Boriani, A., Bonafede, M., Piccardo, G. B., and Vai, G. B.) (Academia Nazionale de Lincei, Atti dei Convegni Lincei, 80, Roma 1989) pp. 93–109.

DELLA VEDOVA, B., MARSON, I., PANZA, G. F., and SUHADOLC, P. (1991), *Upper Mantle Properties of the Tuscan-Tyrrhenian Area: A Key for Understanding the Recent Tectonic Evolution of the Italian Region*, Tectonophysics *195*, 311–318.

GABRIELOV, A. M., DMITRIEVA, O. E., KEILIS-BOROK, V. I., KOSOBOKOV, V. G., KUZNETSOV, I. V., LEVSHINA, T. A., MIRZOEV, K. M., MOLCHAN, G. M., NEGMATULLAEV, S. Kh., PISARENKO, V. F., PROZOROV, A. G., RINEHART, W., ROTWAIN, I. M., SHEBALIN, P. N., SHNIRMAN, M. G., and SCHREIDER, S. Yu. (1986), *Algorithms of Long-Term Earthquakes' Predictions*. International School for Research Oriented to Earthquake Prediction-Algorithms, Software and Data Handling, Lima, Perù.

HABERMANN, R. E., and CREAMER, F. (1994), *Catalogue Errors and the M8 Earthquake Prediction Algorithm*, Bull. Seismol. Soc. Am. *84*, 1551–1559.

ING. (1995), *Seismological Reports 1980–1995.* Istituto Nazionale di Geofisica, Roma, Italy (computer file).

KAGAN, Y. Y., and KNOPOFF, L. (1981), *Stochastic Synthesis of Earthquake Catalogs*, Geophys. J. R. Astr. Soc. *86*, 303–320.

KEILIS-BOROK, V. I., KNOPOFF, L., and ROTWAIN, I. (1980), *Bursts of Aftershocks, Long-term Precursors of Strong Earthquakes*, Nature *283*, 259–263.

KEILIS-BOROK, V. I., and KOSOBOKOV, V. S. (1986), *Time of Increased Probability for the Great Earthquake of the World*, Computational Seismology *19*, 48–57.

KEILIS-BOROK, V. I., KUZNETSOV, I. V., PANZA, G. F., ROTWAIN, I. M., and COSTA, G. (1990), *On Intermediate-term Earthquake Prediction in Central Italy*, Pure and Appl. Geophys. *134*, 79–92.

KEILIS-BOROK, V. I., and ROTWAIN, I. (1990), *Diagnosis of Time of Increased Probability of Strong Earthquakes in Different Regions of the World: Algorithm CN*, Phys. Earth Planet. Inter. *61*, 57–72.

MARSON, I., PANZA, G. F., and SUHADOLC, P. (1995), *Crust and Upper Mantle Models along the Active Tyrrhenian Rim*, Terra Nova *7*, 348–357.

MOLCHAN, G. M., KRONROD, T. L., and DMITRIEVA, O. E. (1995), *Statistical Analysis of Seismicity and Hazard Estimation for Italy (Mixed Approach)*, ICTP, IAEA, UNESCO, Internal Report, IC/95/27, 85 pp. Trieste, Italy.

MUELLER, S., *Deep structure and recent dynamics in the Alps.* In *Mountain Building Process* (ed. K. J. Hsu) (Academic Press 1982) pp. 181–199.

NEIC. (1992), *Worldwide earthquake catalogue*, National Earthquake Information Center (NEIC), USGS, Denver, Colorado, U.S.A. (computer file).

PANZA, G. F., MUELLER, S., CALCAGNILE, G., and KNOPOFF, L. (1982), *Delineation of the North Central Italian Upper Mantle Anomaly*, Nature *296*, 238–239.

PATACCA, E., and SCANDONE, P., *Post-Tortonian mountain building in the Apennines. The role of the passive sinking of a relic lithospheric slab.* In *The Lithosphere in Italy* (eds. Boriani, A., Bonafede, M., Piccardo, G. B., and Vai, G. B.) (Academia Nazionale dei Lincei, Atti dei Convegni Lincei, 80, Roma 1989) pp. 157–176.

PATACCA, E., SATORI R., and SCANDONE, P. (1990), *Tyrrhenian Basin and Apenninic Arcs: Kinematic Relation since Late Tortonian Times*, Mem. Soc. Geol. It. *45*, 425–451.

PAVONI, N., AHJOS, T., FREEMAN, R., GREGERSEN, S., LANGER, H., LEYDECKER, G., ROTH, Ph., SUHADOLC, P., and USKI, M., *Seismicity and focal mechanisms.* In *A Continent Revealed—The European Geotraverse: Atlas of Compiled Data* (eds. Freeman, R. and Mueller, S.) (Cambridge University Press, Cambridge 1992) pp. 14–19.

PFG (1985), *Catalogo dei terremoti italiani dall'anno 1000 al 1980* (ed. Postpischl, D.), CNR-P. F. Geodinamica.

RUNDKVIST, D. V., and ROTWAIN, I. M. (1994), *Present-day Geodynamics and Seismicity of Asia Minor*, Computation of Seismology *27*, 201–245.

SUHADOLC, P., and PANZA, G. F. (1988), *The European-African Collision and its Effects on the Lithospheric-astenosphere System*, Tectonophysics *146*, 59–66.

VOROBIEVA, I. A., and PANZA, G. F. (1993), *Prediction of Occurrence of Related Strong Earthquakes in Italy*, Pure and Appl. Geophys. *141*, 25–41.

(Received July 14, 1995, accepted November 6, 1995)

Proc. 30th Int'l. Geol. Congr., Vol. 5 pp. 193-201
Ye Hong (Ed)

CN Algorithm in Italy: Intermediate-term Earthquake Prediction and Seismotectonic Model Validation.

GIOVANNI COSTA[1),2)], ANTONELLA PERESAN[1)], IVANKA OROZOVA[1,2], GIULIANO FRANCESCO PANZA[1),2)] AND IRINA M. ROTWAIN[3)]
1) Dipartimento di Scienze della Terra, Universita degli Studi di Trieste, via E. Weiss 1, 34127 Trieste, Italy
2) International Center for Theoretical Physics - SAND Group - ICTP, 34100 Trieste Miramar, Italy
3) International Institute of Earthquake Prediction Theory and Mathematical Geophysics, Russian Academy of Sciences, Warshavskoye, 79, K.2, 113556, Moscow, U.S.S.R.

Abstractt

The CN algorithm is here utilized both for the intermediate-term earthquake prediction and to validate the seismotectonic model of the Italian territory. Using the results of the previous analysis, made through the CN algorithm and taking into account the seismotectonic model, three main areas, one for Northern Italy, one for Central Italy and one for Southern Italy, are defined. The separation among them is not marked by sharp boundaries, and on the basis of different zonations, it is possible to identify intersection areas, which can be assigned to either bordering main areas. The earthquakes occurred in these areas contribute to the precursor phenomena identified by the CN algorithm in each main area when the TIPs duration decreases when the intersection areas are included.

In a further step we have constructed a revised catalogue using the most recent information about the seismicity in Italy, and we have considered a regionalization that follows strictly the boundaries of the areas defined in the seismotectonic model of Italy. Each of these new regions contains only the zones with similar seismotectonic characteristics. The results obtained in this way are good and stable and represent an improvement with respect to the previous investigations.

Keywords: CN Algorithm, intermediate-term earthquake prediction, seismotectonic model, Italy

INTRODUCTION

The analysis of the Time of Increased Probability (TIP) of a strong earthquake with magnitude greater than, or equal to a given threshold M_0, based on the algorithm CN, makes use of normalized functions, which describe the seismicity pattern of the analyzed area. Therefore the original algorithm, developed for the California-Nevada region, can be directly used, without any adjustment, in areas with different size and level of seismicity. The algorithm CN is described in full detail by Keilis-Borok et al.[5,6].

It has been shown [3, 4] that a regionalization, supported by seismological and tectonic arguments, leads to the reduction of the alarm duration (TIP) and of the failures to predict, and increases the stability of the algorithm compared with the results obtained when the borders of the studied area are defined simply according to the completeness of the used catalogue [7]. Therefore, the CN algorithm permits to deal with the development of modern regional geodynamic models, involving relationships between the key structural features which control the seismicity, and the selection of the optimal causative fault system for

prediction purposes [12].

Considering the information contained in the seismotectonic model of Italy [10] and the spatial distribution of the epicentres, the country can be divided into three main areas (Fig. 1) [4]. Each of them is characterized by a dominant seismotectonic behavior, with varying seismicity level, therefore the appropriate M_0 is used in each area.

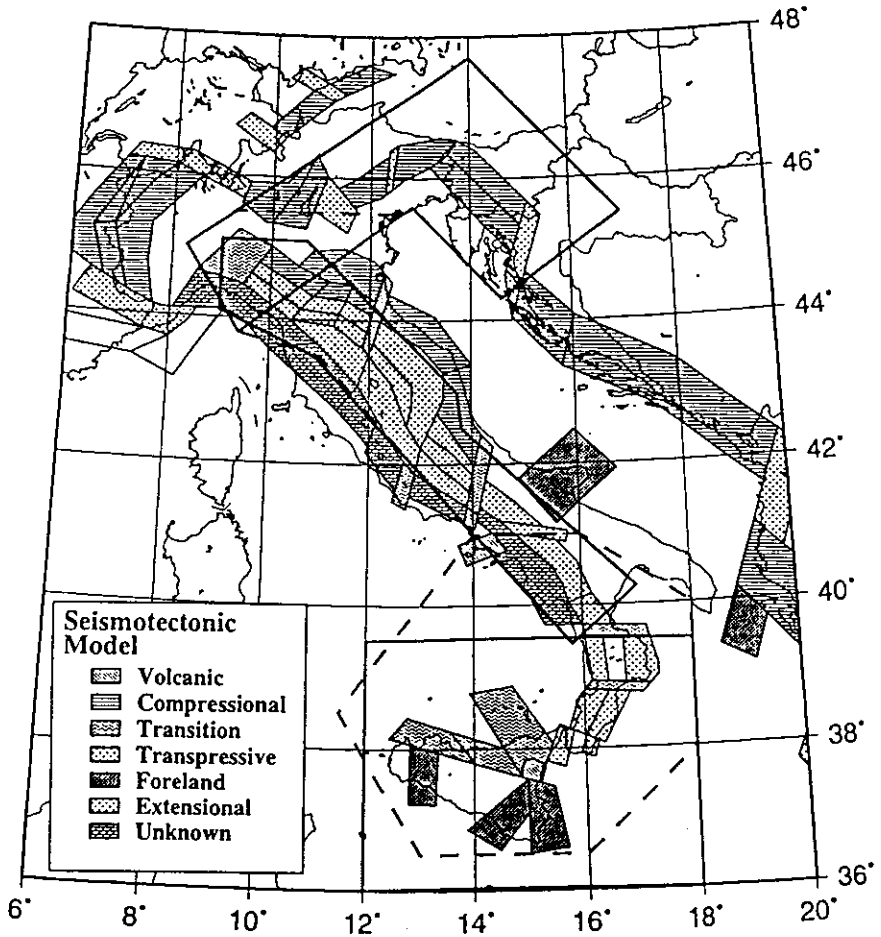

Fig. 1 Seismotectonic model of Italy [10] and regionalization into three main and two transition areas.

We introduce here a more detailed regionalization for Nord, South and Central Italy which follows strictly the boundaries of the seismotectonic zones [10]. Only the seismotectonic zones with the same characteristic, and with transitional behavior between them, are contained in each new area.

In the present analysis a new catalogue "CCI96" is routinely used for the application of the CN algorithm in Italy. The catalogue has been compiled revising the PFGING [2,3, 11] catalogue with the recently published data about the seismicity, mainly historical [1]. Some relevant differences, also for large magnitudes, have been found between the PFGING catalogue and the new CCI96 catalogue, mainly for Southern Italy where maximum magnitude is used.

REGIONALIZATION

To minimize the spatial uncertainty, the area where a strong earthquake has to be predicted, should be as small as possible, but there are three rules that limit its minimum dimensions: 1) the border of the area must be drawn following as much as possible the minima in the seismic activity; 2) the annual number of earthquakes with magnitude greater or equal to the completeness threshold of the catalogue has to be greater or equal to 3; 3) the linear dimension of the region must be about 5L to 10L, where L is the length of the expected source.

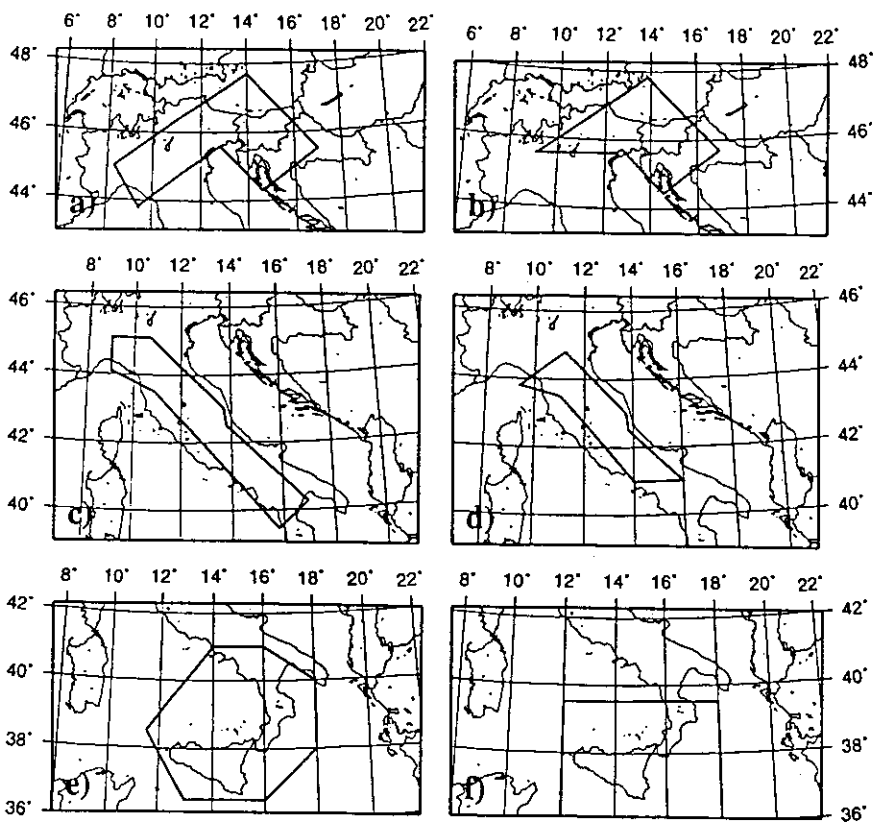

Fig. 2 Regionalization considered in [4]: first variant in Northern Italy (area 1); b) second variant in Northern Italy (area 2); c) first variant in Central Italy (area 1); d) second variant in Central Italy (area 2); e) first variant in Southern Italy (area 1); f) second variant in Southern Italy (area 2).

In the regionalization proposed by Costa et al. [4], the borders between the three main areas: Northern, Central and Southern are not sharply defined and they can be better represented by a transition domain (Fig. 1). In fact, the division of the Italian territory in three main areas, separated by two transition areas, seems to be consistent with the indications given about the properties of seismicity by the CN algorithm. In each main region, in order to analyze the effect on the prediction of the transition domains seismicity, two different regions have been tested, which blandly follow the border of the seismotectonic zones (Fig. 1, 2). In all the cases considered, the best results are obtained for the regions which include the transition areas [4].

The earthquakes information contained in ALPOR[1] has been used to construct the new catalogue, CCI96, used in the CN analysis performed in the framework of a new regionalization (Fig. 3), which follows strictly the borders of the seismotectonic zones, and in the forward monitoring in Italy.

CN ANALYSIS IN NORTHERN ITALY

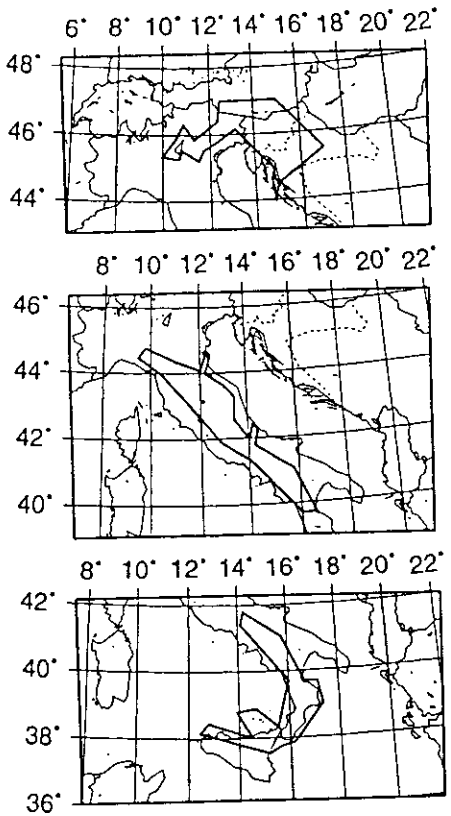

Fig. 3 Regionalization considered in the present study (solid line) Italy; b) Central Italy; c) Southern Italy; dashed lines indicate some of the variants used in [4].

The Alpine arc, the most important tectonic feature in Northern Italy, is crossed by different political borders and consequently the catalogue PFGING is fairly incomplete for our purposes [4]; to fill in the gap the information contained in two other catalogues, ALPOR [1] and NEIC [9] , has been included.

According to the standards used in the CN algorithm [3], the magnitude threshold for the definition of strong earthquakes is chosen to be M_0=5.4. The period 1960-1992 is analyzed, because of the significant incompleteness of the catalogue before 1960 [4]. In the region (Fig. 2a), only 2 strong earthquakes occurred during the last 30 years (M=6.5, May 6, 1976 and M=5.4, January 2, 1988), in fact the M=6.0 September 15, 1976 event is a strong aftershock, identified as Related Strong Earthquake [8], and therefore it is not a target of the CN algorithm.

The seismogenic region, thus defined, is shown in Fig. 2a. The two strong events are predicted and the TIP duration is 27% of the total time (see Fig 4a). There is only one false alarm after the strong earthquake of 1988.

In order to test the hypothesis that the earthquakes, concentrated on the edges of a tectonic structure or in the areas of intersection with other structures, cannot be neglected for the purposes of intermediate term earthquake prediction, a second regionalization (Fig. 2b), which includes only the compressive domains in the Eastern Alps (Fig. 2b), is considered by Costa et al. [4]. The two strong events are predicted (Fig 4b), but the TIP duration increases to 34% of the total time, and there are three false alarms.

The new regionalization considered here follows the compressional zones of the seismotectonic model for Northeast Italy and therefore is disconnected from Central Italy (Fig. 3a). In the Austrian and Slovenian territory the seismotectonic zones have been defined only near the border with Italy and a complete zonation is not available, therefore the border outside Italy is defined by seismicity only. The results obtained with such regionalization and using the CCI96 catalogue (Fig. 5a) are: the two strong events are predicted and the TIP duration is 28.8% of the total time with two false alarms. The reduction of the spatial uncertainty is about 28%.

CN ANALYSIS IN CENTRAL ITALY

The CN algorithm has been initially applied to Central Italy [3, 6], because the catalogue PFGING is rather complete here. Subsequently a regionalization based on seismotectonic consideration has been proposed [3] (see Fig. 2c). Only the crustal earthquakes occurred in Central Italy are used, even if, according to the model proposed by Costa et al.[4] few intermediate and deep earthquakes belong to Central Italy and should be considered when using the CN algorithm. In fact, their inclusion in the data set does not affect the results, and this is not surprising since the number of these events and their size is small. The magnitude threshold for the definition of the strong earthquakes is chosen to be M_0=5.6. The two strong events are predicted and the alarm occupies about 30% of the total time with two false alarms (see Fig. 4c).

The definition of the areas in Northern and Southern Italy [4] make it necessary a revision of the regionalization proposed by Costa et al.[3] for Central Italy. This revised regionalization is presented in Fig. 2d. Due to the smaller dimension of the area, the magnitude threshold is M_0=5.4. Four strong earthquakes occuned in the area. As it can be seen from Fig. 4d, three of them are predicted by the CN algorithm, while the 1979 event is a failure to predict; there are 4 false alarms and the TIPs increase, with respect to the previous study, from 30% to 38% of the total time.

The new regionalization (Fig. 3b) , which follows strictly the border of the seismotectonic zones, includes the extensional zones and some transitional ones. The magnitude threshold for the definition of the strong earthquakes is M_0=5.6 and the catalogue used is the CCI96. All the three strong events are predicted and the alarm occupies about 21% of the total time, with three false alarms (Fig. 5b).

CN ANALYSIS IN SOUTHERN ITALY

The catalogue PFGING can be considered complete in this part of Italy only after 1950, and for magnitude above 3. The magnitude threshold in the definition of the strong earthquakes, used by Costa et al.[4], is M_0=6.5.

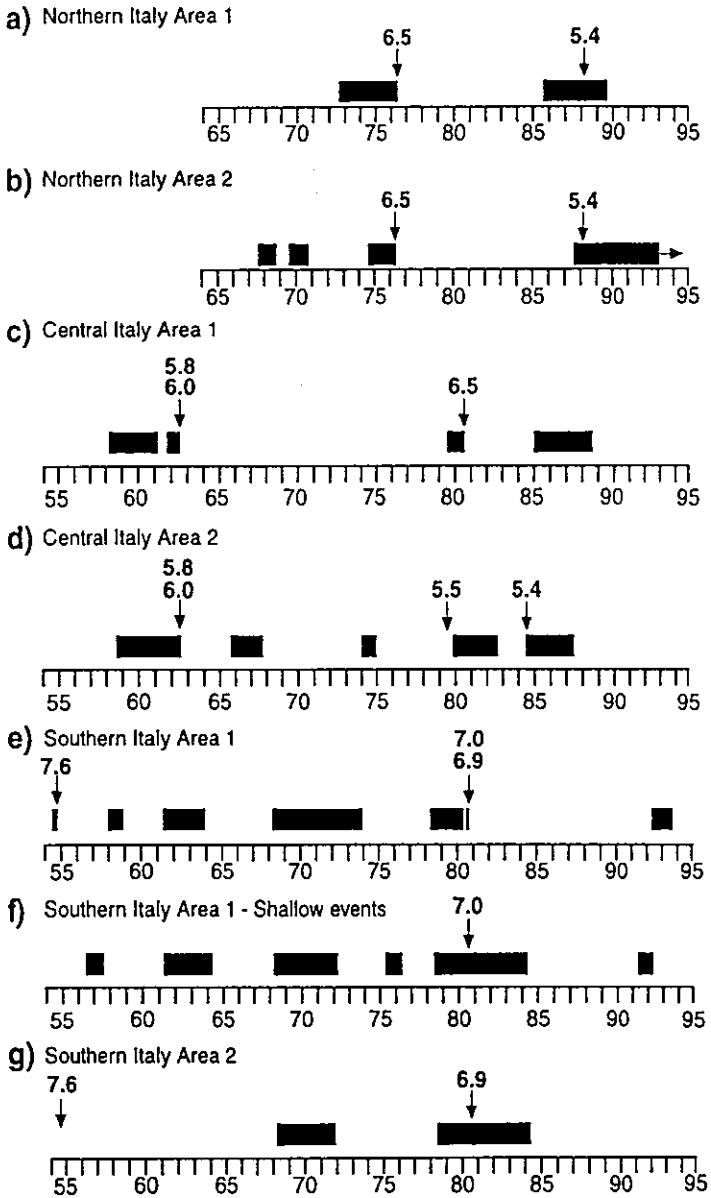

Fig. 4 Results of the CN analysis in Italy using the regionalization of figure 2. The catalogue used is the PFGING. The arrows indicate earthquakes with $M \geq M_0$, TIPs are marked by black rectangles. In e) and g) the magnitude 6.9 marks an intermediate-depth earthquake in the Tyrrhenian sea; in e) and f) the magnitude 7 marks the Irpinia, 1980, earthquake and in a) and b) the magnitude 6.5 marks the Friuli 1976 event. In the Southern Italy the maximum magnitude present in the catalogue is used for the analysis, while in Northern and Central Italy the priority magnitude M_p (M_L, M_l, M_d, M_p) [3] is used.

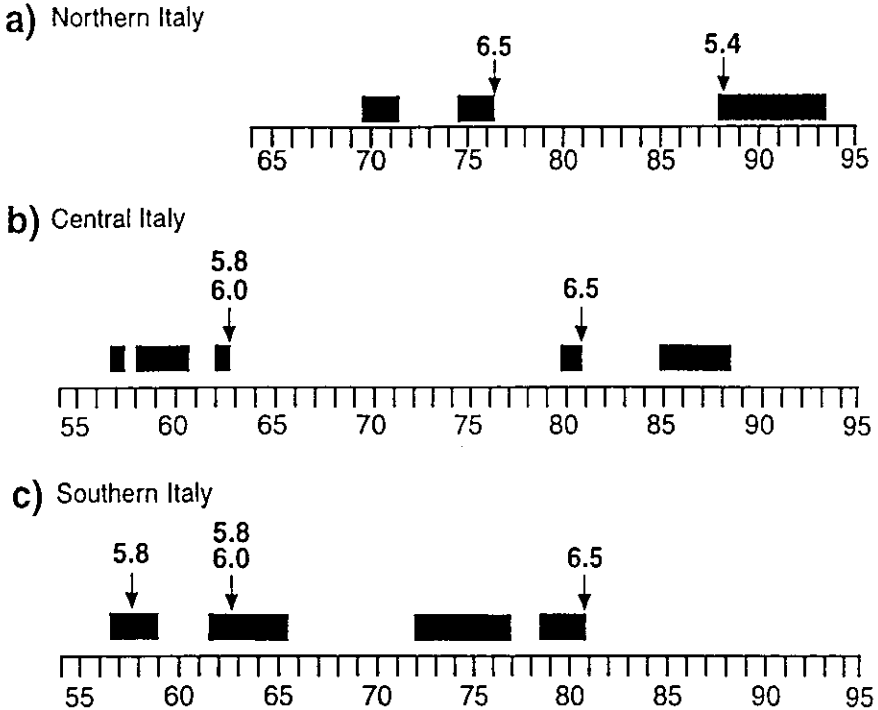

Fig. 5 Results of the CN analysis in Italy using the regionalization of figure 3. The catalogue used is the CCI96. The arrows indicate earthquakes with $M \geq M_0$. TIPs are marked by black rectangles. The priority magnitude M_p (M_L, M_l, M_d, M_p)[3] is used.

Following the idea that the 41°N parallel divides the Apennines into two completely different tectonic domains [10], for Southern Italy the area shown on Fig. 2e has been considered. The results of the CN algorithm applied to this area [4] are reported in Fig. 4e. All three strong earthquakes (M=7.6, November 23, 1954, M=7.0 November 23, and M=6.9, November 24, both in 1980) are predicted and the duration of TIP is 33% of the total time. There are 5 false alarms.

To study the influence of the relevant deep seismicity [4] only the shallow earthquakes is considered and thus the strong event to be predicted is the M=7.0, November 23, 1980 earthquake. The diagnosis of the CN algorithm is given in Fig. 4f. The strong event is predicted, but the duration of TIP increases up to 44% of the total time and there are six false alarms.

As a second test, according to the regionalization for Central Italy [3], the northern border of Southern Italy is traced along the 39.5° parallel (Fig. 2f). In this area the two strong earthquakes to be predicted are the M=7.6, November 23, 1954 and the M=6.9, November 23, 1980 events. The 1980 earthquake is predicted with a TIP duration lasting for 25% of the total time; the 1954, M=7.6, event is a failure to predict and there are two false alarms (Fig. 4g).

The new regionalization (Fig. 3c) follow strictly the extensional and transitional seismotectonic zones present in South Italy (below the 42°N parallel). The small, but with a intense seismicity, volcanic zone present in Sicily is included as well, while the foreland seismotectonic zones have been excluded, as it was done in Central Italy in [3].

In Southern Italy the differences in the magnitude between the PFGING catalogue and the CCI96 catalogue are very large also for the events with $M>M_0$. Therefore a direct comparison with the results obtained by Costa et al. [4] is not possible. The improvement introduced by the new catalogue and the new regionalization permits to use for Southern Italy the same criteria used in Northern and Central Italy. The magnitude threshold is $M_0=5.4$ and the strong events to be predicted are 4. All of them are predicted and the duration of TIP is 31.8% of the total time (Fig. 5c). There are 3 false alarms. The spatial uncertainty reduction with respect to the results of Costa et al.[4] is relevant, about 72%.

CONCLUSIONS

The CN algorithm has been here utilized both for the intermediate term earthquake prediction and to validate the seismotectonic model of the Italian territory.

The catalogue PFGING used by Costa et al. [3, 4] has been revised using the earthquakes information contained in ALPOR [1] and a new catalogue, the CCI96, has been compiled and used here. Some relevant differences, for large magnitudes, have been found between the PFGING catalogue and the new catalogue, mainly for Southern Italy, when maximum magnitude is considered.

A new detailed regionalization for Northern, Southern and Central Italy, which follows strictly the boundaries of the seismotectonic zones [10], has been proposed. Only the seismotectonic areas with the same characteristic, or with transitional behavior, are contained in each new area. This regionalization represent an improvement of the regionalization proposed by Costa et al. [4], the average spatial uncertainty reduction of the prediction is about 45% with a general reduction of the TIPs duration and of the false alarms. The improvement of the results is particularly relevant in Southern Italy.

On the basis of the results obtained, Costa et al. conclude that the separation among the three regions proposed is not marked by sharp boundaries, and on the basis of different zonations, it is possible to identify intersection areas, which can be assigned to either bordering main areas[4]. When these intersection areas are included in the CN analysis, an improvement of the results is obtained. This result hasbeen confirmed, for Southern and Central Italy, by the results obtained using the newregionalization proposed here. In Northern Italy, the compressional seismotectonic zones are disconnected from the transitional and compressional seismotectonic zones included in the regionalization proposed by Costa et al. [4]. Therefore, a comparison is possible only with the region shown in Fig. 2b: there is an improvement with respect to the previous results, but the best result remains the one obtained when the intersection areas are included.

Acknowledgments

The authors are very grateful to Prof. V.I.Keilis-Borok for stimulating discussions. We acknowledge financial support from MURST funds, CNR-Gruppo Nazionale per la Difesa dai Terremoti contracts n.° 95.00608.54 and 96.02968.54 and INTAS grant 94-0232.

REFERENCES

1. ALPOR., *Catalogug of the Eastern Alps*, Osservatorio Geofisico Sperimentale, Trieste, Italy (computer file) (1987).
2. E. Boschi G. Ferrari P. Gasperini, E. Guidoboni, G. Smriglio and G. Valensise. *Catalogo dei forti terremoti in Italia dal 461 a.C. al 1980*. Istituto Nazionale di Geofisica SGA storia geofisica ambiente (1995)..
3. G. Costa, G.F. Panza, and I.M. Rotwain, Stability of premonitory seismicity pattern and intermediate-term earthquake prediction in Central Italy. *PAGEOPH*,144, in press.
4. G. Costa I. Orozova-Stanishkova G.F. Panza, and I.M. Rotwain. Seismotectonic models and CN algorithm: the case of Italy. *PAGEOPH*, 147 No. 1, 119-130 (1996).
5. A.M. Gabrielov, O.E. Dmitrieva, V.I. Keilis-Borok, V.G. Kosobokov, I.V. Kuznetsov, T.A. Levshina, K.M. Mirzoev, G.M., Molchan, S.K. Negmatullaev, V.F. Pisarenko, A.G. Prozorov, W. Rinehart, I.M. Rotwain, P.N. Shebalin, M.G. Shnirman, and S.Yu. Schreider, Algorithms of Long-Term Earthquakes' Prediction. International School for Research Oriented to Earthquake Prediction-Algorithms, Software and Data Handling, Lima, Peru (1986).
6. V.I.Keilis-Borok, and I. Rotwain, Diagnosis of Time of Increased Probability of strong earthquakes in different regions of the world: algorithm CN. *Phys. Earth Planet. Inter.*, 61, 57-72 (1990).
7. V.I. Keilis-Borok, I.V. Kuznetsov, G.F. Panza, I.M. Rotwain, and G. Costa, On Intermediate-Term Earthquake Prediction in Central Italy. *PAGEOPH*, 134, 79-92 (1990).
8. I., Marson, G.F. Panza, and P. Suhadolc, Crust and upper mantle models along the active Tyrrhenian Rim, *Terra Nova*, 7, in press.
9. NEIC. *World-wide earthquake catalogue*. National Earthquake Information Center (NEIC), USGS, Denver, USA. (computer file) (1992).
10. E. Patacca, R. Sartori and P. Scandone, Tyrrenian basin and Apenninic arcs: kinematic relation since late Tortonian times. *Mem. Soc. Geol. It.*, 45, 425-451(1990).
11. PFG. *Catalogo dei terremoti italiani dall'anno 1000 al 1980* (ed. Postpischl, D.), CNR-P.F. Geodinamica. Roma, Italy (computer file) (1985).
12. D.V Rundkvist, and I.M. Rotwain, Present-day geodynamics and seismicity of Asia Minor. *Computation of Seismology*, 27, (in press) .
13. I. A. Vorobieva, and G.F. Panza, Prediction of Occurrence of Related Strong Earthquakes in Italy. *PAGEOPH*, 141, 25-41(1993).

united nations
educational, scientific
and cultural
organization

international atomic
energy agency

the
abdus salam
international centre for theoretical physics

H4.SMR/1150 - 7

Fifth Workshop on Non-Linear Dynamics
and Earthquake Prediction

4 - 22 October 1999

Experiments with CN in Italy and Seismic Hazard

Part II

G. F. Panza

Department of Earth Sciences
Trieste, Italy

Pure appl. geophys. 154 (1999) 281–306
0033–4553/99/020281–26 $ 1.50 + 0.20/0

Pure and Applied Geophysics

Seismotectonic Model and CN Earthquake Prediction in Italy

A. PERESAN,[1] G. COSTA[1,2] and G. F. PANZA[1,2]

Abstract—The choice of the regions is essential in the application of the algorithm CN, therefore a seismotectonic criterion for their definition is tested. In order to take into account the geodynamic complexity characterising the Italian peninsula, we established to strictly follow the seismotectonic zones, including in each region only zones with similar seismogenic behaviour and the transitional zones connected to them. Three regions have been successfully defined in this way, corresponding approximately to the North, Centre and South of Italy. The reduction of the space-time uncertainty and the increase of the stability of prediction results obtained with this regionalisation, with respect to the previous applications of CN in Italy (KEILIS-BOROK *et al.*, 1990; COSTA *et al.*, 1995, 1996), can be interpreted as a validation of the seismotectonic model.

Key words: CN algorithm, earthquake prediction, Italy, seismotectonic model.

Introduction

The algorithm CN is structured according to a pattern recognition scheme to allow a diagnosis of the Time of Increased Probability (TIPs) for events with magnitude above a fixed threshold M_0. CN is based on the quantitative analysis of the premonitory phenomena, which can be detected in the seismic flow preceding the occurrence of strong earthquakes. The quantification of the seismicity patterns is obtained through a set of empirical functions of time, evaluated on the sequence of the main shocks which occurred in the analysed region. The seismicity traits considered are: level of seismic activity, quiescence, space-time clustering and space concentration of events. At each time, a vector formed by the values, coarsely discretized, assumed by the different functions, describes the seismic flow (KEILIS-BOROK, 1996). Although CN has been originally designed by retrospective analysis of seismicity in the California–Nevada region, the normalisation of its functions

[1] Department of Earth Sciences, University of Trieste, via E. Weiss 4, 34127 Trieste, Italy. Fax: + 39-40-676-2111, e-mail: anto@geosun0.univ.trieste.it

[2] International Centre for Theoretical Physics—SAND Group—ICTP, 34100 Trieste, Miramare, Italy.

allows application of the algorithm, without any adjustment of parameters, even to regions with different dimensions and seismicity.

The first application of CN to the central part of the Italian territory was performed by KEILIS-BOROK *et al.* (1990), over a region chosen considering simply the completeness of the used catalogue. Subsequently COSTA *et al.* (1995) showed that seismological and tectonic arguments permit a narrowing of the region, leading at the same time to a reduction of failures to predict and of TIPs, while increasing the stability of the algorithm. In a further step the analysis has been extended to the whole Italian territory by COSTA *et al.* (1996), selecting three main regions, Northern, Central and Southern Italy, according both to the seismotectonic model (SCANDONE *et al.*, 1990) and to the spatial distribution of epicentres. These experiments evidence that the CN algorithm allows for dealing with the development of the regional geodynamic models, since it involves relationships between the structural features that control the seismicity and the selection of the optimal causative fault system for prediction purposes (RUNDKVIST and ROTWAIN, 1996).

In this work we want to advance one step further in this direction, testing the possibility of tracing the boundary of regions following closely the seismotectonic zones, independently defined by GNDT (SCANDONE *et al.*, 1990, 1994), to investigate the possibility of reducing the time-space uncertainty and the number of false alarms.

A new catalogue, the CCI1996 (COSTA *et al.*, 1997; PERESAN *et al.*, 1997) has been compiled which revises the PFGING catalogue (POSTPISCHL, 1985; COSTA *et al.*, 1995) to take into account recent information, mainly concerning historical seismicity, supplied by BOSCHI *et al.* (1995). In order to guarantee homogeneous and timely catalogue upgrading, monitoring is currently performed which updates the CCI1996 catalogue with the NEIC Preliminary Determinations of Epicentres; the procedure of data upgrading is fully described in PERESAN and ROTWAIN (1998).

The Regionalization

The choice of the region in which a strong earthquake must be predicted, is a relevant factor to obtain reliable results and to minimise the time-space uncertainty. Regions defined for prediction purposes have to be as small as possible, in order to reduce the space uncertainty, and must include the zones with higher seismicity level, where stronger earthquakes are likely to occur. Therefore, considering the fractal character of the spatial distribution of events (KAGAN and KNOPOFF, 1980; TURCOTTE, 1992), the region must contain the major clusters of epicentres, characterised by a high density of epicentres and by large magnitudes. This choice clearly affects the frequency-magnitude distribution for events which occurred within each region, because the log-linearity of the Gutenberg–Richter relation is

preserved only on a global scale or, according to a multiscale approach (MOLCHAN *et al.*, 1996, 1997), within an area of the appropriate hierarchical scale, depending on the maximum magnitude considered. To reduce the spatial uncertainty of predictions, the area must be relatively small; therefore the frequency-magnitude distribution exhibits a good linearity only for lower magnitudes, with increasing fluctuations due to the small number of events for larger magnitudes. Generally an upward bend can be observed in this pattern, starting at a certain magnitude, depending both on the particular choice of the region that must include the more seismically active zones and on the possible occurrence of a characteristic earthquake for the major faults included in it (SCHWARTZ and COPPERSMITH, 1984). According to the standard procedure (MOLCHAN *et al.*, 1990), the magnitude threshold M_0, for the selection of the events to be predicted, is chosen close to this minimum in the number of events, and this guarantees the stability of the results (e.g., COSTA *et al.*, 1995). In other words, CN makes use of the information engendered by small and moderate earthquakes, registering good statistics, to predict the stronger earthquakes, which are rare events.

The area selected for predictions, using the algorithm CN, must satisfy three general rules: (1) its linear dimensions must be greater or equal to 5L–10L, where L is the length of the expected source; (2) on average, at least 3 events with magnitude exceeding the completeness threshold should occur inside the region each year; (3) the border of the region must correspond, as much as possible, to minima in the seismicity (KEILIS-BOROK *et al.*, 1996). This indicates that the detection level controls, to some extent, the time-space uncertainty of prediction (KEILIS-BOROK, 1996) and then the possibility of reducing the spatial uncertainty is limited by the difficulty of keeping a high level of detection, due to unavoidable logistic problems.

CN algorithm has been designed by the retrospective analysis of seismicity in the California–Nevada region, whose geodynamic can be related to a main driving mechanism, controlled by the relative displacement between the Pacific and the North-American plates. Compared to the California–Nevada, the Italian peninsula and the entire Mediterranean area exhibit a considerable heterogeneity in the tectonic regime, revealed by the coexistence of fragmented seismogenic structures of greatly differing kinds, where a very complex and apparently paradoxical kinematic evolution can be observed within very narrow regions (MELETTI *et al.*, 1998). Although the normalisation of CN functions guarantees the applicability of the algorithm to regions with a different level of seismic activity, we believe that this aspect should not be neglected. For instance, the number of aftershocks generated by an earthquake of a given magnitude is not independent from the fault mechanism, and consequently to mix sources of different kinds may compromise precursors based on the time cluster of events. More specifically, the selection of the region can influence the thresholds of discretisation of the function associated to the "bursts of aftershocks," even if this is a precursor observed in very diverse regions (MOLCHAN *et al.*, 1990).

Wishing to account for the seismotectonic complexity of the Italian area, we decided to test a new criterion for the definition of the regions, strictly based on the seismotectonic model. Considering the general rules and the sizes of the seismotectonic zones (Fig. 1), we establish to include in a single region adjacent zones with the same seismogenic characteristics (e.g., only compressive or only extensive) and zones with transitional properties. A transitional zone is included in a region if it is between zones of the same kind or if it separates two zones with different regimes and the space distribution of the aftershocks reveals a possible connection. For this purpose the selection of aftershocks is performed (MOLCHAN *et al.*, 1995) using the

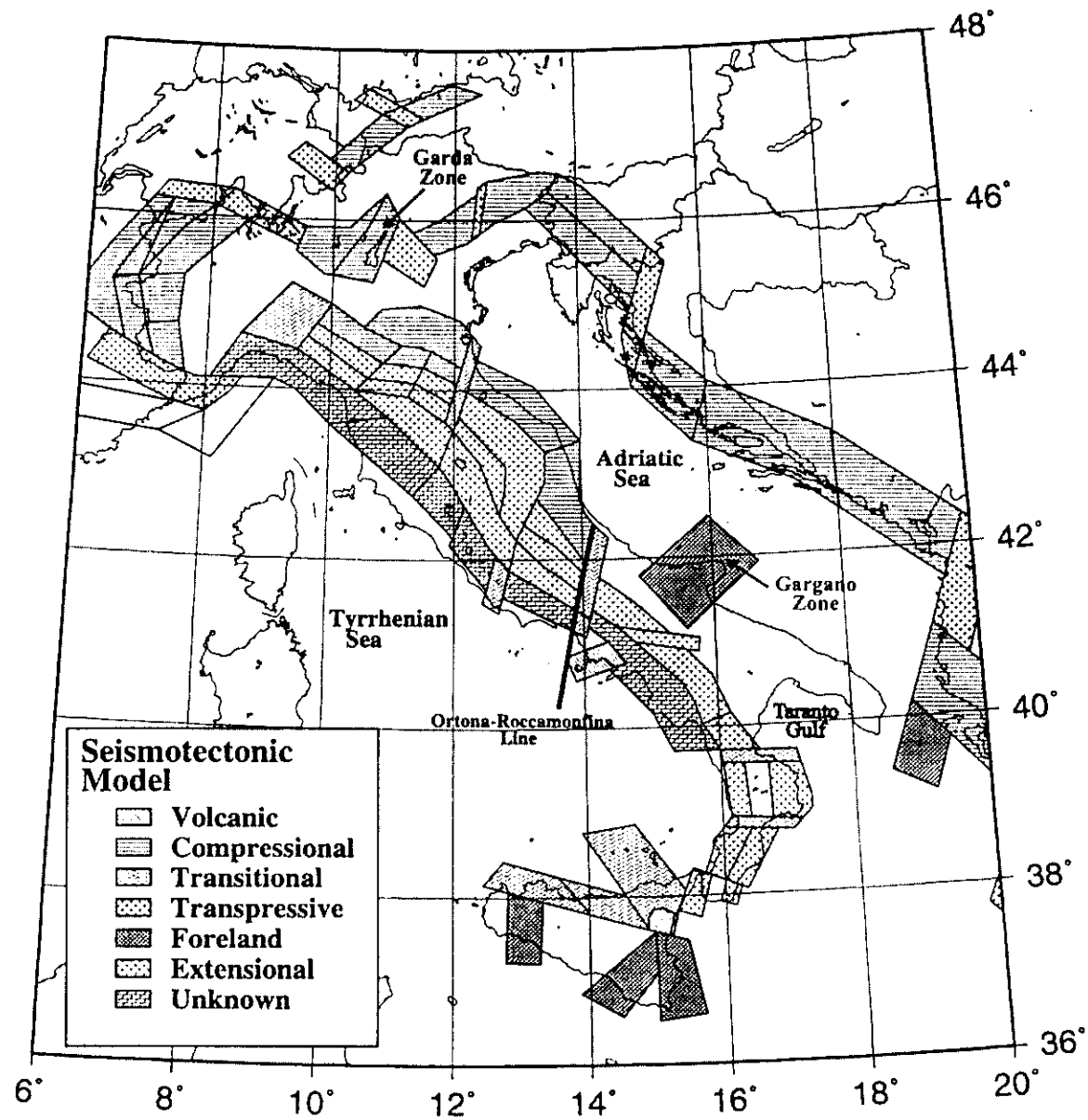

Figure 1
Seismotectonic model of Italy (SCANDONE *et al.*, 1994), revised version of the preliminary zoning described in SCANDONE *et al.* (1990).

"minimax" method proposed by MOLCHAN and DMITRIEVA (1992), since it allows a better spatial identification of aftershocks than the method proposed by KEILIS-BOROK *et al.* (1980), which is used in the selection of the subcatalogue of main shocks for prediction purposes.

Northern Italy

Northern Italy is characterised by the presence of a main structure, the Alpine arc, which is generally uplifting (MUELLER, 1982) with some westerly strike-slip motion (PAVONI *et al.*, 1992) and therefore the majority of focal mechanisms are compressive or transpressive.

The presence of many different political borders across the Alpine arc introduces two problems. Firstly the catalogue CCI1996 covers an area that, towards the North, follows the Italian border and consequently is fairly incomplete for our purposes; this problem has been solved (COSTA *et al.*, 1996) by filling the gap with data contained in two other catalogues, ALPOR (CATALOGO DELLE ALPI ORIENTALI, 1987) and NEIC (1992). The catalogue obtained for Northern Italy can be considered complete for $M \geq 3.0$ starting from 1960. The operating magnitude is selected as follows:

$$M = \mathrm{MAX} \begin{vmatrix} M_{\mathrm{ALPOR}}(M_L, M_I) \\ M_{\mathrm{CCI}}(M_L, M_d, M_I) \\ M_{\mathrm{NEIC}}(M_L, M_S, m_b) \end{vmatrix} . \tag{1}$$

This means that the operating magnitude is the maximum of the three magnitudes selected for each catalogue, according to the priority order given in brackets. Magnitudes are indicated as follows: M_L is the local magnitude, M_d the duration magnitude, M_I is the magnitude from intensities, while M_S and m_b are the magnitudes from surface and body waves. Aftershocks are removed following the criteria proposed by KEILIS-BOROK *et al.* (1980) and, according to the general rules of the algorithm CN, the magnitude for the selection of the events to be predicted is fixed at $M_0 = 5.4$.

The second problem, due to the presence of political borders, arises from the necessity to use an adequate seismotectonic zoning for the neighbouring countries. Until recently, the available zones for the Slovenian–Croatian region were designed with different purposes and criteria (LAPAJNE *et al.*, 1995), consequently the easternmost border of the region could only be defined on the base of seismicity. Recently, following criteria quite similar to those used for Italy by SCANDONE *et al.* (1990, 1994), a seismotectonic zoning was proposed by ZIVCIC and POLJAK (1997) and consequently it became possible to redraw the boundaries of the northeastern part of the region closely following the seismogenic zones (Figs. 2c and 3).

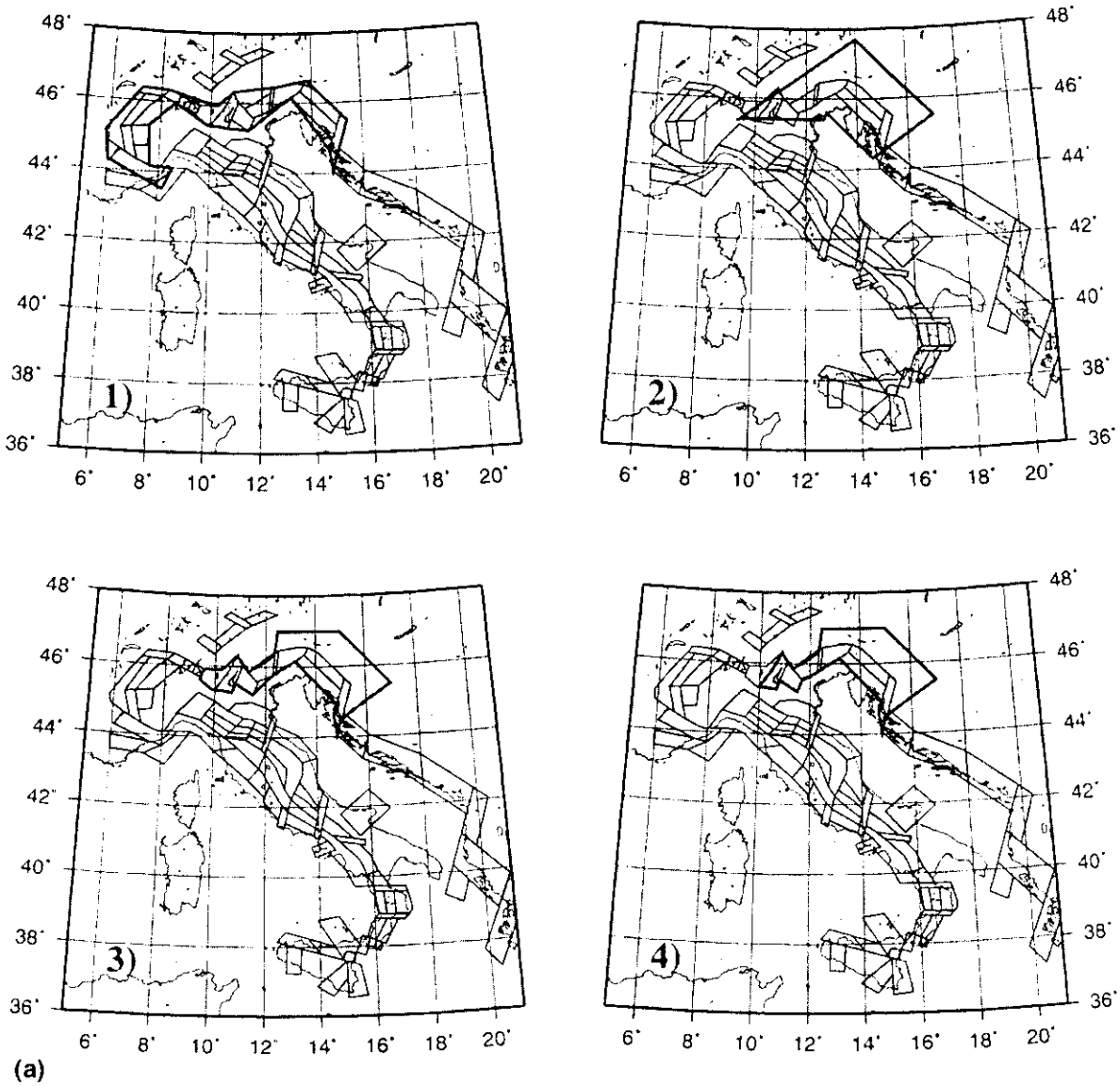

Figure 2a
Regionalisation for Northern Italy, considering simply connected seismogenic zones: (1) first variant based on the seismotectonic model, including the whole Alpine arc; (2) "small" region defined by COSTA *et al.* (1996); (3) second variant, including the zone at the west of Garda's Lake (GZ); (4) third variant, excluding the GZ zone.

Our final choice of the region to be used with CN algorithm is based on the prediction experiments described below. When performing prediction experiments, with the aim to optimise the regionalisation, we must preserve the predictive power reached with the previous regionalisations. Therefore, since the old regionalisations allow us to predict all the strong earthquakes, in the following we define as successful only the experiments with no failures to predict.

Experiment 1. We consider the region formed by the compressional band and the adjacent transpressive zones that cover the entire Alpine arc, from the Istrian peninsula to Liguria (Fig. 2a-1 and Table 1). This experiment is unsuccessful,

probably due to the different completeness of the catalogue (MOLCHAN *et al.*, 1995) and to the different level of seismic activity in different parts of the Alpine arc.

Experiment 2. Within the smaller region defined by COSTA *et al.* (1996) for Northern Italy (Fig. 2a-2) we keep only the compressional and transpressive adjacent zones in Italy, while in Austria, Slovenia and Croatia we keep the boundaries proposed by COSTA *et al.* (1996), except towards the North, where we follow the minimum of seismicity located in correspondence of the 47°N parallel. The seismogenic properties of the zone at the west side of Lake Garda (central part of Southern Alps) have been the subject of debate, as can be seen by recent

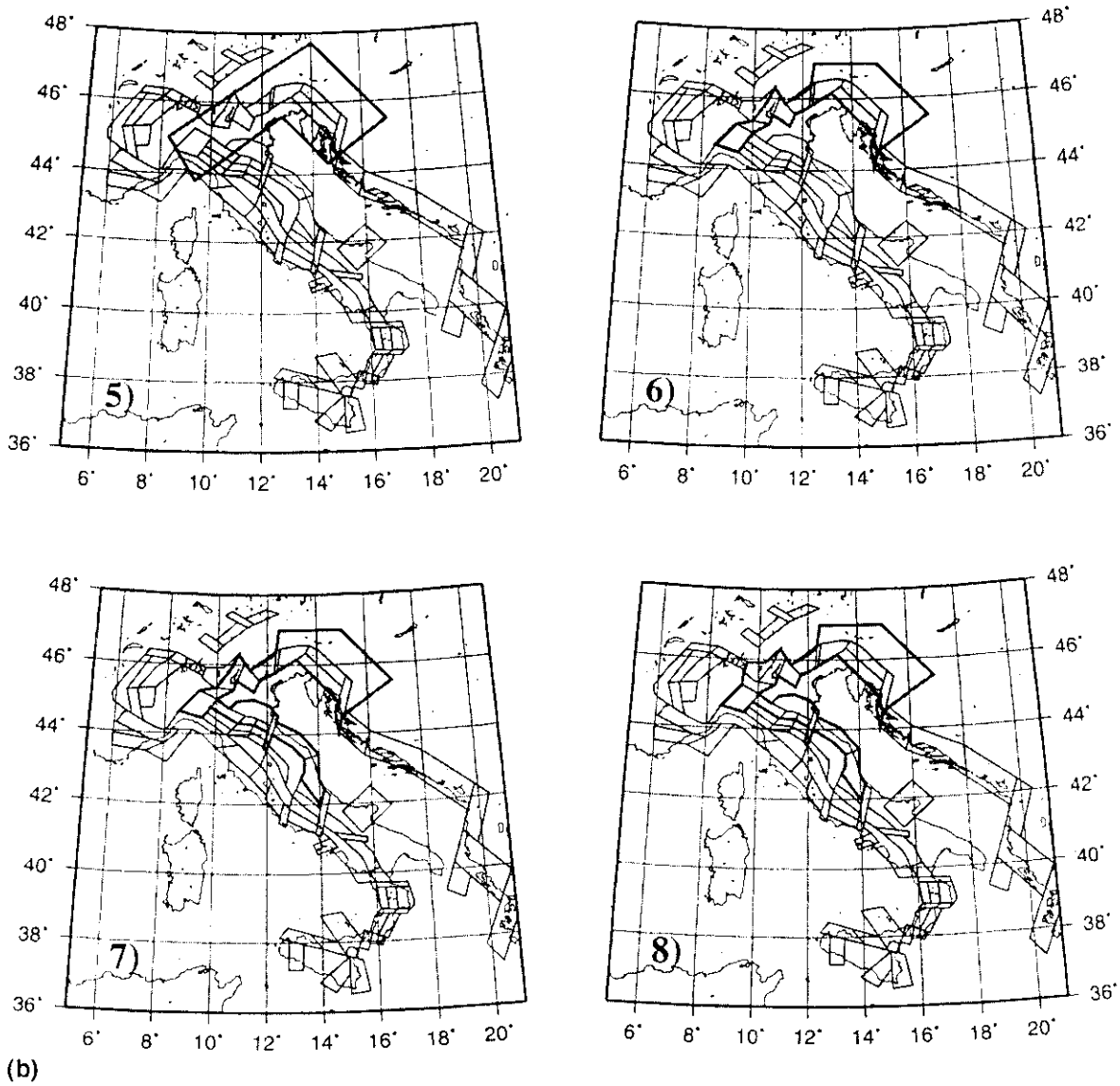

Figure 2b

Regionalisation for Northern Italy, considering also disconnected zones: (1) "extended" region defined by COSTA *et al.* (1996); (2) first variant based on the seismotectonic model, including the transitional zone at the northern edge of the Apennines; (3) second variant, including the whole compressional band, but without the GZ zone; (4) third variant, including also the GZ zone.

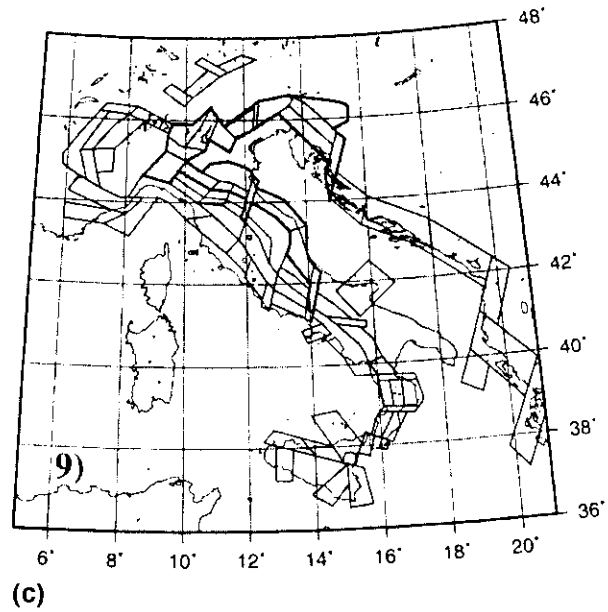

Figure 2c
Regionalisation for Northern Italy that takes into account the seismogenic zoning of the Slovenian Croatian territory (ZIVCIC and POLJAK, 1997); the transition zones are included at both edges.

revisions of the seismotectonic model (SCANDONE *et al.*, 1990, 1994). Therefore we define two regions, one including and the other excluding the zone west of Garda (GZ), as shown respectively in Figures 2a-3 and 2a-4. The results obtained for these two regions are given in Table 1 and can be considered satisfactory only for the region shown in Figure 2a-4. Then we deduce that the seismicity contained in this small zone plays a critical role, revealing a certain instability with respect to the choice of the areas represented in Figures 2a-2, 3 and 4 (see also Fig. 4).

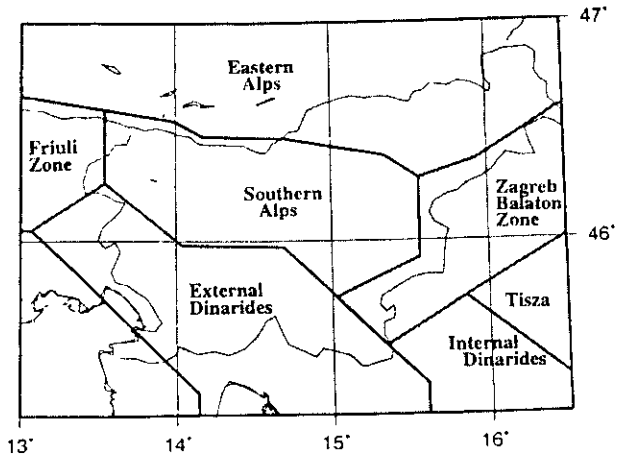

Figure 3
Preliminary seismogenic zoning of Slovenia and adjacent regions proposed by ZIVCIC and POLJAK (1997).

Table 1

Results obtained with the algorithm CN in Northern Italy, using the different regions represented in Figures 2a, 2b and 2c. For regions 2 and 5 the catalogue PFGING has been used by COSTA *et al. (1996). The last line indicates results updated on September 1, 1998, whose corresponding TIPs diagram is shown in Figure 10-a*

Northern Italy							
Region	Time	Learning period	M_0	Events predicted	Failure to predict	TIPs %	False alarms
1	1960–1995	1964–1995	5.4	0	2	32.5	6
2*	1960–1994	1964–1994	5.4	2	0	34	2
3	1960–1995	1964–1995	5.4	1	1	35.1	4
4	1960–1995	1964–1995	5.4	2	0	28.8	2
5*	1960–1994	1964–1994	5.4	2	0	27	1
6	1960–1995	1964–1995	5.4	2	0	24.7	2
7	1960–1995	1964–1995	5.4	2	0	24.7	3
8	1960–1995	1964–1995	5.4	2	0	20.5	2
9	1960–1995	1964–1995	5.4	2	0	19.9	2
9**	1960–1998	1964–1995	5.4	4	0	25.1	2

* Catalogue: PFGING.
** Updated Catalogue: CCI1996(1960–1994) + NEIC(1995–1998).

Experiment 3. For a deeper analysis of the instability detected with experiment 2, we remember the hypothesis that the seismicity at the northern edge of the Apennines may be related to the seismicity of the Alpine arc (COSTA *et al.*, 1996), which led to a definition of the region in Figure 2b-5. Therefore we extend the region of Figure 2a-4 to the transition seismogenic zone at the northern edge of the Apennines, even if it is not directly connected to the others (Fig. 2b-6). In such a way the percentage of total TIPs is reduced. Subsequently the area is further extended to the whole compressional band along the Adriatic coast (Fig. 2b-7). With this extension the destabilising effect of the zone at the west side of Lake Garda's zone is removed (Figs. 2a-3, 4 and Table 1).

Experiment 4. The northeastern border of the region shown in Figure 2b-8 is modified considering the seismotectonic zoning for the Slovenian–Croatian territory (ZIVCIC and POLJAK, 1997) and including only compressional and transpressive zones. Where there is an overlapping of the two zoning the priority is given to the model proposed by SCANDONE *et al.* (1994) (Figs. 2c and 3).

The results obtained for the area finally selected (Fig. 2c) can be summarised as follows: both events with $M \geq M_0$, which occurred in the period under analysis ($M = 6.5$, May 6, 1976 and $M = 5.4$, February 1, 1988) are predicted with 20% of the total time considered occupied by TIPs and 2 false alarms. The improvement with respect to the results obtained by COSTA *et al.* (1996) is a reduction in the percentage of TIPs (from 27% to 20%) and in the spatial uncertainty (around 38%).

These results are stable with respect to changes in the learning period and to the exclusion of the transition zone containing the Ortona–Roccamonfina line (Fig. 4).

The new regionalisation is compatible with the kinematic model of rotation and subduction of the Adriatic microplate and supports the hypothesis of a possible connection between the earthquakes that occur within the compressional band, marking the zone of subduction along the Southern Alps and Northern Apennines (WARD, 1994; ANDERSON and JACKSON, 1987).

The diagram of the time distribution of TIPs, obtained in the monitoring updated to September 1998, is presented in Figure 10-a. The catalogue for the monitoring in the Northern region is updated with the NEIC data since January

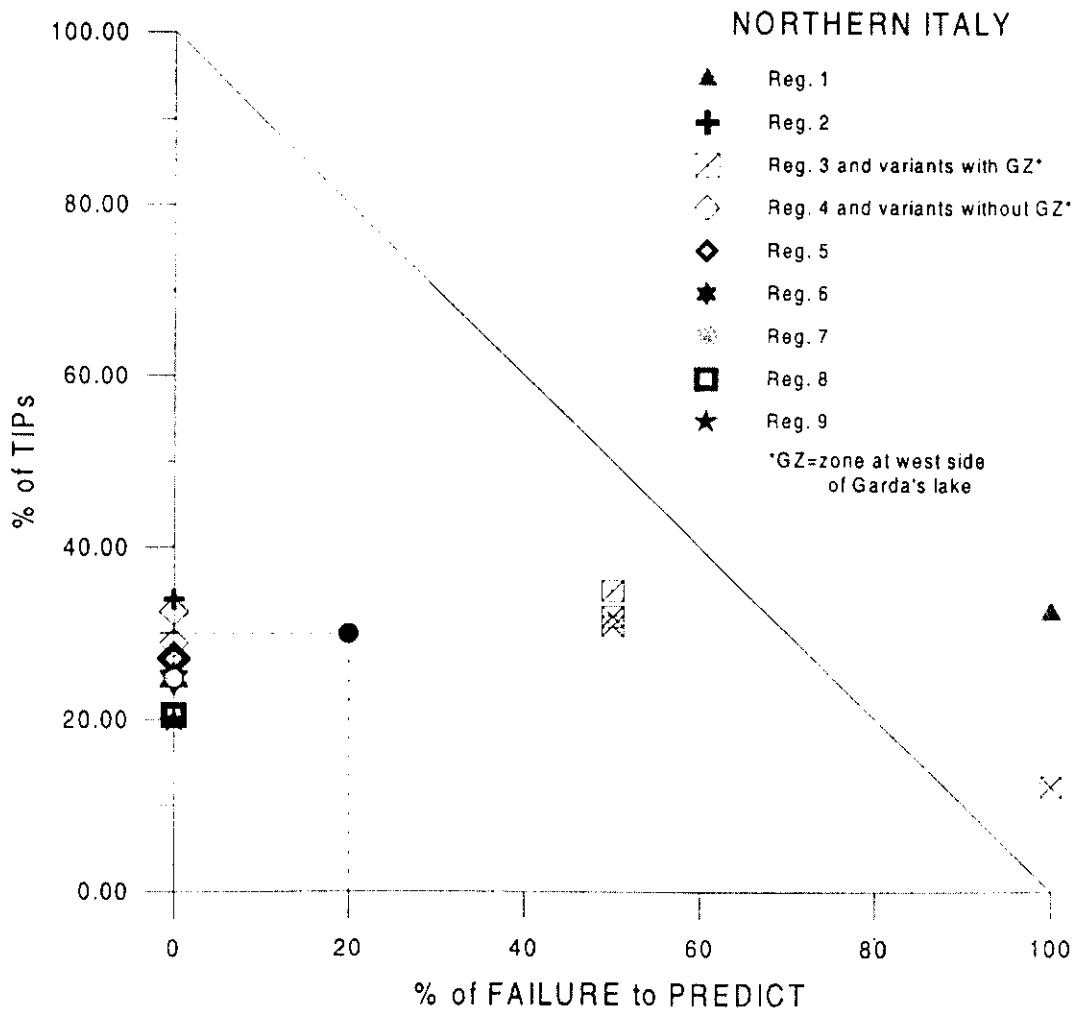

Figure 4

n-τ diagram of the percentage of total TIPs versus the percentage of failures to predict for the results obtained in Northern Italy for the different regions shown in Figures 2a, 2b and 2c. Other variants (not shown) including or not the GZ zone have been considered. All the regions with GZ (zone at west side of Lake Garda) correspond to unsuccessful experiments. The diagonal line indicates the results of a random guess (MOLCHAN, 1990). The large full dot represents the worldwide performance of CN.

1995. The operating magnitude from NEIC is chosen to be the maximum given in the Preliminary Determinations of Epicentres database (PERESAN and ROTWAIN, 1998). The results of the application of CN algorithm to this updated catalogue can be summarised as follows: all the four strong earthquakes with $M \geq M_0 = 5.4$ which took place within the region since 1964, are preceded by TIPs, with alarms (including two false alarms) covering about 25% of the total time. Only two strong events occurred during the learning period, while the two recent events ($M = 5.8$, October 15, 1996 and $M = 6.0$, April 12, 1998) are real predictions.

A common feature to the different successful regionalisation experiments performed is the persistence of a TIP in the time interval from 1972 to 1976. Starting in January 1973, remarkable tilt perturbations have been recorded by the horizontal pendulums of Grotta Gigante, near Trieste (ZADRO, 1978). These anomalies have been interpreted as a "slow earthquake" (DRAGONI *et al.*, 1985) and therefore it seems reasonable to formulate the hypothesis that the persisting TIP, from September 1972 to January 1976, is related to these creeping phenomena. A less clear-cut, but similar phenomenon, seems to characterise the false alarm following the $M \geq M_0 = 5.4$ event, correctly predicted in 1988. Long-term tilt variations, with periods of several years, have been detected for both the NS and EW components of the tiltmeters in the stations of Villanova and Cesclans, located in the Friuli region and working since 1977. Among them a strong anomalous deformation with a shorter period can be evidenced by the EW component of tilt in Cesclans (near Tolmezzo, Udine), from 1987 to 1991 (ROSSI and ZADRO, 1996). The occurrence of the $M = 5.4$ earthquake did not slow down the deformations nor the alarm. Therefore the symptoms of instability detected by the algorithm CN could reveal a stress accumulation, partially released seismically and not terminated with a strong earthquake, because of creep. This interpretation is an alternative to the explanation given within the framework of the dilatancy model, in which a volume increase is expected under the effect of tectonic stresses, due to fluid migration in a volume of cracked rocks; accordingly the anomalies can be seen as precursors, indicating accumulation rather than relaxation of stress.

Central Italy

The central part of the Italian peninsula along the Apennines is characterised by a band with tensional seismotectonic behaviour, with prevailing dip-slip focal mechanism. Two belts run parallel to it: the western belt comprises the extensional zones near the Tyrrhenian coast and the eastern consists of the compressional zones along the Adriatic Sea, from the Ortona–Roccamonfina line (Fig. 1) to the Po Plain. COSTA *et al.* (1996) evidenced that the central band may be considered individually and this fact seems to be supported by the model proposed by MELETTI *et al.* (1995) for the deep structure of the Northern Apennines. The model

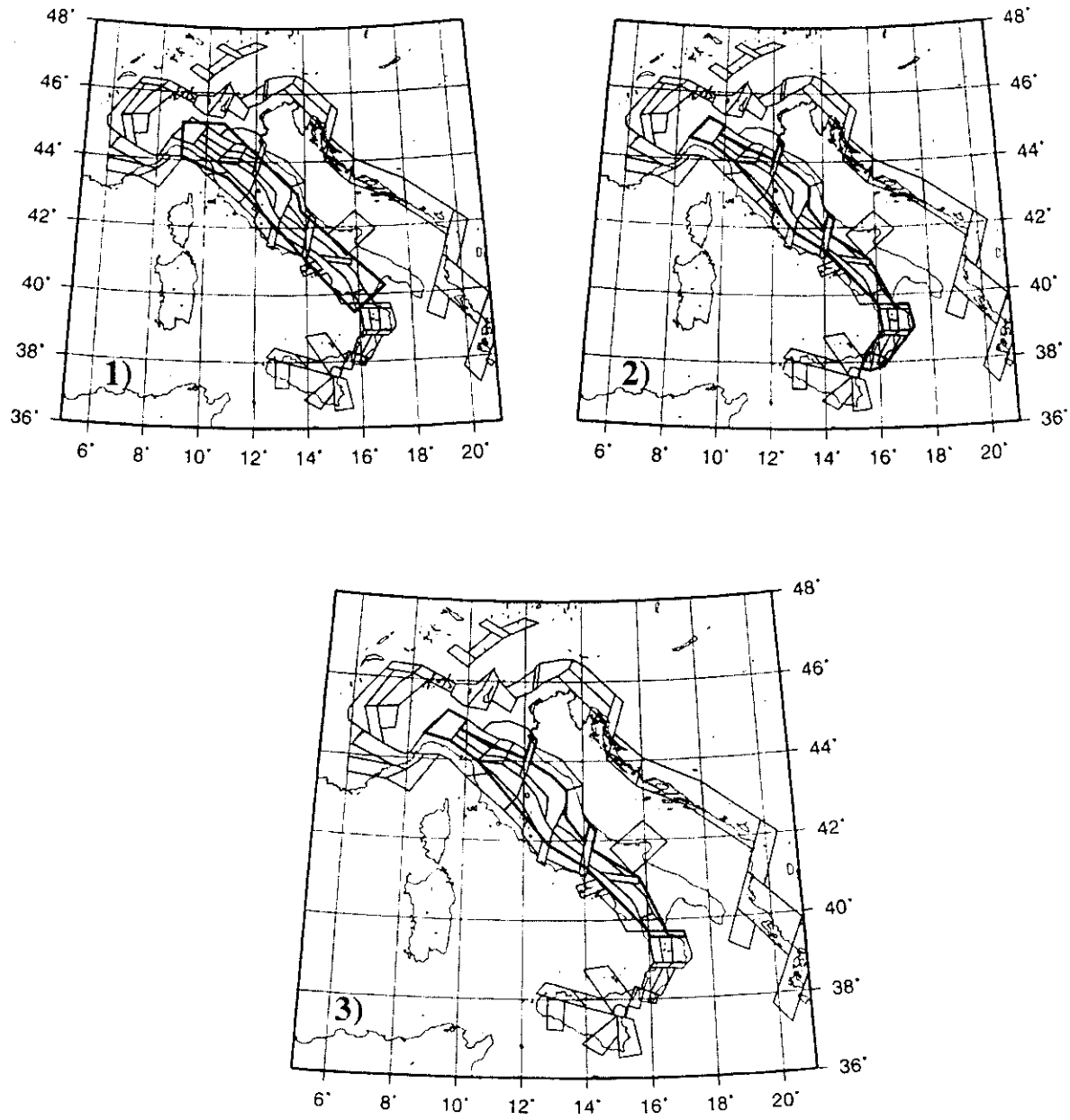

Figure 5
(1) Regionalisation for Central Italy defined by COSTA *et al.* (1996); (2) region including the whole extensional band; (3) region defined following the seismotectonic model, including the transition zones at the edges.

indicates a connection at depth between the Adriatic compressional front and the uplifting asthenosphere along the Tyrrhenian Sea, in agreement with the geometry of the lithosphere–asthenosphere system outlined by CALCAGNILE and PANZA (1981), DELLA VEDOVA *et al.* (1991) and MARSON *et al.* (1995) on the basis of the available relevant geophysical data (surface waves, body waves tomography, heat flow, gravity). According to the seismogenic zoning, the foreland Gargano region must be excluded from the region of Central Italy.

The region defined for Central Italy is presented in Figure 5-3. In this region the catalogue CCI1966, starting from 1950, can be considered complete for $M \geq 3.0$ (MOLCHAN *et al.*, 1995). The operating magnitude is chosen following the priority: M_L, M_d, M_I. Aftershocks are removed as in Northern Italy and, according to the general rules of the algorithm CN, only crustal earthquakes are considered, and the threshold for the selection of strong events is $M_0 = 5.6$. The events to be predicted inside this region (Fig. 5-3) are three: $M = 5.8$ and $M = 6.0$, both on August 21, 1962 and the Irpinia's earthquake, with $M = 6.5$, on November 23, 1980. All of them are predicted with TIPs covering 19% of the total time and with two false alarms (Table 2). The exclusion of the transition zones at both edges of the extensional band does not significantly affect the results, which are very stable over this area (COSTA *et al.*, 1995).

The entire extensional band, extending along the peninsula from the Po Plain to the Messina Strait, can be considered to form a single region (Fig. 5-2), although this leads only to an increase of the spatial uncertainty (Table 2 and Fig. 6). On the contrary, the attempt to divide this tensional band along the Ortona–Roccamonfina discontinuity demonstrates that a proper retrospective description of seismicity is impossible, because the strong Irpinia's earthquake and its precursors seem to significantly affect the activation in the entire peninsula.

Comparing the region defined in Figure 5-3 to that defined for Central Italy by COSTA *et al.* (1996) (Fig. 5-1), we observe that the new criteria allow us a reduction of the spatial uncertainty by about 30%.

The monitoring of seismicity in the Central region is currently performed using the CCI1966 catalogue updated with the NEIC data since January, 1986. The operating magnitude from NEIC is chosen according to the priority order: $M_{\text{NEIC}}(M2, M1, M_S)$, where M_S is the magnitude from surface waves, while $M1$ and $M2$ are two estimations contributed from different agencies, mainly local and

Table 2

Results obtained over the regions defined for Central Italy and shown in Figure 5. The first line indicates the results given by COSTA et al. (1996), using the PFGING catalogue. The diagram of TIPs for the updated catalogue and with the new region is shown in Figure 10-b

Central Italy							
Region	Time	Learning period	M_0	Events predicted	Failure to predict	TIPs %	False alarms
1*	1950–1994	1950–1986	5.6	3	0	23	2
2	1950–1995	1950–1986	5.6	3	0	22.3	3
3	1950–1995	1950–1986	5.6	3	0	18.7	2
3**	1950–1998	1950–1986	5.6	5	0	22.2	2

* Catalogue: PFGING.

** Updated Catalogue: CCI1996(1960–1985) + NEIC(1996–1998).

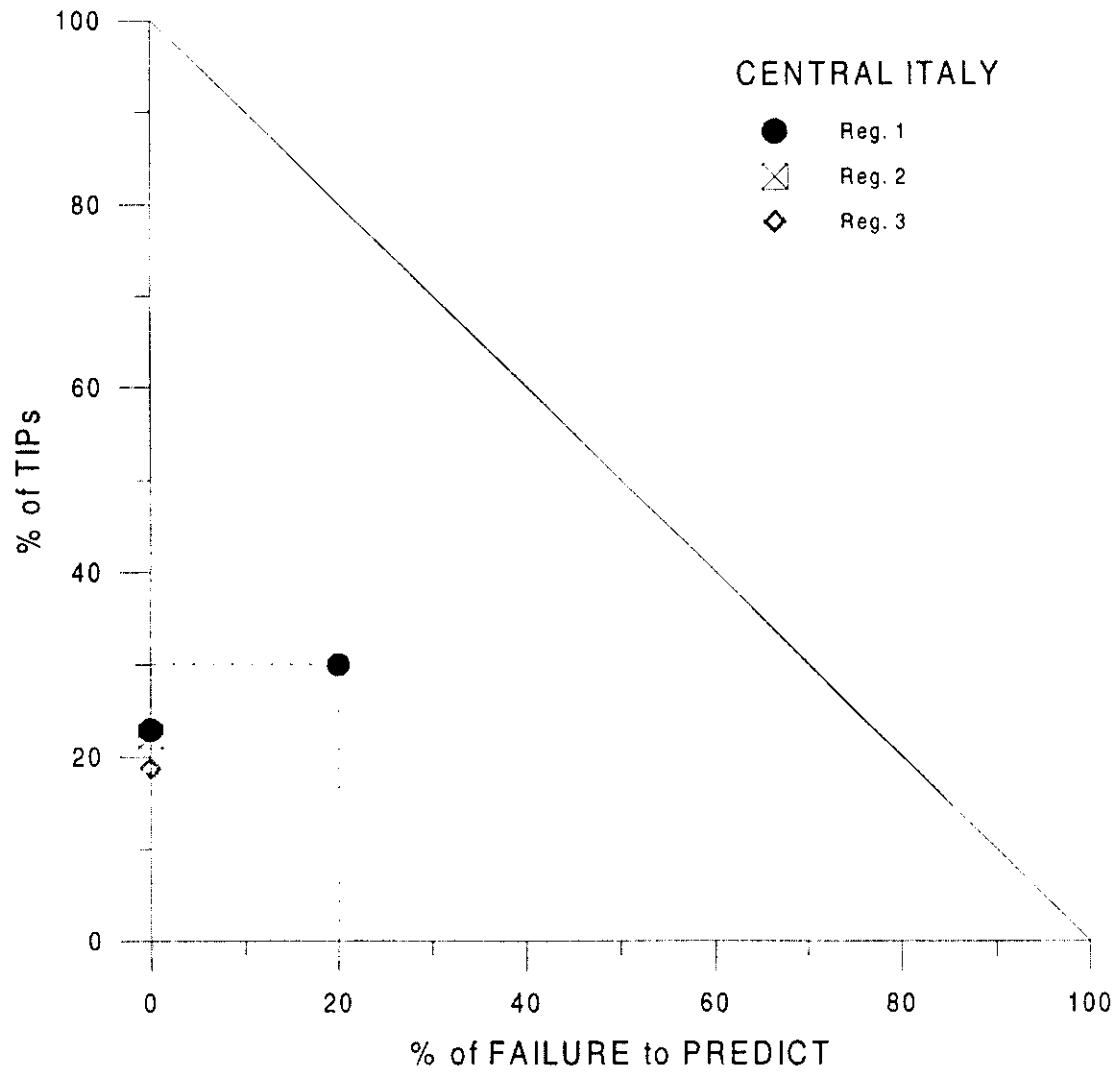

Figure 6
n-τ diagram for the results obtained in Central Italy considering the different regions shown in Figure 5. The large full dot represents the worldwide performance of CN.

duration magnitude (PERESAN and ROTWAIN, 1998). The results obtained with this catalogue are the following: all five strong earthquakes with $M \geq M_0 = 5.6$ which occurred within the region since 1954, are identified by TIPs covering about 22% of the total time, including two false alarms. The forward monitoring updated to September 1998 indicates a current alarm for this region continuing to September 1999. The distribution of TIPs is shown in Figure 10-b.

The results obtained using different regionalisations for Central Italy (KEILIS-BOROK *et al.*, 1990; COSTA *et al.*, 1996), all show the persistence of a false alarm which spans a period from July 1984 to March 1988. Similar to the case observed in Northern Italy, anomalous deformations, modelled as aseismic dislocation processes (DRAGONI, 1988), have been recorded in this region during 1985 (BELLA *et al.*, 1987).

Southern Italy

The extremity of the Italian peninsula, together with Sicily, is characterised by a seismotectonic connected with the sinking of the Adriatic–Ionic plate under the Southern Apennines and the Calabrian arc. The kinematic model proposed by SCANDONE *et al.* (1990, 1994) for Southern Italy seems to indicate a possible relation among the events occurring along the arc which reaches from the Ortona–Roccamonfina discontinuity to the western edge of Sicily. This hypothesis is supported by the unsuccessful CN-prediction experiment reported by COSTA *et al.* (1996) for the region that excludes the Irpinia's area (Fig. 7-2 and Table 3).

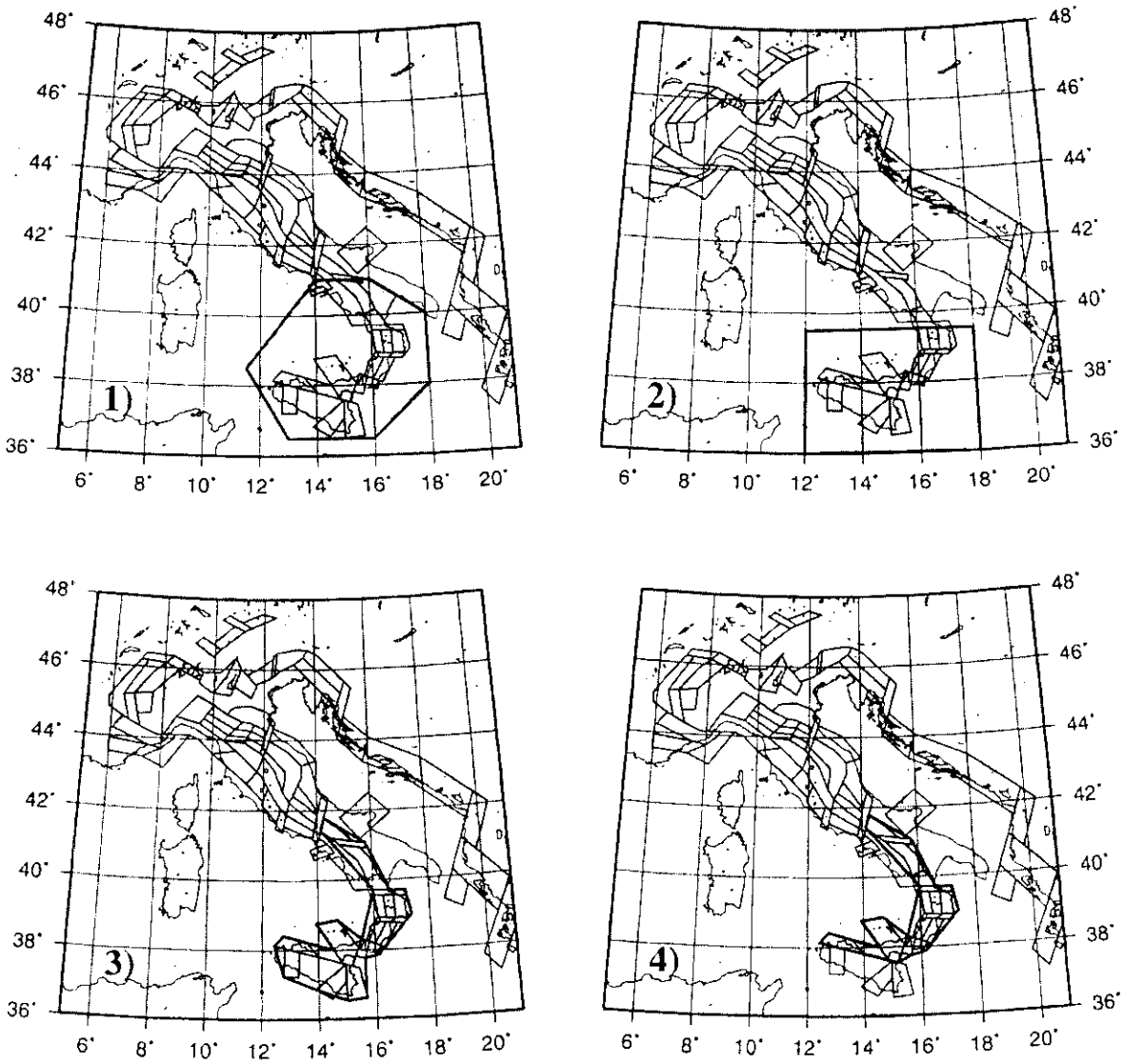

Figure 7
(1) Region defined for Southern Italy by COSTA *et al.* (1996); (2) region tested by COSTA *et al.* (1995); (3) region defined following the seismotectonic model and including the foreland zones of Sicily; (4) region defined for Southern Italy, excluding all the foreland zones.

Table 3

Results obtained for the four variants of the Southern Italy region shown in Figure 7. The results given by COSTA *et al. (1996) for regions 1 and 2 were obtained using the PFGING catalogue, including deep events and considering their maximum magnitude. Updated predictions (September 1, 1998) for the new region are represented with a TIPs diagram in Figure 10-c*

Southern Italy							
Region	Time	Learning period	M_0	Events predicted	Failure to predict	TIPs %	False alarms
1*	1950–1994	1954–1994	6.5	3	0	33	5
2*	1950–1994	1954–1994	6.5	1	1	25	2
3	1948–1995	1952–1995	6.5	0	1	42.6	7
4	1950–1995	1954–1986	5.6	4	0	34.6	5
4**	1950–1998	1954–1986	5.6	4	0	30.8	5

* Magnitude = MAX. Catalogue: CCI1996. Also deep events are included.
** Updated Catalogue: CCI1996(1960–1991) + NEIC(1992–1998).

The role played by foreland zones is particularly critical in Southern Italy, because their inclusion in the analysis leads to unsuccessful or very unstable experiments. When they are excluded, both in the Gargano region and in Sicily, the experiments are successful (Figs. 7-3, 4 and Table 3).

The transition zone corresponding to the Ortona–Roccamonfina line is not included in the South-Italy region, though it is adjacent to the region, since the distribution of the aftershocks of the strong events which occurred over this area (MOLCHAN *et al.*, 1995) does not indicate a connection between the transition zone and the southward part of the tensional band (Fig. 9).

Following the standard priority (M_L, M_d, M_I) for the operating magnitude in the region shown in Figure 7-4, we can fix the completeness threshold for the catalogue CCI1996, starting from 1950, at $M = 3.0$ and choose $M_0 = 5.6$. All four events ($M = 5.8$, May 20, 1957; $M = 5.8$ and $M = 6.0$ in August, 1962; $M = 6.5$ on November 23, 1980) with $M \geq M_0$ are predicted with TIPs occupying about 34% of the total time interval and 5 false alarms. With respect to the region defined by COSTA *et al.* (1996) and shown in Figure 7-1, the reduction of the spatial uncertainty can be estimated around 72%, although it is necessary to consider that the threshold M_0 has been lowered.

The updated catalogue for Southern Italy has been compiled using the CCI1996 for the period: 1954–1991, followed by the NEIC (1992–1998), with priority $M_{\mathrm{NEIC}}(M2, M1, M_s)$. Results of the monitoring, updated to September 1, 1998, indicate that all four strong events are correctly identified by the retrospective analysis, with TIPs covering about 31% of total time, including 5 false alarms. The time distribution of alarm periods and the time of occurrence of strong events are represented in Figure 10-c. Particular attention must be paid, however, to the forward monitoring in the Southern region, where the lower completeness level of NEIC data increases the probability of failures to predict (PERESAN and ROTWAIN, 1998).

Evaluation of the Results

To reduce the spatial uncertainty of predictions, the area indicated as the place where a strong event is expected to occur, must be as small as possible. Therefore, even if on a global scale strong earthquakes are not infrequent, within such small regions they are rare events, with long interevents time. Since the compilation of reliable catalogues started quite recently, on a regional scale the statistical properties of the sequence of strong earthquakes remain undefined and therefore alternative approaches must be used for predictions.

A crucial problem that generally arises with empirical methods, such as CN and *M*8 (KEILIS-BOROK, 1996), is the evaluation and comparison of results together with the estimation of the reliability of forward predictions.

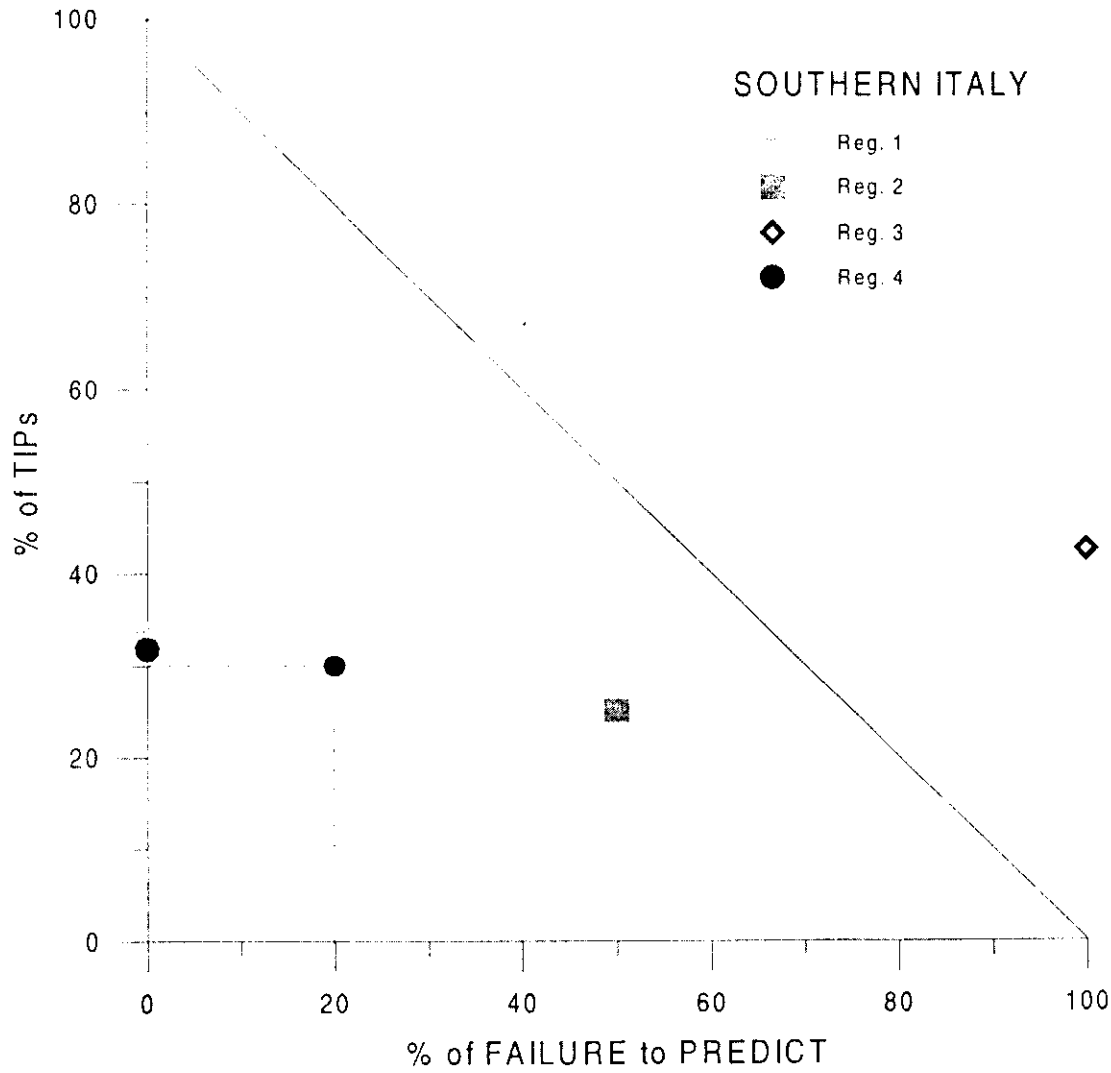

Figure 8

η-τ diagram of the results, obtained using algorithm CN, for the different regions tested for Southern Italy and shown in Figure 7. The large full dot represents the worldwide performance of CN.

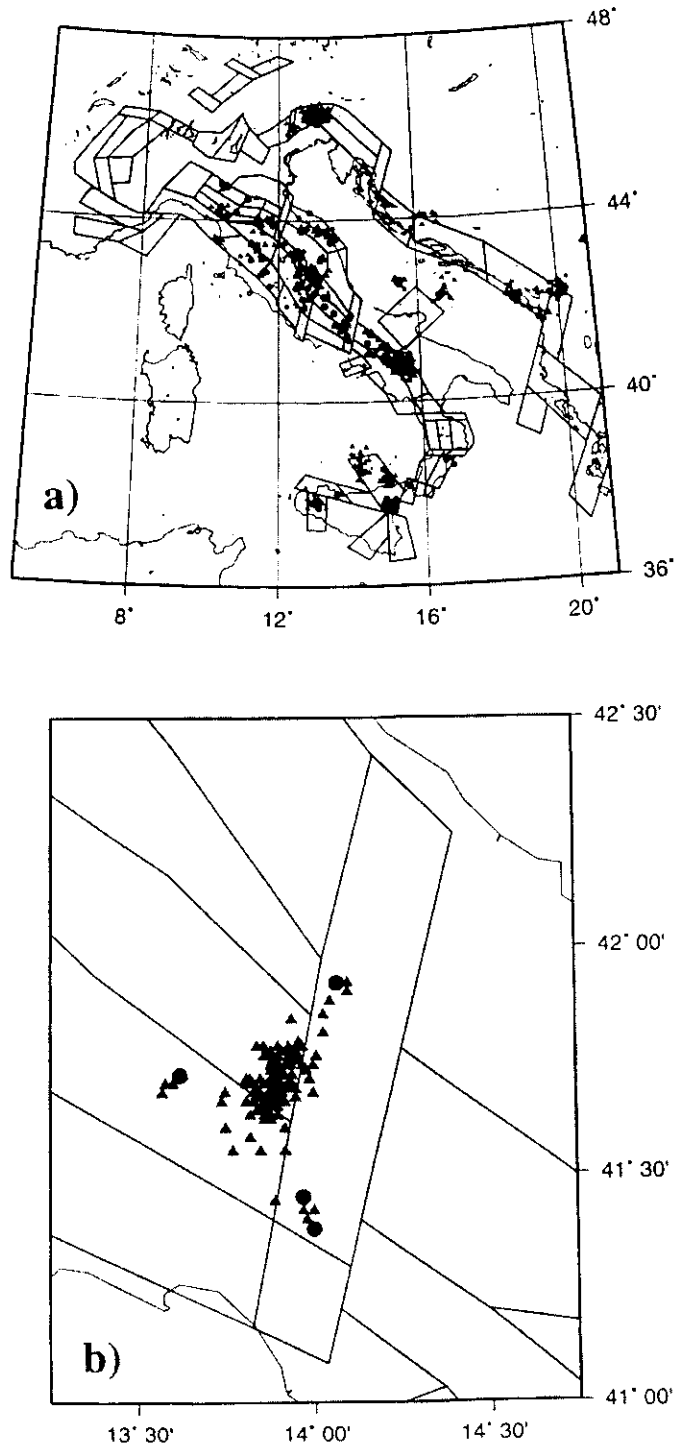

Figure 9

(a) Map of the main shocks (dots) and corresponding aftershocks (triangles) selected with the "minimax" method proposed by MOLCHAN *et al.* (1995). Only events with at least 10 aftershocks and which occurred in the time span 1900–1993 are considered. The small box indicates the area shown in detail in part (b) centred around the transitional zone corresponding to the Ortona–Roccamonfina line. Aftershocks indicate a possible connection only with the northward part of the extensional band.

In the previous paragraphs we have compared the results obtained with different choices of the regional boundaries. Particularly in Northern Italy we performed a series of experiments, defining as successful only those which provided an indication of the occurrence of all the strong events. This is not a general rule for evaluation however, but simply represents the choice to preserve the predictive power of the algorithm with respect to the regionalisation used by COSTA *et al.* (1996). Obviously declaring an alarm covering 100% of the time all the events are predicted, while if no alarm is indicated there are only failures to predict. Therefore

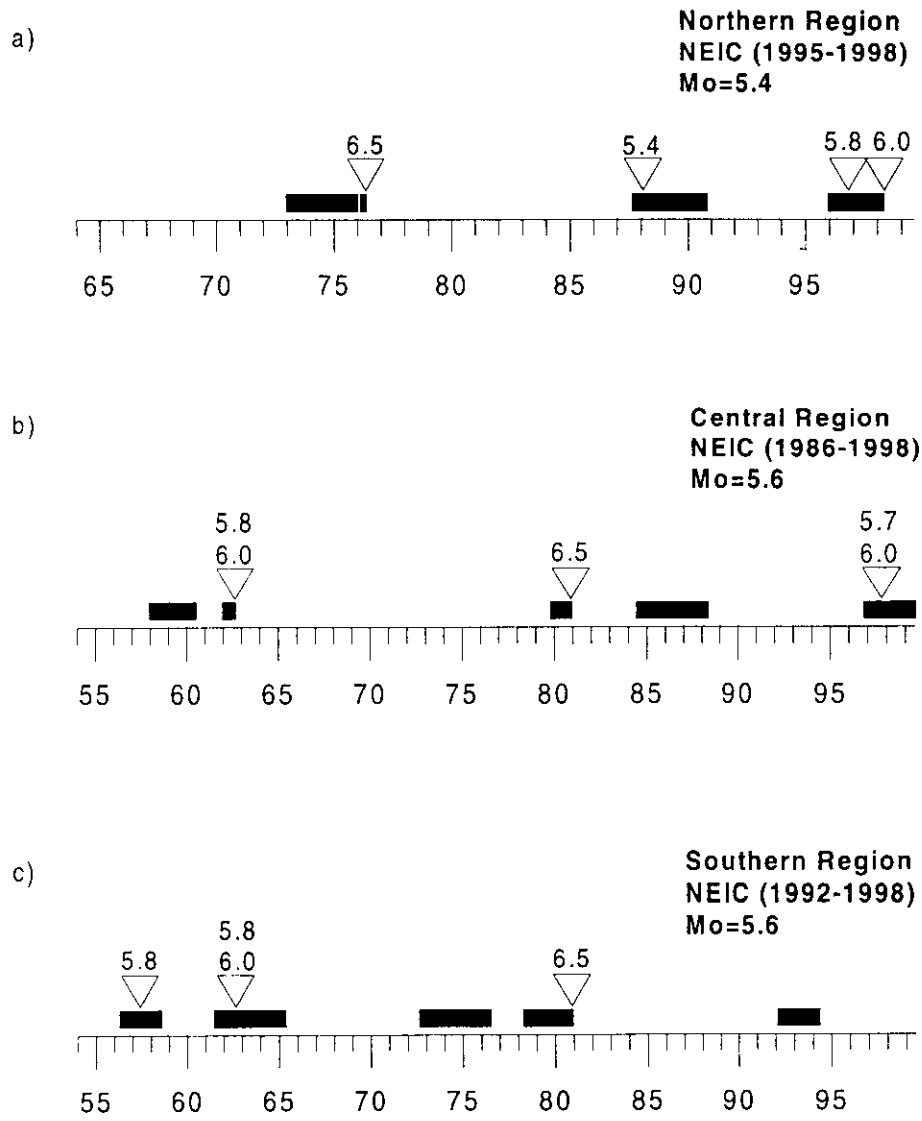

Figure 10

Diagrams of the TIPs obtained with the updated catalogue: CCI1996 + NEIC (up to September 1, 1998), over the regions defined for: (a) Northern (Fig. 2c-9), (b) Central (Fig. 5-3) and (c) Southern Italy (Fig. 6-4). NEIC data are used for the period of time indicated in brackets. The time of occurrence of a strong earthquake is indicated by a triangle with a number above giving its magnitude. These diagrams correspond to the results indicated in Tables 1, 2 and 3, respectively. On a global scale, about 50% of the TIPs continuing after strong events become false alarms.

an algorithm must trade between these extremes, trying to minimise both the time uncertainty and the number of failures to predict. The condition can be properly described through the so called n-τ error diagrams (MOLCHAN, 1996), representing the percentage of failures to predict versus the percentage of total alarm duration (Figs. 4, 6 and 8). The diagonal line between the extreme points (0, 1) and (1, 0) represents the results of a random guess, therefore we expect that the results associated with a useful prediction method will lie below this line. Once chosen the set of information to be used for prediction, for instance earthquake catalogues, the set of errors corresponding to the different possible strategies will lay in the portion of plane between the diagonal line and a convex downward monotonic curve. This curve represents the set of optimal prediction strategies and is characteristic of the set of information itself. Once a loss function is defined, taking into account both the costs of possible false alarms and of failures to predict, the n-τ diagram allows us to evaluate the quality of results. The best result, and therefore the best prediction strategy, corresponds to the first point (for increasing n and τ errors) that lies on the convex upward, monotonic curve corresponding to a contour of the loss function (MOLCHAN, 1996).

Figures 4, 6 and 8 represent the empirical results obtained for Northern, Central and Southern Italy, respectively. The diagram corresponding to the Northern regions shows the evident instability of the results when slight variations of region 3 (including Garda's zone) are considered, while for the other regionalisation the results lie on the τ axis. For all three regions the results obtained with the new regionalisation appear to be the best, as their τ has been reduced, and there is still no failure to predict. Nevertheless the small number of events to be predicted limits the statistical significance of the description with the n-τ diagram, whose proper use would require a multitude of predictions.

We now describe the problem of the evaluation CN results and of the reliability of forward predictions from a slightly different point of view, simply showing on the basis of the concept of "base-rate effect," the consequences which the chances of occurrence of an event have on the ability to predict it. This effect is characteristic of rare phenomena and, in the case of earthquakes, it determines innumerable false alarms, in spite of the great accuracy that a prediction method may reach (MATTEWS, 1996).

From the global retrospective tests performed, it results that the algorithm CN is able to indicate the occurrence of some 80% of the strong events, with TIPs occupying, on average, about 30% of the total time (KEILIS-BOROK, 1996). When dangerous conditions are recognised by CN an earthquake is expected to occur within one year and a TIP is declared. In practice alarms may be longer or shorter than one year, due to the merging of consecutive TIPs or to the occurrence of a strong earthquake. Nevertheless, for an average description, it appears appropriate to use for TIPs the value of 1 year, neglecting their possible correlation in time. Once a region is fixed, according to the general rules for the application of the

Table 4

Contingency table for the algorithm CN, for a time period of 100 years. The yearly base-rate of earthquakes is the probability of occurrence of a strong event during one year, and it is obtained considering the average return period of six years (condition for the applicability of the algorithm). The accuracy in the prediction of earthquakes and the percentage of total alarm are drawn from global results in retrospective and forward analysis, while the other quantities have been calculated in the hypothesis of the yearly duration of TIPs. The accuracy here refers to prediction within a single class of objects (dangerous or non-dangerous) and gives a measure of their predictability with algorithm CN. The conditional probability of predictions is given by the ratios: "true alarms/total alarms" and "true no alarm/total no alarm"

	Prediction of earthquake	Prediction of no earthquake	Total	Accuracy of predictions
Years with earthquake	12	3	15	80%
Years with no earthquake	18	67	85	79%
Total	30	70	100	
Conditional probability of predictions	40%	96%		

Yearly base-rate of earthquakes: 15% (one earthquake every 6 years, on average, within the considered region).

Average performance (forward and retrospective) in intermediate-term prediction of earthquakes: 80%.

Average percentage of total TIPs: 30%.

algorithm CN, the events with magnitude $M \geq M_0$ must have an average recurrence time of about six years and the probability of occurrence of a strong earthquake during one year (base-rate) is around 15%. Therefore, considering a period of 100 years, 15 years are expected to contain an event with $M \geq M_0$, while during the remaining 85 no strong earthquake will occur (Table 4). According to global results, 12 out of the 15 earthquakes will be correctly forecasted, with 3 failures to predict and alarms will occupy about 30 years. Because there are only 12 strong events, we can expect that at least 18 TIPs will correspond to false alarms. Consequently, if we try to evaluate the accuracy in recognition of non-dangerous years, we ascertain that it is about 79% (18 out of 85 years are identified as dangerous by mistake) and then 80% seems a reasonable measure of CN performance. From Table 4 it is possible to see that only 12 of the 30 predictions of an incoming earthquake are correct, therefore the conditional probability for a TIP can be estimated at roundly 40%. This percentage increases to about 96% when the conditional probability for predictions of no earthquake is considered (67 successes out of 70 forecasts). These estimations, in any case, must be viewed as approximate and averaged values, because they are based on global results, both forward and retrospective, and on the assumption of a yearly duration of alarms. The values given in Table 4 have been calculated neglecting the properties of the time distribution of TIPs and earthquakes, such as possible correlation or periodicity, which can be very different from region to region. A proper evaluation of the reliability of the monitoring for a single region must take into account these specific

properties and a similar table must be compiled which considers the real time distribution of the true and false alarms. Regretfully, the small number of events to be predicted in all three regions defined for Italy, and particularly for the Northern region, compromises the statistical significance of this type of evaluation, just as it occurs with the n-τ diagrams. Therefore the real predictive power of CN algorithm and the reliability of its predictions within a fixed region could be evaluated only on the basis of future results. Approximately, however, it is possible to deduce from Table 4 that when a TIP is declared, it has a 60% probability of being a false alarm. Conversely, if no TIP is indicated, at 96% no strong earthquake will occur.

Conclusions

The new regionalisation of the Italian territory, based on the seismotectonic zoning, allows us to both improve the predictions and to validate the seismotectonic model.

Three regions have been selected for Northern, Central and Southern Italy respectively, strictly following the boundaries of the seismogenic zones; each region contains only adjacent zones with the same characteristics or with transitional properties.

The Northern Italy region appears compatible with the kinematic model of rotation and subduction of the Adriatic microplate, and the results of the analysis with the CN algorithm support the hypothesis of the connection between earthquakes that occur within the compressional band along the subduction zone in the Southern Alps and Northern Apennines. Similarly, the Southern Italy region is defined by the seismotectonic structures associated with the sinking of the Adriatic–Ionian plate under the Calabrian Arc. The choice of the Central region, instead, is related to the deep structure of the Northern Apennines, characterised by the subduction of the Adria plate and by the uplifting of the asthenosphere along the Tyrrhenian rim.

The results obtained for the three regions exhibit a general reduction of time and space uncertainty of the predictions of strong events, with respect to the regionalisations that do not closely follow the seismotectonic zones (COSTA *et al.*, 1996). The border of the regions defined according to the tested criterion might appear too complex and the regions too tiny. However the hypothesis, derived by this regionalisation, that precursors can be found inside seismogenically homogeneous areas associated with a dominating geodynamic process, seems supported by the corresponding improvement of results.

The results of the forward monitoring (Fig. 11), show that the strong earthquakes which occurred in the Northern and Central regions can be correctly predicted using this regionalisation. Nevertheless only a statistically significant number of forward predictions can firmly validate the regionalisation and the method itself.

Earthquake catalogues, as complete and homogeneous as possible, are essential for intermediate-term predictions. For this reason we have used a revised version of

the PFGING catalogue, named CCI1996 (PERESAN *et al.*, 1997), obtained considering the most recently available revisions of source parameters of individual events (BOSCHI *et al.*, 1995; ICS, 1976–1990). Nevertheless, it appears particularly difficult to compile a suitable updated catalogue, especially when the studied area is crossed by political boundaries, and this calls for a strengthening of data collection at the European level. For the time being we have bypassed this shortcoming using the NEIC global catalogue, which guarantees the space homogeneity and the timely upgrading of the catalogue necessary for CN application in the three Italian regions.

The discretisation of the functions which describe the seismic flow, however, makes the algorithm CN quite robust with respect to the small, sporadic errors that

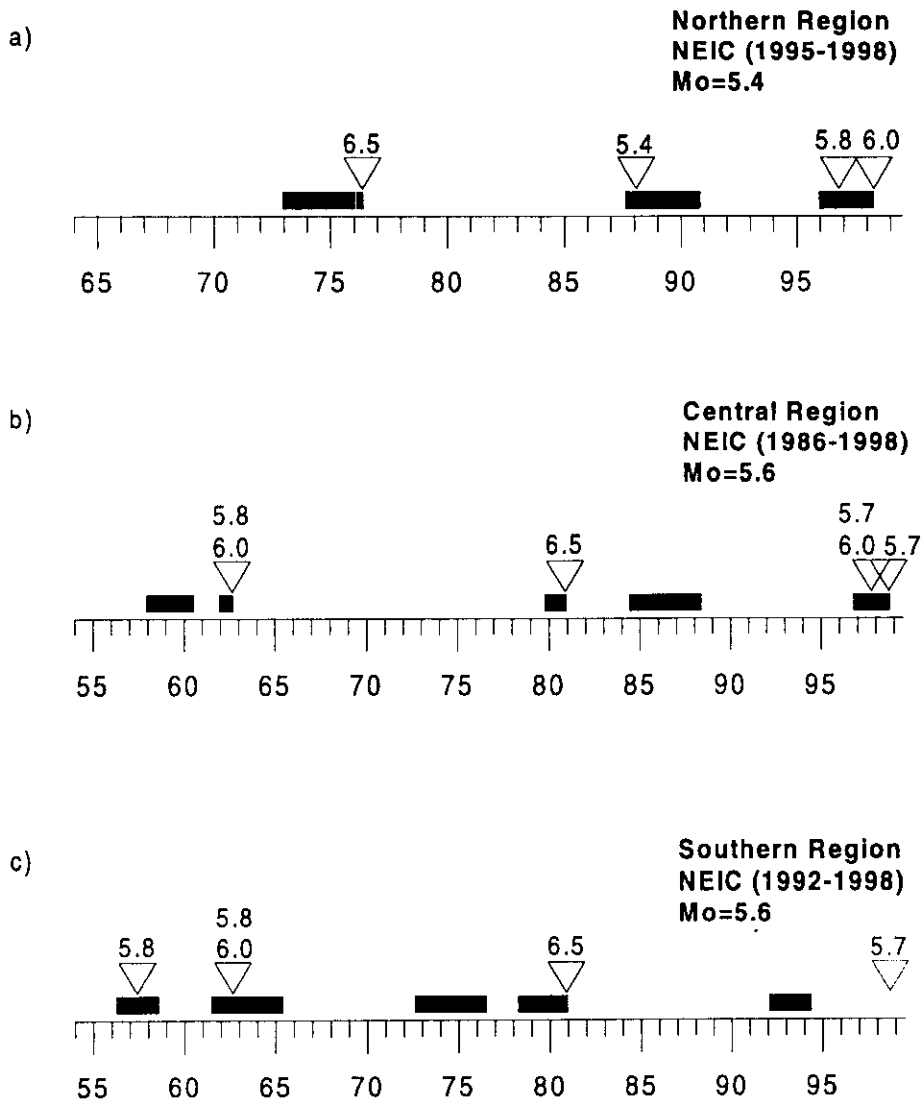

Figure 11

(Information added during the revision of the proofs in January 1999). Prediction results updated to January 1, 1999. On September 9, 1998 an earthquake with $M = 5.7$ occurred within the area common to the Central (Fig. 5-3) and Southern (Fig. 7-4) regions. The TIPs diagram shows that the event is predicted. The event terminates an alarm that continued after the Umbria-Marche events, occurred on September, 26 1998 (see Fig. 10). The failure to predict when considering the Southern region is not a surprise, due to the lower completeness level of the data (see text for more details).

inevitably affect earthquake catalogues. For instance, the inadvertent increase in magnitude indicated by ZUNIGA and WYSS (1995) for the Italian catalogue, from 1980 to 1981, does not seem to affect the results of predictions (during this period there are alarms of different length in Central and Southern Italy and no alarm in Northern Italy).

From this work emerges the necessity to integrate and compare the data contained in earthquake catalogues with the available information pertinent to deformations and silent earthquakes, in order to analyse whether aseismic processes can affect the precursory patterns. Indeed, even if a direct connection between TIPs and creeping phenomena must still be verified, some similarities can be detected, analysing the functions of seismic flow (GABRIELOV *et al.*, 1986) for Northern and Central Italy during the false alarms associated with angular deformations. In both cases there is a relatively high space-time clustering of events (triggering the TIPs), while the release of seismic energy throughout minor events is small, if compared to that of a strong earthquake, and therefore insufficient to stop the alarm.

Acknowledgements

We are grateful to Prof. I. M. Rotwain for her active and critical contribution in this work, to Prof. P. Scandone and to Prof. L. Pietronero for their useful discussions and to Prof. G. M. Molchan and N. Cabibbo for their precious suggestions. We also wish to thank Prof. M. Zadro and Dr. G. Rossi for their helpful comments and critical revision. This research has been developed in the framework of the project 414 UNESCO-IGCP and has been supported by funds MURST (40% and 60%) and by funds CNR (contracts Nos. 95.00608.PF54 and 96.02968.PF54).

REFERENCES

ALPOR (1987), *Catalogue of the Eastern Alps*. Osservatorio Geofisico Sperimentale, Trieste, Italy (computer file).

ANDERSON, H., and JACKSON, J. (1987), *Active Tectonics in the Adriatic Region*, Geophys. J. R. Astron. Soc. *91*, 937–983.

BELLA, F., BELLA, R., BIAGI, P. F., DELLA MONICA, G., ERMINI, A., and SGRIGNA, V. (1987), *Tilt Measurements and Seismicity in Central Italy over a Period of Approximately Three Years*, Tectonophysics *139*, 333–338.

BOSCHI, E., FERRARI, G., GASPERINI, P., GUIDOBONI, E., SMRIGLIO, G., and VALENSISE, G. (1995), *Catalogo dei forti terremoti in Italia dal 461 a.C. al 1980*, Istituto Nazionale di Geofisica e Storia Geofisica Ambiente.

CALCAGNILE, G., and PANZA, G. F. (1981), *The Main Characteristics of the Lithosphere–Asthenosphere System in Italy and Surrounding Regions*, Pure appl. geophys. *119*, 865–879.

COSTA, G., PANZA, G. F., and ROTWAIN, I. M. (1995), *Stability of Premonitory Seismicity Pattern and Intermediate-term Earthquake Prediction in Central Italy*, Pure appl. geophys. *145*(2), 259–275.

COSTA, G., STANISHKOVA, I. O., PANZA, G. F., and ROTWAIN, I. M. (1996), *Seismotectonic Models and CN Algorithm: The Case of Italy*, Pure appl. geophys. *147*, 1–12.

COSTA, G., PERESAN, A., OROZOVA, I., PANZA, G. F., and ROTWAIN, I. M. (1997), *CN Algorithm in Italy: Intermediate-term Earthquake Prediction and Seismotectonic Model Validation*, Proceedings of the 30th International Geological Congress, Vol. 5, Beijing, 1996, China.

DELLA VEDOVA, B., MARSON, I., PANZA, G. F., and SUHADOLC, P. (1991), *Upper Mantle Properties of the Tuscan-Tyrrhenian Area: A Key for Understanding the Recent Tectonic Evolution of the Italian Region*, Tectonophys. *195*, 311–318.

DRAGONI, M., BONAFEDE, M., and BOSCHI, E. (1985), *On the Interpretation of Slow Ground Deformation Precursory to the 1976 Friuli Earthquake*, Pure appl. geophys. *122*, 784–792.

DRAGONI, M. (1988), *Aseismic Propagation of Dislocations: A Model for Tilt Anomalies*, Proceedings National Meeting, National Research Council of Italy, ESA ed., Rome, 923–939.

GABRIELOV, A. M., DMITRIEVA, O. E., KEILIS-BOROK, V. I., KOSSOBOKOV, V. G., KUTZNETSOV, I. V., LEVSHINA, T. A., MIRZOEV, K. M., MOLCHAN, G. M., NEGMATULLAEV, S. KH., PISARENKO, V. F., PROZOROV, A. G., RINHEART, W., ROTWAIN, I. M., SHELBALIN, P. N., SHNIRMAN, M. G., and SCHREIDER, S. YU (1986), *Algorithms of Long-term Earthquakes' Prediction*, International School for Research Oriented to Earthquake Prediction-algorithms, Software and Data Handling (Lima, Peru 1986).

KAGAN, Y. Y., and KNOPOFF, L. (1980), *Spatial Distribution of Earthquakes: The Two-point Correlation Function*, Geophys. J. R. Astron. Soc. *62*, 303–320.

KEILIS-BOROK, V. I. (1996), *Intermediate-term Earthquake Prediction*, Proc. Natl. Acad. Sci. USA *93*, 3748–3755.

KEILIS-BOROK, V. I., KNOPOFF, L., and ROTWAIN, I. M. (1980), *Bursts of Aftershocks, Long-term Precursors of Strong Earthquakes*, Nature *283*, 259–263.

KEILIS-BOROK, V. I., KUTZNETSOV, V. I., PANZA, G. F., ROTWAIN, I. M., and COSTA, G. (1990), *On Intermediate-term Earthquake Prediction in Central Italy*, Pure appl. geophys. *134*, 79–92.

KEILIS-BOROK, V. I., and ROTWAIN, I. M. (1990), *Diagnosis of Time of Increased Probability of Strong Earthquakes in Different Regions of the World: Algorithm CN*, Phys. Earth Planet. Inter. *61*, 57–72.

ISC (1976–1990), Bulletins of the International Seismological Centre, *13*(1) - *27*(3).

LAPAJNE, J. K., SKET MOTNIKAR, B., and ZUPANCIC, P. (1995), *Delineation of Seismic Hazard Areas in Slovenia. Seismic Zonation.* Proceedings of the 5th International Conference on Seismic Zonation, 1995, Nice, France, *1*, 429–436.

MARSON, I., PANZA, G. F., and SUHADOLC, P. (1995), *Crust and Upper Mantle Models along the Active Tyrrhenian Rim*, Terra Nova *7*, 348–357.

MATTEWS, R. (1997), *How Right Can You Be?* New Scientist *3*, 28–31.

MELETTI, C., PATACCA, E., and SCANDONE, P., *Il sistema compressione-distensione in Appennino.* In *Cinquanta anni di attività didattica e scientifica del Prof. Felice Ippolito* (eds. Bonardi, G., De Vivo, B., Gasperini, P., Vallario, A.) (Liguori–Napoli 1995) pp. 361–370.

MELETTI, C., PATACCA, E., and SCANDONE, P. (1998), *Construction of a Seismotectonic Model: The Case of Italy*, Pure appl. geophys., submitted.

MOLCHAN, G. M. (1990), *Strategies in Strong Earthquake Prediction*, Phys. Earth Planet. Inter. *61*, 84–98.

MOLCHAN, G. M. (1996), *Earthquake Prediction as a Decision-making Problem*, Pure appl. geophys. *147*(1), 1–15.

MOLCHAN, G. M., DMITRIEVA, O. E., ROTWAIN, I. M., and DEWEY, J. (1990), *Statistical Analysis of the Results of Earthquake Prediction, Based on Bursts of Aftershock*, Phys. Earth Planet. Inter. *61*, 128–139.

MOLCHAN, G. M., and DMITRIEVA, O. E. (1992), *Aftershocks Identification: Methods and New Approaches*, Geophys. J. Int. *190*, 501–516.

MOLCHAN, G. M., KRONROD, T. L., and DMITRIEVA, O. E. (1995), *Statistical Parameters of Main Shocks and Aftershocks in the Italian Region*, ICTP, Internal report.

MOLCHAN, G. M., KRONROD, T. L., and PANZA, G. F. (1996), *Hazard Oriented Multiscale Seismicity Model: Italy*, International Centre for Theoretical Physics. Internal report IC/96/23, Trieste, Italy.

MOLCHAN, G. M., KRONROD, T. L., and PANZA, G. F. (1997), *Multiscale Seismicity Model for Seismic Risk*, Bull. Seismol. Soc. Am. *87*(5), 1220–1229.

MUELLER, S., *Deep structure and recent dynamics in the Alps.* In *Mountain Building Process* (ed. K. J. Hsu) (Academic Press 1982), pp. 181–199.

NEIC, *National Earthquake Information Center: Italy*, U.S.G.S., Denver, USA.

PANZA, G. F., CALCAGNILE, G., SCANDONE, P., and MUELLER, S. (1980), *Struttura profonda dell'area mediterranea*, Le Scienze *24*, 60–69.

PANZA, G. F., PERESAN, A., and COSTA, G. (1997), *Zone sismogenetiche e previsione a medio termine dei terremoti in Italia*, Il Quaternario *10*(2), 281–284.

PAVONI, N., AHJOS, T., FREEMAN, R., GREGERSEN, S., LANGER, H., LEYDECKER, G., ROTH, PH., SUHADOLC, P., and USKI, M. (1992), *Seismicity and focal mechanism.* In *A Continent Revealed—The European Geotraverse: Atlas of Compiled Data* (eds. R. Freeman and S. Mueller) (Cambridge University Press 1992) pp. 14–19.

PERESAN, A., COSTA, G., and VACCARI, F. (1997), *CCI1996: The Current Catalogue of Italy*, International Centre for Theoretical Physics, Internal report IC/IR/97/9. Trieste, Italy.

PERESAN, A., and ROTWAIN, I. M. (1998), *Analysis and Definition of Magnitude Selection Criteria for NEIC (PDE) Data, Oriented to the Compilation of a Homogeneous Updated Catalogue for CN Monitoring in Italy*, International Centre for Theoretical Physics. Internal report, Trieste, Italy.

POSTPISCHL, D. (1980), *Catalogo dei terremoti italiani dall'anno 1000 al 1980*, C.N.R.-Progetto Finalizzato Geodinamica.

RUNDKVIST, D. V., and ROTWAIN, I. M. (1996), *Present-day Geodynamics and Seismicity of Asia Minor*, Computational Seism. and Geodyn. *3*, 130–149.

ROSSI, G., and ZADRO, M. (1996), *Long-term Crustal Deformations in NE Italy Revealed by Tilt-strain Gauges*, Phys. Earth Planet. Inter. *97*, 55–70.

SCANDONE, P., PATACCA, E., MELETTI, E., BELLATALLA, M., PERILLI, N., and SANTINI, U. (1990), *Struttura geologica, evoluzione cinematica e schema sismotettonico della penisola italiana*, Atti del Convegno GNDT 1990 *1*, 119–135.

SCANDONE, P., PATACCA, E., MELETTI, C., BELLATALLA, M., PERILLI, N., and SANTINI, U. (1994), *Seismotectonic Zoning of the Italian Peninsula: Revised Version*, Working file NOV94.

SCHWARTZ, D. P., and COPPERSMITH, K. J. (1984), *Fault Behaviour and Characteristic Earthquakes: Examples from the Wasatch and San Andreas Fault Zones*, J. Geophys. Res. *89*, 5681–5698.

TURCOTTE, D. L., *Fractals and Chaos in Geology and Geophysics* (Cambridge University Press 1992).

WARD, S. N. (1994), *Constraints on the Seismotectonics of the Central Mediterranean from Very Long Baseline Interferometry*, Geophys. J. Int. *117*, 441–452.

ZADRO, M. (1978), *Use of Tiltmeters for the Detection of Forerunning in Seismic Areas*, Boll. Geod., Sci. Aff. *37*, 597–618.

ZIVCIC, M., and POLJAK, M. (1997), *Seismogenetic Areas of Slovenia.* Quantitative Seismic Zoning of the Circum Pannonian Region. QSEZ-CIPAR. Project CIPA CT 94-0238. Second year report.

ZUNIGA, F. R., and WYSS, M. (1995), *Inadvertent Changes in Magnitude Reported in Earthquake Catalogs: Their Evaluation through the b-value Estimates*, Bull. Seismol. Soc. Am. *5*, 1858–1866.

(Received January 11, 1998, accepted October 5, 1998)

IC/98/97

United Nations Educational Scientific and Cultural Organization
and
International Atomic Energy Agency

THE ABDUS SALAM INTERNATIONAL CENTRE FOR THEORETICAL PHYSICS

ANALYSIS AND DEFINITION OF MAGNITUDE SELECTION CRITERIA FOR NEIC (PDE) DATA, ORIENTED TO THE COMPILATION OF A HOMOGENEOUS UPDATED CATALOGUE FOR CN MONITORING IN ITALY

A. Peresan
Department of Earth Sciences, University of Trieste, Trieste, Italy

and

I.M. Rotwain
Russian Academy of Sciences,
International Institute of Earthquake Prediction Theory and Mathematical Geophysics,
Moscow, Russian Federation
and
The Abdus Salam International Centre for Theoretical Physics, SAND Group,
Trieste, Italy.

Abstract

In the present work we describe the construction of an updated catalogue for the Italian territory, necessary for intermediate-term earthquake prediction using algorithm CN. Due to the inaccessibility of data from the local network, we established to update the Italian catalogue CCI1996 using the Preliminary Determinations of Epicentres (PDE) from NEIC. Since CN requires an input catalogue that must be, as much as possible, homogeneous in space and time, it has been necessary to perform a preliminary analysis. Therefore, the completeness of the PDE catalogue is studied and the relations between different kind of magnitudes reported in the CCI1996 and PDE catalogues are analysed, in order to formulate a rule for the choice of magnitude priority in PDE, similar to that used for CCI1996. The results of CN monitoring of Italian seismicity, updated to July 1998, are given here.

MIRAMARE - TRIESTE
July 1998

Introduction

The algorithm CN (Gabrielov et al., 1986; Keilis-Borok and Rotwain, 1990) allows us to indicate, on the basis of the analysis of seismicity, the Times of Increased Probability (TIP) for the occurrence of an event with magnitude greater than a fixed threshold M_0. Thanks to the normalisation of its functions, CN can be applied to regions with a different seismicity level without any adjustment of parameters, when the general conditions of applicability of the algorithm are satisfied. CN application to a fixed region consists of two steps: at a first stage, referred to as learning step, the magnitude M_0, the magnitudes for normalisation of functions and the thresholds for discretization of functions are defined. In the second step the monitoring of seismicity is performed using the parameters fixed in the learning phase. The catalogue homogeneity among the different steps of the analysis is a relevant question, because it can significantly influence the results.

The regionalization used for the application of the algorithm in Italy has been defined by Peresan et al. (1997a), on the basis of the seismotectonic model of the Italian territory proposed by Scandone et al. (1990; 1994) and it is composed of three regions, corresponding approximately to the North, Centre and South of Italy (Fig. 1).

The catalogue used for CN application in Italy up to July 1997 was the CCI1996 (Peresan et al., 1997b); this catalogue is composed of the revised PFG catalogue (Postpischl, 1985), for the period 1000-1979, and since 1980 was updated by us with the ING bulletins. Due to the inaccessibility of the ING (Istituto Nazionale di Geofisica) data set since July 1997, we established to update the catalogue using different data. Among the currently available databases, the only one suitable for CN application seems to be the catalogue of Preliminary Determinations of Epicentres (PDE) from NEIC. This catalogue is updated timely enough and it is quite complete for our purposes, even if its completeness appears lower than that of the CCI1996, especially going back in the past.

Nevertheless, the upgrading performed using data from a different source could make the catalogue inhomogeneous, influencing the values of functions. Therefore, in order to construct a homogeneous updated catalogue for CN application, it is necessary to perform the following preliminary analysis:

- Study of the completeness of the PDE catalogue;
- Study of the relations between different kinds of magnitudes reported in the CCI1996 and PDE catalogues;

- Formulation of a rule for the choice of magnitude priority in PDE, similar to the priority used for CCI1996.

In the present study all these aspects will be analysed and the results of monitoring of seismicity, updated to May 1998, will be given.

Scheme of the analysis

The monitoring of seismicity with algorithm CN, for intermediate-term earthquake prediction purposes, is performed with a time step of two months and requires a catalogue updated with a time delay of a couple of weeks. Since the Italian catalogue of earthquakes, currently compiled by ING, ceased to be distributed after June 1997, the necessity arose to make use of a different data set for the upgrading. Among the available data-base we established to use the PDE data (Preliminary Determinations of Epicentres yearly, monthly and weekly revised versions) and the QED (Quick Epicentral Determinations), officially distributed by NEIC via ftp (Earthquake Hypocentres Data File version).

The PDE catalogue, analysed for the entire Italian area (rectangle with Lat: 35-50N and Lon: 5-20E), appears to satisfy the general conditions required for CN application in Italy, since it can be considered complete for magnitudes greater than 3.0, at least after 1985, and it is updated rapidly enough. Besides, CN requires an input catalogue that must be, as much as possible, homogeneous also in space and time and this has to be checked for each one of the three subcatalogues for the areas corresponding to Northern, Central and Southern regions.

The time homogeneity of the catalogue can be evaluated on the basis of the Gutenberg-Richter distribution. In the present case we are mainly concerned about the possible inhomogeneity that may result appending the PDE catalogue to the CCI1996 catalogue (briefly indicated as CCI in the following). Therefore we wish that the slope of the frequency-magnitude distribution does not change significantly passing from one catalogue to the other. Moreover we'll expect that, for a fixed common interval of time, the two distributions will be comparable in terms of G-R parameters and number of events. Both these comparisons however depend on the choice of magnitude that is made for PDE catalogue, that must be performed with a criterion homogeneous to the priority order selected for the CCI catalogue.

Indeed, CCI contains four estimations of magnitude: duration magnitude M_d, magnitude from intensities M_I, local magnitude M_L and body wave magnitude m_b from ISC; the priority used to select the operating magnitude in CCI is: M_L, M_d, M_I; m_b from ISC is not used, since it is given just for a few events and for a limited period of time. In the PDE catalogue, for each record, there are four possible different estimations of magnitude: m_b from NEIC, M_S from NEIC, M1 and M2; the last two values may correspond to magnitudes of a different kind provided from different agencies. A preliminary analysis of the catalogue allowed us to evidence that, for the Italian area, both M1 and M2 contain mainly M_d and M_L (M_L are more frequent than M_d, with a rate of 10/1). Since it is necessary to define a priority for PDE catalogue that allows a choice of magnitude similar to that of the CCI catalogue, we established to perform the following analysis, for each one of the three regions:

1. a subcatalogue of events common to the CCI and PDE is selected and all magnitudes from one catalogue are compared to the four estimations of the other catalogue. The linear regression (minimising distances normal to the fitting line), the standard deviation σ and the percentage P of points falling outside 2σ are calculated for each pair of magnitudes;
2. for each of the three magnitudes M_L, M_d and M_I from the CCI catalogue a corresponding magnitude from PDE is selected, according to the rule that the standard deviation σ is minimal for this magnitude, P is small, and the parameters A and B of the straight-line: M(CCI)=BM(PDE)+A are as close as possible to zero and one, respectively. Once the correspondence between magnitudes is found, the priority defined for the CCI catalogue can be transferred to the PDE;
3. the operating magnitude is selected from PDE according to the priority fixed as in step 2, both using original values of M and for M'=BM+A, recalculated using the parameters A and B of the corresponding M(CCI)-M(PDE) regression;
4. the operating magnitude from CCI and PDE are compared, considering the $M_{priority}$(CCI)-$M_{priority}$(PDE) distribution and the G-R relation. Among the possible choices (for equivalently good priorities and with or without recalculation of magnitudes), the one giving a good linear extrapolation and, above all, producing a frequency-magnitude relation closer to that from CCI, is retained.

Once selected the operating magnitude, the catalogue for monitoring is compiled using the CCI data for the learning period and the PDE data during the period of forward analysis. In this way the learning is performed using the best available data, since the Italian catalogue is more complete than the PDE, especially in the past, while real monitoring is done using the currently updated available data.

Priority choice for the three different regions

Northern region

The comparison of magnitudes for the Northern region is performed extracting a subcatalogue of common events for the PDE and the catalogue used for CN monitoring in Northern Italy. Indeed, here the data from the CCI catalogue were integrated with the information contained in the ALPOR(1987) and NEIC catalogues, because the Italian catalogue was fairly uncomplete outside the political boundaries. Here we will refer to the catalogue CCI+ALPOR+NEIC as Northern catalogue. The area considered for this analysis is the rectangle of coordinates: Lat:41.0-46.6N, Lon:8.0-16.0E, including the whole polygon that delimits the Northern region, while the time interval goes from the beginning of 1950 to the end of 1985. The selection of common events is performed considering equivalent the records differing in time less than 1 minute and 1 degree in epicentral coordinates, while depth and magnitudes are not considered.

In the Northern catalogue the operating magnitude is chosen as the maximum among $M_{ALPOR}(M_L, M_I)$, $M_{CCI}(M_L, M_d, M_I)$ and $M_{NEIC}(M1, M_S, m_b)$, selected from initial catalogues according to the priority order reported in brackets. Each one of the 1620 equivalent events extracted can be consequently associated to 3 estimations of magnitude from the Northern catalogue and 4 estimations of magnitude, m_b, M_S, M1 and M2 in the PDE catalogue. Therefore it appears necessary to find out for each magnitude given in the Northern catalogue a different representative priority from the PDE catalogue and after to select the maximum among these corresponding values.

The relations between different kinds of magnitudes have been evaluated calculating the parameters for the linear fitting, the standard deviation σ and the percentage P of events outside 2σ. Considering the diagrams of M_{ALPOR} versus different magnitudes from PDE, we observe that M_{ALPOR} is well fitted

by M1(PDE) and M2(PDE), while just a few points are available for M_S(PDE) and dispersion becomes very large for m_b(PDE). Consequently, to select from PDE a magnitude corresponding to M_{ALPOR} a proper priority order can be: M1, M2, M_S.

To select a magnitude corresponding to M_{CCI}, all the possible regression between the different magnitudes given in the CCI and in the PDE catalogue have been considered for the equivalent events which occurred within the fixed space-time interval. In this case a good linear extrapolation has been obtained between M_L(CCI) and M1(PDE) and between M_d(CCI) and M2(PDE), for M_S(PDE) the small number of points does not allow to establish any clear relation, while m_b(PDE) does not seem representative of any of the CCI magnitudes. Therefore M_{CCI} should be also properly represented by PDE magnitudes selected according to the priority: M1, M2, M_S.

Finally, for M_{NEIC} magnitude, we established to keep for the PDE data, that are provided from the same NEIC agency, the same priority order M1, M_S, m_b used to construct the Northern catalogue.

Once the three priority magnitudes, corresponding to M_{ALPOR}, M_{CCI} and M_{NEIC}, are selected from PDE, the operating magnitude can be taken as the maximum among them, just as it is routinely done for the Northern catalogue. The diagram of the operating magnitudes $M_{Max}(PDE_{priority})$ versus $M_{Max}(M_{Alpor}, M_{CCI}, M_{NEIC})$ for the common events, allows a good linear extrapolation y=A+Bx, with B=0.92 and A=0.30. The standard deviation for the fitted line is 0.22 and 5% of the points lie outside 2σ.

Nevertheless we observed that this complex priority choice is practically equivalent to pick directly the maximum magnitude from PDE, since the distribution M_{Max}(PDE) versus $M_{Max}(M_{Alpor}, M_{CCI}, M_{NEIC})$ is identical to that obtained using $M_{Max}(PDE_{priority})$ and gives the same values for A, B, for the linear extrapolation reported in Fig. 2. This observation is confirmed by the Gutenberg-Richter relations obtained with these two different choices of M (Fig. 3), that are almost identical; therefore it has little meaning to use the complex procedure and in the forward monitoring the operating magnitude will be selected simply as M_{Max}(PDE).

From Fig. 3 we can observe that the PDE catalogue, using $M=M_{Max}$(PDE) and for the time interval 1986-1997, can be considered complete for $M \geq 3.0$;

besides it has a slope very close to that of the Northern catalogue in the previous period of time (1950-1985), at least in the range of intermediate size earthquakes (3.0-4.5). Therefore PDE determination, with this magnitude priority choice, appears adequate for the catalogue upgrading in the Northern region.

Central Region

The analysis of magnitudes for Central Italy is performed within the rectangle of coordinates: Lat:39.0-45.5N, Lon:8.0-17.5E. The time interval considered goes from the beginning of 1900 to the end of 1997.

As a first step we extracted a subcatalogue of events common to both CCI and PDE catalogue, which occurred from 1900 up to the whole 1985; the selection of common events is made allowing a difference in origin time equal to 1 minute and 1 degree for epicentral coordinates, while depth and magnitudes are not considered. For the 1520 common events extracted from the two catalogues, the relations between different kinds of magnitudes in the CCI and PDE catalogue are considered (Figures 4a,b,c,d). For each diagram the values of the parameters for the linear fitting, the standard deviation and the percentage P of points outside 2 standard deviations from the line, are reported. For each kind of magnitude used in the CCI catalogue a corresponding magnitude from PDE is selected, according to the rule that the standard deviation is minimum and the parameters A and B of the linear extrapolation are closer to zero and one, respectively (see Figures 4a,b,c,d). Consequently M_L(CCI) can be associated to M2(PDE) and M_d(CCI) to M1(PDE); for M_S(PDE) the statistic is very poor, hence it will be kept only as a last chance, while m_b(PDE) does not seem representative of any one of the magnitudes considered in the CCI catalogue. According to this analysis, the choice of priority: M2, M1, M_S from PDE, should be similar to the priority used in the learning period in this region.

The magnitudes from PDE, however, can be used in two different ways: they can be recalculated into the corresponding CCI magnitude, using the coefficients obtained from the linear regression, or they can be used without any recalculation. The cumulative frequency-magnitude graph (Fig. 5), normalised by time, shows that the differences between the three curves obtained for CCI (time: 1900-1985) and PDE (time: 1986-1997), both

recalculated or not, are almost negligible for magnitude greater than the completeness level. Besides, for earthquakes with magnitude between 4.5 and 5.5 (that is the range of magnitude considered for the evaluation of functions), the PDE operating magnitude obtained without recalculation gives a curve closer to CCI. Therefore we established to select the magnitude from PDE according to the priority order: M2, M1, M_S, without any recalculation.

Southern Region

An analysis similar to that described for the Central region, has been performed for Southern Italy, checking the catalogue within the rectangular area of coordinates: Lat: 37.0-42.0N, Lon: 12.0E-17.5E. Magnitudes for the common events extracted from the CCI1996 and PDE catalogues have been compared for the time interval 1900-1985, considering the relations between all the different M(CCI)-M(PDE) pair of magnitudes. From Fig. 6a,b,c,d it is possible to observe that the best linear extrapolation for M_L(CCI) is obtained for M1(PDE), but also M2(PDE) and m_b(PDE) provide a good estimation for M_L(CCI), while no clear correspondence can be established for M_d(CCI) and M_I(CCI) magnitudes. Besides, just as in the Northern and Central regions, we observed that recalculation of magnitudes does not improve significantly the homogeneity among the CCI and PDE catalogues (Figs. 7 and 8). Therefore we established to choose the operating magnitude for the Southern region according to the priority order: M1, M2, m_b without recalculation.

Comparing the frequency-magnitude relations, normalised by time, obtained for the two catalogues CCI1996 (1900-1985) and PDE (1986-1997) the seismic activity appears to be significantly lower in the PDE determinations, even if the total number of events it is even larger (Fig. 7). Nevertheless, this difference almost disappears when considering the catalogue of main shocks only (Fig. 8) and this can be explained by the fact that in this area many events are reported in the PDE catalogue without any estimation of magnitude. A further analysis of PDE completeness for Southern Italy shows us that this catalogue cannot be considered complete for magnitudes lower than M=4.0 before 1992, and for M=3.5 up to the present time. The lower completeness level must be taken into account both during the construction of the catalogue for the monitoring of seismicity and in the evaluation of results, since it increases the risk of failures to predict.

Results of CN monitoring in Italy

The analysis and comparison of PDE and CCI catalogues described in this work allows us to construct an updated catalogue as homogeneous as possible, indicating for each region the proper selection of the operating magnitude from the PDE catalogue. Wishing to perform the learning step with the best quality and homogeneous set of data, we established to compile the catalogue for CN monitoring using CCI1996 data for the learning period and the PDE data during the period of forward analysis, since the Italian catalogue is more complete than PDE, especially in the past.

Northern region

The updated catalogue for the Northern Region (Fig. 1a) is composed by the Northern catalogue (ALPOR+CCI+NEIC) for the time interval 1964-1994, corresponding to the learning period, and by the PDE determinations since 1995, that is the period of forward predictions. According to the results of our analysis, the operating magnitude for PDE in this area is chosen to be the maximum M_{Max}(PDE), while for the Northern catalogue it is the maximum among $M_{ALPOR}(M_L, M_I)$, $M_{CCI}(M_L, M_d, M_I)$ and $M_{NEIC}(M_L, M_S, m_b)$.

The results of application of CN algorithm, updated at May, 1st 1998, can be summarized as follows: all the four strong earthquakes with $M \geq M_0 = 5.4$, which occurred within the region from March 1964 to May 1998, are correctly preceded by a TIP, with alarms covering about 25% of the total time and two false alarms. The diagram showing the time distribution of TIPs and the occurrence of strong events in the Northern region is given in Fig. 9a. No alarm is currently indicated for this region.

Central region

The catalogue for CN application in Central Italy (Fig. 1b) is constructed using the CCI from 1954 to 1985, that corresponds to the learning period, and the PDE catalogue since 1986. The priority used for the CCI catalogue is $M_{CCI}(M_L, M_d, M_I)$, while for the PDE in the Central region the operating magnitude is $M_{PDE}(M2, M1, M_S)$.

The results of application of CN algorithm in Central Italy are represented in Fig. 9b and can be described as follows: all the five strong earthquakes with $M \geq M_0 = 5.6$, which occurred within the region from 1954 to May 1998, are correctly identified with TIPs covering about 22% of the total time and there are two false alarms. The forward monitoring, updated to May 1998, indicates a current alarm for this region from 26.9.1997 to 1.5.1999.

Southern region

The completeness threshold for the PDE catalogue in Southern Italy is about M=4.0 up to 1992, and reaches M=3.5 only since 1992 (Fig. 8). Therefore, due to the lower completeness level of data in this area, it is not possible to compile the catalogue using the PDE for the whole period of forward analysis, but it is necessary to keep CCI at least up to 1991. Indeed, the functions of seismic flow in Southern region are evaluated using the events with $M \geq 3.8$, while for the counting of aftershocks the earthquakes with $M \geq 3.0$ are considered. Hence using PDE data since 1992, we must bear in mind that one precursor, based on bursts of aftershocks, could be lost due to the lack of aftershocks, and this increases the probability of failures to predict. Keeping into account these necessary warnings, the updated catalogue for Southern Italy can be compiled using the CCI for the period: 1954-1991, with magnitude priority $M_{CCI}(M_L, M_d, M_I)$, followed by the PDE (1992-1998), with priority $M_{PDE}(M1, M2, m_b)$.

The results of the monitoring updated to May, 1 1998 are the following: all the four strong events with $M \geq M_0 = 5.6$ are correctly identified by retrospective analysis, with TIPs covering about 31% of total time and with 5 false alarms. The time distribution of alarm periods and the time of occurrence of strong events are represented in Fig. 9c. No current alarm is indicated for Southern Italy.

Conclusions

The results obtained indicate that the PDE catalogue is appropriate for forward prediction of strong earthquakes in Italy, once the proper operating magnitude is chosen. Indeed, using the updated CCI+PDE catalogue compiled according to the rules defined here, all the four strong earthquakes, which occurred during the period of forward monitoring both in the Northern and

Central regions, are correctly predicted. This means that CN algorithm can detect the symptoms of instability in the PDE catalogue, with the same parameters and discretization thresholds fixed during the learning period with the CCI catalogue. Special attention must be payed however to the Southern region, where the lower completeness level of data increase the probability of failures to predict.

Acknowledgements

The authors are very grateful to Professor G. F. Panza for the critical observations and stimulating discussions.

This research has been developed in the framework of the UNESCO-IGCP project 414 and has been supported by INTAS funds (n° 94-0232). This work has been partly supported from MURST (40% and 60%) funds, CNR- Gruppo Nazionale per la Difesa dai Terremoti contracts nos. 95.00608.PF54 and 96.02968.PF54.

References

ALPOR (1987): Catalogue of the Eastern Alps. *Osservatorio Geofisico Sperimentale, Trieste, Italy.*

GABRIELOV, A.M., O.E. DMITRIEVA, V.I. KEILIS-BOROK, V.G. KOSSOBOKOV, I.V. KUTZNETSOV, T.A. LEVSHINA, K.M. MIRZOEV, G.M. MOLCHAN, S.KH. NEGMATULLAEV, V.F. PISARENKO, A.G. PROZOROV, W. RINHEART, I.M. ROTWAIN, P.N. SHELBALIN, M.G. SHNIRMAN and S.YU SCHREIDER (1986): Algorithms of long-term earthquakes' prediction. *International School for Research Oriented to Earthquake Prediction-algorithms, Software and Data Handling (Lima, Perù, 1986).*

KEILIS-BOROK, V.I. and I.M. ROTWAIN (1990): Diagnosis of time of increased probability of strong earthquakes in different regions of the world: algorithm CN. *Phys. Earth Planet. Inter.*, **61**, 57-72.

PDE, *Preliminary Determinations of Epicenters: Italy.* Computer files from anonymous ftp: gldcs.cr.usgs.gov. National Earthquake Information Center. U.S.G.S. Denver, USA.

PERESAN, A., G. COSTA AND G.F. PANZA (1997a): Seismotectonic model and CN earthquake prediction in Italy. *Pageoph.* Submitted.

PERESAN, A., G. COSTA AND F. VACCARI (1997b): CCI1996: the Current Catalogue of Italy. *International Centre for Theoretical Physics.* Internal report IC/IR/97/9. Trieste. Italy.

POSTPISCHL, D. (1985): Catalogo dei terremoti italiani dall'anno 1000 al 1980. C.N.R.-*Progetto Finalizzato Geodinamica.*

SCANDONE, P., E. PATACCA, C. MELETTI, M. BELLATALLA, N. PERILLI and U. SANTINI (1990): Struttura geologica, evoluzione cinematica e schema sismotettonico della penisola italiana. *Atti del Convegno GNDT 1990*, **1**, 119-135.

SCANDONE, P., E. PATACCA, C. MELETTI, M. BELLATALLA, N. PERILLI and U. SANTINI (1994): Seismotectonic zoning of the italian peninsula: revised version. Working file NOV94.

Figure captions

Fig. 1 - Regionalization of the Italian territory proposed by Peresan et al. (1997a) and following closely the seismotectonic model. a) Northern Region; b) Central Region; c) Southern Region.

Fig. 2 – Relation between the operating magnitude in the Northern catalogue (Alpor+CCI+NEIC), selected as $M_{Max}(M_{Alpor}, M_{CCI}, M_{NEIC})$, and the maximum magnitude from PDE, without recalculation. Only the events common to both catalogues, which occurred within the fixed rectangle in the period of time 1950-1985, are considered here.

Fig. 3 – Cumulative frequency-magnitude relations, normalised by time, obtained for the Northern catalogue (Alpor+CCI+NEIC) and for the PDE catalogue, considering both $M_{Max}(PDE_{priority})$ and $M_{Max}(PDE)$ simply. All the events which occurred within the rectangle with coordinates: Lat:37.0-42.0N Lon:12.0-18.0E are considered. Mc is the completeness threshold required.

Fig. 4a,b,c,d – Relations between different kinds of magnitudes in the CCI1996 catalogue and the PDE catalogue for the common events which occurred in the Central part of Italy (Lat: 39.0-45.5N, Lon: 8.0-17.5E). The parameters a and b of the linear fitting Y=bX+a are given for each diagram, together with the number of events N used to evaluate the linear extrapolation (with both nonzero magnitudes); sd is the standard deviation and P is the percentage of points outside two standard deviations.

Fig. 5 - Cumulative frequency-magnitude relations, normalised by time, obtained for the CCI1996 and PDE catalogues in the Central part of Italy. For the PDE catalogue two different operating magnitudes are considered: $M_{PDE}(M2, M1, M_S)$ recalculated, according to the linear extrapolations of Fig. 4, and $M_{PDE}(M2, M1, M_S)$ not recalculated.

Fig. 6a,b,c,d – Relations between different kinds of magnitudes in the CCI1996 catalogue and the PDE catalogue for the common events which occurred in the Southern part of Italy (Lat: 37.0-42.0N, Lon: 12.0-17.5E). The parameters a and b of the linear fitting, the number of events N, the standard deviation sd and the percentage P of points outside two standard deviations, are given for each diagram.

Fig. 7a,b - Cumulative frequency-magnitude relations, normalised by time, obtained for a) all the events and b) main shocks only contained in the CCI1996 and PDE catalogues for Southern Italy. For the PDE catalogue two different operating magnitudes are considered: $M_{PDE}(M1, M2, m_b)$ recalculated, according to the linear extrapolations of Fig. 6, and $M_{PDE}(M1, M2, m_b)$ not recalculated. Mc is the completeness threshold required.

Fig. 8a,b – Frequency-magnitude distributions, obtained for the PDE catalogue in the Southern part of Italy, considering six different time intervals of two years duration, a) from 1986 to 1991 and b) from 1992 to 1997, respectively. The operating magnitude is $M_{PDE}(M1, M2, m_b)$ not recalculated.

Fig. 9 – Results of application of CN algorithm in Italy, updated at May, 1st 1998, using the catalogue CCI+PDE composed by the CCI1996, for the learning period, and by the PDE for the forward monitoring. Black boxes indicate the periods of alarm, while triangles indicate the occurrence of the strong earthquakes with $M \geq M_0$. The learning period and the threshold M_0 are reported for each region.

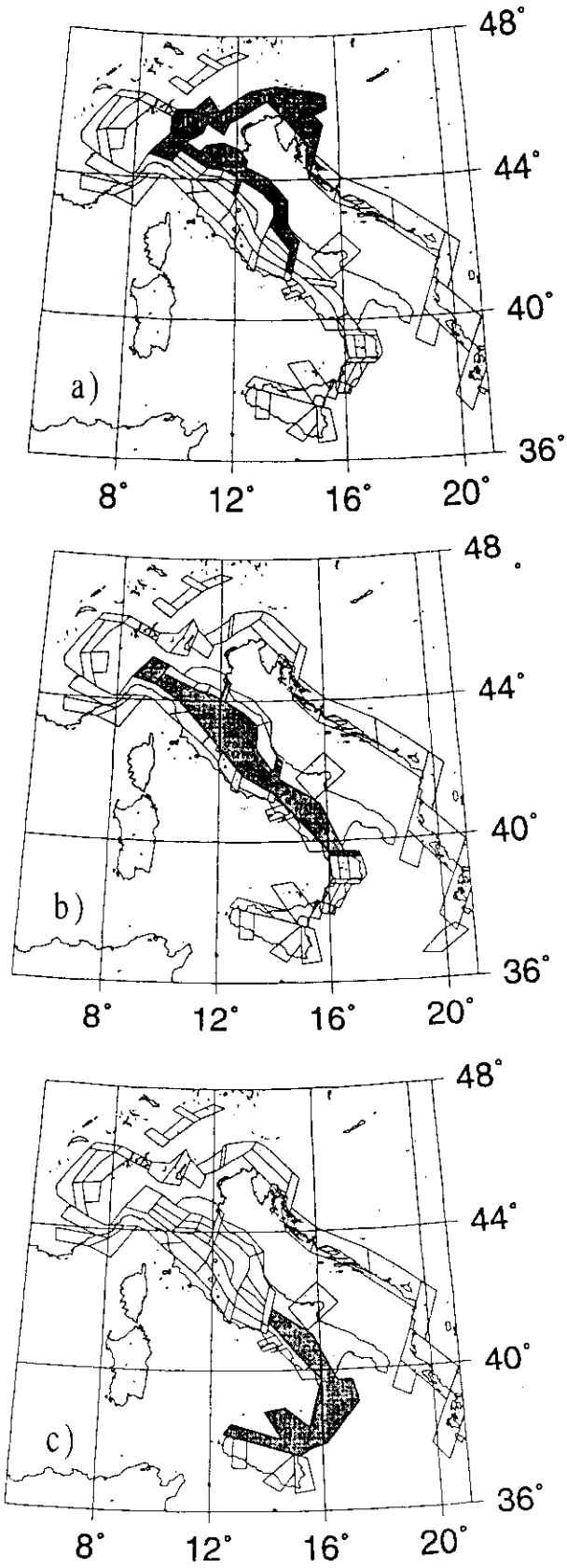

Fig. 1

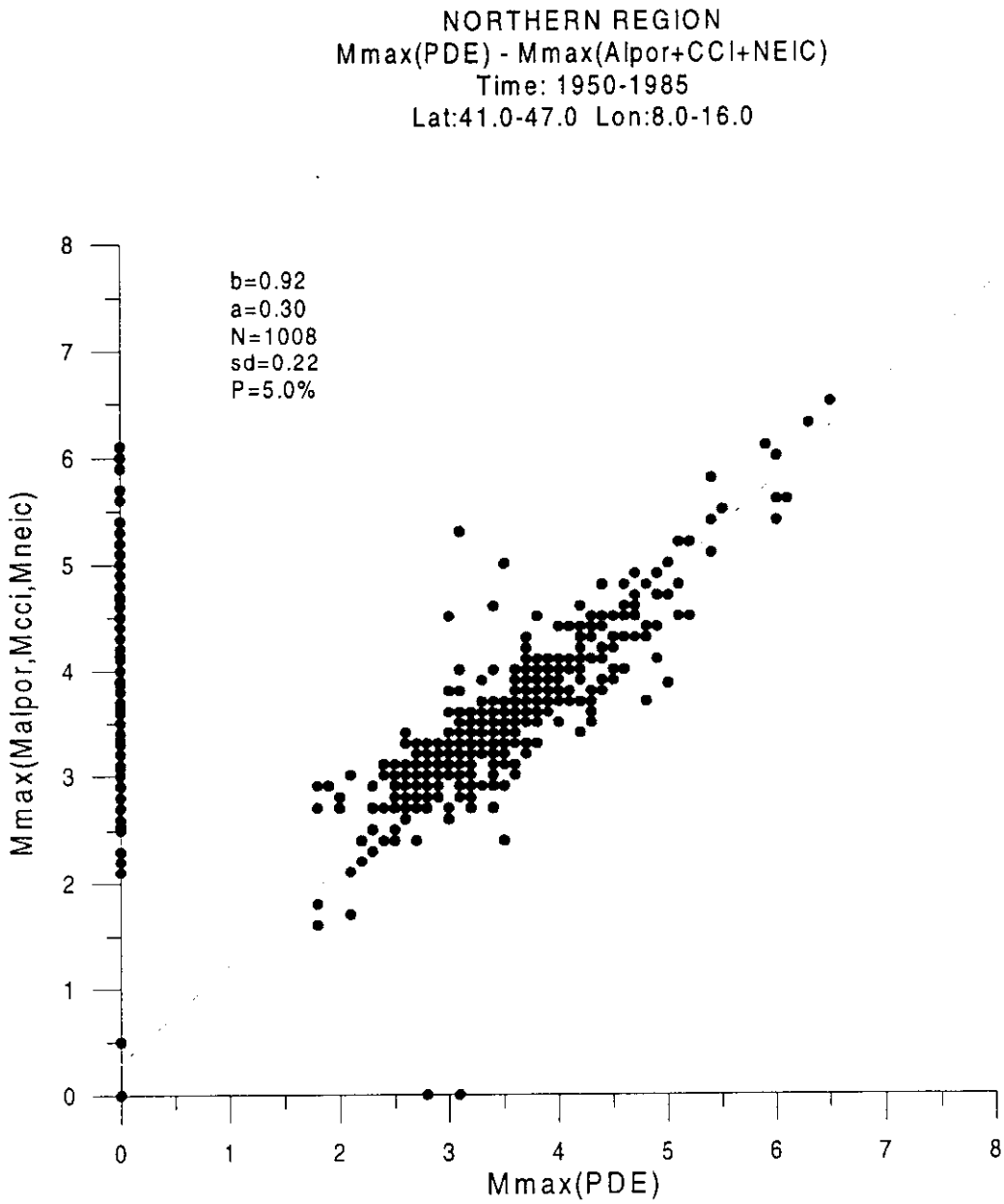
NORTHERN REGION
Mmax(PDE) - Mmax(Alpor+CCI+NEIC)
Time: 1950-1985
Lat:41.0-47.0 Lon:8.0-16.0
b=0.92
a=0.30
N=1008
sd=0.22
P=5.0%
Mmax(Malpor,Mcci,Mneic)
Mmax(PDE)
0
1
2
3
4
5
6
7
8

Fig. 2

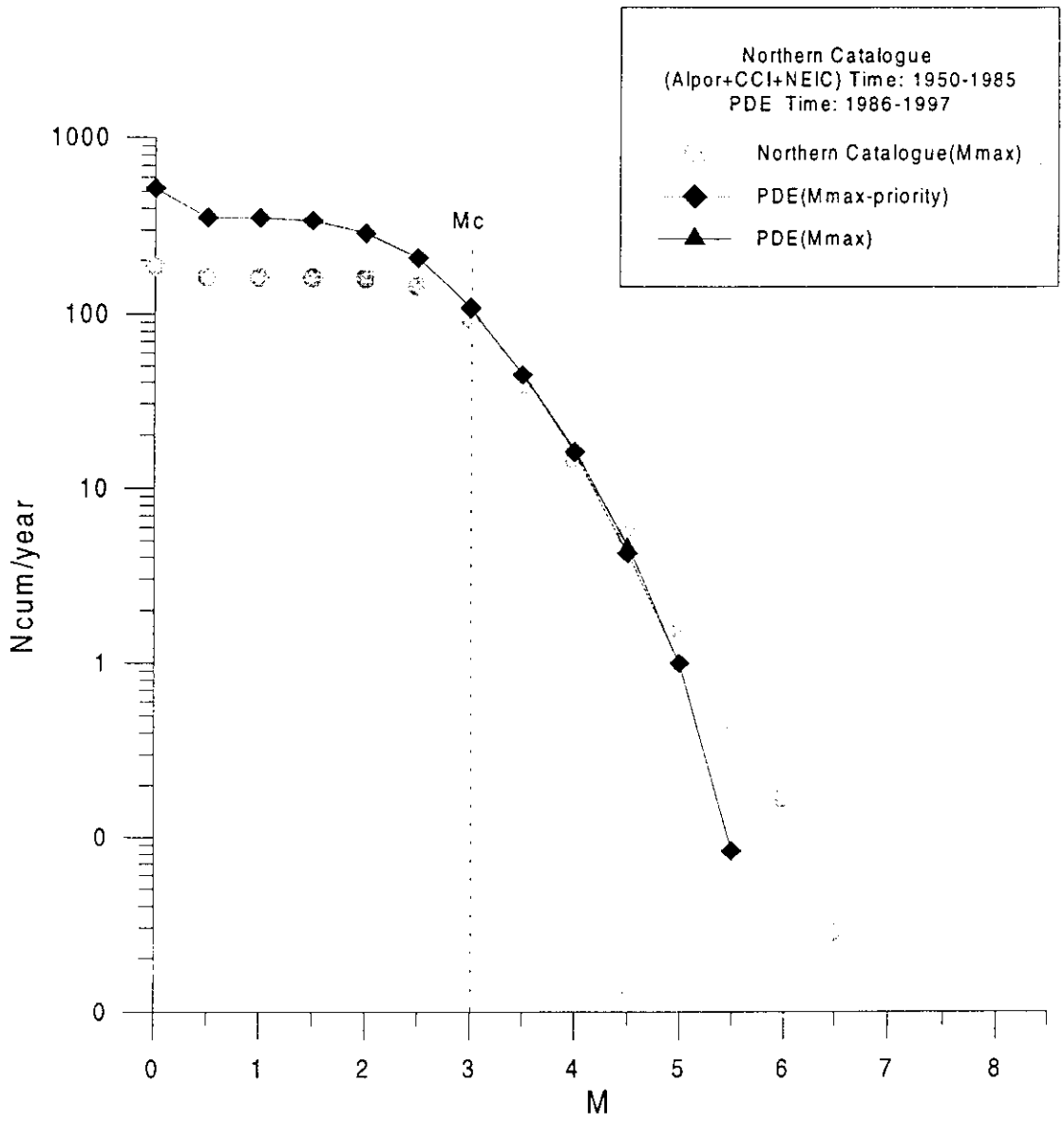
Northern Catalogue
(Alpor+CCI+NEIC) Time: 1950-1985
PDE Time: 1986-1997
Northern Catalogue(Mmax)
PDE(Mmax-priority)
PDE(Mmax)
Mc
Ncum/year
M
1000
100
10
1
0
0
1
2
3
4
5
6
7
8

Fig. 3

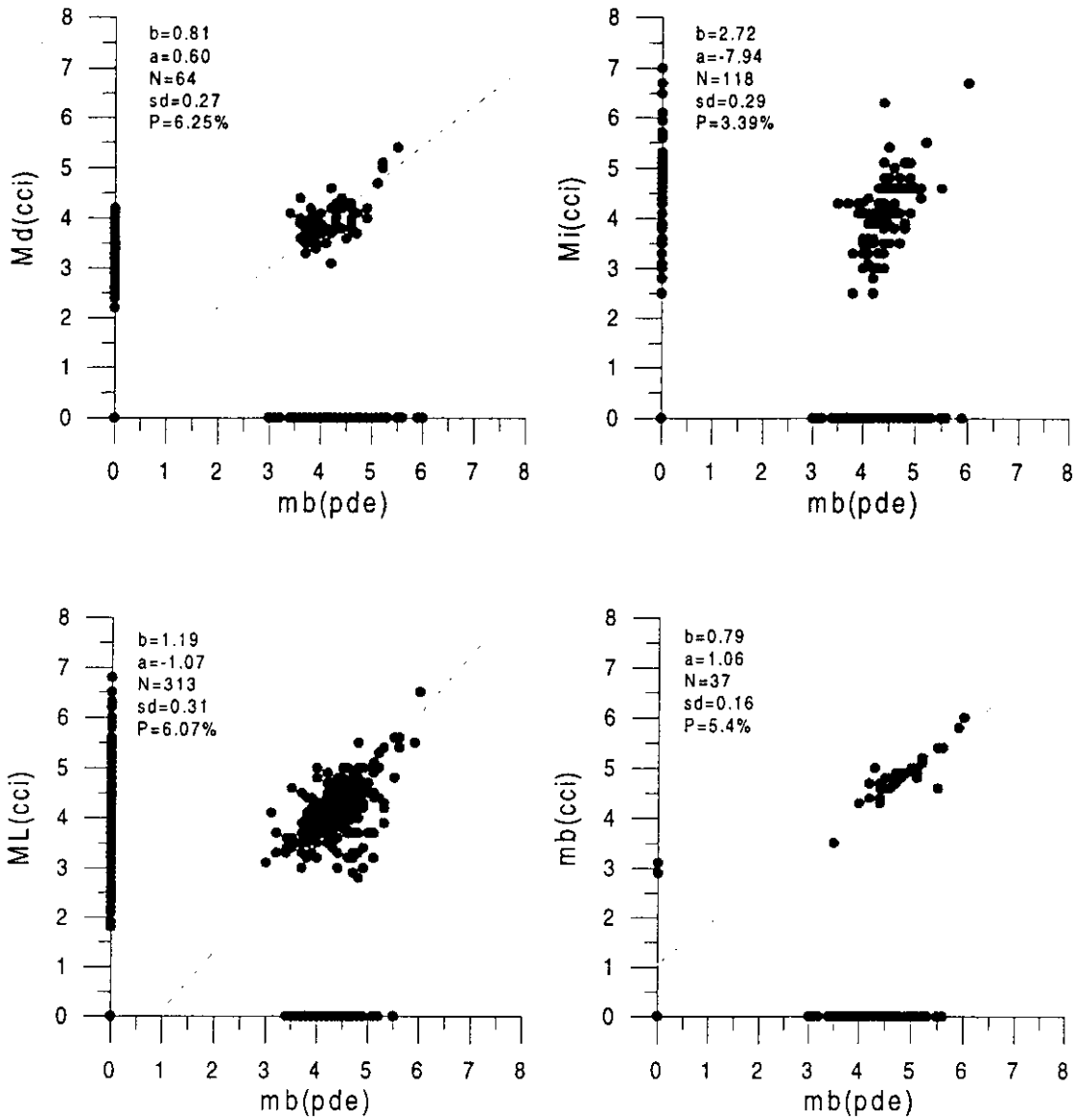
b=0.81
a=0.60
N=64
sd=0.27
P=6.25%
Md(cci)
mb(pde)
b=2.72
a=-7.94
N=118
sd=0.29
P=3.39%
Mi(cci)
mb(pde)
b=1.19
a=-1.07
N=313
sd=0.31
P=6.07%
ML(cci)
mb(pde)
b=0.79
a=1.06
N=37
sd=0.16
P=5.4%
mb(cci)
mb(pde)

Fig. 4a

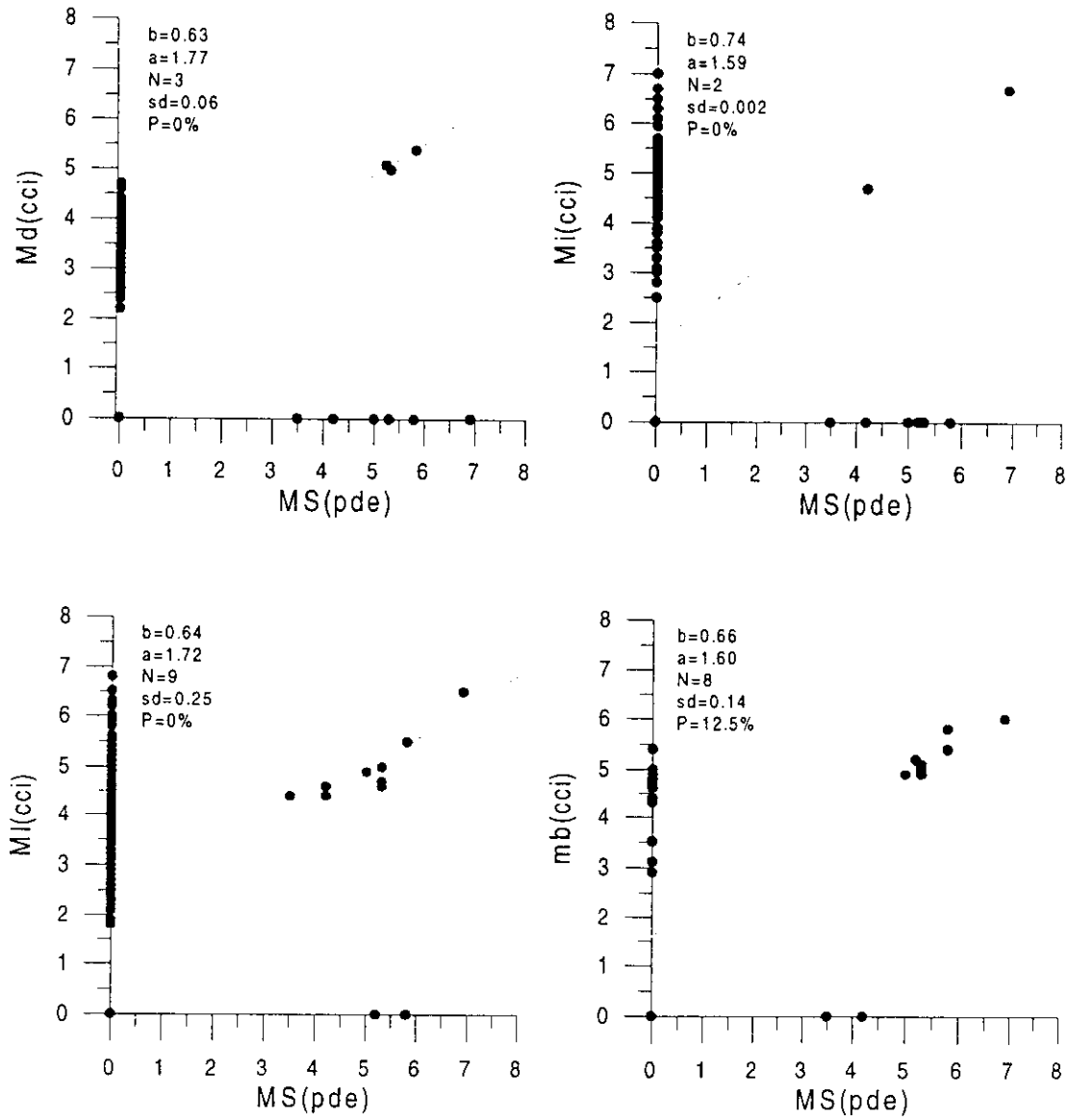
b=0.63
a=1.77
N=3
sd=0.06
P=0%
Md(cci)
MS(pde)
b=0.74
a=1.59
N=2
sd=0.002
P=0%
Mi(cci)
MS(pde)
b=0.64
a=1.72
N=9
sd=0.25
P=0%
Ml(cci)
MS(pde)
b=0.66
a=1.60
N=8
sd=0.14
P=12.5%
mb(cci)
MS(pde)

Fig. 4b

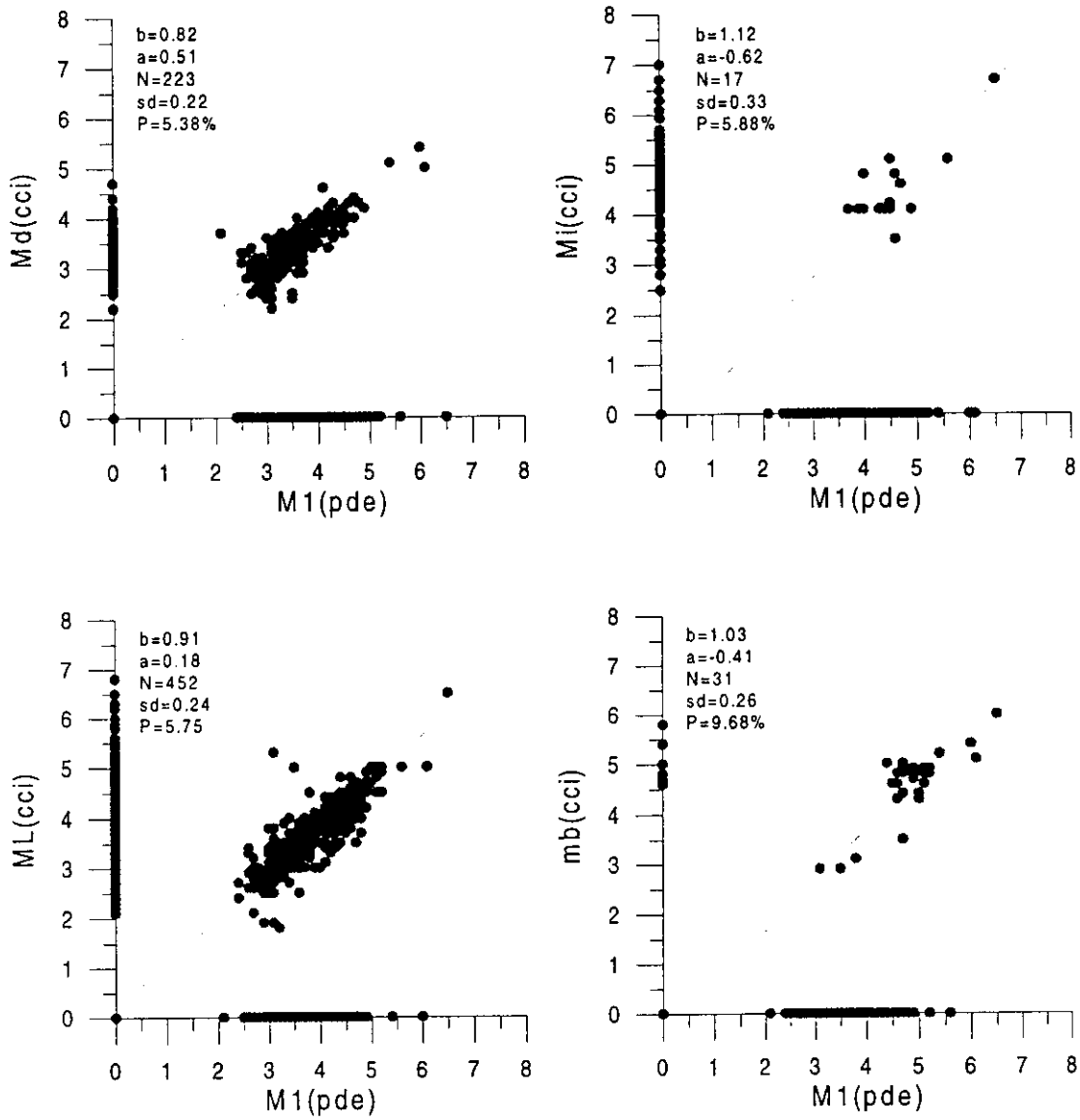
b=0.82
a=0.51
N=223
sd=0.22
P=5.38%
Md(cci)
M1(pde)
b=1.12
a=-0.62
N=17
sd=0.33
P=5.88%
Mi(cci)
M1(pde)
b=0.91
a=0.18
N=452
sd=0.24
P=5.75
ML(cci)
M1(pde)
b=1.03
a=-0.41
N=31
sd=0.26
P=9.68%
mb(cci)
M1(pde)

Fig. 4c

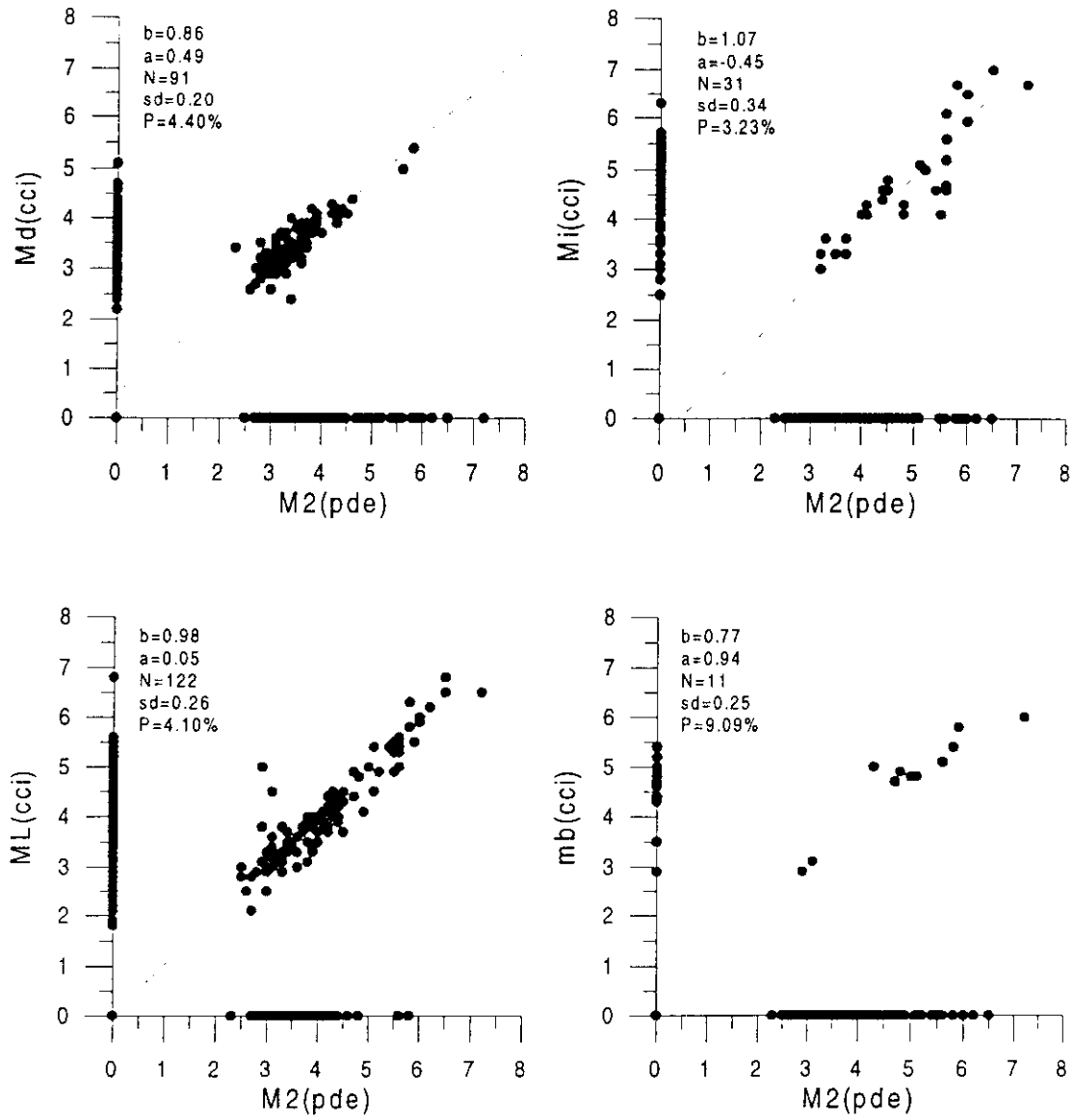
b=0.86
a=0.49
N=91
sd=0.20
P=4.40%
Md(cci)
M2(pde)
b=1.07
a=-0.45
N=31
sd=0.34
P=3.23%
Mi(cci)
M2(pde)
b=0.98
a=0.05
N=122
sd=0.26
P=4.10%
ML(cci)
M2(pde)
b=0.77
a=0.94
N=11
sd=0.25
P=9.09%
mb(cci)
M2(pde)

Fig. 4d

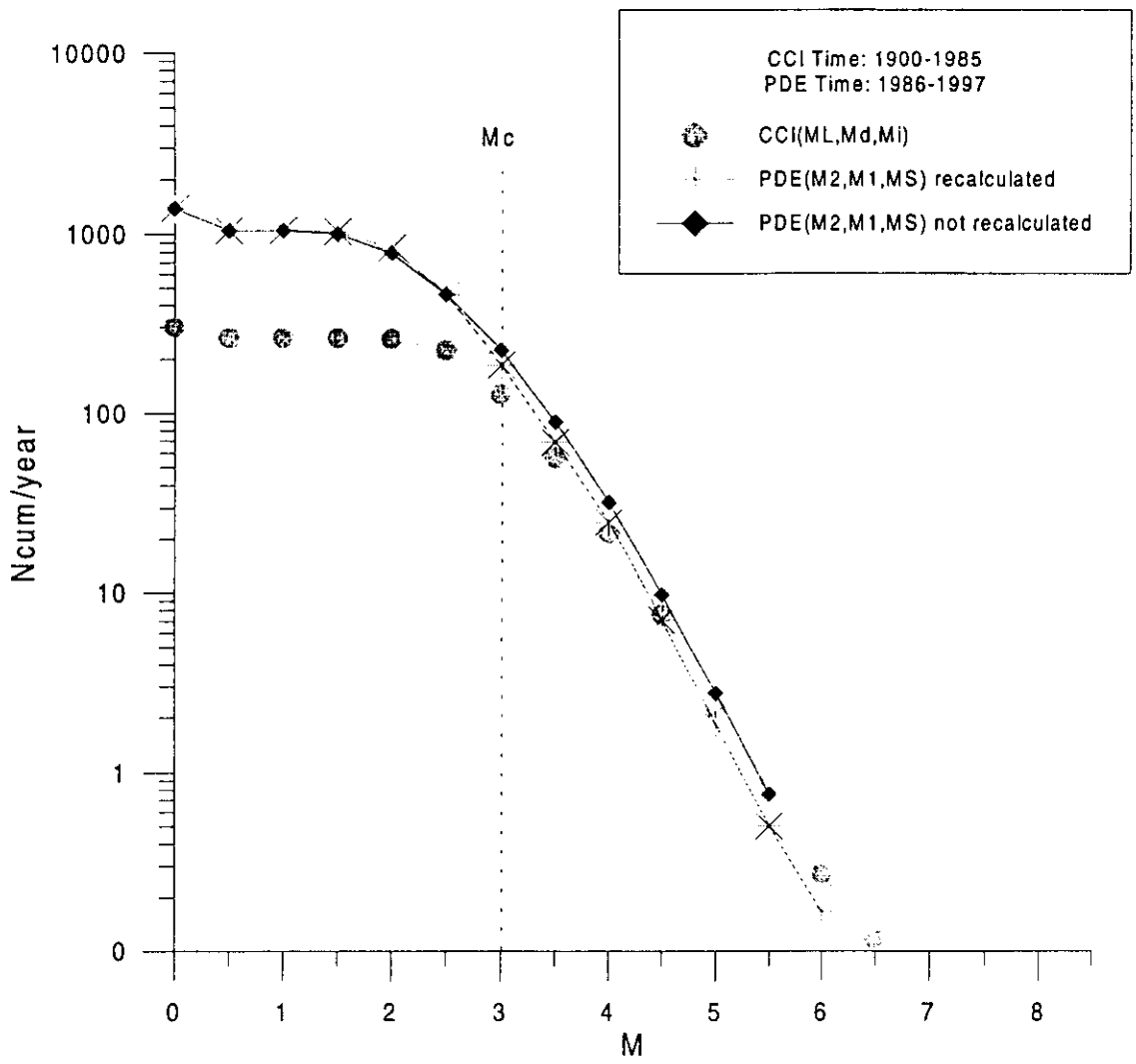
CCI Time: 1900-1985
PDE Time: 1986-1997
CCI(ML,Md,Mi)
PDE(M2,M1,MS) recalculated
PDE(M2,M1,MS) not recalculated
Mc
Ncum/year
M
10000
1000
100
10
1
0
0
1
2
3
4
5
6
7
8

Fig. 5

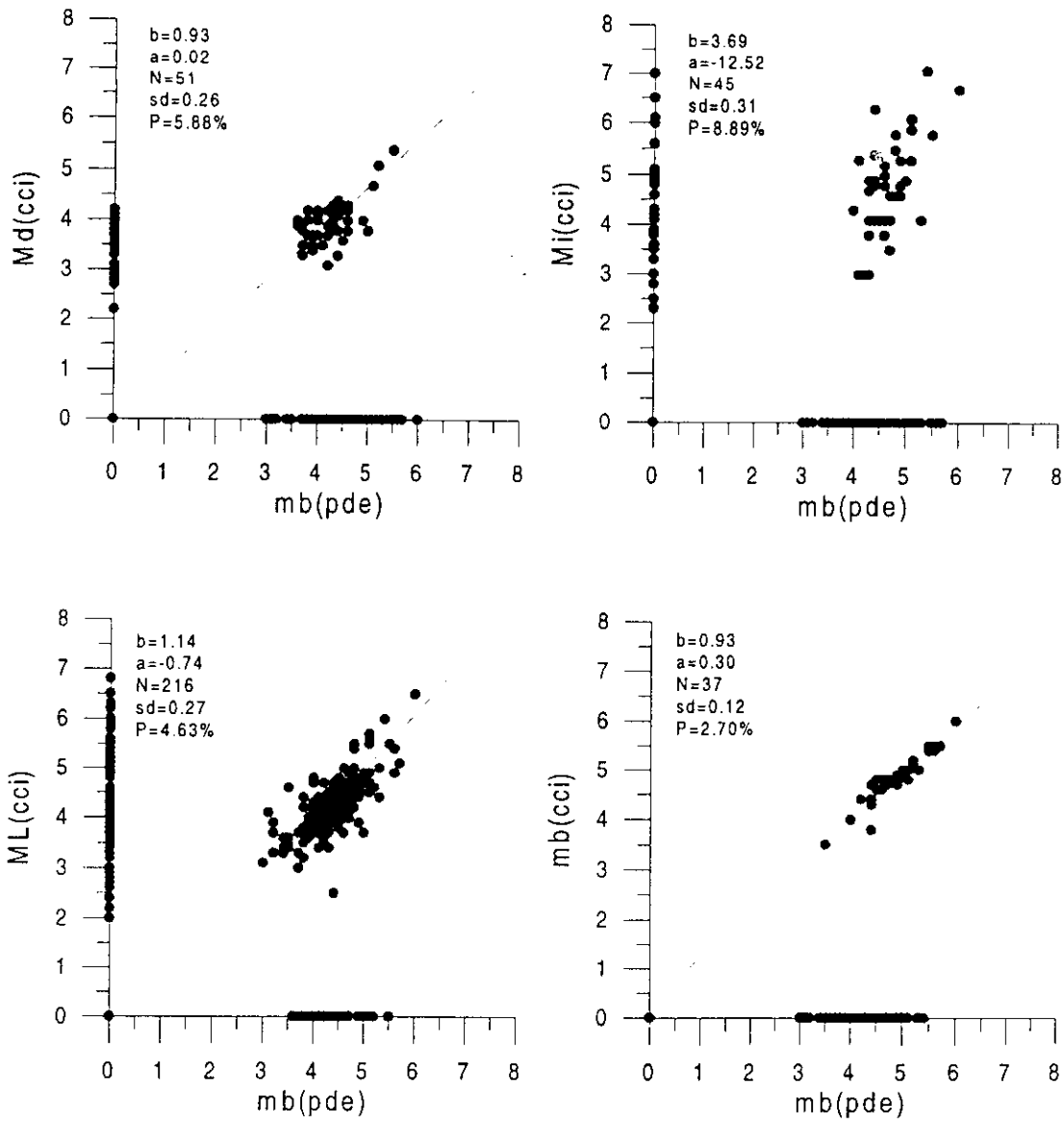
b=0.93
a=0.02
N=51
sd=0.26
P=5.88%
Md(cci)
mb(pde)
b=3.69
a=-12.52
N=45
sd=0.31
P=8.89%
Mi(cci)
mb(pde)
b=1.14
a=-0.74
N=216
sd=0.27
P=4.63%
ML(cci)
mb(pde)
b=0.93
a=0.30
N=37
sd=0.12
P=2.70%
mb(cci)
mb(pde)

Fig. 6a

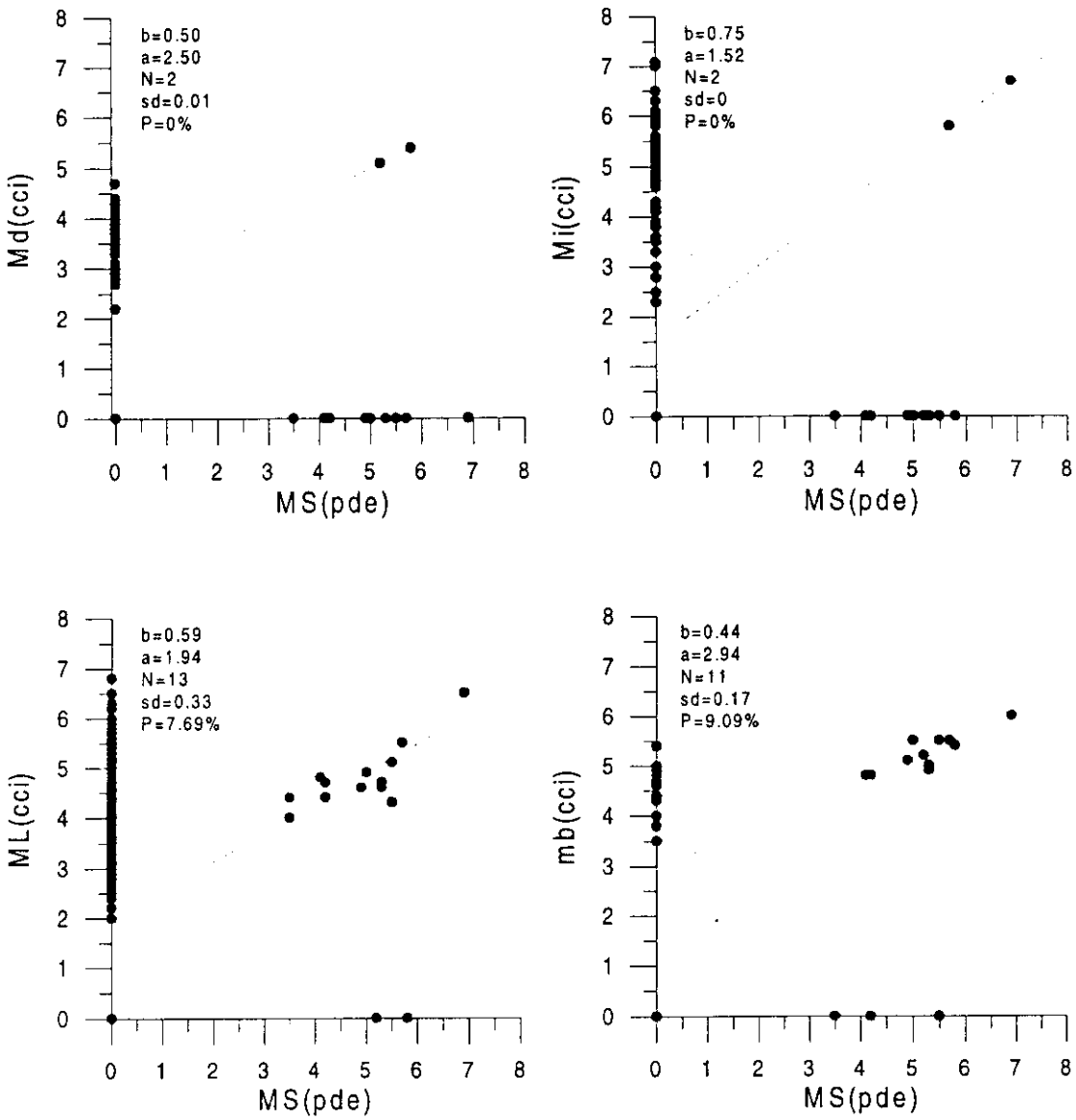
b=0.50
a=2.50
N=2
sd=0.01
P=0%
Md(cci)
MS(pde)
b=0.75
a=1.52
N=2
sd=0
P=0%
Mi(cci)
MS(pde)
b=0.59
a=1.94
N=13
sd=0.33
P=7.69%
ML(cci)
MS(pde)
b=0.44
a=2.94
N=11
sd=0.17
P=9.09%
mb(cci)
MS(pde)

Fig. 6b

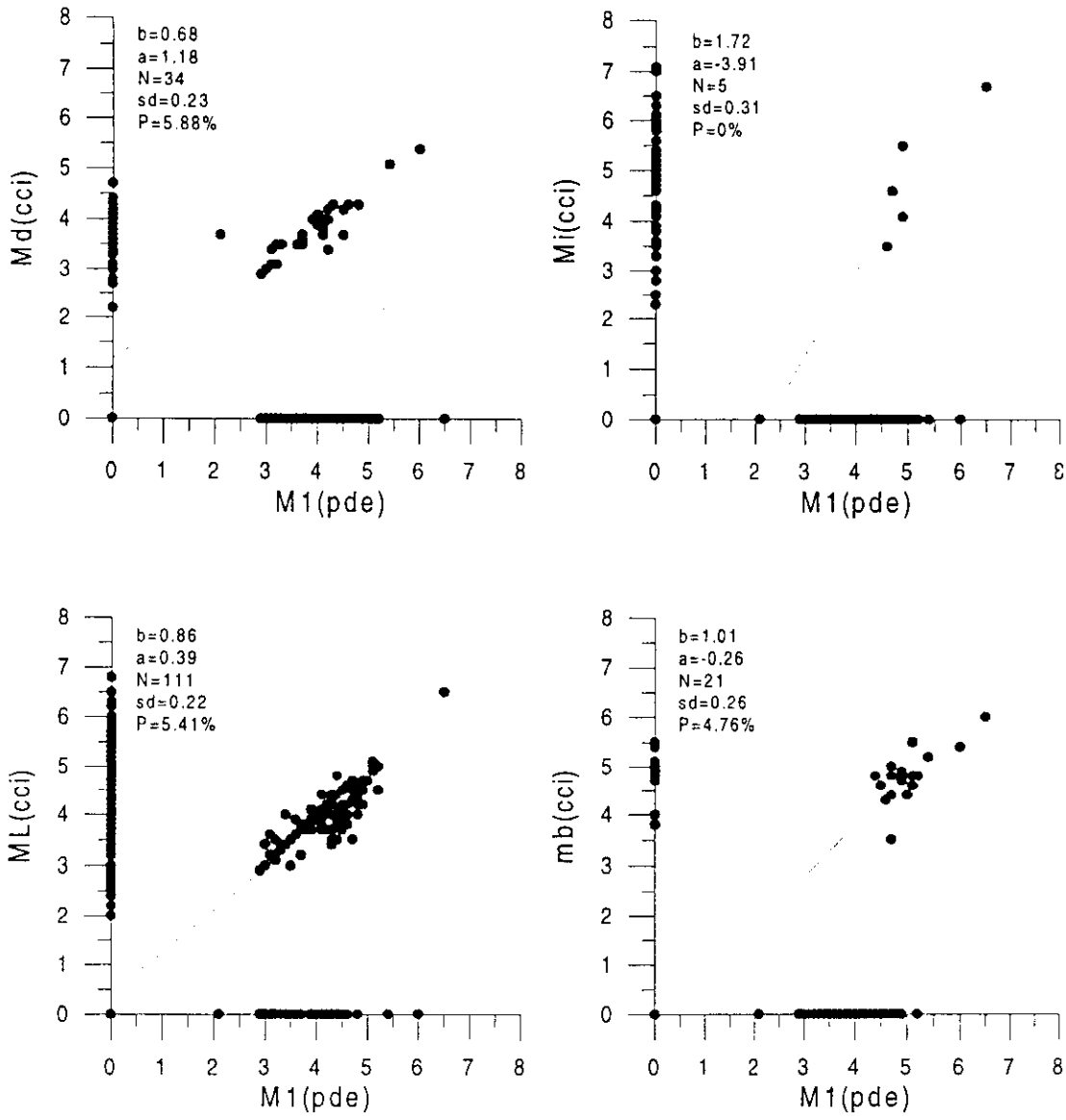
b=0.68
a=1.18
N=34
sd=0.23
P=5.88%
Md(cci)
M1(pde)
b=1.72
a=-3.91
N=5
sd=0.31
P=0%
Mi(cci)
M1(pde)
b=0.86
a=0.39
N=111
sd=0.22
P=5.41%
ML(cci)
M1(pde)
b=1.01
a=-0.26
N=21
sd=0.26
P=4.76%
mb(cci)
M1(pde)

Fig. 6c

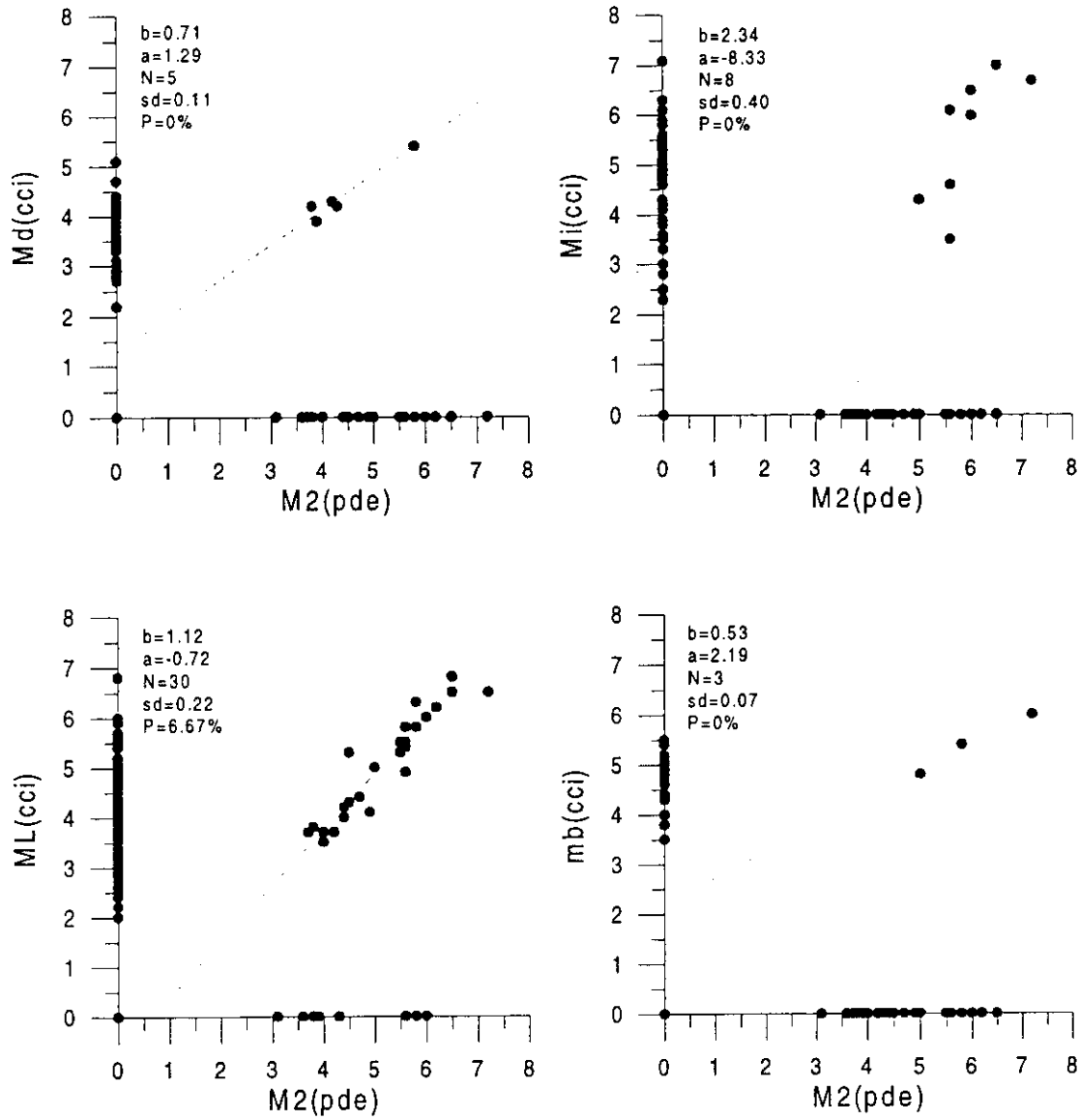
b=0.71
a=1.29
N=5
sd=0.11
P=0%
Md(cci)
M2(pde)
b=2.34
a=-8.33
N=8
sd=0.40
P=0%
Mi(cci)
M2(pde)
b=1.12
a=-0.72
N=30
sd=0.22
P=6.67%
ML(cci)
M2(pde)
b=0.53
a=2.19
N=3
sd=0.07
P=0%
mb(cci)
M2(pde)

Fig. 6d

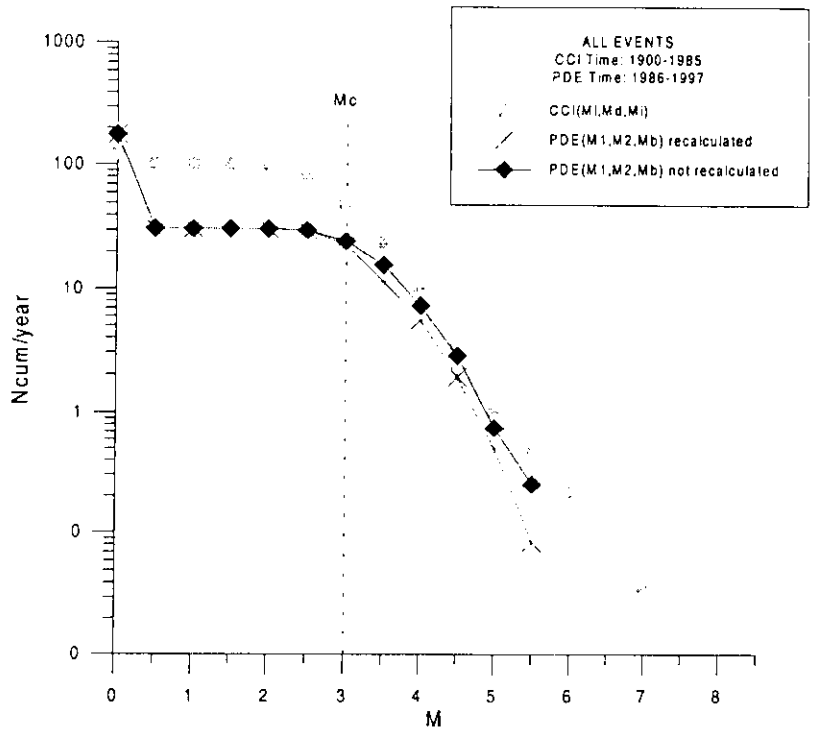
ALL EVENTS
CCI Time: 1900-1985
PDE Time: 1986-1997
CCI(Ml,Md,Mi)
PDE(M1,M2,Mb) recalculated
PDE(M1,M2,Mb) not recalculated
Mc
Ncum/year
M
1000
100
10
1
0
0
1
2
3
4
5
6
7
8

Fig. 7a

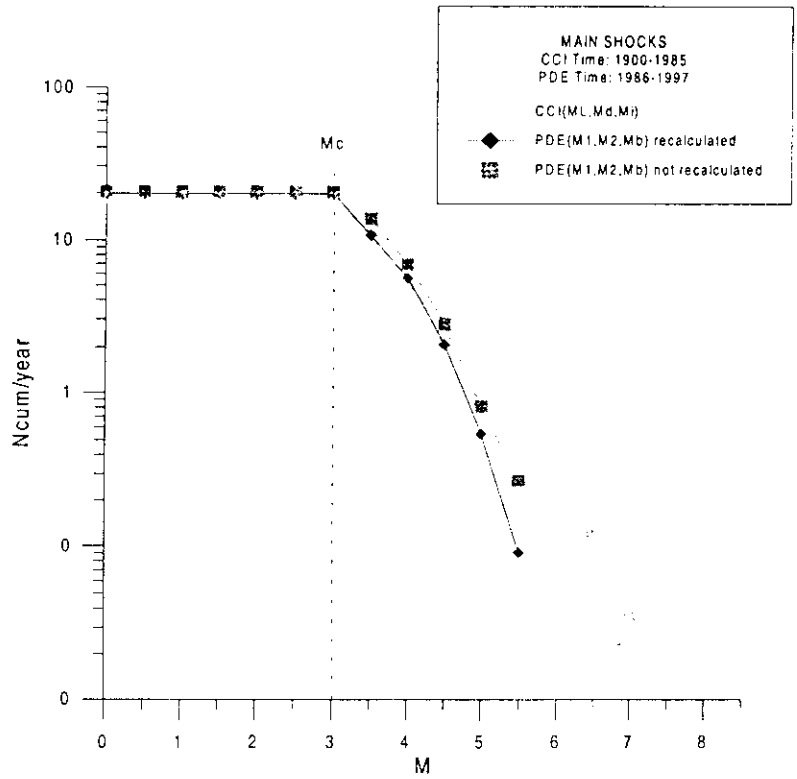
MAIN SHOCKS
CCI Time: 1900-1985
PDE Time: 1986-1997
CCI(ML,Md,Mi)
PDE(M1,M2,Mb) recalculated
PDE(M1,M2,Mb) not recalculated
Mc
Ncum/year
M
100
10
1
0
0
1
2
3
4
5
6
7
8

Fig. 7b

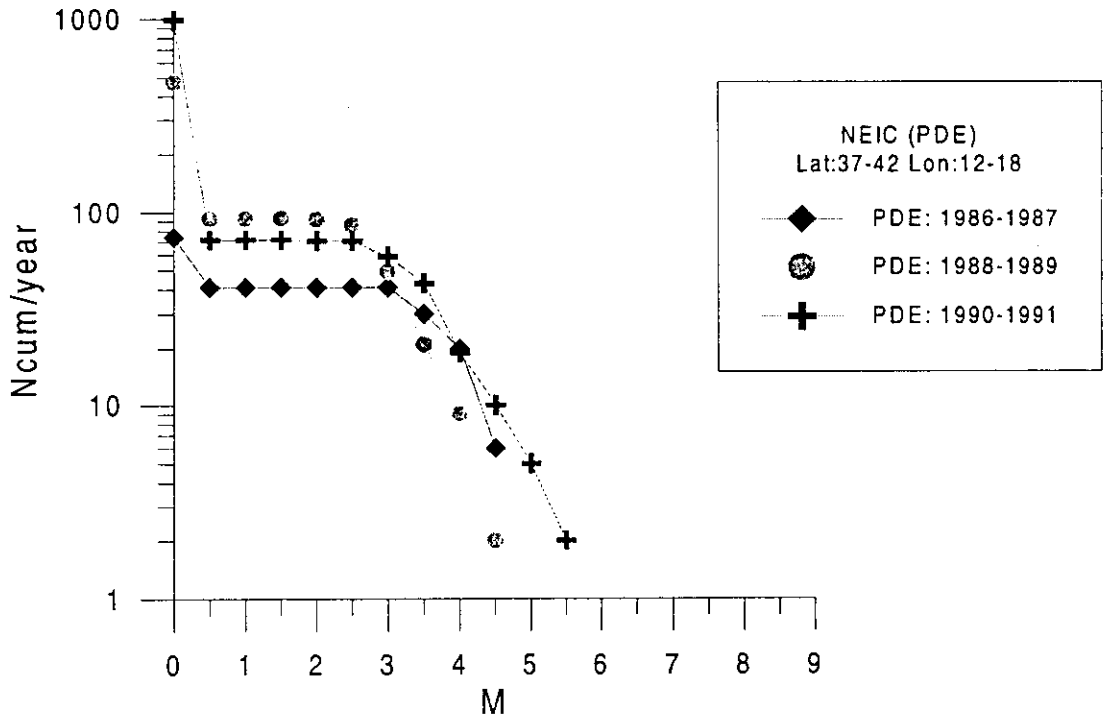
1000
100
10
1
Ncum/year
0
1
2
3
4
5
6
7
8
9
M
NEIC (PDE)
Lat:37-42 Lon:12-18
PDE: 1986-1987
PDE: 1988-1989
PDE: 1990-1991

Fig. 8a

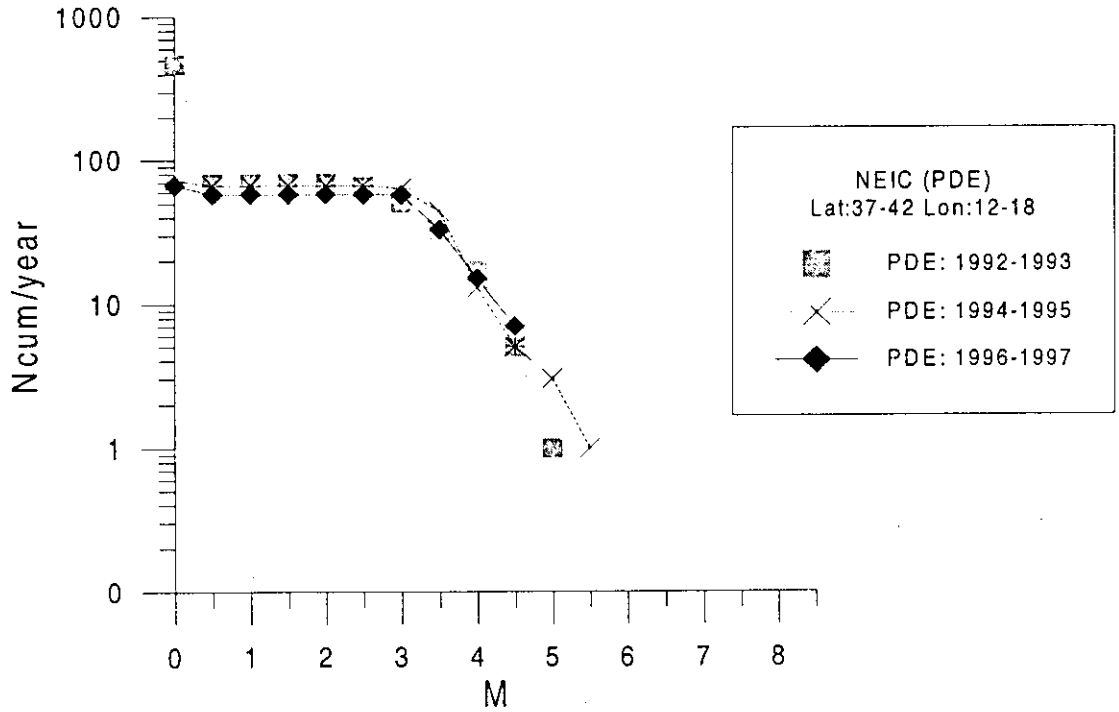
1000
100
10
1
0
Ncum/year
0
1
2
3
4
5
6
7
8
M
NEIC (PDE)
Lat:37-42 Lon:12-18
PDE: 1992-1993
PDE: 1994-1995
PDE: 1996-1997

Fig. 8b

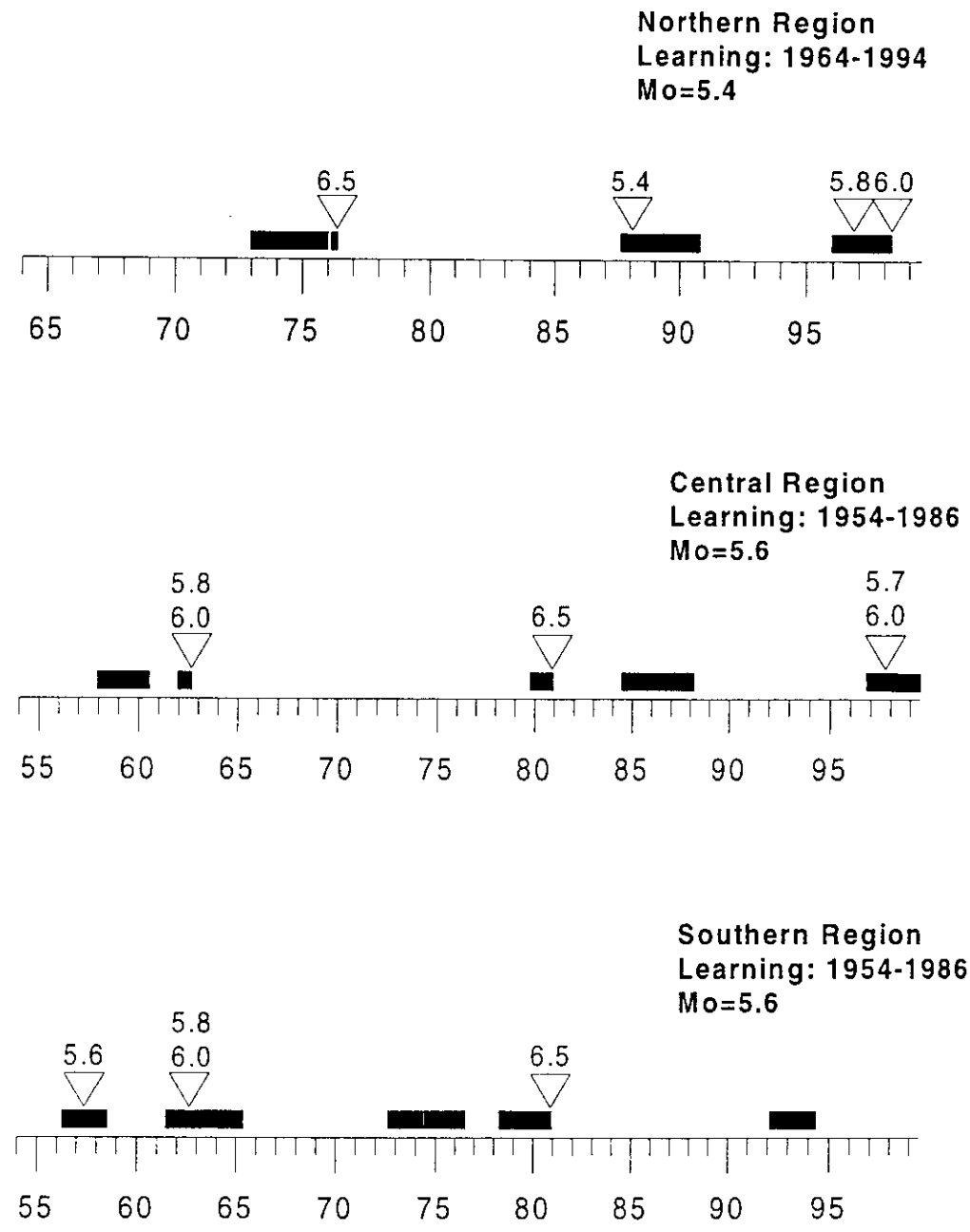
Northern Region
Learning: 1964-1994
Mo=5.4
6.5
5.4
5.86.0
65
70
75
80
85
90
95
Central Region
Learning: 1954-1986
Mo=5.6
5.8
6.0
6.5
5.7
6.0
55
60
65
70
75
80
85
90
95
Southern Region
Learning: 1954-1986
Mo=5.6
5.6
5.8
6.0
6.5
55
60
65
70
75
80
85
90
95

Fig. 9

IC/99/72

United Nations Educational Scientific and Cultural Organization
and
International Atomic Energy Agency
THE ABDUS SALAM INTERNATIONAL CENTRE FOR THEORETICAL PHYSICS

CN ALGORITHM AND LONG LASTING CHANGES IN REPORTED MAGNITUDES: THE CASE OF ITALY

A. Peresan[1]
Department of Earth Sciences, University of Trieste, via E. Weiss 1, 34127 Trieste, Italy,

G.F. Panza
Department of Earth Sciences, University of Trieste, via E. Weiss 1, 34127 Trieste, Italy
and
The Abdus Salam International Centre for Theoretical Physics, SAND Group, Trieste, Italy

and

G. Costa
Department of Earth Sciences, University of Trieste, via E. Weiss 1, 34127 Trieste, Italy.

MIRAMARE – TRIESTE
August 1999

[1]E-mail: anto@geosun0.univ.trieste.it Fax: +39-40-676-2111.

Abstract

Prediction methods based on seismic precursors, and hence assuming that catalogues contain the necessary information to predict earthquakes, are sometimes criticised for their sensitiveness to the unavoidable catalogue errors and possible undeclared variations in the evaluation of reported magnitudes. We consider a real example and we discuss the effect, on CN predictions, of a long lasting underestimation of the reported magnitudes.

Starting approximately in 1988, the CN functions in Central Italy evidence an anomalous behaviour, not associated with TIPs, which indicates an unusual absence of moderate events. To investigate this phenomenon, the magnitudes given in the used catalogue, that since 1980 is defined by the ING bulletins, are compared to the magnitudes reported by different global catalogues, such as NEIC, ISC and IDC.

The comparison is initially performed between the ING bulletins and the NEIC catalogue, considering the local, M_L, and duration, M_d, magnitudes, first within the Central region, and then extending the analysis to the whole Italian territory. To check the consistency of the conclusions drawn from ING and NEIC data, the comparison is extended to a third catalogue (ISC or IDC, depending on the considered interval of time) and, for the common events occurred within the whole Italian area, the maximum magnitudes are compared.

The difference between duration magnitudes M_d, that are reported by ING since 1983, appear quite small and constant with time. Starting in 1987, an average underestimation of about 0.5 can be attributed to M_L reported by ING, for the Central region and this difference decreases to about 0.2, when the whole Italian territory is considered. The anomalous behaviour of the CN functions disappears if a magnitude correction of +0.5 is applied to M_L reported in the ING bulletins. However, such simple magnitude shift cannot restore the real features of the seismic flow and ING bulletins are not suitable for CN algorithm application.

Introduction

CN is an intermediate-term earthquake prediction algorithm, based on the quantitative analysis of premonitory phenomena, which can be detected in the seismic flow preceding the occurrence of strong earthquakes (Gabrielov et al., 1986; Keilis-Borok and Rotwain, 1990). The quantification of the properties of the seismic flow is performed by mean of a set of functions of time (tab. 1), which evaluate variations in the seismic activity, seismic quiescence and space-time clustering of events. The normalisation of the functions allows us to apply CN to regions with different seismic activity (Keilis-Borok, 1996; Rotwain and Novikova, 1997).

The algorithm CN is applied for the monitoring of seismicity in Central Italy since 1990 (Keilis-Borok et al., 1990; Costa et al., 1996; Peresan, Costa and Panza, 1998a). The analysis of the time behaviour of CN functions for the different regionalisations defined for Central Italy (fig. 1), allowed us to observe the common anomalous flat values of some functions (see $Z_{\max}, S_{\max}, Sigma, K, G$ in fig. 2), starting approximately in 1988. The flat trend of the functions, never observed before, indicates the absence of moderate events and hence evidences an unusual decrease of the seismicity rate, suggesting us to check for possible changes in the magnitudes reported by the used catalogue.

Up to July 1997 the catalogue used for CN monitoring in Italy is the CCI1996 (Peresan, Costa and Vaccari, 1997); this catalogue is composed of the revised PFG catalogue (Postpischl, 1985), for the period 1000-1979, and since 1980 it is updated by us with the bulletins distributed by the Istituto Nazionale di Geofisica (ING). For the years 1980-1985 we use the ING paper bulletins, while beginning from 1986 the upgrading is done with the digital ING bulletins made available via e-mail till July 1997. In order to check a possible change in reported magnitudes, the ING data are compared with the following three global catalogues (tab. 2):

- the Preliminary Determinations of Epicenters distributed by NEIC (USGS), for the time period 1980-1997;
- the ISC Catalogue (International Seismological Centre), from January 1980 to December 1995;
- the Reviewed Event Bulletin of the IDC (International Data Centre) since January 1996.

A comparison for the whole interval of time 1980-1997 is feasible only between ING and NEIC data, while the test with a third data set, ISC or IDC, is possible for the periods January 1980 - December 1995 and January 1996 – June 1997, separately.

The ING bulletins contain two estimations of magnitude: the local magnitude M_L and, since 1983, the duration magnitude M_d. The NEIC global catalogue reports the magnitude m_b and M_S, both computed by NEIC, plus two values M1 and M2, that correspond to magnitudes of a different kind contributed by different agencies. A previous analysis of the NEIC catalogue (Peresan and Rotwain, 1998) allowed us to evidence that, for the Italian area, both M1 and M2 are mainly M_d and M_L, and that M_L is ten times more frequent than M_d. Furthermore, ING is among the contributors to the NEIC Preliminary Determinations of Epicentres and it supplied information for more than 600 events, from 1987 to 1997, as it can be observed simply listing the events with network code ROM reported in the PDE catalogue. The largest part of these events has magnitude below 4.0, especially when M_d is considered, while about one hundred of them have M_L greater than 4.0. The revised bulletins distributed by ISC and IDC, instead, report two and four different magnitudes respectively, specified in each case.

In order to perform the magnitude comparison, the events common to the different catalogues are identified according to the following rules: a) time difference $\Delta t \leq 1$ second; b) epicentral distance: $\Delta \mathrm{Lat} = \Delta \mathrm{Lon} \leq 1^\circ$ (Storchak,

Bird and Adams, 1998). No limitation is imposed to magnitude or depth differences.

The analysis is performed evaluating, for a fixed kind of magnitude, the quantities:

$$\Delta M = M(C1) - M(C2) \qquad (1)$$

that are the differences between the magnitudes of the same kind reported in the catalogues C1 and C2 for each of the common earthquakes.

The comparison between ING and NEIC estimations is performed considering M_L and M_d separately, among the events for which M_L and M_d is reported in both the catalogues. The events contributed to NEIC by ING, which represent a relatively small fraction of the set of the common events (less than 10%), are obviously excluded from the analysis. Initially the comparison is focussed on the Central region (fig. 1) and the yearly average values ΔM_L and ΔM_d are evaluated from the common events, contained in the area monitored with the CN algorithm. Subsequently, the analysis between ING and NEIC catalogues is extended to the whole Italian territory and its surroundings, as shown in figure 9.

Finally the events common to three different catalogues, that is to ING-NEIC-ISC and to ING-NEIC-IDC, are selected and compared for the entire Italian territory, considering all the possible couples of catalogues.

Changes in reported magnitudes for Central Italy

The analysis of the behavior of CN functions in Central Italy, allows us to identify the anomalous flat trend of some of them (fig. 2), starting approximately in 1988. Such a flat trend indicates an unusual absence of moderate events.

To look for an explanation for this anomaly we focus our attention on the magnitudes variations within the Central region currently used for the monitoring of seismicity (in dark gray in figure 1). The subcatalogue of earthquakes common to ING and NEIC contains about 800 events. The operating magnitude for CN monitoring is chosen from the Italian catalogue CCI1996, and hence from ING

bulletins, according to the priority order: M_L, M_d, M_I (Costa et al., 1996; Peresan et al., 1998a), therefore local magnitudes play a relevant role in CN analysis of seismicity. Hence, at a first stage, we study the discrepancies among the M_L reported in the two catalogues, that is the quantity:

$$\Delta M_L = M_L(\text{NEIC}) - M_L(\text{ING}) \qquad (2)$$

The histograms of ΔM_L are plotted for three contiguous ranges of magnitude (fig. 3), chosen corresponding to the CN magnitude thresholds for Central Italy. The events with $M_L < 3$ are not used by CN, the events with $3.0 \le M_L < 4.2$ are included only in the counting of aftershocks and those with $M_L \ge 4.2$ can enter into the calculation of functions. For most of the events $\Delta M_L > 0$, while a secondary peak around $\Delta M_L = 0$ can be seen in figure 3 for the smaller events.

In order to detect a possible undeclared long lasting change in the estimation of the reported M_L, the time behavior of the yearly average of ΔM_L is analysed considering only earthquakes with $M_L(\text{NEIC}) > 3.0$. The yearly number of such events is around 20-25, with two exceptions: there are 83 earthquakes in 1980 (mainly associated to the Irpinia event occurred on November 23, 1980) and, at the opposite, only 4 events in 1987.

The time distribution of ΔM_L yearly averages, shown in figure 4b, indicates the presence of a main discontinuity in 1987. The average ΔM_L, estimated using equation (2) for two subsequent periods of time, excluding the year of transition 1987, are the following (the errors correspond to the 95% confidence interval of the mean):

(1980-1986) $\Delta M_L = 0.13 \pm 0.05$

(1988-1997) $\Delta M_L = 0.64 \pm 0.04$

According to these average results, assuming $M_L(\text{NEIC})$ as reference value, an underestimation of about 0.5 can be assigned to M_L values reported by ING since 1987.

A similar analysis, performed replacing M_L with M_d in equation (2), does not evidence a significant change for M_d(ING). The relevant uncertainty associated to the value of ΔM_d (fig. 4a) for the years 1985 and 1991 is mainly due to the reduced sample size (only two events in 1985 and four in 1991). The average magnitude difference for the whole period 1983-1995, during which the sample is available, is estimated to be ΔM_d=0.30±0.04.

CN: a detective of anomalous variations in reported magnitudes

In order to understand if the evidenced variation in reported magnitudes can account for the anomalous behavior of the CN functions observed in the Central region, the quantity D=0.5 is added to the M_L reported by the ING bulletins, beginning in 1987. M_d values do not need to be modified because no significant time variation has been detected. CN is then applied to the Central region using the "corrected" catalogue and following the standard procedure of forward monitoring of seismicity: learning is not repeated and the parameters are kept unchanged.

The time diagram obtained is reported in figure 5 and clearly shows that the anomalous behavior of some CN functions, shown in figure 2, is no longer present.

Obviously this magnitude transformation cannot be used to correct the catalogue and the magnitude revision must be performed using all the available information (especially concerning variations in the acquisition system) and not only that provided by the catalogue itself. Furthermore, a simple magnitude shift, estimated from a limited sample, cannot restore all the properties of the real seismic sequence.

Several tests performed, systematically increasing or decreasing the operating magnitude in the catalogue currently used for CN monitoring (Peresan and Rotwain, 1998), show that the functions *G*, *Sigma*, Z_{max} and S_{max} (tab. 1) are

sensitive to magnitude under-estimations: they became anomalously constant for relatively long periods of time but do not cause any TIP activation. Magnitude over-estimations, instead, determine unusually high values, especially for the functions N_2 and N_3; hence the TIPs, that can be caused by relevant systematic magnitude increases, can be identified through the analysis of these functions and discarded.

Extension of the analysis to the whole Italian region

The magnitude differences have been analysed also within the Northern and Southern regions defined for the application of CN to the Italian territory (Peresan et al., 1998a). In the Northern region, the results are in very good agreement with those obtained for the Central region and, on the average, an increase of +0.5 is observed for ΔM_L in 1987. The variation in reported M_L does not affect the CN functions in the Northern region as clearly as in the Central one, because the Italian catalogue (Postpischl, 1985) covers an area that, toward the North, follows the Italian border and consequently it's fairly incomplete for CN application. This incompleteness has been filled in by Costa et al. (1996) and by Peresan et al. (1998a) with data provided by two other catalogues: ALPOR (Catalogo delle Alpi Orientali, 1987) and NEIC, thus reducing the influence of M_L(ING) in the computation of CN functions in the Northern region. The small number of common events, and hence the insufficient sample size, does not allow any conclusive analysis in the Southern region.

The analysis of the NEIC catalogue, performed by Peresan and Rotwain (1998) for the Italian area, evidenced that, among the magnitudes M_d and M_L contributed to NEIC by other agencies, M_L is ten times more frequent than M_d. From figure 6 it is possible to observe that the total yearly number of common events varies quite significantly with time. The number of common events

considerably increases after 1988, both for M_L and M_d, especially when the smaller earthquakes are considered.

The frequency distributions of ΔM_L and ΔM_d versus NEIC magnitude, are analyzed to evaluate their possible correlation with the earthquakes size (fig. 7). The linear correlation between ΔM_L and M_L(NEIC) appears quite weak, while the correlation is relevant for ΔM_d versus M_d(NEIC), the correlation coefficient being about 0.7 (significant at $p<0.05$). The distributions of ΔM_L and ΔM_d are rather different, as can easily be seen from their histograms constructed for three subsequent ranges of magnitude (fig. 8). The values of ΔM_d appear normally distributed around mean values increasing with M_d. The histograms of ΔM_L, instead, are centered around $\Delta M_L=0$, with a tail towards positive values. It seems that the set of common events can be divided into two subsets: a) events having ΔM_L distributed around zero, and b) the remaining events, having ΔM_L distributed around 0.5.

A deeper analysis, suggested by the bi-modal distribution of ΔM_L, shows that the events giving $\Delta M_L \equiv 0$ are pretty well localized in space (fig. 9). The peak in the ΔM_L histograms seems to be due to the coincidence of M_L(ING) with the M_L contributed to NEIC by some local networks, mainly from GEN (Dipartimento Scienze della Terra, Università di Genova, Italy), LDG (CEA, Laboratoire de Detection et de Geophysique, Bruyeres-le-Chatel, France), TTG (Seismological Institute of Montenegro, Podgorica, Yugoslavia) and TRI (OGS, Osservatorio Geofisico Sperimentale, Trieste, Italy), according to the standard station codes used by NEIC.

Figure 6 indicates that the size of the sample becomes relatively stable for magnitudes larger than 3.0, even if the yearly number of common events generally increases in 1988. Hence, also in this step of the analysis, the time

behavior of the yearly average of ΔM_L and ΔM_d is evaluated including only earthquakes with NEIC magnitude larger than 3.0.

The yearly average values of ΔM_L and ΔM_d are shown in figure 10. The remarkable uncertainty on the average value of ΔM_L during the year 1983 and, similarly, of ΔM_d in 1985, is due to the large dispersion of the reported values rather than to the sample size.

For the whole period 1983-1997, the yearly average of ΔM_d appears almost constant around a mean value 0.30±0.02 (fig. 10a), in very good agreement with the results obtained for the Central region. Therefore, this analysis seems to confirm that since 1983, when they started to be reported, there are no changes in the M_d provided by ING. A linear relation between the M_d reported by the two agencies, can be evaluated using the set of common events:

$$M_d(\mathrm{ING}) = 0.6\, M_d(\mathrm{NEIC}) + 1.1 \qquad (3)$$

According to this relation, the events with $M_d(\mathrm{ING}) > 3.0$ appear generally underestimated with respect to $M_d(\mathrm{NEIC})$, while smaller events turn out to be overestimated.

The diagram of the yearly average ΔM_L (fig. 10b), instead, seems to indicate the presence of two main discontinuities: the first in 1987 and the second in 1994. The average ΔM_L, estimated for the three subsequent periods of time, are the following (the error correspond to the 95% confidence interval of the mean):

(1980-1986) $\Delta M_L = 0.08 \pm 0.05$

(1988-1993) $\Delta M_L = 0.30 \pm 0.04$

(1995-1997) $\Delta M_L = 0.77 \pm 0.06$

The ΔM_L increase observed during 1987, appears less relevant within the whole Italian area than for the Central region (figures 10b and 4b). This reduction of ΔM_L can be explained by the inclusion of the M_L values contributed to NEIC by some of the neighbouring local networks, whose information often coincides

with that provided by ING. Indeed the events producing the spike around $\Delta M_L = 0$ (see fig. 8), are located close to local networks, near to the French and Slovenian borders and along the Croatian coast.

Comparison of maximum magnitudes

The use of equation (2) for M_L and M_d reported by the catalogues ING and NEIC, gives positive values for ΔM_L and ΔM_d. To establish if these differences represent a real underestimation by ING, it is necessary to extend the comparison to a third data set and to evaluate ΔM between the three possible couples of catalogues.

The heterogeneity of the magnitudes reported in the various catalogues and the reduced number of events common to three data sets, suggest us to perform the comparison considering for each event the maximum magnitude reported in each catalogue. Indeed, this criterion of magnitude selection can be applied to every catalogue and permits to take into account all the earthquakes for which at least one magnitude is reported.

The global catalogues available for our purposes during the period 1980-1995 are the NEIC and the ISC catalogues. Over the whole Italian territory, the events common to these three catalogues are about 450, while their number exceeds 4000 when only NEIC and ING are intersected. Nevertheless, most of the earthquakes excluded by the intersection with the ISC catalogue has magnitude below 3.5, hence the subset of events common to the three catalogues permits to keep a significant number of events, for which magnitude determinations can be considered quite reliable in global catalogues.

The average values of ΔM_{max}, obtained from equation (2) for the two couples of catalogues NEIC-ING and ISC-ING, are always significantly greater than zero, even with some fluctuations in time, while ΔM_{max} between the two global catalogues NEIC and ISC is within the standard errors in magnitude

determination. The differences ΔM_{max}, estimated for each pair of catalogues and for the period 1980-1995, give the following average values:

(NEIC-ING) $\Delta M_{max} = 0.43 \pm 0.04$

(ISC-ING) $\Delta M_{max} = 0.30 \pm 0.05$

(NEIC-ISC) $\Delta M_{max} = 0.12 \pm 0.04$

For the subsequent period of time (January 1996-June 1997), the analysis is performed among ING, NEIC and IDC catalogues. The average values estimated for ΔM_{max}, using the 200 common events, are:

(NEIC-ING) $\Delta M_{max} = 0.31 \pm 0.05$

(IDC-ING) $\Delta M_{max} = 0.30 \pm 0.04$

(NEIC-IDC) $\Delta M_{max} = 0.01 \pm 0.06$

These values are in good agreement with those estimated considering M_L and M_d in the catalogues NEIC and ING. According to Bath (1973), even in the best cases we have to expect errors as large as ±0.3 units in a calculated magnitude, nevertheless average differences between ING and the global catalogues are systematically equal or larger than +0.3, therefore, the magnitude reported by ING bulletins is generally underestimated with respect to the global catalogues.

Conclusions

Prediction methods based on seismic precursors are sometimes criticised for their sensitivity to the unavoidable catalogue errors and undeclared changes in the evaluation of the reported magnitudes (Habermann, 1991; Habermann and Creamer, 1994). This study provides a real example, showing the effect of a long lasting systematic magnitude underestimation on CN predictions.

The absence of moderate events detected by CN functions and consequently the unusual decrease of the seismicity rate within the Central region, used for the

CN monitoring in Italy, suggested us to check for possible systematic errors in the reported magnitudes.

A detailed comparative analysis, focused on M_L and M_d, has been performed between ING and NEIC catalogues, within the area corresponding to the Central region. The ΔM_d provided by ING appear quite stable in time and small, while a variation of about 0.5 has been evidenced in ΔM_L, starting in 1987. This difference decreases to about 0.2 when the analysis is extended to a wider area including the whole Italian territory, but always indicates that M_L values given by ING are underestimated.

The comparison, extended to a third catalogue corroborates the hypothesis of a general magnitude underestimation in the Italian ING bulletins, with respect to the global catalogues.

The robustness of CN algorithm has been successfully tested with respect to the catalogue substitution, once the homogeneity of data is preserved (Peresan and Rotwain, 1998; Peresan et al., 1998b), and with respect to the short-term inadvertent increase in reported magnitude, indicated by Zuniga and Wyss (1995) for the Italian catalogue, which does not seem to affect the results of predictions (Peresan et al., 1998a).

Therefore, our study indicates that a careful analysis of CN functions allows us to detect relevant long lasting undeclared changes in the reported magnitudes and may permit to separate such effects from the anomalies in the seismic flow that define the Times of Increased Probability (TIPs) for the occurrence of a strong event. The results of our analysis cannot be used for catalogue correction, therefore the ING catalogue cannot be used for CN monitoring and one has to make use of a different data set like NEIC catalogue.

Acknowledgements

We are grateful to Prof. I.M. Rotwain and V.I. Kossobokov for their relevant contribution in the catalogues analysis. We wish to thank Prof. G. Molchan and

T. Kronrod for the useful discussions and their precious suggestions. This research has been supported by MURST (40% and 60% funds), by CNR (contracts n° 96.02968.PF54 and n° 97.00507.PF54) and by INTAS (n° 94-0232).

References

ALPOR, 1987. Catalogue of the Eastern Alps. Osservatorio Geofisico Sperimentale, Trieste, Italy (computer file).

Bath, M., 1973. Introduction to seismology. Birkhauser. Basel, pp.365.

Costa, G., Panza, G.F. & Rotwain, I.M., 1995. Stability of premonitory seismicity pattern and intermediate-term earthquake prediction in central Italy. *Pure and Appl. Geophys.* **145**, 2, 259-275.

Costa, G., Stanishkova, I.O., Panza, G.F., & Rotwain, I.M., 1996. Seismotectonic models and CN algorithm: the case of Italy. *Pure and Appl. Geophys.* **147**, 1, 1-12.

Gabrielov, A.M., O.E. Dmitrieva, V.I. Keilis-Borok, V.G. Kossobokov, I.V. Kutznetsov, T.A. Levshina, K.M. Mirzoev, G.M. Molchan, S.Kh. Negmatullaev, V.F. Pisarenko, A.G. Prozorov, W. Rinheart, I.M. Rotwain, P.N. Shelbalin, M.G. Shnirman & Schreider, S.Yu, 1986. Algorithms of long-term earthquakes' prediction. International School for Research Oriented to Earthquake Prediction-algorithms, Software and Data Handling (Lima, Perù, 1986).

Habermann, R.E., 1991. Seismicity rate variations and systematic changes in magnitudes in teleseismic catalogs. *Tectonophysics*, **193**, 277-289.

Habermann, R.E. & Creamer, F., 1994. Catalog errors and the M8 earthquake prediction algorithm. *Bull. Seism. Soc. Am*, **84**, 1551-1559.

Keilis-Borok, V.I., 1996. Intermediate term earthquake prediction. *Proc. Natl. Acad Sci.* USA, **93**, 3748-3755.

Keilis-Borok, V.I., Kutznetsov, I.V., Panza, G.F., Rotwain, I.M., & Costa, G., 1990. On intermediate-term earthquake prediction in Central Italy. *Pure and Appl. Geophys.* **134**, 79-92.

Keilis-Borok, V.I. & Rotwain, I.M., 1990. Diagnosis of time of increased probability of strong earthquakes in different regions of the world: algorithm CN. Phys. *Earth Planet. Inter.*, **61**, 57-72.

Peresan, A., Costa, G. & Vaccari, F., 1997, CCI1996: the Current Catalogue of Italy. International Centre for Theoretical Physics. Internal report IC/IR/97/9. Trieste. Italy.

Peresan, A., Costa G. & Panza, G.F., 1998a. Seismotectonic model and CN earthquake prediction in Italy. *Pure and Appl. Geophys.* **154**, 281-306.

Peresan, A., I.M. Rotwain & Panza, G.F., 1998b. Evaluation of the stability of algorithm CN with respect to random errors in magnitude: Central Italy. *Annales Geophysicae*. Abstract supplement, **16**, 1091.

Peresan, A. & Rotwain, I.M., 1998. Analysis and definition of magnitude selection criteria for NEIC (PDE) data, oriented to the compilation of a homogeneous updated catalogue for CN monitoring in Italy. International Centre for Theoretical Physics. Internal report. Trieste. Italy.

Postpischl, D., 1985. Catalogo dei terremoti italiani dall'anno 1000 al 1980. C.N.R.-Progetto Finalizzato Geodinamica.

Rotwain, I., & Novikova, O., 1997. Performance of the Earthquake Prediction Algorithm CN in 21 Regions of the World. Fourth Workshop on Non-Linear Dynamics and Earthquake Prediction, 6 - 24 October 1997, Trieste: ICTP, H4.SMR/1011-21.

Storchak, D.A., A.L. Bird & Adams, R.D., 1998. Location Discrepancies. XXVI General Assembly of E.S.C., Tel Aviv, Israel. 1998.

Zuniga, F.R., & Wyss, M., 1995. Inadvertent changes in magnitude reported in earthquake catalogs: their evaluation through the b-value estimates. *Bull. Seism. Soc. Am.*, **5**, 1858-1866.

Table captions

Tab. 1 – Definition of the time functions used in the CN algorithm for the quantification of the properties of the seismic flow (from Keilis-Borok et al., 1990). The magnitude thresholds m_1, m_2, m_3, that allow the normalisation of the functions, are fixed accordingly to the average yearly frequency of the main shocks, which occurred within the region during the learning period (1954-1986). For the Central region (in dark grey in fig. 1): $m_1 = 4.2$, $m_2 = 4.5$, $m_3 = 5.0$, corresponding to the standard yearly average frequencies $n_1 = 3.0$, $n_2 = 1.4$, $n_3 = 0.4$.

Tab. 2 – Data set used for the catalogue comparison. For each agency are indicated: the period of time, the kind of catalogue and how the data are made available.

$N_2(t)$ Number of main shocks with $M \geq m_3$, which occurred in the time interval (t-3 years, t).

$K(t)$ $K(t) = K_1 - K_2$, where K_i is the number of main shocks with $M_i \geq m_2$ and origin time (t-2j years)$\leq t_i \leq$(t-2(j-1) years).

$G(t)$ $G(t)=1-P$, where P is the ratio among the number of the main shocks with $M_j \geq m_2$ ($m_2 > m_1$) and the number of the main shocks with $M_j \geq m_1$. Only main shocks with origin time t_j in the interval (t-1 year)$\leq t_j \leq$t are considered.

SIGMA(t)$=\Sigma 10^{\beta(M_i-\alpha)}$; the main shocks with $m_1 \leq M_i \leq M_0-0.1$ and origin time (t-3 years)$\leq t_i \leq$t are included in the summation; $\alpha=4.5$, $\beta=1.00$.

$S_{max}(t)$ $S_{max}(t)=\max\{S_1/N_1, S_2/N_2, S_3/N_3\}$ where S_j is calculated as SIGMA(t) for the events with the origin time (t-j years)$\leq t_i \leq$(t-(j-1) years), and N_j is the number of earthquakes in the sum.

$Z_{max}(t)$ $Z_{max}(t)=\max\{Z_1/N_1^{2/3}, Z_2/N_2^{2/3}, Z_3/N_3^{2/3}\}$ where Z_j is calculated as S_j, but with $\beta=0.5$ and N_j is the number of earthquakes in the sum.

$N_3(t)$ Number of main shocks with $M \geq m_2$, which occurred in the time interval (t-10 years, t-7 years)

$q(t)$ $q(t)=\sum_{j=1}^{6} \max\{0,6a_2-n_j\}$, where a_2 is the average annual number of main shocks with $M_j \geq m_2$, n_j is the number of main shocks with $M_j \geq m_2$ and origin time (t-(8+j) years)$\leq t_i \leq$(t-(2+j) years).

$B_{max}(t)$ Maximum number of aftershocks for each main shock, counted within a radius of 50 km for the first 2 days after the main shock.

Tab. 1

IDC - Prototype International Data Centre		
1996-1997	*REB-Reviewed Event Bulletin*	web
ING - Istituto Nazionale di Geofisica		
1980-1984	*Revised ING bulletins*	printed
1985-1986	*Digital ING bulletins*	floppy-disk
1987-1997	*Digital ING bulletins*	ftp
ISC - International Seismological Centre		
1980-1995	*ISC Catalogue*	cd-rom
NEIC - National Earthquake Information Centre, USGS		
1980-1989	*Global Hypocenters Data Base*	cd-rom
1990-1997	*Earthquake Hypocenters Data Files*	ftp

Tab. 2

Figure captions

Fig. 1 – Different regionalisations defined for CN application to Central Italy. The continuous line delimits the region defined by Keilis-Borok et al. (1990), while the dotted line shows the region proposed by Costa et al. (1995). The region currently used for CN monitoring, defined strictly following the seismotectonic model (Peresan et al., 1998a), corresponds to the dark grey area.

Fig. 2 – Time diagrams of the standard CN functions obtained for the Central region shown in fig. 1. Functions *Sigma*, S_{max} and Z_{max} are evaluated for $4.2 \le M \le 4.6$, functions *K*, *G*, *N3*, *q* for $M \ge 4.5$ and functions N2 for $M \ge 5.0$; magnitude thresholds have been selected according to the general rules for normalisation of functions (Keilis-Borok and Rotwain, 1990). The corresponding diagram of TIPs (Times of Increased Probabilities), obtained using the CCI1996 catalogue, is given at the top of the figure (triangles indicate the occurrence of strong events). The dotted line indicates the beginning of the anomalous behaviour of functions.

Fig. 3 - Histograms of the number of events versus ΔM_L, for three subsequent ranges of magnitude, in the Central region (dark grey area in fig. 1).

Fig. 4 – Yearly average of (a) ΔM_d and (b) ΔM_L between NEIC and ING catalogues, calculated for the common events which occurred within the Central region (fig. 1). Error bars correspond to the 95% confidence interval of the mean.

Fig. 5 – Time diagrams of the CN functions obtained for the Central region using the "corrected" catalogue, in which the quantity D=0.5 is added to M_L(ING) beginning in 1987.

Fig. 6 - Yearly number of common events used for the comparison between ING and NEIC catalogues. (a) Events used for M_d analysis; (b) Events used for M_L analysis.

Fig. 7 - Frequency scatter-plots of (a) ΔM_d and (b) ΔM_L versus the corresponding NEIC magnitude.

Fig. 8 - Histograms of the number of events versus ΔM for three subsequent ranges of magnitude for (a) ΔM_d and (b) ΔM_L. Events with ΔM lower or equal to the upper boundary are counted in each interval.

Fig. 9 - (a) Space histogram of the number of common events used for ΔM_L evaluation. (b) Space distribution of events with $\Delta M_L = 0$.

Fig. 10 - Yearly average of (a) ΔM_d and (b) ΔM_L between NEIC and ING catalogues. Only events with magnitude greater than 3.0 have been considered. Error bars correspond to a 95% confidence level on the calculated average.

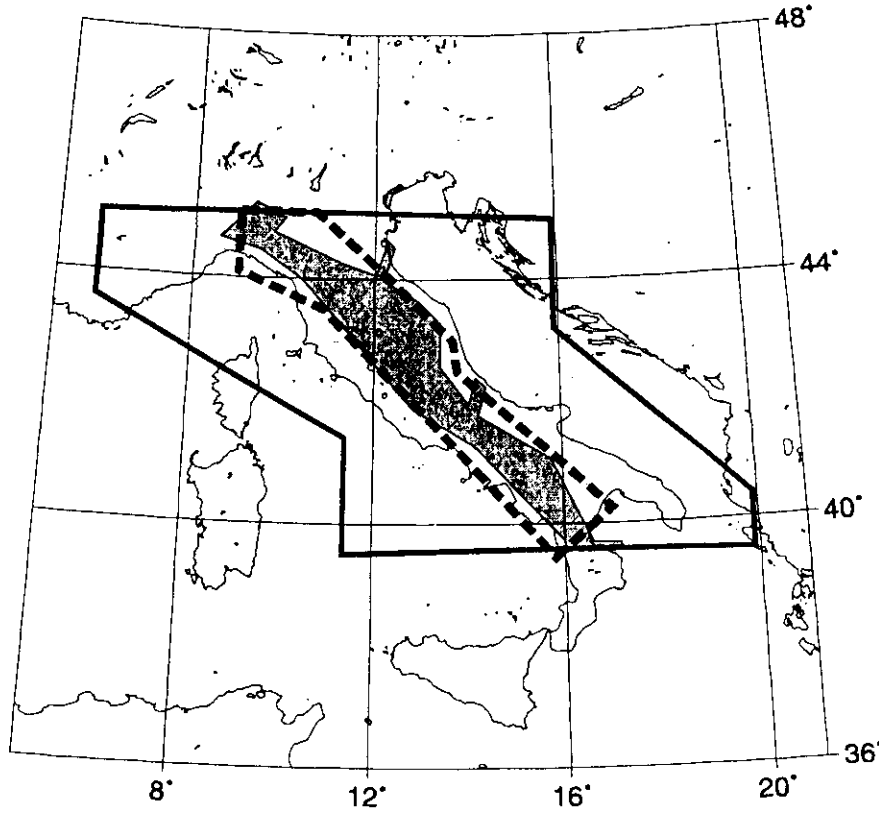

Fig. 1

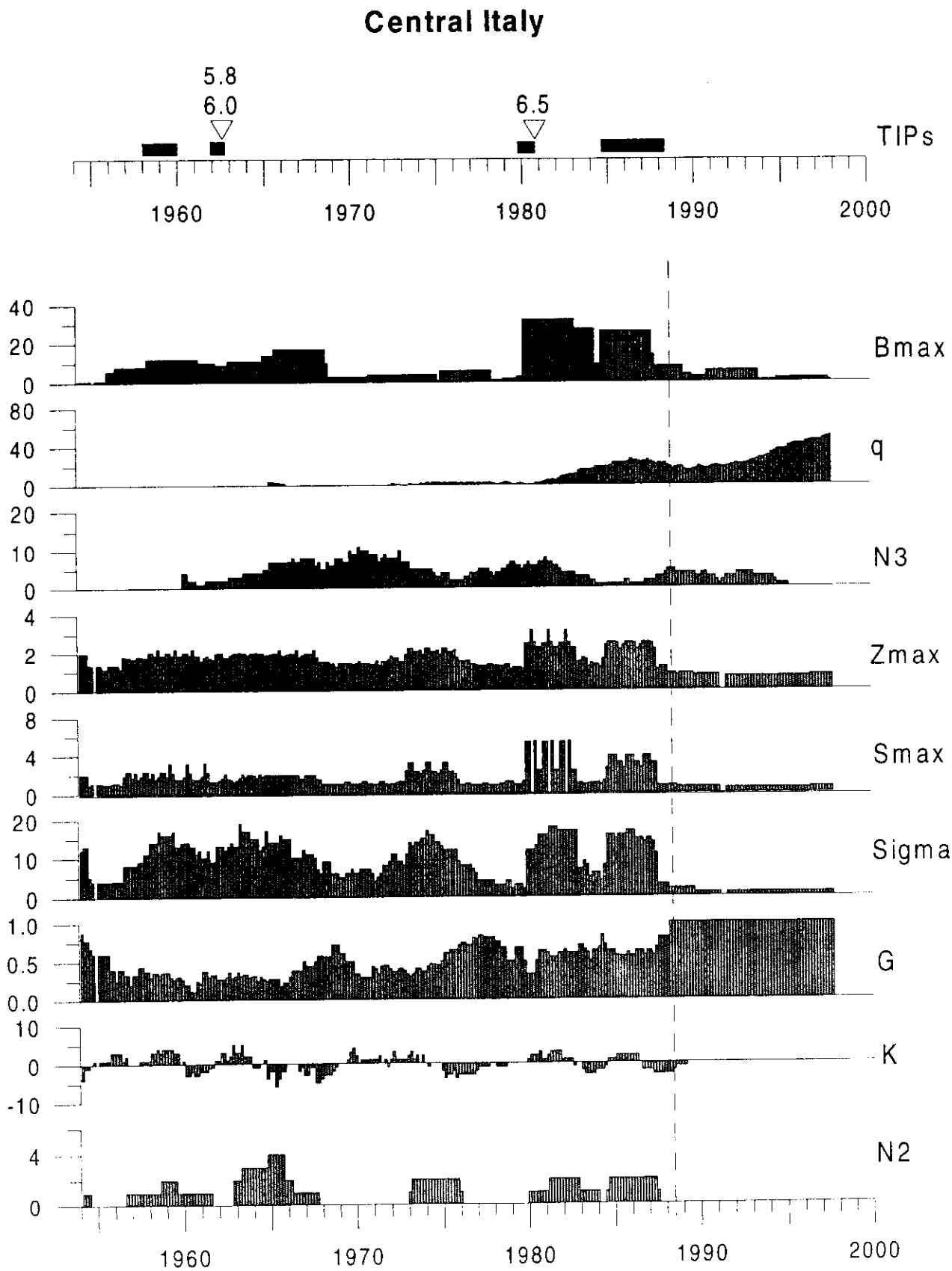
Central Italy
5.8
6.0
6.5
TIPs
1960
1970
1980
1990
2000
40
20
0
Bmax
80
40
0
q
20
10
0
N3
4
2
0
Zmax
8
4
0
Smax
20
10
0
Sigma
1.0
0.5
0.0
G
10
0
-10
K
4
0
N2
1960
1970
1980
1990
2000

Fig. 2

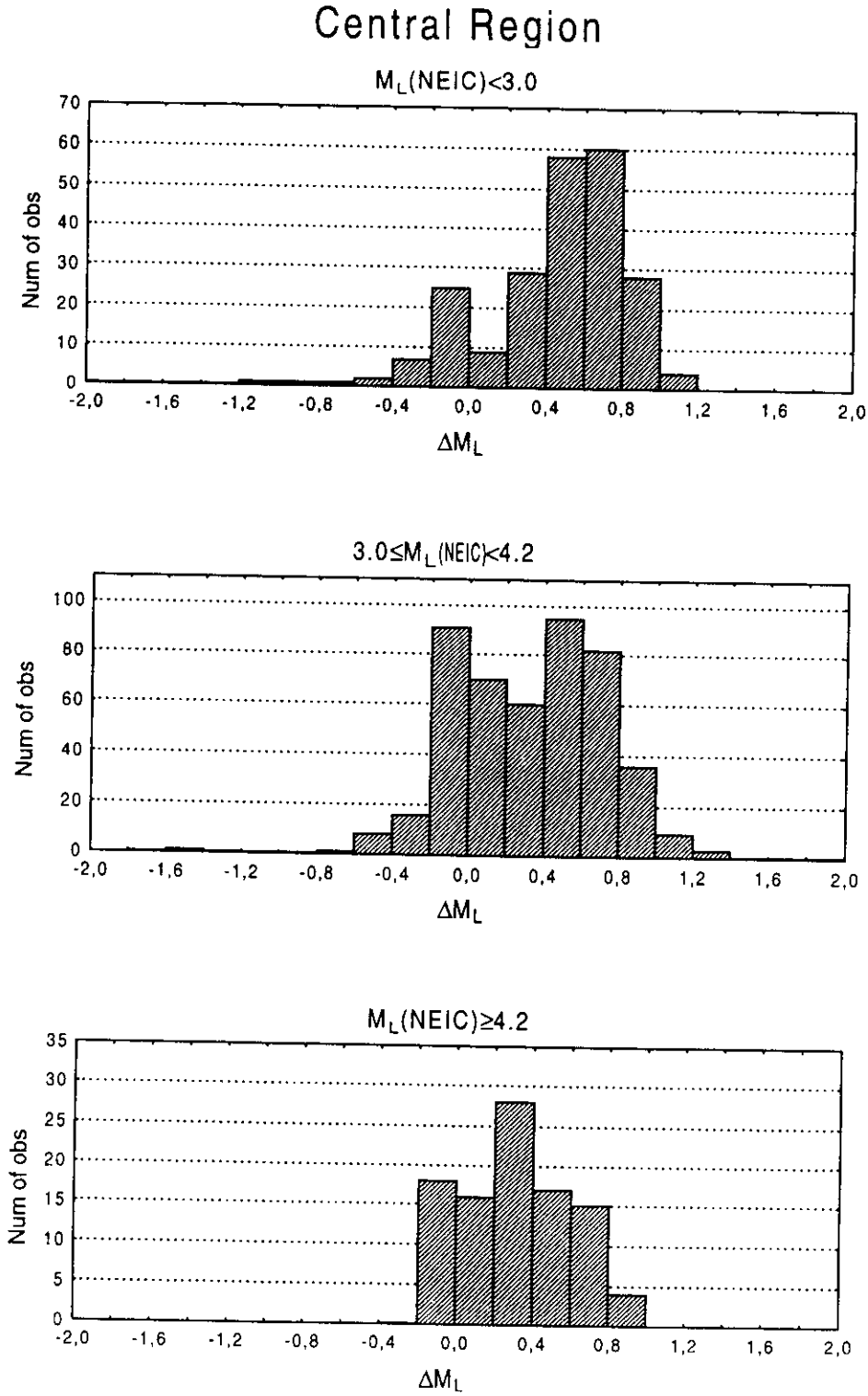
Central Region
M_L(NEIC)<3.0
Num of obs
70
60
50
40
30
20
10
0
-2,0
-1,6
-1,2
-0,8
-0,4
0,0
0,4
0,8
1,2
1,6
2,0
ΔM_L
3.0≤M_L(NEIC)<4.2
Num of obs
100
80
60
40
20
0
-2,0
-1,6
-1,2
-0,8
-0,4
0,0
0,4
0,8
1,2
1,6
2,0
ΔM_L
M_L(NEIC)≥4.2
Num of obs
35
30
25
20
15
10
5
0
-2,0
-1,6
-1,2
-0,8
-0,4
0,0
0,4
0,8
1,2
1,6
2,0
ΔM_L

Fig. 3

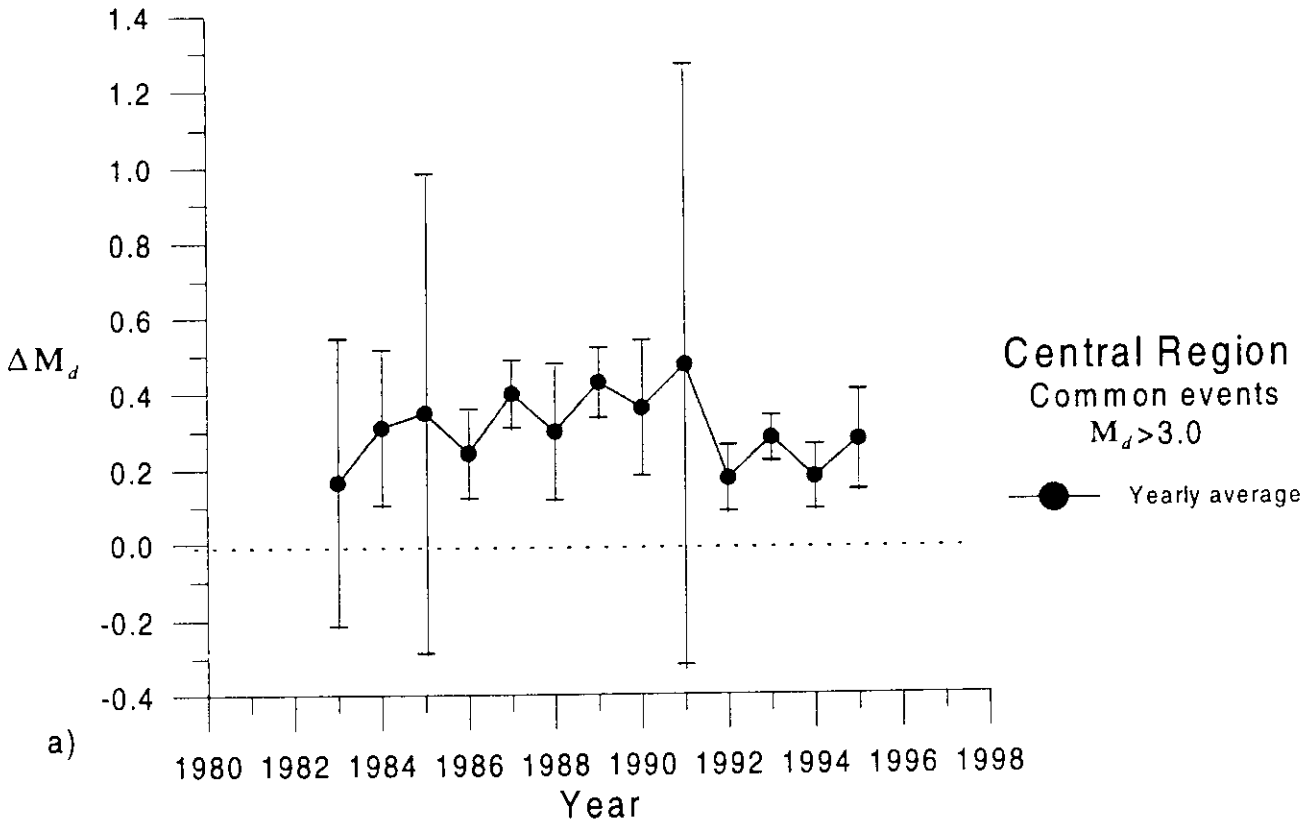
1.4
1.2
1.0
0.8
0.6
0.4
0.2
0.0
-0.2
-0.4
ΔM_d
a)
1980 1982 1984 1986 1988 1990 1992 1994 1996 1998
Year
Central Region
Common events
M_d>3.0
Yearly average

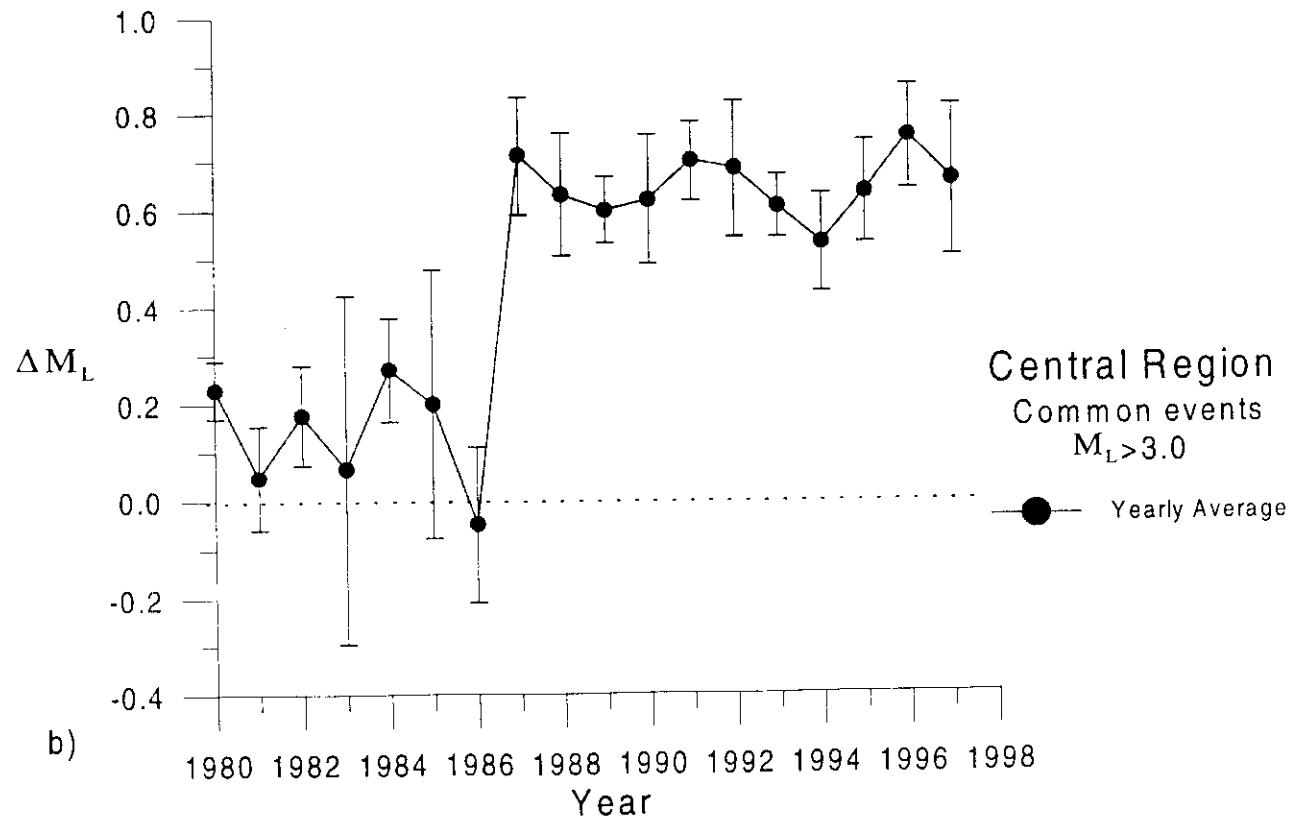
1.0
0.8
0.6
0.4
0.2
0.0
-0.2
-0.4
ΔM_L
b)
1980 1982 1984 1986 1988 1990 1992 1994 1996 1998
Year
Central Region
Common events
M_L>3.0
Yearly Average

Fig. 4

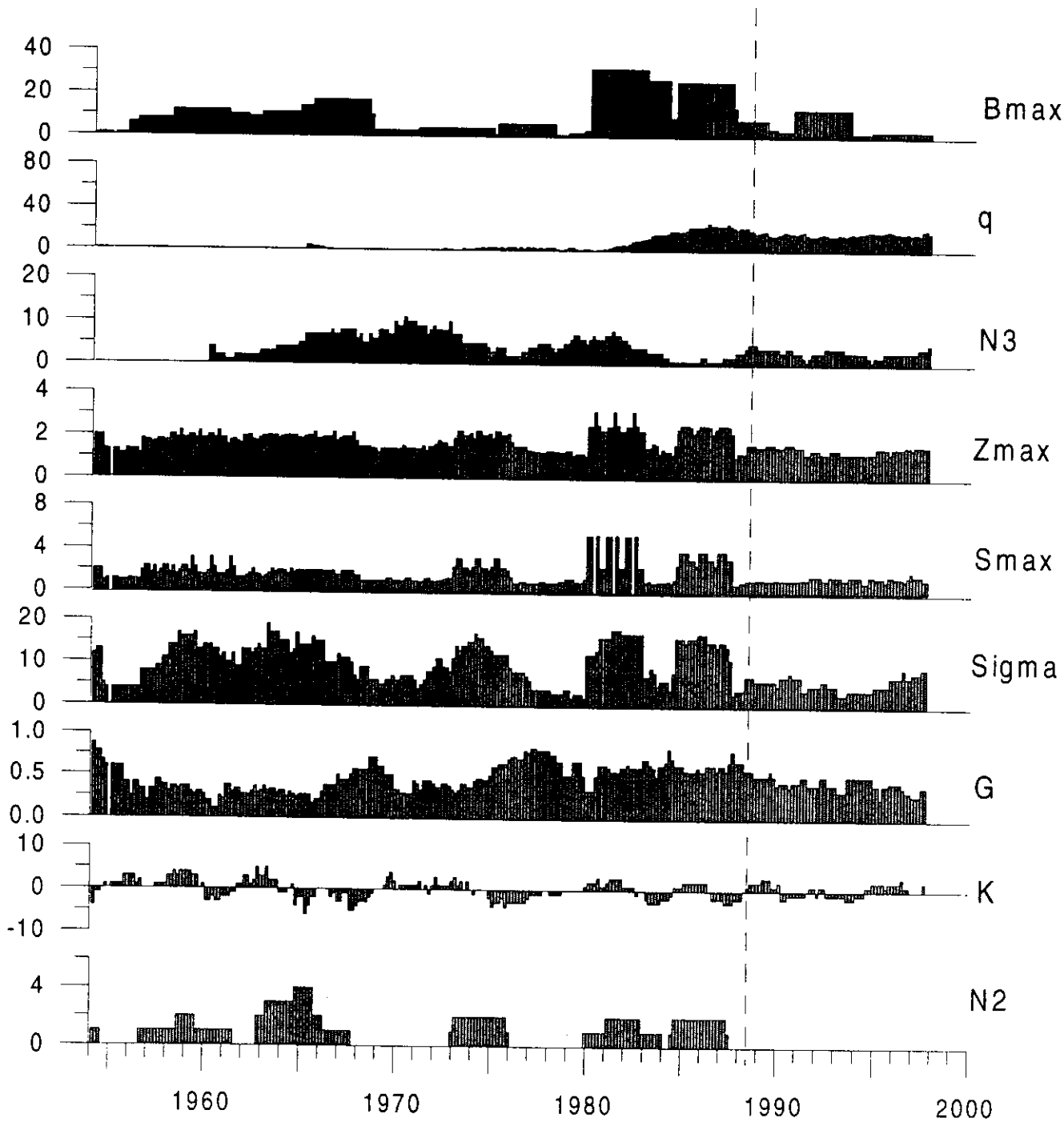
Central Italy
ML(ING)+0.5 since 1987
Bmax
q
N3
Zmax
Smax
Sigma
G
K
N2
1960
1970
1980
1990
2000

Fig. 5

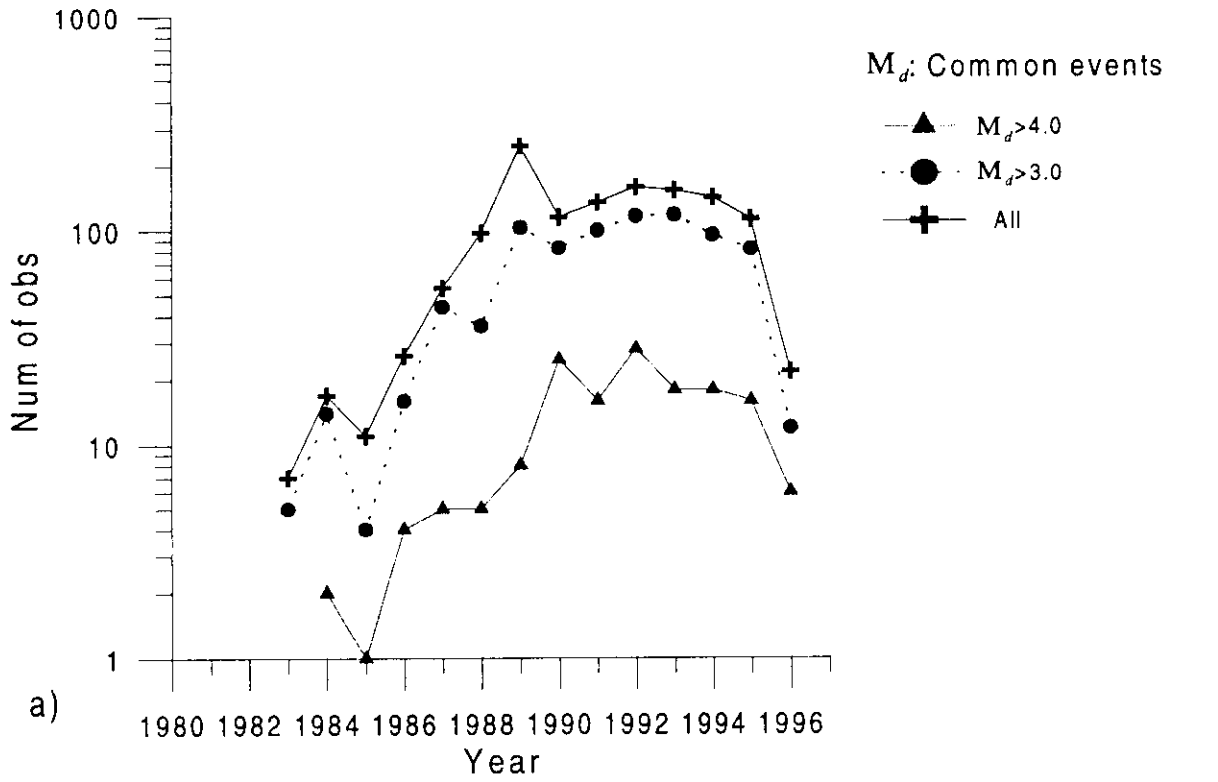
1000
100
10
1
Num of obs
a)
1980 1982 1984 1986 1988 1990 1992 1994 1996
Year
M_d: Common events
M_d>4.0
M_d>3.0
All

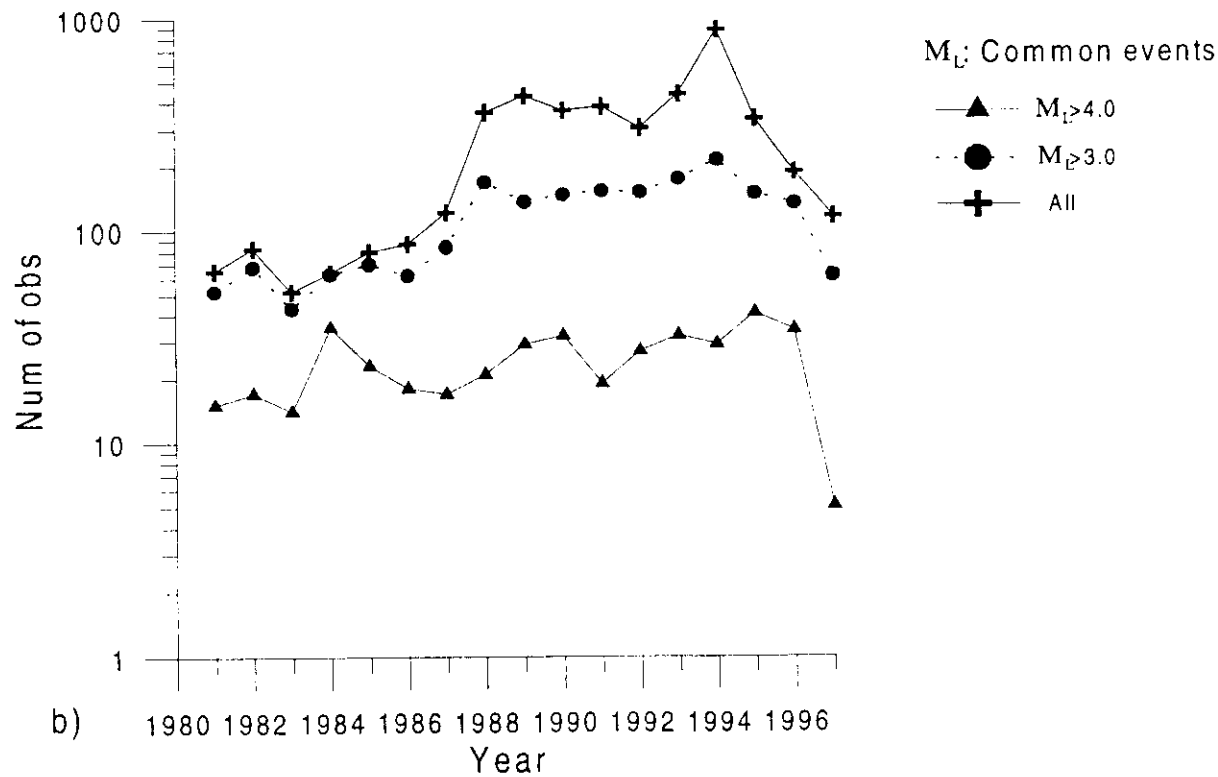
1000
100
10
1
Num of obs
b)
1980 1982 1984 1986 1988 1990 1992 1994 1996
Year
M_L: Common events
M_L>4.0
M_L>3.0
All

Fig. 6

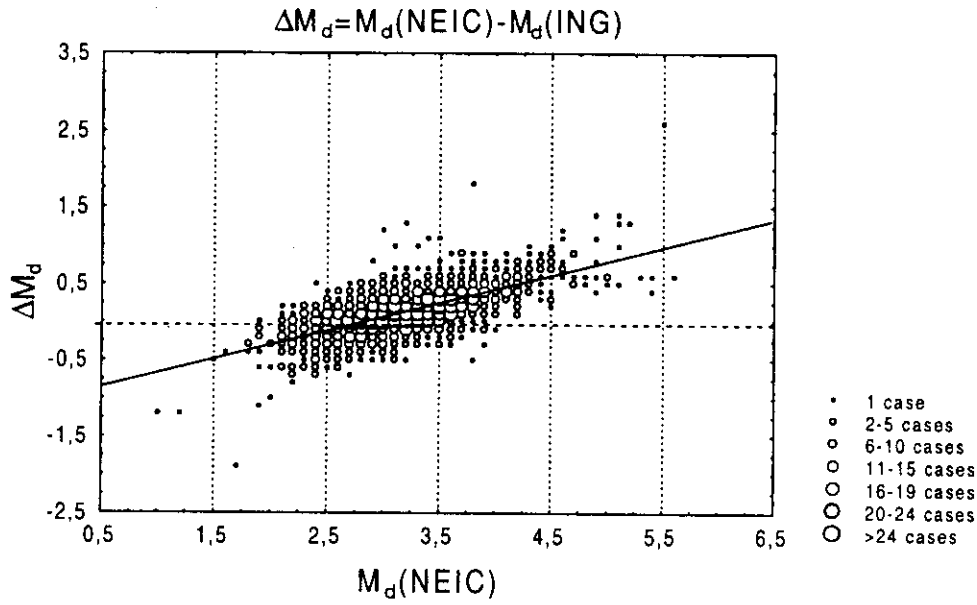
ΔMd=Md(NEIC)-Md(ING)
3,5
2,5
1,5
0,5
-0,5
-1,5
-2,5
ΔMd
0,5
1,5
2,5
3,5
4,5
5,5
6,5
Md(NEIC)
1 case
2-5 cases
6-10 cases
11-15 cases
16-19 cases
20-24 cases
>24 cases

a)

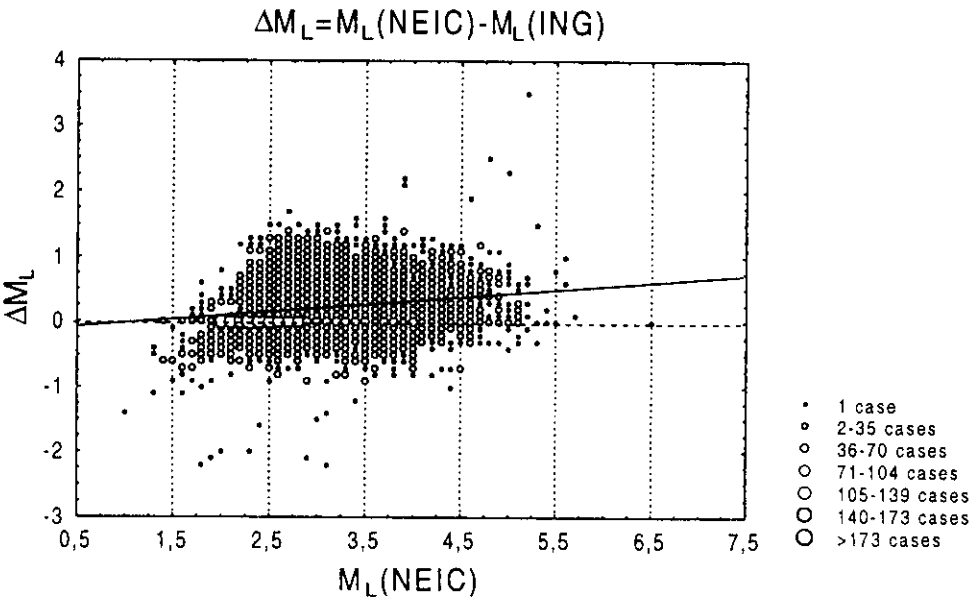
ΔML=ML(NEIC)-ML(ING)
4
3
2
1
0
-1
-2
-3
ΔML
0,5
1,5
2,5
3,5
4,5
5,5
6,5
7,5
ML(NEIC)
1 case
2-35 cases
36-70 cases
71-104 cases
105-139 cases
140-173 cases
>173 cases

b)

Fig. 7

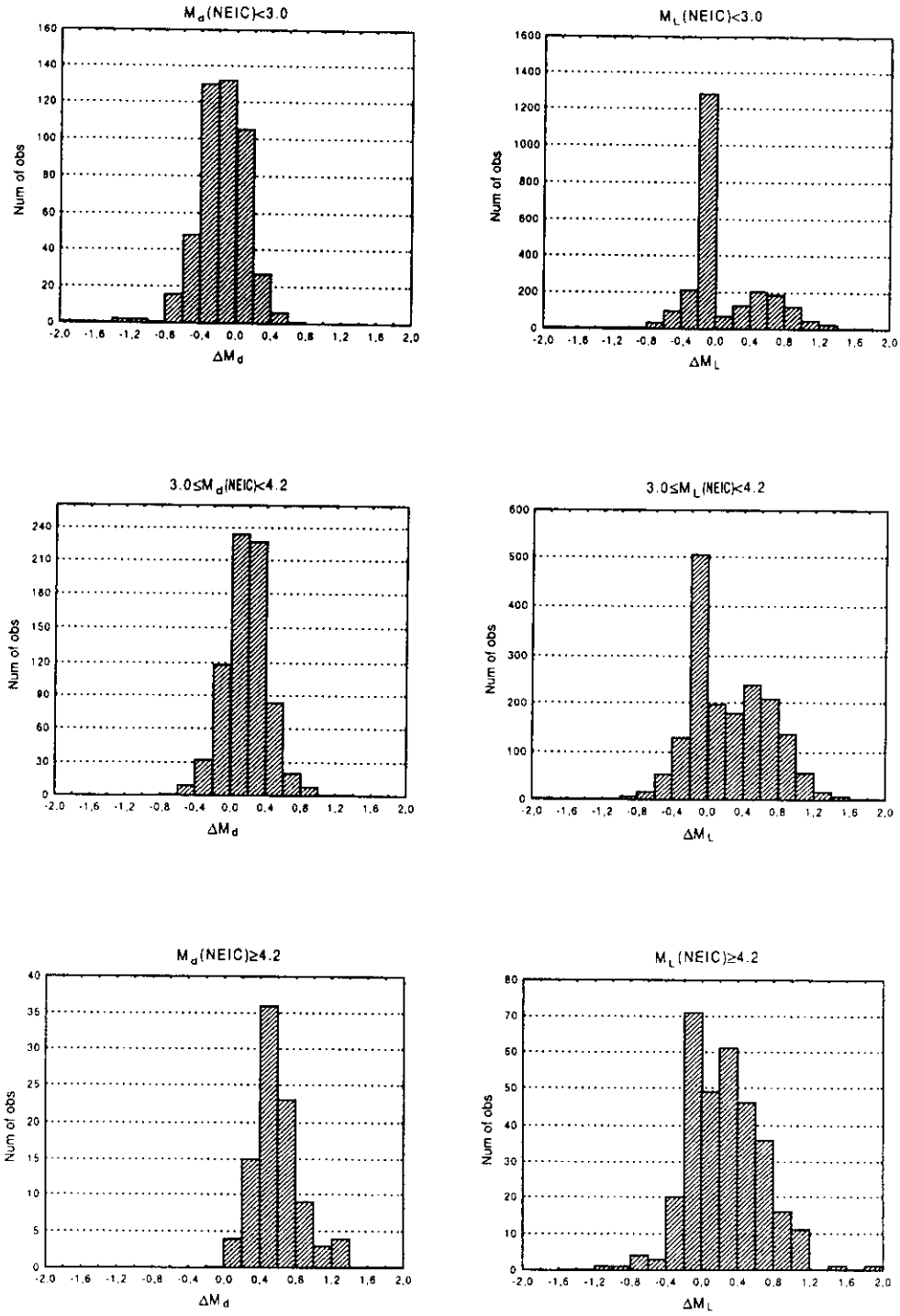
M_d(NEIC)<3.0
Num of obs
ΔM_d
M_L(NEIC)<3.0
Num of obs
ΔM_L
3.0≤M_d(NEIC)<4.2
Num of obs
ΔM_d
3.0≤M_L(NEIC)<4.2
Num of obs
ΔM_L
M_d(NEIC)≥4.2
Num of obs
ΔM_d
M_L(NEIC)≥4.2
Num of obs
ΔM_L

Fig. 8

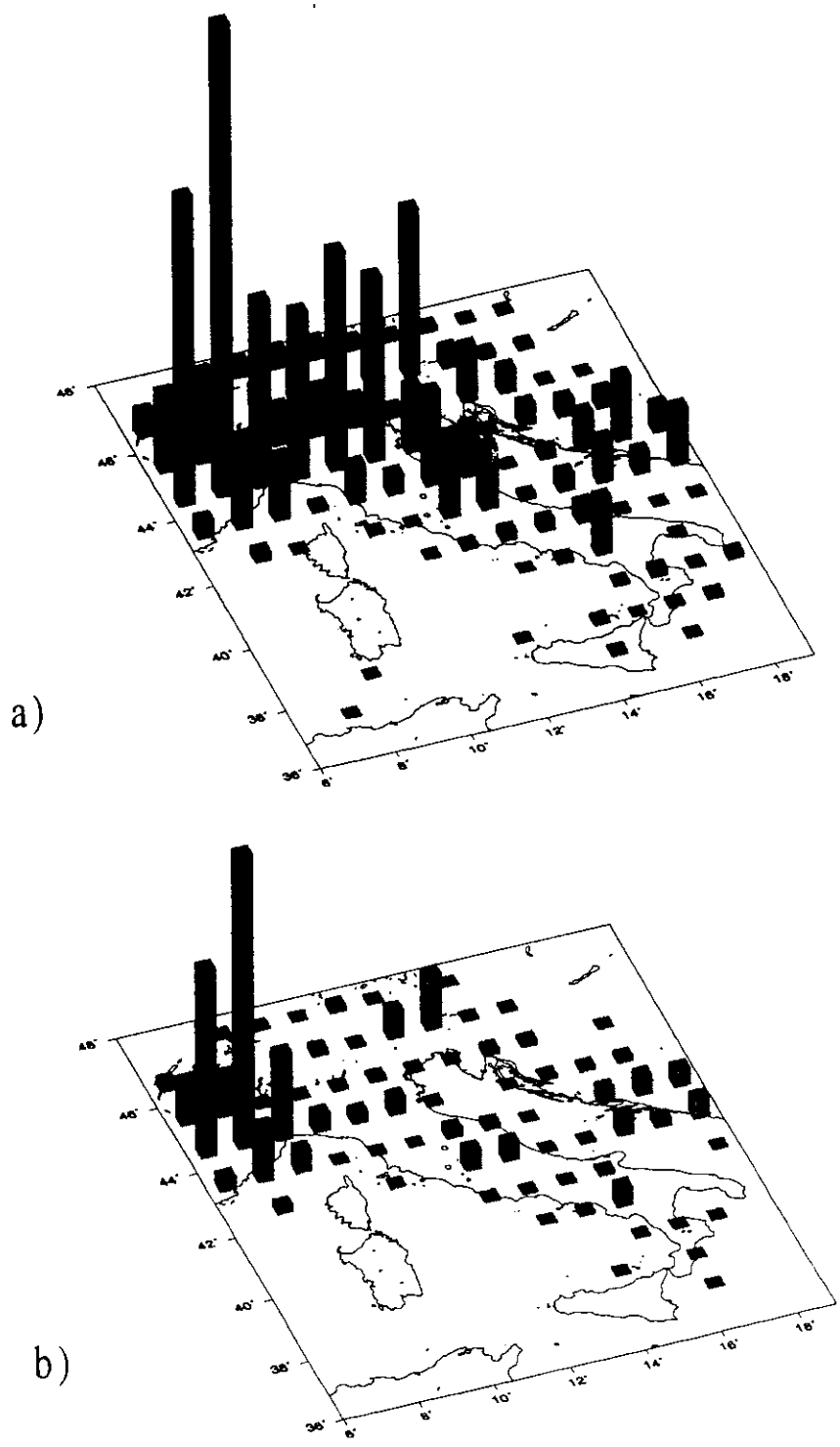

Fig. 9

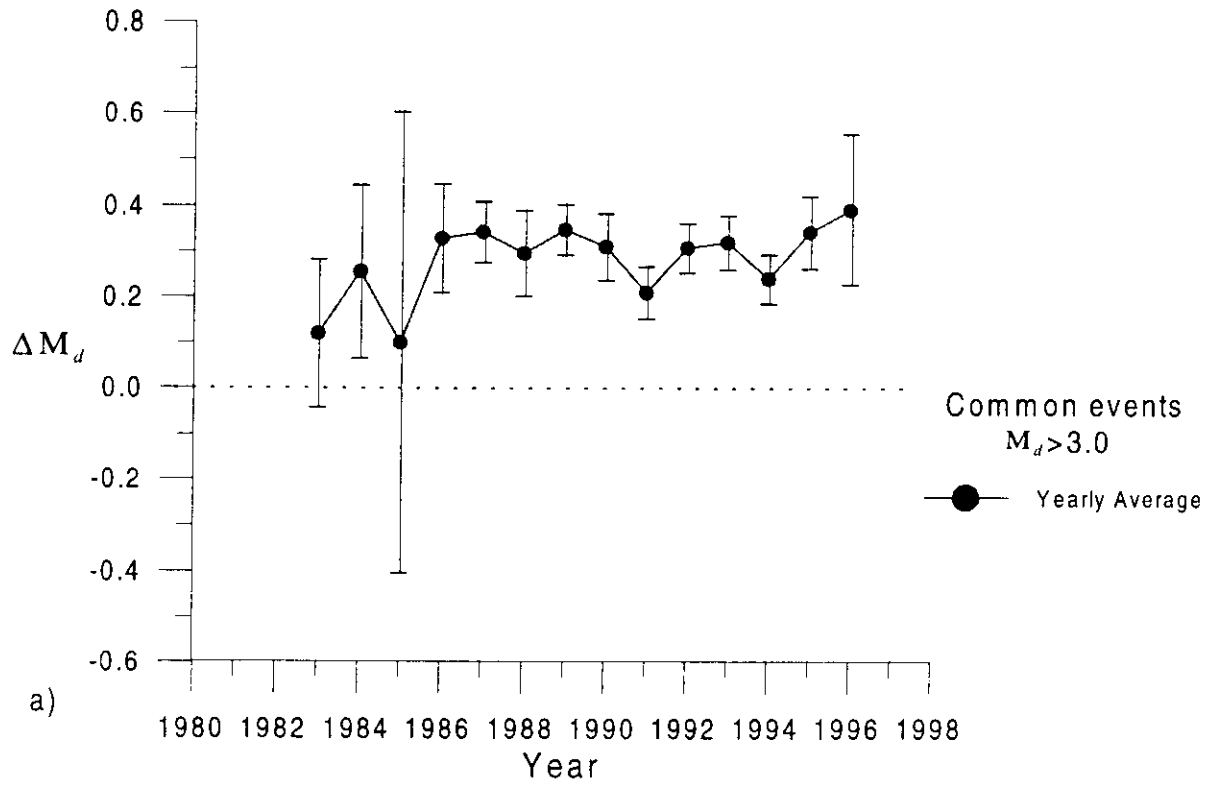
0.8
0.6
0.4
0.2
0.0
-0.2
-0.4
-0.6
ΔM_d
a)
1980 1982 1984 1986 1988 1990 1992 1994 1996 1998
Year
Common events
M_d>3.0
Yearly Average

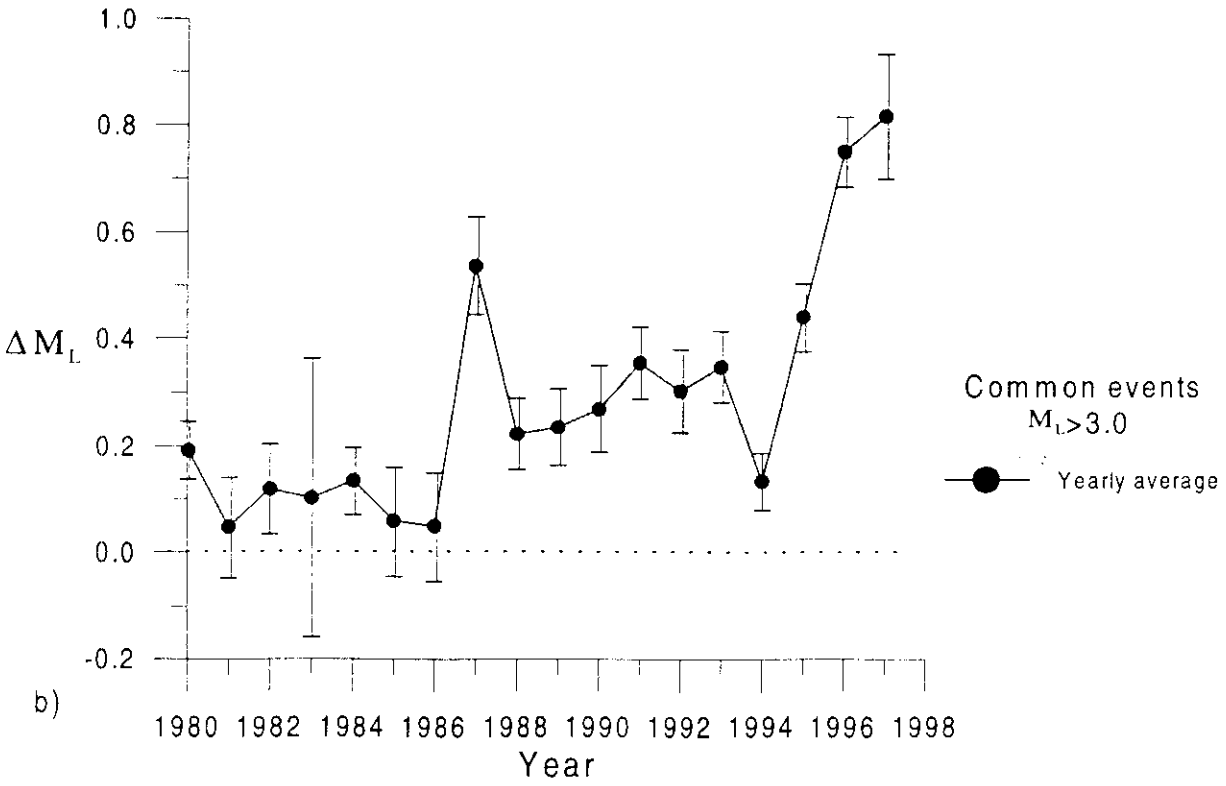
1.0
0.8
0.6
0.4
0.2
0.0
-0.2
ΔM_L
b)
1980 1982 1984 1986 1988 1990 1992 1994 1996 1998
Year
Common events
M_L>3.0
Yearly average

Fig. 10

united nations
educational, scientific
and cultural
organization

international atomic
energy agency

the
abdus salam
international centre for theoretical physics

H4.SMR/1150 - 7

Fifth Workshop on Non-Linear Dynamics
and Earthquake Prediction

4 - 22 October 1999

Experiments with CN in Italy and Seismic Hazard

Part III

G. F. Panza

Department of Earth Sciences
Trieste, Italy

DETERMINISTIC SEISMIC HAZARD ASSESSMENT

Giuliano F. Panza[1,2], F. Vaccari[1,3], R. Cazzaro[1]
[1]Dipartimento di Scienze della Terra - Università di Trieste
[2]The Abdus Salam International Centre for Theoretical Physics, SAND Group, Trieste
[3]GNDT - Gruppo Nazionale per la Difesa dai Terremoti - CNR, Rome

Abstract

Using the available information about regional structural models, past seismicity, and the seismotectonic regime in Italy, we have generated a set of synthetic seismograms covering the whole Italian territory on a 0.2° x 0.2° grid. Peak values of ground motion (displacement, DMAX, and velocity, VMAX) and Design Ground Acceleration (DGA) based on Eurocode 8 (EC8, 1993), extracted from the synthetic signals, have been compared with the macroseismic intensities felt in Italy. The correlation relations that we have obtained are in a good agreement with empirical relationships given by other authors and compare quite well with the few observations available in the Italian territory.

1. Introduction

The procedure for the deterministic seismic zoning developed by Costa et al. (1992, 1993) represents one of the new and most advanced approaches and can, at the same time, be used as a starting point for the development of an integrated procedure that combines the advantages of the probabilistic and of the deterministic methods, thus minimizing their drawbacks.

Synthetic seismograms are constructed to model ground motion at the sites of interest, using the available knowledge of the physical process of earthquake generation and wave propagation in realistic anelastic media. In first-order zoning a database of seismograms covering the area of interest (at a regional scale) is computed, with a low order approximation of the effects of lateral heterogeneities. Synthetic seismograms are very efficiently generated by the modal summation technique (Panza, 1985; Florsch et al., 1991), so it is possible to perform detailed parametric analyses at reasonable costs. For example, different source and structural models can be taken into account in order to create a wide range of possible scenarios from which to extract essential information for decision making.

Once the parametric analysis is performed and the gross features of the seismic haz-

F. Wenzel et al. (eds.), Vrancea Earthquakes: Tectonics, Hazard and Risk Mitigation, 269–286.

ard are defined, a more detailed modelling of ground motion is possible. We can take into account the local geological and geotechnical conditions at a specific site of interest, using either the hybrid method, which combines, for the description of wave propagation in anelastic heterogeneous media, the modal summation with finite differences techniques (Fäh et al., 1990; Fäh, 1992), or the fully analytical modal summation method, extended to laterally varying media (Vaccari et al. 1989; Romanelli et al., 1996; 1997). This deterministic modelling goes well beyond the conventional deterministic approach taken in hazard analyses - in which only a simple wave attenuation relation is invoked - in that it includes full waveform modelling.

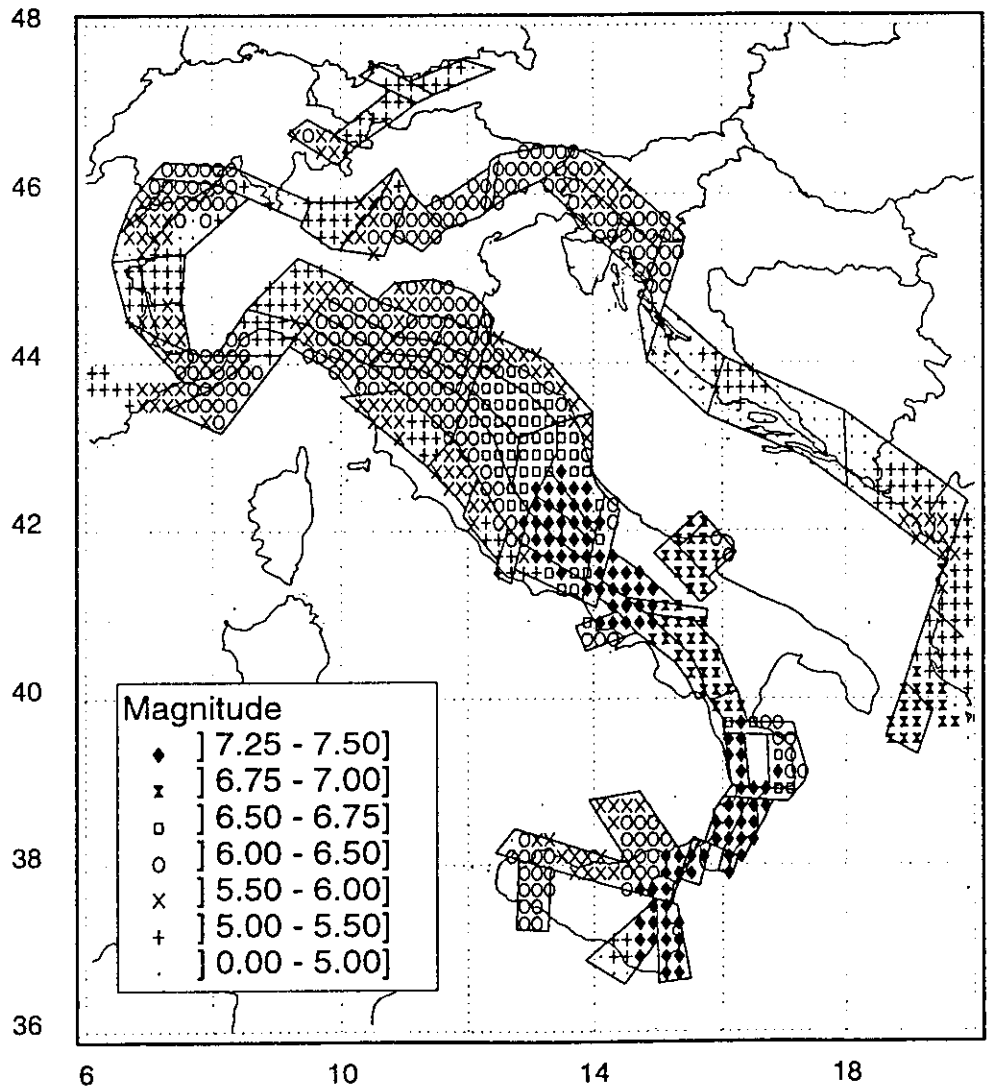

Figure 1. Smoothed magnitude distribution for the cells belonging to the seismogenic zones defined by GNDT (Corsanego et al., 1997).

2. Deterministic zoning using synthetic seismograms

Starting from the available information on the Earth's structure, seismic sources and the level of seismicity of the investigated area, it is possible to estimate the maximum ground velocity and displacement in a given frequency band (VMAX and DMAX respectively), Design Ground Acceleration (DGA) or any other parameter relevant to seismic engineering, which can be extracted from the computed theoretical signals. This procedure allows us to obtain a realistic estimate of the seismic hazard also in those areas for which scarce (or no) historical or instrumental information is available, and to perform the relevant parametric analyses.

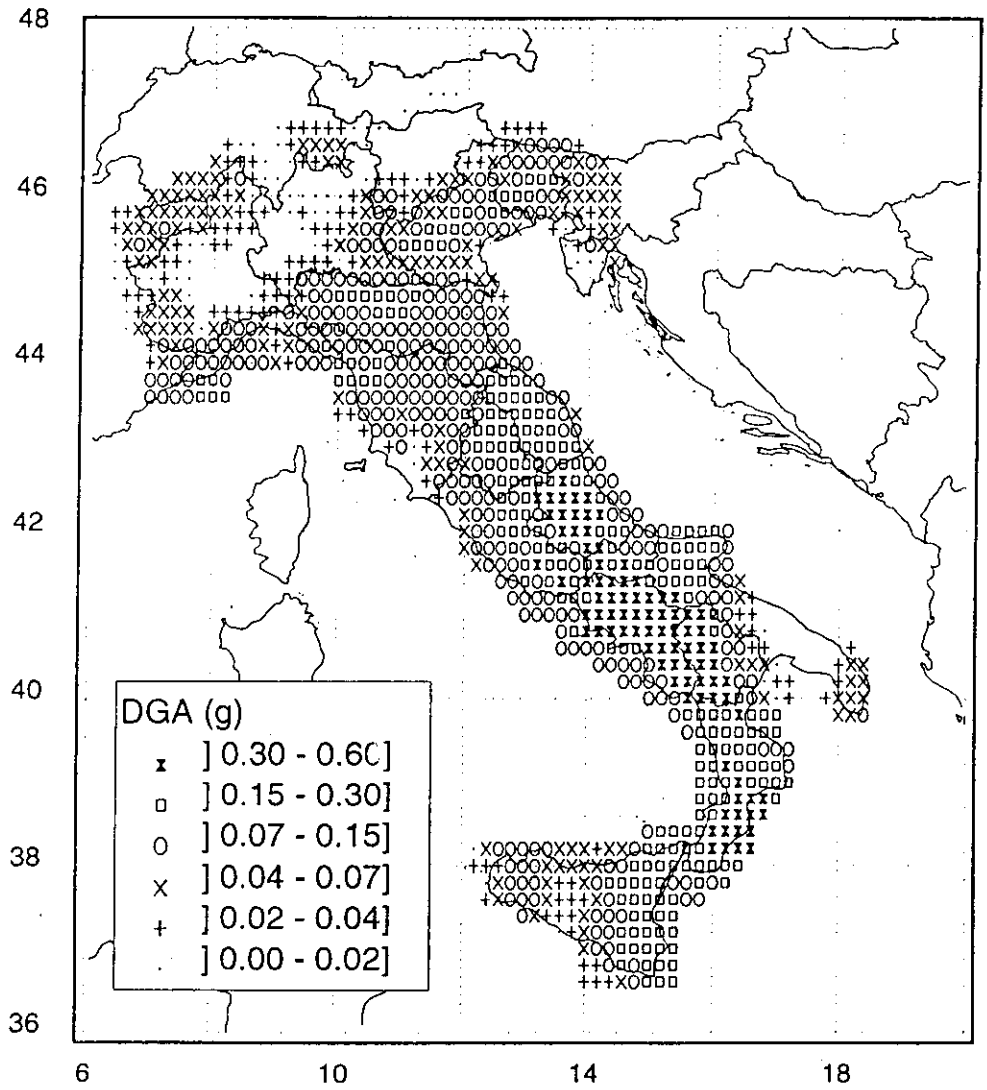

Figure 2. Distribution of DGA, obtained as a result of the deterministic zonation extended to high frequencies using the design spectra of EC8 for soil A.

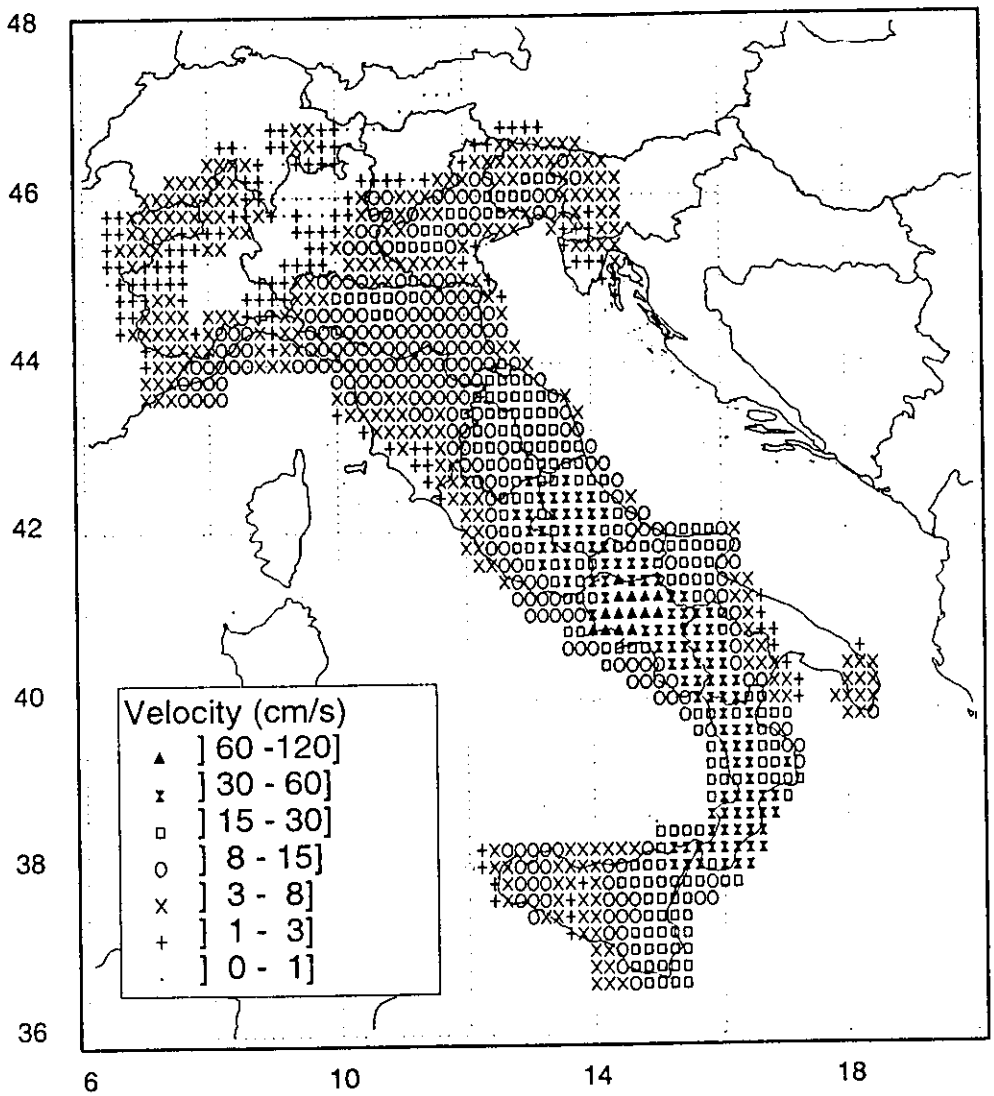

Figure 3a. Horizontal VMAX distribution, obtained as a result of the deterministic zonation.

To reduce the amount of computations, the seismic sources can be grouped into homogeneous seismogenic areas, and for each group a representative focal mechanism can be defined. The scalar seismic moment associated with each source is determined from the analysis of the maximum magnitude observed in the epicentral area.

To derive the distribution of the maximum observed magnitude over the territory, the image of the seismicity given by the earthquake catalogue is smoothed as follows. We divide the considered territory with cells 0.2° by 0.2°. To each cell we assign the magnitude value, M_i, of the most energetic event that occurred within it, and we use a centered smoothing window with a radius of 0.6° in order to take into account the source extension in space, and location uncertainties. Only the cells falling within the seismogenic areas are retained and a double-couple point source, corresponding to a magnitude M_i, is placed in

the centre of each cell, with a depth equal 10 km for $M_i < 7$, and equal to 15 km for the larger events.

If available, reliable values of maximum expected magnitudes can be used in a straightforward way instead of M_i.

Detailed examples of the input data used in the procedure are described by Costa et al. (1993) and Panza and Vaccari (1994).

The file NT (version 4.1) prepared by GNDT (Camassi and Stucchi, 1996) is used for the definition of seismicity. The smoothed magnitude distribution for the cells belonging to the seismogenic zones defined in April 1996 by GNDT (Corsanego et al., 1997) is given in Figure 1.

The synthetic signals are computed for an upper frequency limit of 1 Hz, and are properly scaled according to the (smoothed) magnitude (to be conservative we have assumed that all magnitude values given in the NT file are Ms) associated with the cell of the

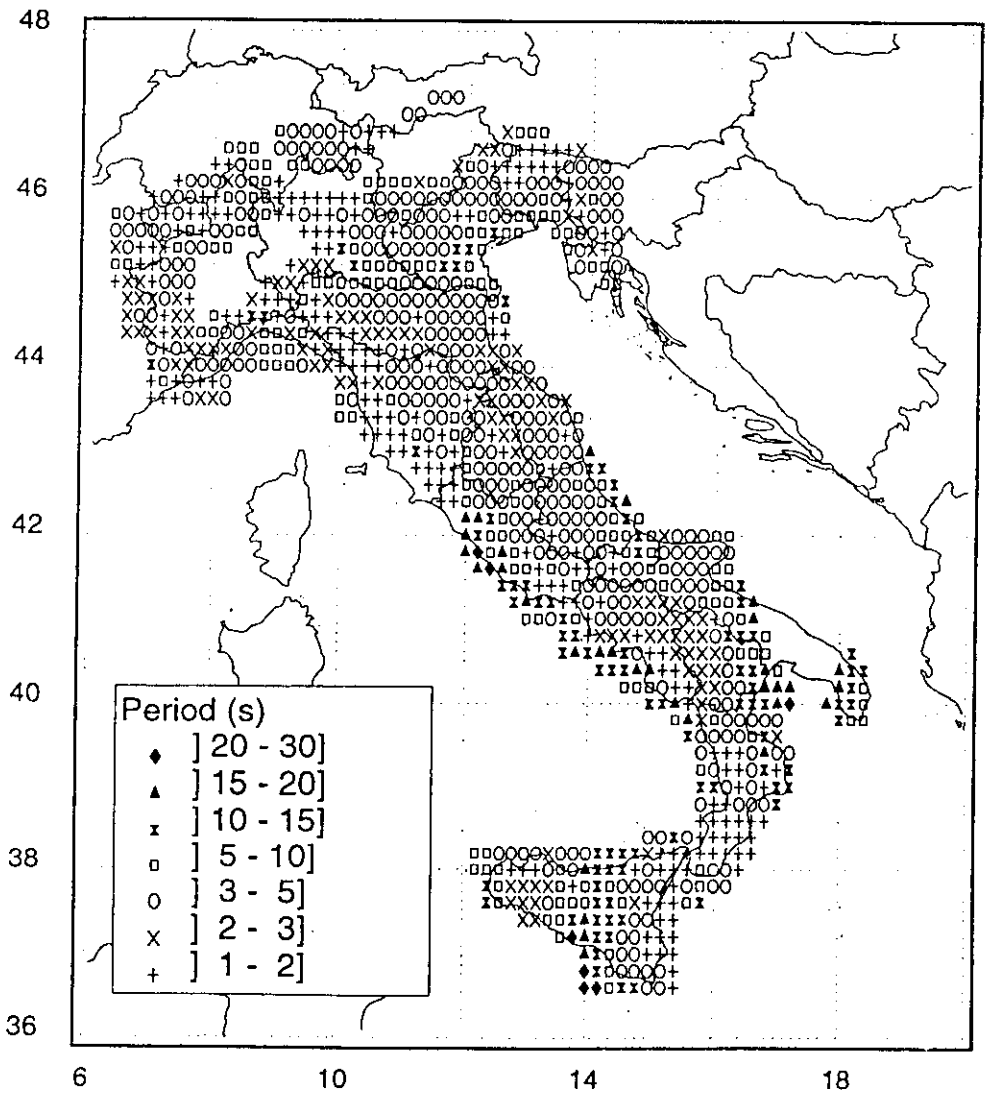

Figure 3b. Period in seconds of the maximum of VMAX at each site.

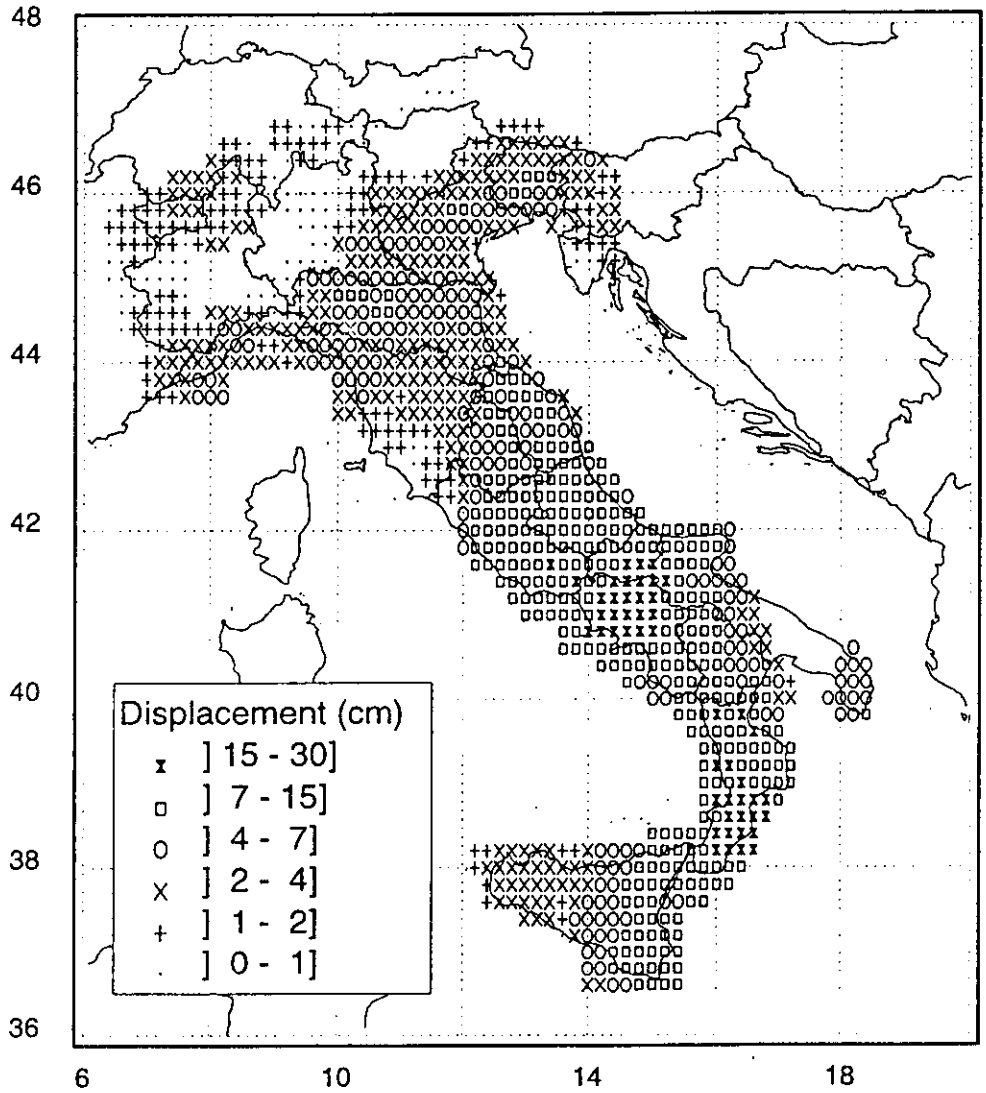

Figure 4a. Horizontal DMAX distribution, obtained as a result of the deterministic zonation.

source, using the moment-magnitude relation given by Kanamori (1977) and the spectral scaling law proposed by Gusev (1983) as reported in Aki (1987). The deterministic results may be extended to higher frequencies by using design response spectra (Panza et al., 1996), for instance Eurocode 8 (EC8, 1993), which define the normalized elastic acceleration response spectrum of the ground motion, for 5% critical damping. In general this operation should be made taking into account the soil type. For Italy, the used regional structural models (Costa et al., 1993) are all of type A, as defined in EC8, therefore we can immediately determine DGA (Figure 2) and the Maximum Spectral Value (MSV) using the EC8 parameters for soil A.

In addition to DGA we focus on the maximum ground velocity, and displacement, VMAX, and DMAX. We compute the complete time series, therefore we are not limited to this choice, and it is possible to consider other parameters, like Arias intensity (Arias, 1970) or other integral quantities that can be of interest in earthquake engineering or

engineering seismology. Since recordings of many different sources are associated to each site, different maps can be produced. If one single value is to be plotted on a map, then only the maximum value of the analyzed parameter is considered - maximum velocity and displacement respectively in Figures 3a and 4a. In Figures 3b and 4b the periods associated with the maxima given in Figures 3a and 4a are shown. It can be seen that in some regions, like for instance Central Italy around latitude 42°N, long periods in the range between 20s and 30s are very frequent. They belong to signals generated by strong earthquakes occurring at a large distance from the site (about 90km), while the magnitude of the closer events, which are responsible for the higher frequencies (between 2 s and 5 s in our computations), is not large enough to let high frequencies dominate the scenario.

The deterministic procedure, for the definition of seismic input, is particularly suitable in a situation like the one of Bucharest where the dominant periods of the larger accelerations are above 1 s. The results of the deterministic zonation of Romania have been shown by Radulian et al. (1997).

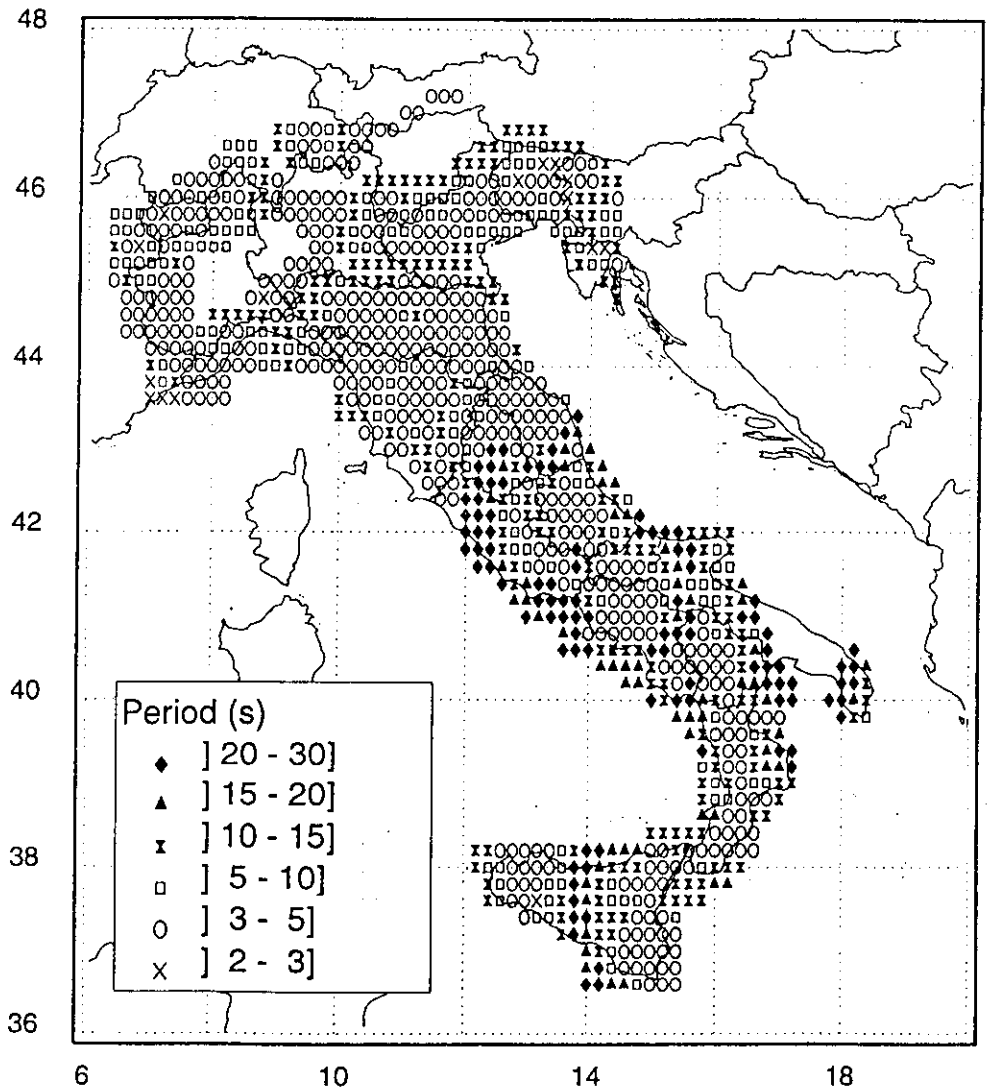

Figure 4b. Period in seconds of the maximum of DMAX at each site.

3. Validation of the synthetic models against independent observations

A quantitative validation is supplied by the observed accelerograms recorded during the Irpinia earthquake (23 November 1980) and the Friuli earthquake (6 May 1976). The source rupturing process of the Irpinia event is very complex (e.g., Bernard and Zollo, 1989) and the dimension of the source has been estimated to be of the order of several tens of km. Nevertheless, it seems that the signal recorded at the station of Sturno is mostly due to a single sub-event that occurred rather close to the station itself, while the energy contributions coming from other parts of the source seem unimportant (Vaccari et al., 1990). With the cutoff frequency at 1 Hz, the horizontal components accelerograms recorded at Sturno have been low-pass filtered to be compared with the computed signals for the Irpinia region. The example shown in Figure 5 refers to the NS component but the same considerations can be applied to the EW component of motion.

The early phases and the maximum (AMAX) of the recorded signal (upper trace) and the synthetic one computed in the point-source approximation (middle trace), are in very

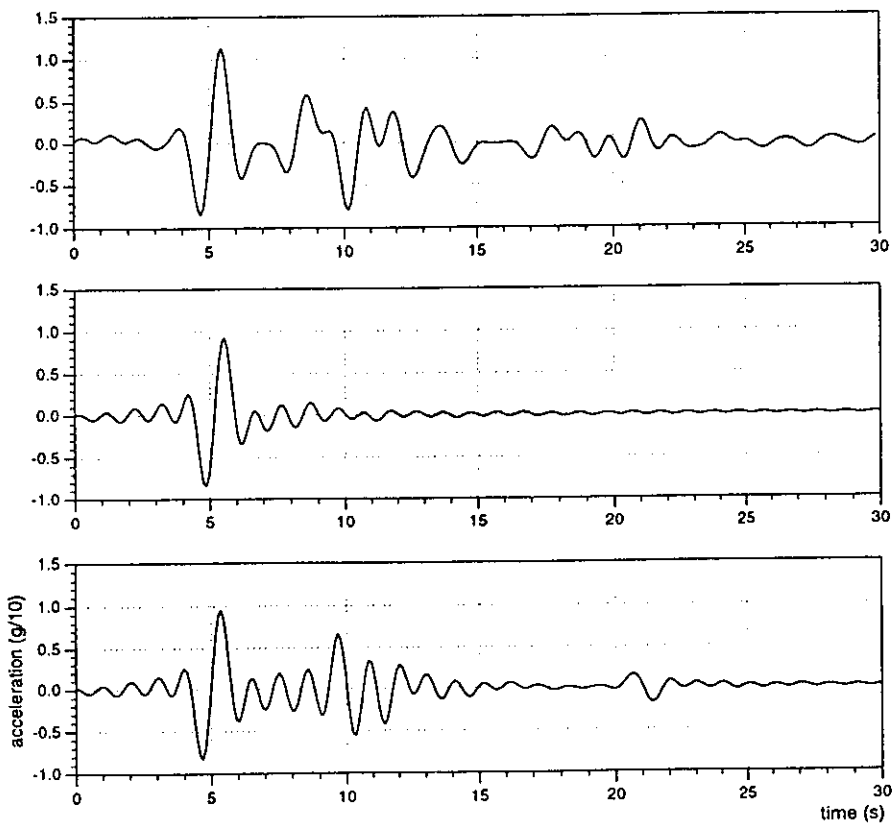

Figure 5. NS component accelerogram recorded at Sturno (upper trace), low-pass filtered to be compared with the computed signals for the Irpinia region (middle trace). The lower trace is the result of a superposition of four sub-events, each one modelled with the middle trace properly weighted and shifted in time, accordingly with the model by Vaccari et al. (1990).

good agreement. The late part of the observed recording is more complicated and this is mostly related to the complexity of the source, which is deliberately neglected in the computation of the synthetic signal used in the first-order zoning. The lower trace is shown as an example of modelling of the source complexity.

For the same Irpinia event Nunziata et al. (1995) show results of the deterministic modelling of ground motion in good agreement with the accelerometric record in Torre del Greco, near Naples.

Sufficient agreement between observations and modelling is obtained considering the Tolmezzo record of the Friuli (1976) earthquake (Panza et al., 1996), and, in this case, the point-source seems to be a satisfactory approximation for an event with Ms=6.1.

4. Ground motion models and intensity observations

The deterministic modelling can be used to derive correlation relations between the maximum felt macroseismic intensity, I, and DMAX, VMAX, and DGA (Panza et al., 1997a). This possibility is particularly relevant for countries with a long seismological history since it facilitates the engineering use of historical events, that are quantified only in terms of macroseismic intensity.

In this case the maximum observed magnitude is smoothed as follows. To each cell we assign the magnitude value of the most energetic event that occurred within it, and for events with $M_i > 6.75$, we use a centered smoothing window with a radius of 0.2° in order to take into account the source extension in space. Only the cells falling within the seismogenic areas are retained and a double-couple point source, corresponding to a magnitude M_i, is placed in the centre of each cell, with a depth equal to 10 km for $M_i < 7$ and equal to 15 km for the larger events.

Panza et al. (1997a) have used two sources for intensity data: (1) a map of maximum macroseismic intensity felt in Italy, made by Istituto Nazionale di Geofisica (ING intensity) (Boschi et al., 1995), where the intensity ranges between the V and the XI grade of MCS scale, the intensity value V including values below V; and (2) a set of maximum intensity felt in every municipal land, compiled jointly by ING, SSN and GNDT (ISG intensity) (Molin et al.,1996), where the intensity ranges between the VI and the X grade of the MCS scale. Grade VI includes values below VI and grade X includes values above X.

Peak values of ground motion and intensity are poorly correlated and their scatter is considerable (Ambraseys, 1974, Decanini et al., 1995). If we apply the correlation hypothesis:

$$\log(y) = b_0 + b_1 I \qquad (1)$$

(where y is a peak value or DGA and I is the intensity) to the whole set of data, the χ^2 test indicates that hypothesis (1) must be rejected (the hypothesis is statistically significant), while equation (1) becomes acceptable if average values of y, determined in correspondence of each intensity, are used.

TABLE I. Results of regression (1) for ING data.

Displacement	Velocity	Acceleration	DGA
$b_0 = -2.0 \pm 0.5$	$b_0 = -1.85 \pm 0.35$	$b_0 = -4.25 \pm 0.35$	$b_0 = -3.5 \pm 0.3$
$b_1 = 0.31 \pm 0.06$	$b_1 = 0.32 \pm 0.05$	$b_1 = 0.32 \pm 0.04$	$b_1 = 0.28 \pm 0.04$
$\chi^2_5 = 4.1$	$\chi^2_5 = 4.2$	$\chi^2_5 = 4.3$	$\chi^2_5 = 4.1$

TABLE II. Results of regression (1) for ISG data.

Displacement	Velocity	Acceleration	DGA
$b_0 = -2.0 \pm 0.2$	$b_0 = -2.1 \pm 0.1$	$b_0 = -4.6 \pm 0.1$	$b_0 = -3.7 \pm 0.1$
$b_1 = 0.31 \pm 0.03$	$b_1 = 0.35 \pm 0.01$	$b_1 = 0.35 \pm 0.01$	$b_1 = 0.30 \pm 0.01$
$\chi^2_3 = 1.9$	$\chi^2_3 = 2.0$	$\chi^2_3 = 2.2$	$\chi^2_3 = 2.1$

The application of (1) to ING and ISG data gives the coefficients reported in Table I and Table II, where the χ^2 is determined assigning to the value obtained from the regression coefficients an error of 2σ. For each intensity data set (ING and ISG) the slopes of (1) are comparable between themselves, but the slopes obtained with ING data are systematically smaller than the slopes obtained with ISG data. In Figures 6 and 7 we compare our log-linear relations with some earlier results, obtained considering global data, and in Table III we give the conversion between Intensity, I, and Maximum Spectral Value, MSV.

At a fixed intensity, means of peak values, in general, decrease with epicentral distance. Decanini et al. (1995) show an example of 9 events with I=VII, for which the mean of PGA for $R \leq 50$ km is almost 110 cm/s^2, while for $50 < R < 80$ km the mean PGA is 42 cm/s^2, and introduce the regression law for peak values:

$$\log(y) = b_0 + b_1 I + b_2 \log R \qquad (2)$$

with $R=\sqrt{(D^2+h^2)}$, where D is the epicentral distance and h the focal depth.

Tables IV and V contain the results of the regression with synthetic data, that are quite close to the ones given by Decanini et al. (1995) for observations. These tables contain the values obtained using the NT4.1 catalogue instead of the preliminary version NT3.1 (Stucchi et al., 1995) used by Panza et al. (1997a). The new regressions have been performed with a larger set of data, including intensities VI, VII and VIII, not considered by Panza et al. (1997a). A remarkable agreement with the observation in South Eastern Sicily and Irpinia (Decanini et al., 1995) is obtained when considering MSV and velocity. As an example, in Figures 8 and 9 we show the results we obtained with ISG data (the results obtained with

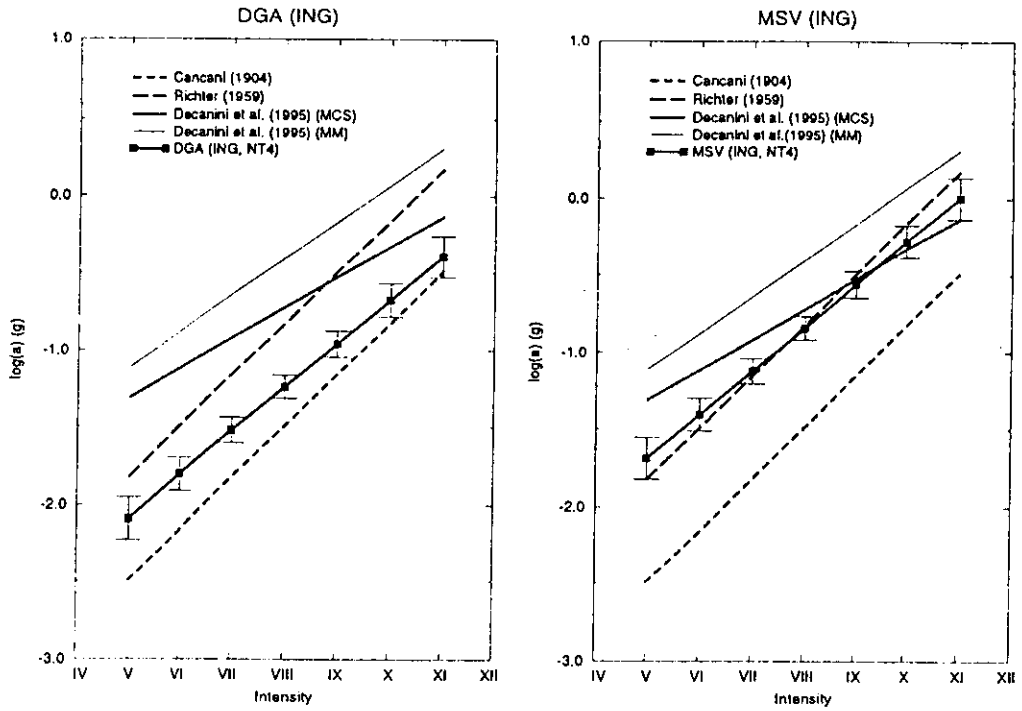

Figure 6. Experimental curves, taken from literature (Decanini et al., 1995; Richter, 1959 and Cancani, 1904) and our estimated values ($\pm\sigma$) of DGA and MSV (ING data set).

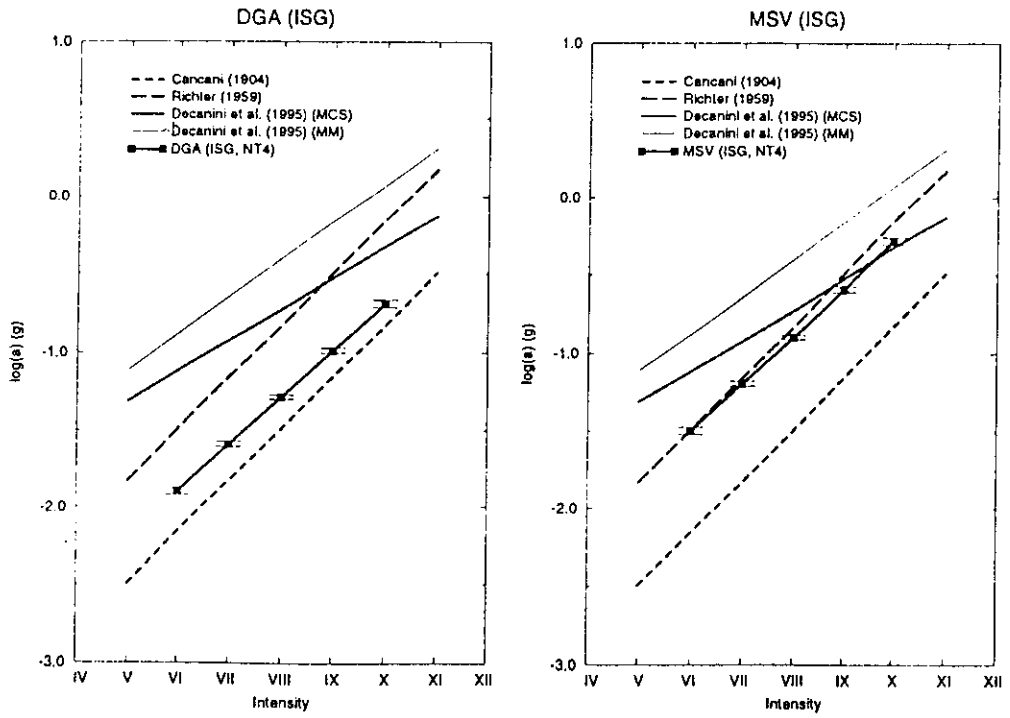

Figure 7. Experimental curves, taken from literature (Decanini et al., 1995; Richter, 1959 and Cancani, 1904) and our estimated values ($\pm\sigma$) of DGA and MSV (ISG data set).

ING data are very similar). In these figures we have plotted observations as solid squares and the modelled values as open circles. The solid and dashed lines are respectively the regression for the observations and for our modeled values. For accelerations we have plotted a(1)=log(PGA)-0.07I and a(2)=log(MSV)-0.1I (single points), a(1)=-0.24-0.8log(R) and a(2)=-0.85-0.5log(R) (regressions). For velocity we have plotted b(1)=log(PGV)-0.15I and b(2)=log(Velocity)-0.15I (single points), b(1)=1.00-0.7log(R) and b(2)=0.43-0.53log(R) (regressions). The values of b_2 are, in the case of displacement, lower than the ones obtained for velocity and DGA; they range from 0.1 (ING data set) to 0.3 (ISG data set), and indicate a weak dependence on distance.

The χ^2 test, applied to the modelled values and to the experimental data plotted in Figures 8 and 9, indicates that hypothesis (2) is statistically significant.

TABLE III. Correspondence between macroseismic intensity, I, and MSV, in units of g, for ING data set. Values in parentheses correspond to ISG data.

I	MSV (g)
V	0.02 ± 0.02
VI	0.04 ± 0.03 (0.030 ± 0.005)
VII	0.08 ± 0.04 (0.065 ± 0.005)
VIII	0.15 ± 0.12 (0.13 ± 0.01)
IX	0.28 ± 0.15 (0.26 ± 0.03)
X	0.53 ± 0.36 (0.52 ± 0.07)
XI	1.01 ± 0.90

TABLE IV. Results of regression (2) for ING data.

Displacement	Velocity	DGA
$b_0 = -0.4 \pm 0.3$	$b_0 = 0.5 \pm 0.5$	$b_0 = -0.6 \pm 0.5$
$b_1 = 0.12 \pm 0.02$	$b_1 = 0.16 \pm 0.03$	$b_1 = 0.07 \pm 0.03$
$b_2 = 0.1 \pm 0.1$	$b_2 = -0.6 \pm 0.2$	$b_2 = -0.7 \pm 0.2$
$\chi^2_{46} = 212$	$\chi^2_{40} = 139$	$\chi^2_{38} = 141$

TABLE V. Results of regression (2) for ISG data.

Displacement	Velocity	DGA
$b_0 = -1.3 \pm 0.4$	$b_0 = 0.4 \pm 0.5$	$b_0 = -1.25 \pm 0.45$
$b_1 = 0.17 \pm 0.03$	$b_1 = 0.15 \pm 0.03$	$b_1 = 0.11 \pm 0.03$
$b_2 = 0.3 \pm 0.2$	$b_2 = -0.5 \pm 0.2$	$b_2 = -0.5 \pm 0.2$
$\chi^2_{39} = 118$	$\chi^2_{38} = 111$	$\chi^2_{37} = 109$

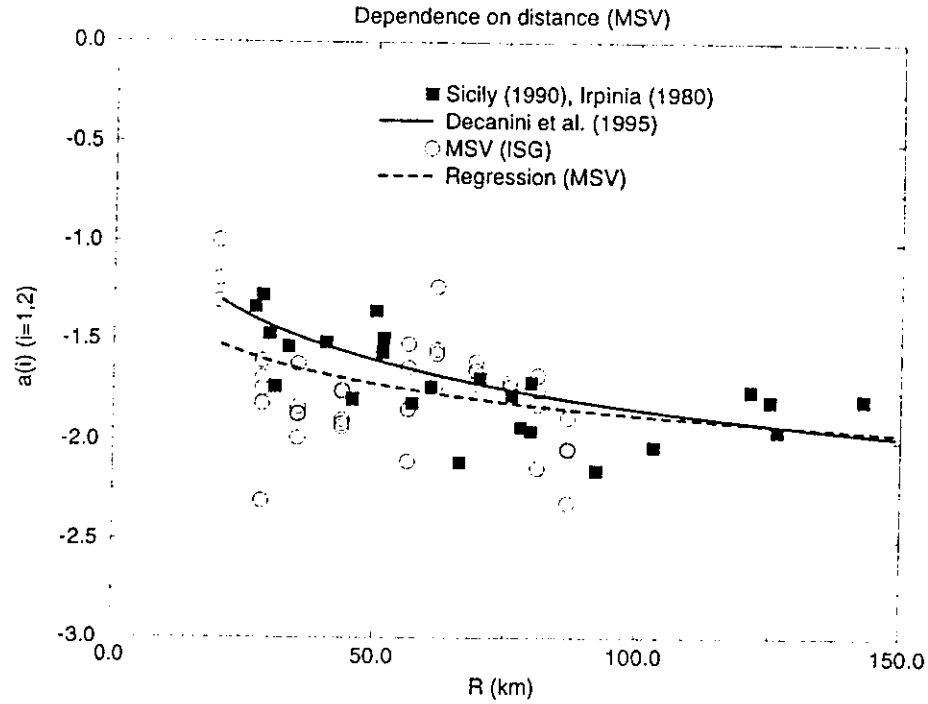

Figure 8. Variation with hypocentral distance, R, (attenuation relationship) of PGA (solid squares) and MSV (open circles), normalized with respect to I. The solid line represents a(1)=-0.24-0.8 log(R), and the dashed line a(2)=-0.85-0.5log(R).

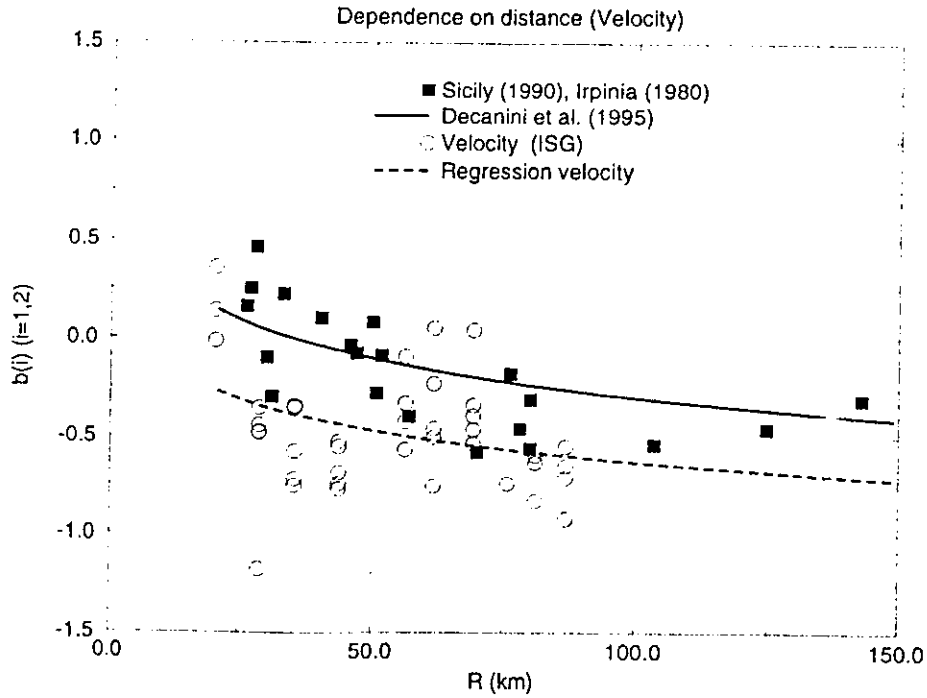

Figure 9. Variation with hypocentral distance, R, (attenuation relationship) of PGV (solid squares) and velocity (open circles), normalized with respect to I. The solid line represents b(1)=1.00-0.7log(R), and the dashed line b(2)=0.43-0.53log(R).

5. Detailed zoning combining observation and modelling of ground motion

The results obtained with a first-order zoning cannot be refined by simply assuming a higher cutoff frequency (> 1 Hz) in the computation of the synthetic seismograms. A more detailed zoning requires a better knowledge of the seismogenic process in the region. Furthermore, to model wave propagation in greater detail the structural models used in the computation of synthetic seismograms must take into account lateral heterogeneities.

Detailed numerical simulations play an important role in the estimation of ground motion in regions of complex geology. They can provide synthetic signals for areas where recordings are absent, that are particularly relevant for engineering seismology and earthquake engineering. Numerical simulations are, therefore, very useful for the design of earthquake-resistant structures.

As we have seen in section 2 the deterministic computation can be extended to higher frequencies by the use of the existing standard design spectra. The matching of the long-period portion of the normalized spectra with the ones computed from synthetic accelerograms, allows us to obtain, for any portion of the considered territory, an absolute spectrum, provided a satisfactory classification of soils is available. The preliminary soil classification of EC8 considers three classes, A, B, and C, ranging from hard rock to loose uncemented sands. Accordingly with EC8 for sites with soil conditions not matching the three classes A, B and C, special studies for the definition of the ground acceleration response spectrum are necessary.

When detailed special studies are required by EC8 or by the presence, in the built environment, of special objects, the standard seismic prospecting techniques, used for the detailed definition of the elastic properties of subsurface geology, do not give satisfactory results since they treat wave propagation in laterally heterogeneous structures with asymptotic forms valid for high frequencies. These methods, called "ray methods", can only be applied to smoothly varying media, where the characteristic dimensions of the inhomogeneities are considerably larger than the prevailing wavelength. They fail to predict ground motion at sites close to lateral heterogeneities such as edges of sedimentary basins and at sites above irregular bedrock-sediment interfaces, where excitation of local surface waves and resonance effects can be important.

Far away from lateral heterogeneities, a local structure can sometimes be approximated by a horizontally-layered structural model, and the modal summation method is the most powerful tool for computing broadband synthetic seismograms. This method is still suitable when lateral variations can be schematized with vertical discontinuities (Vaccari et al., 1989, Romanelli et al., 1996; 1997). When dealing with special, detailed investigations the influence of the local and irregular heterogeneities can be included in the numerical modelling combining the modal summation and the finite difference techniques (Fäh et al., 1990; Fäh, 1992).

Examples of possible procedures for the detailed deterministic modelling of ground motion are given by Suhadolc and Marrara (1997) and a specific example referring to Bucharest is given by Moldoveanu and Panza (1997). Here, in Figures 10a and 10b, we give an example describing the results obtained for the microzoning of Rome.

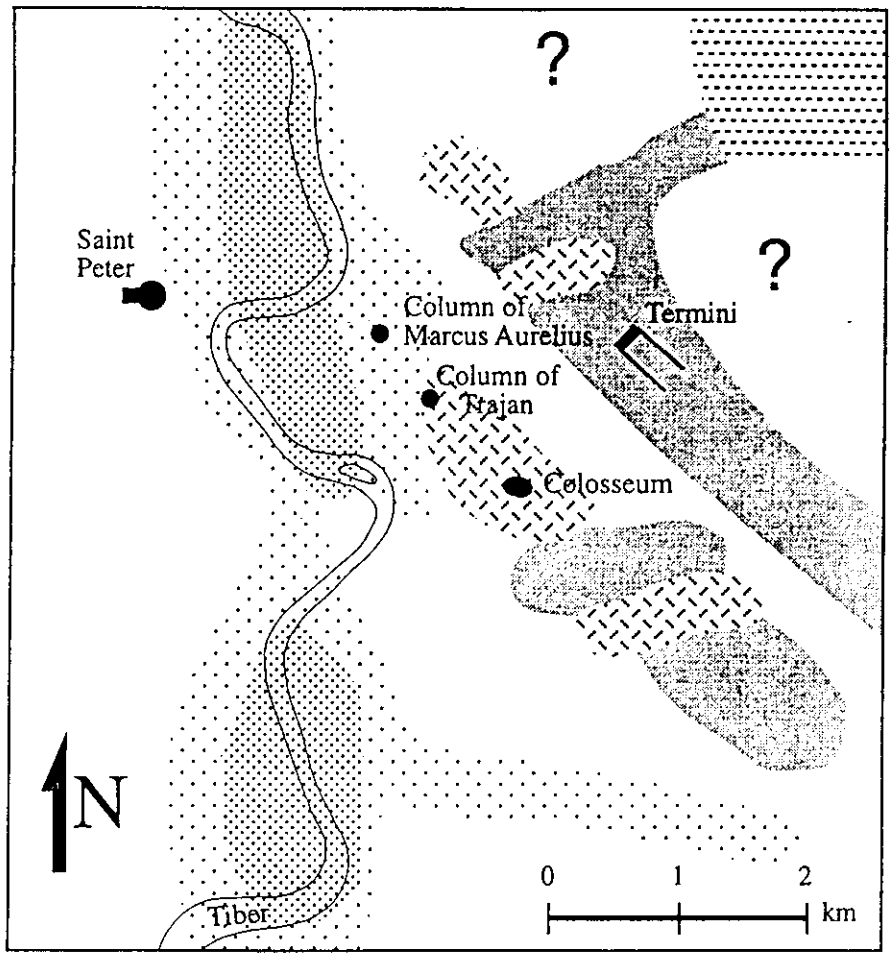

	Zone		Zone
Tiber edges	1	No near-surface volcanic rocks	4
Central Tiber alluvial basin	2	Near-surface volcanic rocks	5
Paleotiber basin edges	3	Near-surface volcanic rocks?	5 ?

Figure 10a. Microzoning for the city of Rome based on local soil classification and on the computation of synthetic spectral amplifications (modified from Panza et al., 1997b).

6. Conclusions

Traditional deterministic methods for seismic zoning can only lead to a kind of "post-event" zoning whose validity cannot easily be extrapolated in time and to different regions and which; therefore, must be considered obsolete.

On the contrary the computation of realistic synthetic seismograms, using methods that make it possible to take source and propagation effects into account, utilizing the

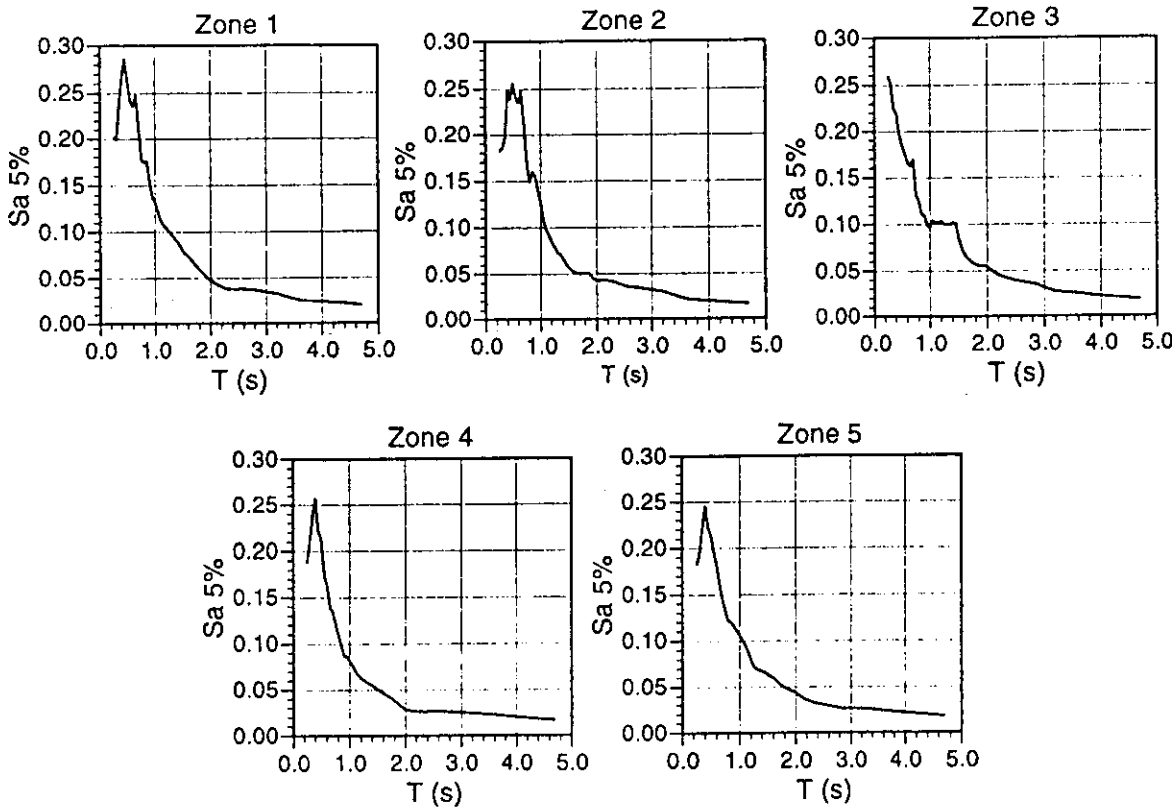

Figure 10b. Maximum absolute spectral accelerations (5% damping) obtained for five zones in the city of Rome (modified from Panza et al., 1997b)

huge amount of geological, geophysical and geotechnical data, already available, goes well beyond the conventional deterministic approach and gives a very powerful and economically valid scientific tool for seismic zonation and microzonation.

Because of its flexibility, the method is suitable for inclusion in new integrated procedures, a kind of compromise between probabilistic and deterministic approaches, that can be developed in order to minimize the drawbacks of each of the two procedures.

The ability to estimate accurately seismic hazard at very low probability of exceedance may be important in protecting, against rare earthquakes, the existence of special objects in the built environment. The deterministic approach, based upon the assumption that several earthquakes can occur within a predefined seismic zone, represents a conservative definition of seismic hazard for pre-event localized planning for disaster mitigation, over a quite broad-band of periods.

With the deterministic modelling it is possible to derive reliable, region specific, correlations between intensity, I, and DMAX, VMAX, and DGA, that facilitate the engineering use of historical data. The availability of correlations, that are valid for a specific region, is quite important, since the use of information collected on a global scale may introduce quite unsatisfactory biases (Trifunac, 1992).

The results of tests made against instrumentally recorded accelerograms show that, even an approximate knowledge of the geometry and of the mechanical properties of the

uppermost layers and the use of commonly available data on the seismic source geometry, is sufficient to make a realistic prediction of the ground motion.

The definition of realistic seismic input can be obtained from the computation of a wide set of time histories and spectral information, corresponding to possible seismotectonic scenarios for different source and structural models. Such a data set can be very fruitfully used by civil engineers in the design of new seismo-resistant constructions and in the reinforcement of the existing built environment, and therefore supply a particularly powerful tool for the prevention aspects of Civil Defence.

The procedure is scientifically and economically valid for the immediate (no need to wait for a strong earthquake to occur), first order, seismic microzonation of any urban area, where the geotechnical data are available.

Acknowledgments

We acknowledge support by European Union grant ENV4-CT96-0491 and EV5V-CT94-0513, Italian MURST 40% and 60% funds (1994-1997), and CNR grants 95.00608.PF54, 96.02986.PF54 and 97.00540.PF54. This research has been carried out in the framework of the UNESCO-IGCP Project 414 "Realistic Modelling of Seismic Input for Megacities and Large Urban Areas".

References

Aki, K. (1987) Strong motion seismology, in M.Ö. Erdik and M.N. Toksöz (eds.), *Strong Ground Motion Seismology*, NATO ASI Series, Series C: Mathematical and Physical Sciences, D. Reidel Publishing Company, Dordrecht, vol. 204, pp. 3-39.

Ambraseys, N. (1974) Notes on engineering seismology, in J. Solnes (ed.), *Engineering Seismology and Earthquake Engineering*, Nato Advanced Study, pp. 33-54.

Arias, A. (1970) A measure of earthquake intensity, in: R. Hansen (ed.), *Seismic design for nuclear power plants*, Cambridge, Massachussets.

Bernard, P. and Zollo, A. (1989) The Irpinia (Italy) 1980 earthquake: detailed analysis of a complex normal faulting, *J. Geophys. Res.* **94**, 1631-1647.

Boschi, E., Favalli, P., Frugoni, F., Scalera, G. and Smriglio, G. (1995) Mappa massima intensita' macrosismica risentita in Italia, Istituto Nazionale di Geofisica, Roma.

Camassi, R. and Stucchi, M. (1996) NT4.1: un catalogo parametrico di terremoti di area italiana al di sopra della soglia del danno. Internet, http://emidius.itim.mi.cnr.it/NT/home.html.

Cancani, A. (1904) Sur l'emploi d'une double échelle seismique des intensites empirique et absolue, *Gerlands Beiträge zur Geophysik Ergänzungsband* **2**, 281-283.

Corsanego, A., Faccioli, E., Gavarini, C., Scandone, P., Slejko, D. and Stucchi, M. (1997) *Gruppo Nazionale per la difesa dai terremoti. L'attività del triennio 1993-1995*, CNR, GNDT, Roma, 1997.

Costa, G., Panza, G.F., Suhadolc, P. and Vaccari, F. (1992) Zoning of the Italian region with synthetic seismograms computed with known structural and source information. *Proc. 10th WCEE, July 1992, Madrid, Balkema*, pp. 435-438.

Costa, G., Panza, G.F., Suhadolc, P. and Vaccari, F. (1993) Zoning of the Italian territory in terms of expected

peak ground acceleration derived from complete synthetic seismograms, in: R. Cassinis, K. Helbig and G.F. Panza (eds.), Geophysical Exploration in Areas of Complex Geology, II, *J. Appl. Geophys.* **30**, 149-160.

Decanini, L., Gavarini, C. and Mollaioli, F. (1995) Proposta di definizione delle relazioni tra intensita' macrosismica e parametri del moto del suolo, *Atti del 7° Convegno Nazionale "L'ingegneria sismica in Italia"* **1**, pp. 63-72.

EC 8 (1993) Eurocode 8 structures in seismic regions - design - part 1 general and building, Doc TC250/SC8/N57A.

Fäh, D. (1992) *A hybrid technique for the estimation of strong ground motion in sedimentary basins*. Ph.D. thesis Nr. 9767, Swiss Federal Institute of Technology, Zürich.

Fäh D., Suhadolc, P. and Panza, G.F. (1990) Estimation of strong ground motion in laterally heterogenenous media: modal summation - finite differences. *Proceedings of the 9-th European Conference of Earthquake Engineering*, Sept. 11-16, 1990, Moscow, 4A, pp. 100-109.

Florsch, N., Fäh, D., Suhadolc, P. and Panza, G.F. (1991) Complete synthetic seismograms for high-frequency multimode Love waves, *Pure Appl. Geophys.* **136**, 529-560.

Gusev, A.A. (1983) Descriptive statistical model of earthquake source radiation and its application to an estimation of short period strong motion, *Geophys. J.R. Astron. Soc.* **74**, 787-800.

Kanamori, H. (1977) The energy release in great earthquakes, *J. Geophys. Res.* **82**, 2981-2987.

Moldoveanu, C. and Panza, G.F. (1997) Modelling, for microzonation purposes, of the seismic ground motion in Bucharest, due to the Vrancea earthquake of May 30, 1990, *this volume*.

Molin, D., Stucchi, M. and Valensise, G. (1996) *Massime intensità macrosismiche osservate nei comuni italiani*, elaborato per il Dipartimento della Protezione Civile. GNDT, ING, SSN, Roma.

Nunziata, C., Fäh, D. and Panza, G.F. (1995) Reduction of seismic vulnerability of a megacity: the case of Naples, Proc. of the conference "Terremoti e civiltà abitative", Accademia Nazionale dei Lincei, Roma, *Ann. Geofis.* **38**, 649-661.

Panza, G.F. (1985) Synthetic seismograms: the Rayleigh waves modal summation, *J. Geophys.* **58**, 125-145.

Panza, G. F. and Vaccari, F. (1994) Advanced criteria of seismic zoning and synthetic seismograms, in G. Verri (ed.), Proc. Europrotech, CISM, Udine, pp. 63-92.

Panza, G.F., Vaccari, F., Costa, G., Suhadolc, P. and Fäh, D. (1996) Seismic input modelling for zoning and microzoning, *Earthquake Spectra* **12**, 529-566.

Panza, G.F., Cazzaro, R. and Vaccari, F. (1997a) Correlation between macroseismic intensities and seismic ground motion, *Ann. Geofis.* **40**, 1371-1382 .

Panza, G.F., Sanò, T., Pugliese, A. and Vaccari, F. (1997b) Studies performed in Italy for the definition of seismic input for isolated structures, *Proceedings of the International Post-SMiRT Conference Seminar on Seismic Isolation, Passive Energy Dissipation and Active Control of Seismic Vibrations of Structure, Taormina*, in press.

Radulian, M., Mandrescu, N., Vaccari, F. and Panza, G.F. (1997) Seismic hazard of Romania: a deterministic approach, *Abstracts book of the 29th General Assembly of the International Association of Seismology and Physics of the Earth's Interior (IASPEI)*, August 18-28 1997, Thessaloniki, Greece, p. 292.

Richter, C.F. (1959) Seismic regionalization, *Bull. Seism. Soc. Am.* **49**, 123-162.

Romanelli, F., Bing, Z., Vaccari, F. and Panza, G.F. (1996) Analytical computation of reflection and transmission coupling coefficients for Love waves, *Geophys. J. Int.* **125**, 132-138.

Romanelli, F., Bekkevold, J. and Panza, G.F. (1997) Analytical computation of coupling coefficient in non-Poissonian media, *Geophys. J. Int.*, **129**, 205-208.

Stucchi, M., Camassi, R. and Monachesi, G. (1995) NT3.1: Un catalogo di lavoro del GNDT, GNDT, Rapporto Interno, Milano.

Suhadolc, P. and Marrara, F. (1997) 2-D modeling of site response and seismic microzoning, *this volume*.

Trifunac, M.D. (1992) Should peak accelerations be used to scale design spectrum amplitudes? Earthquake engineering, Tenth World Conference, Rotterdam, pp. 5817-5822.

Vaccari, F., Gregersen, S., Furlan, M. and Panza, G.F. (1989) Synthetic seismograms in laterally heterogeneous, anelastic media by modal summation of P-SV waves, *Geophys. J. Int.* **99**,285-295.

Vaccari, F., Suhadolc, P. and Panza, G.F. (1990) Irpinia, Italy, 1980 earthquake: waveform modelling of strong motion data, *Geophys. J. Int.* **101**, 631-647.

by G. F. Panza[1,2], F. Vaccari[1,3], and F. Romanelli[1,3]

IGCP Project 414: Realistic Modeling of Seismic Input for Megacities and Large Urban Areas

1 Dipartimento di Scienze della Terra - Università di Trieste, Via Weiss, 4 34127 Trieste, Italy. Fax: +39-40-6762111, Tel: +39-40-6762117, E-mail: <Panza@geosun0.univ.trieste.it>.
2 The Abdus Salam International Centre for Theoretical Physics, Miramar, Italy.
3 Gruppo Nazionale per la Difesa dai Terremoti - CNR, Rome, Italy.

The project addresses the problem of pre-disaster orientation: hazard prediction, risk assessment, and hazard mapping, in connection with seismic activity and man-induced vibrations. The definition of realistic seismic input can be obtained from the computation of a wide set of time histories and spectral information, corresponding to possible seismotectonic scenarios for different source and structural models. The availability of realistic numerical simulations enables us to estimate the amplification effects in complex structures exploiting the available geotechnical, lithological, geophysical parameters, topography of the medium, tectonic, historical, palaeoseismological data, and seismotectonic models. The realistic modeling of the ground motion is a very important base of knowledge for the preparation of groundshaking scenarios that represent a valid and economic tool for seismic microzonation. This knowledge can be very fruitfully used by civil engineers in the design of new seismo-resistant constructions and in the reinforcement of the existing built environment, and, therefore, supplies a particularly powerful tool for the prevention aspects of Civil Defense. At present, the project is active in Antananarivo, Bangalore, Beijing, Bucharest, Budapest, Cairo, Catania, Damascus, Delhi, Kathmandu, Ljubljana, Mexicali, Mexico City, Naples, Rome, Santiago de Chile, Santiago de Cuba, Silistra, Sofia, Thessaloniki, Tijuana and Zagreb.

Introduction

The IUGS-UNESCO IGCP Project 414 "Seismic Ground Motion in Large Urban Areas", started in 1997, addresses the problem of pre-disaster orientation: hazard prediction, risk assessment, and hazard mapping, in connection with seismic activity and man-induced vibrations. The major scientific problem is to handle realistic models on a very detailed level. This can now be done by making use of global observations from digital networks, application of modern theories for the forward and the inverse problems, and by the use of very powerful computers.

We can reduce loss of life and property damage by highly detailed, specific prediction of seismic ground motion. With the knowledge of accurate, three-dimensional structures and probable, complex source mechanisms, the detailed ground motion at any site, or all sites of interest, can be determined. To map seismic ground motion we do not have to wait for earthquakes to occur in likely focal regions and then to measure ground motion with an extremely dense set of recording instruments; instead, with the knowledge above we can compute these seismograms from theoretical considerations. Thus, a complete database for all sites and predicted focal mechanisms can be constructed immediately; no delay is necessary while we wait for experimental evidence and recordings. This database would then, naturally, be updated continuously by comparison with incoming new experimental data.

The general plan includes the following large urban areas and megacities: Antananarivo, Bangalore, Beijing, Bucharest, Budapest, Cairo, Catania, Damascus, Delhi, Kathmandu, Ljubljana, Mexicali, Mexico City, Naples, Rome, Santiago de Chile, Santiago de Cuba, Silistra, Sofia, Thessaloniki, Tijuana and Zagreb. This choice is representative of a broad spectrum of seismic hazard levels that require different efforts to reach a satisfactory level of preparedness. We have deliberately chosen objects not situated very close to known seismogenic zones. In fact, the condition of being some tens of kilometers from the epicenter can allow us an optimum exploitation of the results of microzoning, and fill in a gap in preparedness, since, usually, most of the attention is focused on very near seismogenic zones.

At present, the international and interdisciplinary working group is composed by: Prof. E. Paskaleva, Dr. M. Kouteva, Central Laboratory for Seismic Mechanics & Earthquake Engineering, Sofia; Dr. D. Slavov, University of Sofia, Department of Meteorology and Geophysics, Sofia, BULGARIA; Prof. R. Saragoni, Departamento de Ingenieria Civil, Universidad de Chile, Santiago, CHILE; Prof. Y. T. Chen, Dr. Z. Ding, Institute of Geophysics, China Seismological Bureau, Beijing, Dr. R. Sun, Institute of Geophysics, Science Academy of China, Beijing, CHINA; Prof. M. Herak, Dr. I. Lokmer, Geophysical Institute, University of Zagreb, CROATIA; Prof. J. L. Alvarez Gomez, Centro Nacional de Investigaciones Sismologicas, Havana, CUBA; Dr. A. El-Sayed, Geology Department, Mansoura University, Mansoura, EGYPT; Prof. P. Varga, Dr. T. Ziros, Dr. P. Monus, Geodetic and Geophysical Research Institute, Sopron, HUNGARY; Prof. V. Gaur, Indian Institute of Astrophysics, Bangalore, Prof. R. N. Iyengar, Dr. S. K. Agrawal, Central Building Research Institute, Roorkee, INDIA; Prof. G. F. Panza, Prof. P. Suhadolc, Dr. F. Vaccari, Dr. F. Romanelli, Dr. F. Marrara, Dr. A. Sarao', Dr. A. Aoudia, Dipartimento di Scienze della Terra, Universita' di Trieste and International Center for Theoretical Physics, Trieste; Prof. C. Nunziata, Dr. M. Natale, Dr. R. Mele, Dr. A. Sica, Dipartimento di Geofisica e Vulcanologia, University of Naples; Prof. L. Tortorici, Dipartimento di

Scienze Geologiche, University of Catania, ITALY; Prof. G. Rambolamanana, Institut et Observatoire Géophysique d'Antananarivo, Antananarivo, MADAGASCAR; Dr. J. Frez, Centro de Investigacion Cientifica y de Educacion Superior de Ensenada, MEXICO; Prof. G. Marmureanu, Dr. M. Radulian, Dr. C. Moldoveanu, Dr. C. Cioflan, Dr. D. Bratosin, Dr. B. Apostol, National Institute for Earth Physics, Bucharest, ROMANIA; Prof. Acad. V. I. Keilis-Borok, Dr. A. Soloviov, Dr. I. Kuznetzov, Dr. I. Rotwain, Dr. G. Molchan, International Institute of Earthquake Prediction Theory and Mathematical Geophysics, Academy of Sciences, Moscow, RUSSIA; Dr. M. Zivcic, Dr. A. Gosar, Slovenian Association for Geodesy and Geophysics, Geophysical Survey of Slovenia, Ljubljana, SLOVENIA; Dr. H. Abou Roumieh, Dr. A. Hariri, Syrian National Seismic Network, Damascus, SYRIA.

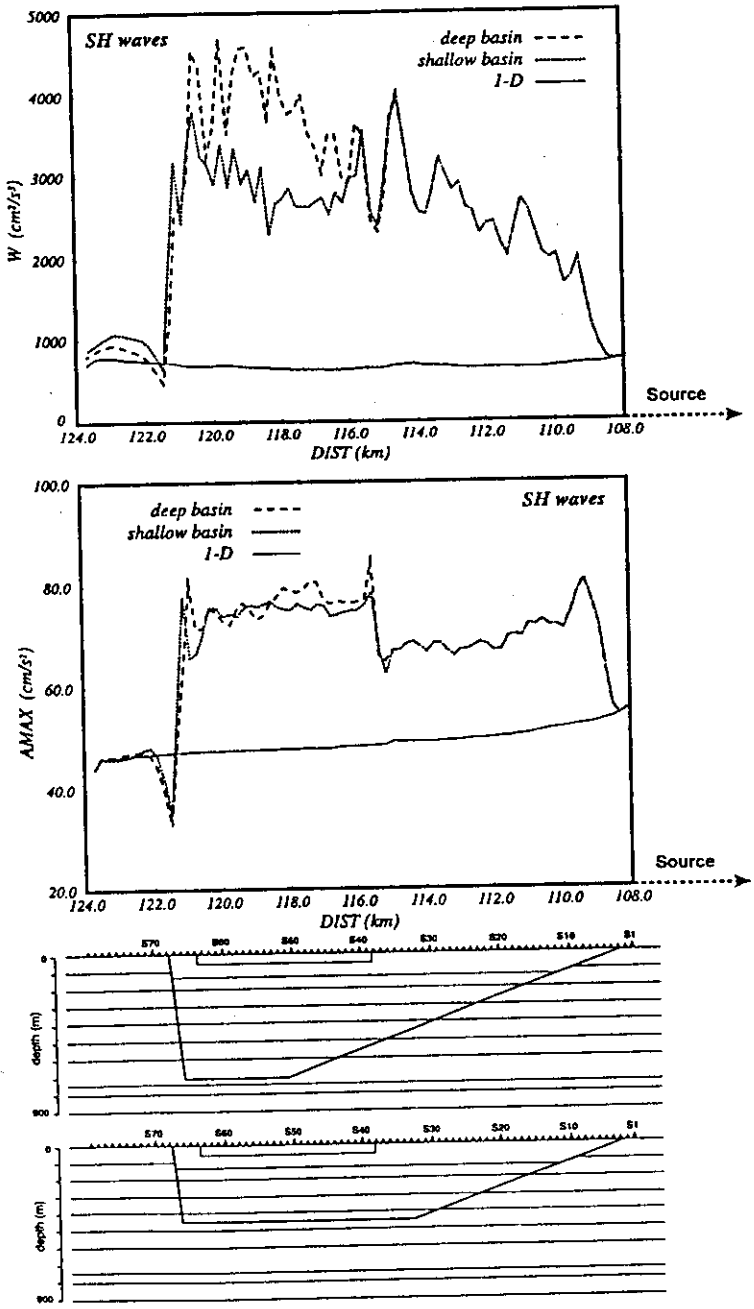

Figure 1 Relative maximum amplitude (A2D/A1D) and total energy of ground motion (W2D/W1D) along a profile across the Xiji Langfu depression, in Beijing area. The thick low velocity deposits are responsible for the large increment of the values inside the basin. On the two sides of the Xiadian fault, A2D/A1D and W2D/W1D can vary by more than 160% and 600%, respectively. The two different geometries of the sedimentary basin are shown in the lower part of the figure, a) deep basin; b) shallow basin. With the existing relationships between acceleration and macroseismic intensity (I) these results can explain the large values of I observed in the Xiji-Langfu area, in connection with the Tangshan 1976 earthquake (from Sun et al., 1998).

Method

The mapping of the seismic ground motion due to the earthquakes originating in a given seismogenic zone can be made by measuring seismic signals with a dense set of recording instruments when a strong earthquake occurs or/and by computing theoretical signals, using the available information about tectonic and geological/geotechnical properties of the medium, where seismic waves propagate. Strong earthquakes are very rare phenomena and this makes very difficult (practically impossible in the near future) the preparation of a sufficiently large database of recorded strong motion signals that could be analyzed in order to define generally valid ground parameters, to be used in seismic hazard estimations.

While waiting for the increment of the strong motion data set, a very useful approach to perform immediate microzonation is the development and use of modeling tools based, on one hand, on the theoretical knowledge of the physics of the seismic source and of wave propagation and, on the other hand, exploiting the rich database about the geotechnical, geological, tectonic, seismotectonic, historical information already available.

The initial stage of our work requires the collection of all available data concerning the shallow geology, and the construction of cross-sections along which to model the ground motion. This work is by its nature multidisciplinary since information is requested from different disciplines as seismology, history, archaeology, geology and geophysics to give engineers reliable building codes. The realistic modeling of ground motion requires, in fact, the simultaneous knowledge of the geotechnical, lithological, geophysical parameters and topography of the medium, on one side, and tectonic, historical, paleoseismological, seismotectonic models, on the other, for the best possible definition of the probable seismic source. In addition, the use of sophisticated computer modeling of wave propagation in heterogeneous anelastic media allows us the best possible exploitation of the existing information on structures and sources. Different advanced methods and approaches, some of them developed and implemented by partners of this project, are used with the goal of determining different indicators of seismic hazard (e.g. Panza et al., 1996).

At the end of the project, maps of various seismic hazard parameters directly measured or numerically modeled, such as peak ground acceleration, and others of practical use for the design of earthquake-safe structures will be produced, taking advantage of modern GIS technology.

The ongoing activity

The methods used for the modeling of the ground motion are described in detail by Panza (1985), Vaccari et al. (1989), Fäh (1991), Florsch et al. (1991), Fäh et al. (1993), Panza (1993), Fäh et al. (1994), Fäh and Panza (1994) and Romanelli et al. (1996), and permit to take into account in a realistic way source, path and local soil effects on the entire wave train. The results obtained so far are all characterized by a large international co-operation and can be divided into two main groups: (1) Urban areas where data collection is still in progress and the modeling is in the preliminary stage; (2) Urban areas

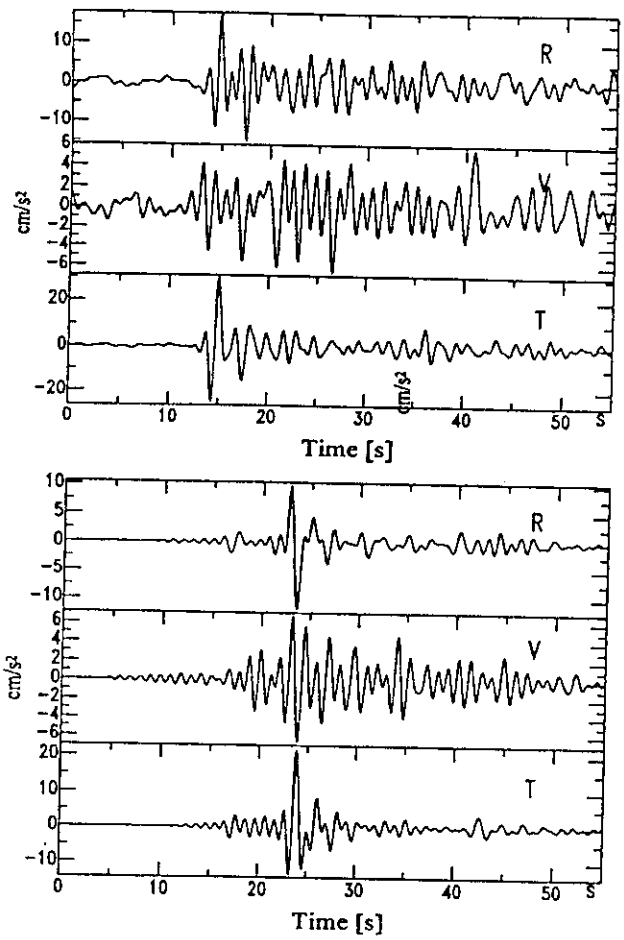

Figure 2 Recorded ground motion in Bucharest (Magurele station) and simulated signal by Moldoveanu and Panza (1998), for periods greater than 1 s, for the event of May 30, 1990.

where the numerical modeling is quite advanced and successfully compared with available observations.

Because of the lack of records, the study of the ground motion in Budapest due to the 1956 Dunaharaszti earthquake, located at about 20 km from the Capital, is based mainly on modeling, using all available information about geological and geotechnical properties. This case represents a typical situation in which the realistic modeling of ground motion is the only tool that permits to estimate the hazard before another event strikes the city.

The ground motion recorded in Mexico City valley during distant earthquakes is often used to illustrate the applicability of the 1-D model with vertically propagating shear waves. However, the analysis of ground displacement waveforms in stations located on firm soil shows that ground displacements are always strongly influenced by Rayleigh waves, with a broad frequency band between 0.08 to 1.0 Hz. No important incident body waves or basin waves are observed (Gomez Bernal and Saragoni, 1997a, b). Therefore, these surface waves greatly contribute to the destructive effects of earthquakes as their frequencies coincide with the site periods encountered at the lake-bed zone (1.0–5.0 s).

In Santiago del Chile, the analysis of the accelerograms recorded for the MS=7.8 Central Chile 1985 earthquake shows ground displacements with important retrograde Rayleigh waves, with strong coupling between horizontal and vertical motion. The study shows that these waves come from the epicenter and from other two sources (Saragoni and Lobos, 1998).

For the microzonation of Santiago de Cuba the initial phase of data collection about the regional crust-upper mantle structure and Santiago de Cuba basin structure has been completed, and the modeling phase just begun.

The site of the city of Sofia falls in the so-called Sofia seismic zone. The main seismogenic zones with influence on the seismic hazard of the Sofia site are: Kresna, Plovdiv, Negotinska Krayna. Vrancea source is located 320 km far from Sofia. The macroseismic effect of Vrancea earthquakes observed on the site of Sofia in 1940 and 1977 correspond to MSK intensities between V and VI. The preliminary results of the deterministic modeling of ground motion for local destructive earthquakes suggest that a reinterpretation of the available studies on the specific attenuation for Sofia Valley is necessary, and that, in the town, the expected intensity may vary between VII and X.

In India, as introductory activity to the microzonation of some Indian megacities, preliminary modeling has been made, taking the Garhwal region of the central sector of Himalaya as an example to carry out seismic microzonation studies for local conditions. Here the 260 m-high earth and rockfill Tehri Dam, across Bhagirathi river, exposes the whole downstream population to high risks. It is, therefore, quite natural, from a socio-economic and scientific point of view, to be speculative about the seismic safety of the dam and its paraphernalia, undertaking a seismic microzonation study for this region. The first preliminary results so far obtained show that, for the Uttarkashi region, despite of the scarce information about the earth crust structure of the area, the comparison of the modeled seismic ground motion with observations is quite satisfactory and realistic (Agrawal, 1998, personal communication), and therefore it is reasonable to extend the seismic microzonation procedure to Indian megacities.

In Naples, the ground motion due to earthquakes occurred in Southern Apennines, with special attention to the November 23, 1980 (MS=6.9, ML=6.5) event, is studied. A quite successful comparison with the strong motion recorded at Torre del Greco has been obtained (Nunziata et al., 1997). In the area studied in detail, the subsoil is mainly formed by alluvial (ash, stratified sand and peat) and pyroclastic materials overlying a pyroclastic rock (yellow neapolitan tuff) representing the neapolitan bedrock. The very detailed information available about the sub-soil mechanical properties and its geometry gives a very good opportunity to compare the results that can be obtained with standard 1-D techniques (Method 1), based on the vertical propagation of waves in a plane layered structure (e.g. computer program Shake, developed by Schnabel et al., 1972) and with our realistic hybrid technique (Method 2). The discrepancies evidenced between the 1-D and the 2-D seismic responses, suggest that serious caution must be taken in the formulation of seismic regulations (Nunziata et al., 1997). As expected, the sedimentary cover causes an increase of the signal's amplitudes and duration. If a thin uniform peat layer is present at depth, the amplification effects at the free surface are reduced, and the peak ground accelerations are similar to those observed for the bedrock model. The study of the effects of the interaction between soil properties and foundations has shown that the peat layer present in a part of the city can act as a seismic isolator (Nunziata et al., 1997).

The study of the ground motion in Beijing area due to earthquakes occurred in its surroundings, such as the Ms=7.8 Tangshan earthquake of July 28, 1976, about 160 km from the City of Beijing, has given satisfactory comparison with observed macroseismic data, especially in Dachang depression (Sun et al., 1998). The special geological conditions in the Xiji-Langfu area are the main reason for the anomalously high macroseismic intensity caused by the Tangshan 1976 earthquake. The area is formed by deep deposits — mainly alluvium sands and clays poorly consolidated and with high water content — that have been trapped by the Xiadian fault.

From the simulated ground motion, quantities commonly used for engineering purposes, like the maximum amplitude (AMAX) and the total energy of ground motion (W), which is related to the Arias Intensity (Arias, 1970), can be computed. The thick low velocity deposits are responsible for the large increment of the values of AMAX and W inside the basin. On the two sides of the Xiadian fault the relative values of AMAX and W, A2D/A1D and W2D/W1D, can vary by more than 160% and 600% respectively, and these variations

are relatively stable with varying thickness of the sedimentary deposit used in the models, as shown in Figure 1. A2D and W2D represent the values computed for the model containing the sedimentary basins, which are shown at the bottom of the figure, while A1D and W1D represent the same quantities computed for the reference bedrock model given by Sun et al. (1998). With the existing relationships between acceleration and macroseismic intensity I (Medvedev, 1977; Panza et al., 1998), these results can explain the large values of I observed in the Xiji-Langfu area, in connection with the Tangshan earthquake.

Macroseismic effects similar to the ones observed in the Dachang depression are predicted by the modeling in the Beijing depression, not much urbanized at the time of the Tangshan event (Ding et al., 1997). This result represents a very good example of the possibility to produce important information for seismic risk mitigation using what is available now and to improve scenarios as new data become available. To further check the modeling, it is now in progress the analysis of the records of the January 10, 1998 earthquake with Ms=6.1, occurred in Zhangbei, Hebei Province, about 180 km NW of Beijing.

The Vrancea seismoactive region, characterized by intermediate-depth earthquakes, is the main quake source that has to be taken into account for the microzonation of Bucharest, that could suffer serious damage because of the severe local site effects. The strong seismic events originating in Vrancea have caused the most destructive effects experienced on the Romanian territory. Since about four destructive earthquakes occur every century in Vrancea, the microzonation of Bucharest, exposed to the potential damages due to these strong intermediate-depth shocks, is an essential step toward the mitigation of the local seismic risk.

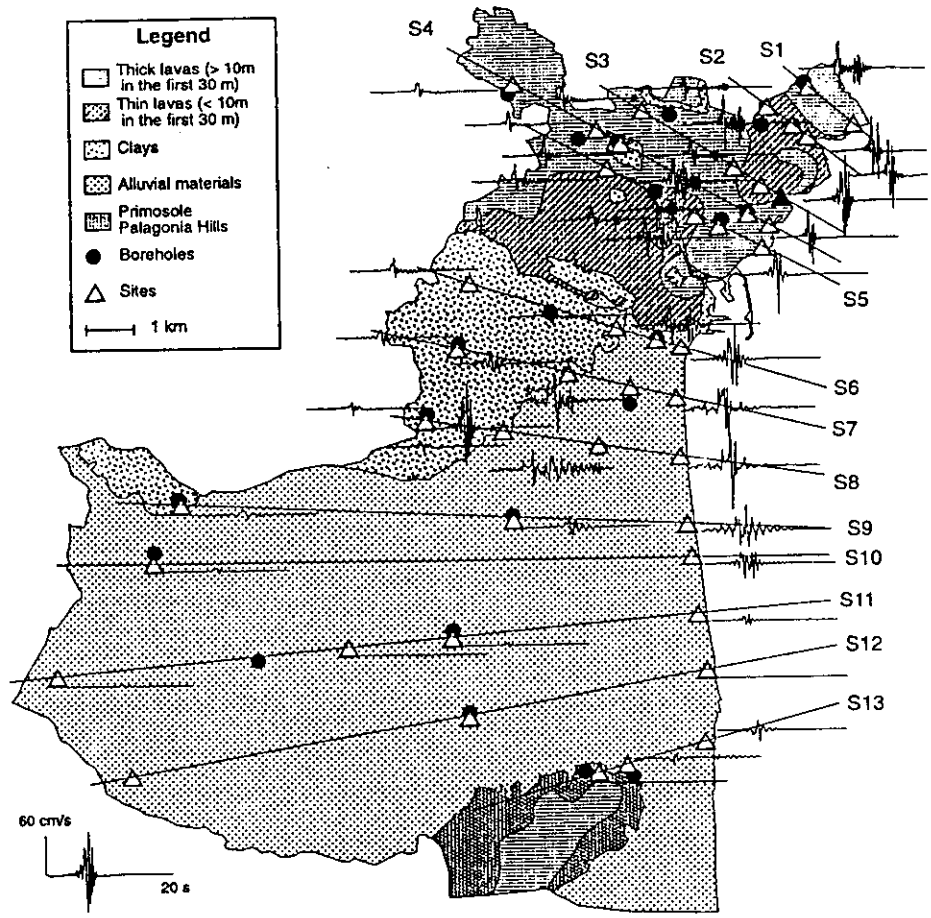

Figure 3 Simplified geotechnical zonation map for the Catania area and the velocities time series calculated, with a cut-off frequency of 10 Hz, at the sites (white triangles) along the thirteen cross-sections shown. The laterally heterogeneous models are built up putting in welded contact (from 2 to 4) different 1-D models: the regional 1-D model is chosen as bedrock model and the geotechnical information related with the selected boreholes are used for the local 1-D models. The site locations are chosen both in the proximity of the boreholes, and at the edges of the section. Each signal is scaled to the maximum value of PGV over the entire area (black triangle) and the time window is 20 s long (from Romanelli et al., 1998).

The study of ground motion in Bucharest, due to earthquakes occurred in Vrancea, has been focused on the May 30, 1990, Mw=6.9 event. Moldoveanu and Panza (1998) succeeded in reproducing, for periods greater than 1 second, the recorded ground motion in Bucharest (Magurele station), at a very satisfactory level for seismic engineering, even if a relatively simple local structure and seismic source have been considered (Figure 2). All the three components of motion are influenced by the presence of the deep alluvial sediments, the strongest local effect being visible (both observed and computed) in the transversal (T) one. Parametric tests, that represent a major advantage of the numerical simulations, have been performed considering the two fault plane solutions representative of the major Vrancea intermediate-depth earthquakes. With varying earthquake scenario, local effects vary in space with frequency. Although the strongest site effect is observed in the transversal component (T), the radial (R) and vertical (V) components are the most sensible to the source mechanism variations of the earthquake scenario (Moldoveanu et al., 1998).

For the complete microzonation of Bucharest, the modeling will be extended to a set of representative cross sections that spans the entire area of the city, and to a set of source parameters typical for the strong Vrancea quakes.

With the modal summation technique, extended to laterally heterogeneous anelastic structural models (Vaccari et al., 1989; Romanelli et al., 1996), a database of synthetic signals has been generated, which can be used for the study of the local response in a set of selected sites, located within the Catania area. The ground shaking scenario so far constructed (Romanelli et al., 1998) corresponds to an earthquake of the same size as the destructive event that occurred on January 11, 1693. Making use of the simplified geotechnical map for the Catania area, we produce maps of the expected ground motion over the entire area (see Figure 3), and, using the detailed geological and geotechnical information along a selected cross section, we study the site response in a very realistic case (see Figure 4). The main result, so far, is that, in order to perform an accurate estimate of the site effects, (1) it is necessary to make a parametric study that takes into account the complex combination of the source and propagation parameters, and (2) obtained with simplified structural models have a limited applicability and detailed models should be preferred (Romanelli et al., 1998).

A large quantity of descriptions of earthquakes that have been felt in Rome is available (Molin et al., 1995). The realistic modeling of the seismic input gives a simple and natural explanation of the damage distribution observed as a consequence of the January 13, 1915 Fucino earthquake — one of the strongest events that have occurred in Italy during this century (intensity XI on the MCS scale). The well-documented distribution of damage in Rome, caused by the Fucino earthquake, is, in fact, successfully compared by Fäh et al.

(1993) with the results of a series of different numerical simulations, using AMAX and W. Since the correlation is good between AMAX, W and the damage statistics, it is possible to extend the zoning to the entire city of Rome, thus providing a basis for the prediction of the expected damage from future strong events.

The highest values of the spectral amplification are observed at the edges of the sedimentary basin of the Tiber, and strong amplifications are observed in the Tiber's river bed. This is caused by the large amplitude and long duration of the ground motion due to (1) low impedance of the alluvial sediments, (2) resonance effects, and (3) excitation of local surface waves (Fäh et al. 1993). A preliminary microzoning map has been produced by Vaccari et al. (1995). The microzonation map and the response spectra, corresponding to the three main seismogenic zones around Rome, are shown in Figure 5.

Conclusions

The project represents a contribution to seismic disasters' preparedness. It produces results using what is available now and it improves scenarios as new data become available.

The availability of realistic numerical simulations allows significant progresses in ground motion mapping. This powerful tool enables us to estimate the amplification effects in complex structures exploiting the available geotechnical, lithological, geophysical parameters, topography of the medium, tectonic, historical, paleoseismological data, and seismotectonic models. The ground motion modeling technique applied in this project proves that it is possible to investigate local effects even at large epicentral distances, taking into account both the seismic source and the propagation path effects.

Traditional methods for seismic microzoning can only lead to a kind of "post-event" action whose validity cannot be easily extrapolated in time and to different regions. On the contrary, the computation of realistic seismic input, taking source and propagation effects into account, utilizing the huge amount of geological, geophysical and geotechnical data already available, goes well beyond the conventional deterministic approach and gives a very powerful and economically valid scientific tool for seismic microzonation. Because of its flexibility, the method is suitable for inclusion in new integrated procedures, a kind of compromise between probabilistic and deterministic approaches.

The ability to estimate realistic seismic hazard at very low probability of exceedance may be important in protecting against rare earthquakes, and the deterministic approach, based upon the assumption that several earthquakes can occur within a predefined seismic zone, represents a conservative definition of seismic hazard for pre-event localized planning for disaster mitigation.

Numerical simulations of the seismic source and of the wave path are a more adequate technique than making estimates based on recorded accelerograms (empirical Green functions), since such records are always influenced by the local soil condition of the recording site. With realistic numerical simulations it is possible to obtain, at low cost and exploiting large quantities of already available data, the definition of realistic seismic input for the existing or planned built environment, including special objects. The definition of realistic seismic input can be obtained from the computation of a wide set of time histories and spectral information, corresponding to possible seismotectonic scenarios for different source and structural models. Such a data set can be very fruitfully used by civil engineers in the design of new seismo-resistant constructions and in the reinforcement of the existing built environment, and, therefore, supply a particularly powerful tool for the prevention aspects of Civil Defense.

A general conclusion of the waveform modeling is that the presence of near surface rigid rocks is not sufficient to classify a

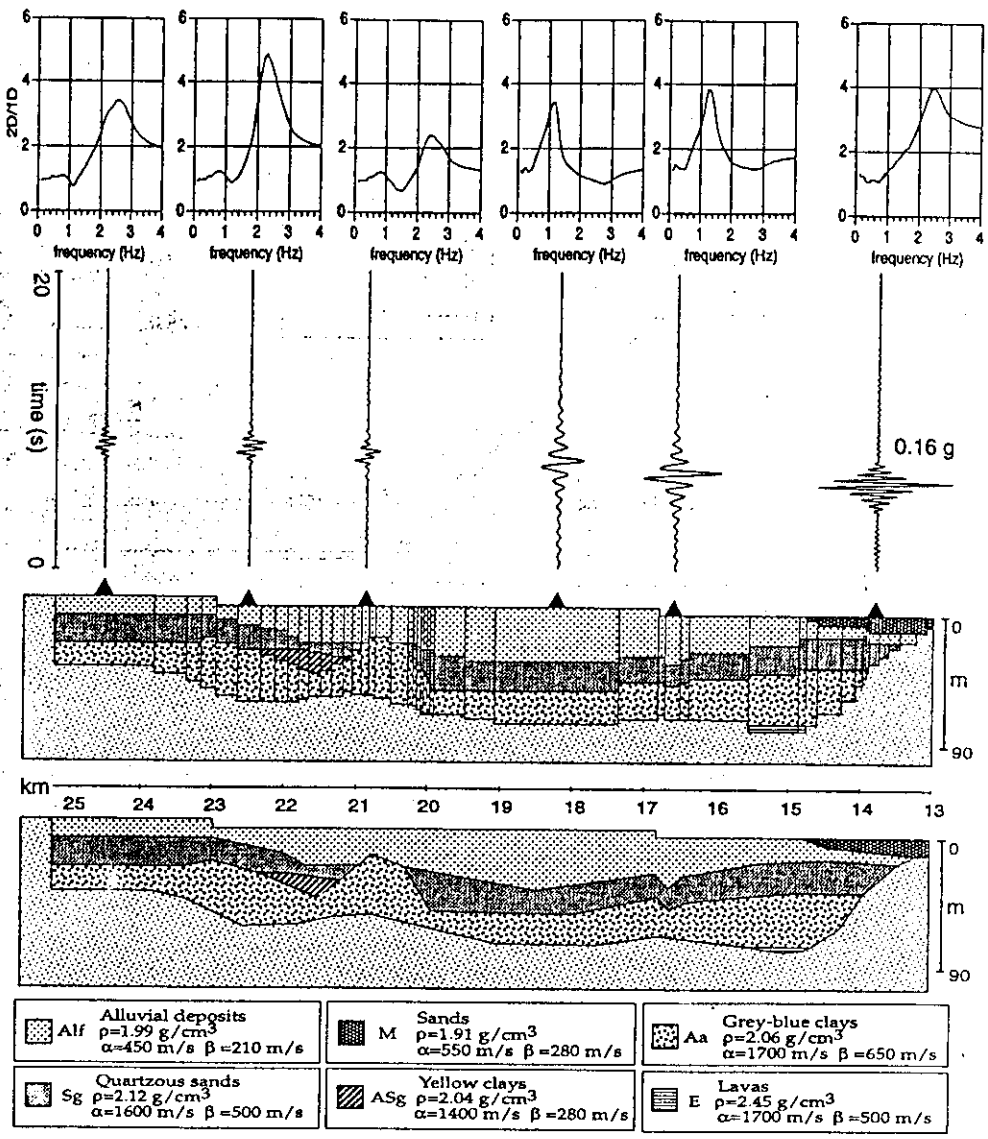

Figure 4 Detailed geotechnical cross-section (bottom) and corresponding model for detailed section S10. The distance along the section is measured in km from the source, while the vertical scale is in m. The acceleration time series and the theoretical site responses are shown at six selected sites along the section (from Romanelli et al., 1998).

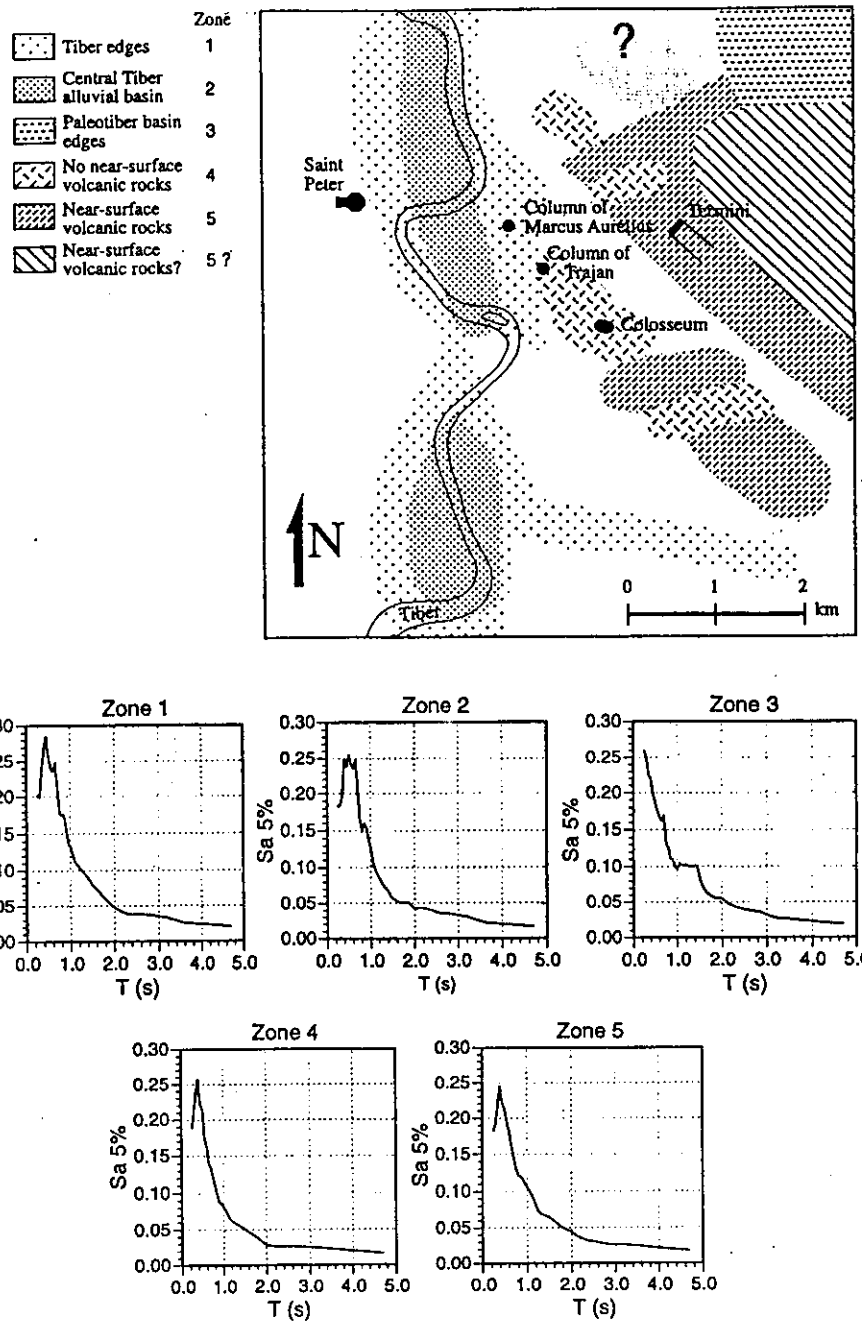

Figure 5 Microzonation map of Rome (top), based on the computation of realistic seismic ground motion due to three seismogenic zones around Rome: the Fucino area, the Alban Hills and the Carseolani Mountains. For the five zones identified in the map, the maximum absolute spectral acceleration (5% damping) is given (bottom).

location as a "hard-rock site", since the existence of underlying sedimentary complex(es) can cause amplifications due to resonance effects. A correct zonation requires therefore knowledge of both the thickness of the surface layer and of the deeper parts of the structure, down to the real bedrock. This is especially important in volcanic areas, where high-rigidity volcanic flows often cover low-rigidity alluvial basins.

The procedure illustrated here, for the mitigation of seismic hazard, is scientifically and economically valid for the immediate (no need to wait for a strong earthquake to occur) seismic microzonation of any urban area, where geotechnical data are available.

Acknowledgements

This project is truly a collaborative and interdisciplinary effort. Many scientists from around the world contribute their ideas, time and work. We would like to express our gratitude in particular for the contribution of the following organizations: UNESCO, IGCP, IUGS, ILP, EC, NATO, ITALIAN MURST, ITALIAN MAE (Div. VII), ICTP.

The supervision of the scientific activity presented in this paper has been performed by the Project Board (Prof. Giuliano Francesco Panza, University of Trieste and International Center for Theoretical Physics, Trieste, President; Prof. Yun Tai Chen, China Seismological Bureau, Beijing, member for Asia; Prof. Gheorge Marmureanu, National Institute Earth Physics, Bucharest, member for Europe; and Prof. Rodolfo Saragoni — University of Chile, Santiago, member for Latin America).

References

Arias, A., 1970, A measure of earthquake intensity, *in* R. Hansen, ed, Seismic design for nuclear power plants, Cambridge, Massachusetts.

Ding, Z., Vaccari, F., Romanelli, F., and Panza, G. F., 1998, Modeling of the SH-wave ground motion in Beijing area: ICTP Report IC/IR/98/11.

Fäh, D., 1991, Stima del moto sismico del suolo in bacini sedimentari, Tesi di dottorato, tutor: G. F. Panza, Trieste University.

Fäh, D., Iodice, C., Suhadolc, P., and Panza, G. F., 1993, A New method for the realistic estimation of seismic ground motion in megacities: the case of Rome: Earthquake Spectra, v. 9, pp. 643-668.

Fäh, D., Suhadolc, P., Mueller, St., and Panza, G. F., 1994, A Hybrid method for the estimation of ground motion in sedimentary basins: Quantitative modeling for Mexico City: Bull. Seism. Soc. Am., v. 84, pp. 383-399.

Fäh, D., and Panza, G. F., 1994, Realistic modeling of observed seismic motion in complex sedimentary basins: Annali di Geofisica, v. 37, pp. 1771-1796.

Florsch, N., Fäh, D., Suhadolc, P., and Panza, G. F., 1991, Complete synthetic seismograms for high-frequency multimode SH-waves: PAGEOPH, v. 136, pp. 529-560.

Gomez Bernal, A., and Saragoni, G. R., 1997a, Influence of surface wave on the design response spectra: Xth National Congress of Structural Engineering, Vol. II, pp. 955-964, Merida, Yucatan, Mexico.

Gomez Bernal, A., and Saragoni, G. R., 1997b, Rayleigh waves and their influence on the amplification and duration of seismic soil response of the Mexico Valley, La Sèrena, Chile, November, 1997 (in Spanish).

Medvedev, S. V., 1977, Seismic intensity scale MSK-76, Publ. Inst. Geophys. Pol. Acad. Sc., vol. 117, pp. 95-102.

Moldoveanu, C. L., and Panza, G. F., 1998, Modeling, for microzonation purposes, of the seismic ground motion in Bucharest, due to the Vrancea earthquake of May 30, 1990, *in* Wenzel, F. and Lungu, D., eds, Vrancea earthquakes; tectonics, hazard and risk mitigation, pp. 85-97, Kluwer Acad. Publishers, Dordrecht, The Netherlands.

Moldoveanu, C. L., Marmureanu, G., Panza, G. F., and Vaccari, F., 1998, Stability of local soil effects in Bucharest. Submitted to PAGEOPH.

Molin, D., Castenetto, S., Di Loreto, E., Guidoboni, E., Liperi, L., Narcisi, B., Paciello, A., Riguzzi, F., Rossi, A., Tertulliani, A., and Traina, G., 1995, Sismicita: Memorie descrittive della carta geologica d'Italia, Vol. L, Chapter VI, pp. 327-408.

Nunziata, C., Costa, G., Marrara, F., and Panza, G. F., 1997, Estimation of response spectra for the 1980 earthquake in the Eastern area of Naples: SDEE 1997 Volume of extended abstracts, July 20-24 1997, Istanbul, Turkey, pp. 82-83.

Panza, G. F., 1985, Synthetic seismograms: the Rayleigh waves modal summation: J. Geophys., v. 58, pp. 125-145.

Panza, G. F., 1993, Synthetic seismograms for multimode summation - theory and computational aspects: Acta Geod. Geoph. Mont. Hyng., v. 28, pp. 197-247.

Panza, G. F., Vaccari, F., Costa, G., Suhadolc, P., and Fäh, D., 1996, Seismic input modeling for zoning and microzoning: Earthquake Spectra, v. 12, pp. 529-566.

Panza, G. F., Vaccari, F., and Cazzaro, R., 1998, Deterministic seismic hazard assessment, *in* Wenzel, F. and Lungu, D., eds, Vrancea earthquakes; tectonics, hazard and risk mitigation, pp. 269-286, Kluwer Acad. Publishers, Dordrecht, The Netherlands.

Romanelli, F., Bing, Z., Vaccari, F., and Panza, G. F., 1996, Analytical computations of reflection and transmission coupling coefficients for Love waves: Geophys.J.Int., v. 125, pp. 132-138.

Romanelli, F., Nunziata, C., Natale, M., and Panza, G. F., 1998, Site response estimation in the Catania area, *in* Irikura, Kudo, Okada and Sasatani, eds, The effects of surface geology on seismic motion, pp. 1093-1100, Balkema, Rotterdam, The Netherlands.

Saragoni Huerta, G. R., and Lobos, C., 1998, Studies performed in Chile for the definition of seismic input for isolated structures: Proceedings International Post - SMIRT Conference Seminar on Seismic Isolation, Passive Energy Dissipation and Active Control of Seismic Vibrations of Structures, Taormina, Italy, 25-27 August 1997.

Schnabel, B., Lysmer, J., and Seed, H., 1972, Shake: A computer program for earthquake response analysis of horizontally layered sites: Rep. E.E.R.C. 70-10, Earthq. Eng. Research Center, Univ. California, Berkeley.

Sun, R., Vaccari, F., Marrara, F., and Panza, G. F., 1998, The main features of the local geological conditions can explain the macroseismic intensity caused in Xiji-Langfu (Beijing) by the Tangshan 1976 earthquake: PAGEOPH, v. 152, pp. 507-522.

Vaccari, F., Gregersen, S., Furlan, M., and Panza, G. F., 1989, Synthetics seismograms in laterally heterogeneous, anelastic media by modal summation of the P-SV waves: Geophys. J. Int., v. 99, pp. 285-295.

Vaccari, F., Nunziata, C., Fäh, D., and Panza, G. F., 1995, Reduction of seismic vulnerability of megacities: the cases of Rome and Naples: Proc. Fifth Int. Conf. Seismic Zonation, pp. 1392-1399, AFPS-EERI, Ouest Editions Presses Academiques.

Giuliano F. Panza is professor of seismology in the Department of Earth Sciences at the University of Trieste, and is head of the SAND Group of the ICTP at Trieste. He received his Laurea in physics (1967) from the University of Bologna and performed PostDoc research at the UCLA University. He is fellow of Accademia Nazionale dei Lincei, of Academia Europae, and of Third World Academy of Sciences. He is leader of several projects funded by EC related to seismic hazard assessment.

Franco Vaccari is a researcher of GNDT (National Group for the Defense against Earthquakes) in the Department of Earth Sciences at the University of Trieste, Italy, where he received Laurea in geology (1986) and Ph.D. (1989) in geophysics. His recent research interests involve seismic hazard assessment, seismic zoning and microzoning, and computational aspects of seismology.

Fabio Romanelli is a researcher of GNDT (National Group for the Defense against Earthquakes) in the Department of Earth Sciences at the University of Trieste, Italy, where he received Laurea in physics (1993) and Ph.D. (1998) in geophysics. His research involves the study of the excitation and the propagation of seismic and tsunami waves in laterally heterogenous media. The recent focus of his work has been the theoretical estimation of site effects.

Earthquake Resistant Engineering Structures II

EDITORS:

Prof. G. Oliveto
University of Catania, Italy

Prof C.A. Brebbia
Wessex Institute of Technology, Southampton, UK

WITPRESS Southampton, Boston

The realistic definition of seismic input: an application to the Catania area

L. Decanini,[1] F. Mollaioli,[2,1] G. F. Panza,[3,4] F. Romanelli [2,4]
[1] *Dip di Ing. Strutturale e Geotecnica, Universita' di Roma "La Sapienza", Rome, Italy*
Email: decanini@hp720.dsg.uniroma1.it
[2] *GNDT, Via Nizza 128, 00198, Rome, Italy*
Email: moll@scilla.ing.uniroma1.it
[3] *SAND Group, ICTP, Miramar, Trieste, Italy*
Email: panza@geosun0.univ.trieste.it
[4] *Dipartimento di Scienze della Terra, Via Weiss 4, 34127 Trieste, Italy*
Email: romanel@geosun0.univ.trieste.it

Abstract

The realistic definition of seismic input can be performed by means of advanced modelling codes based on the modal summation technique. These codes and their extension to laterally heterogeneous structures allow us to accurately calculate synthetic signals, including body waves and of surface waves, corresponding to different source and anelastic structural models, taking into account the effect of local geological conditions. For the estimation of the destructive potential of the calculated signals, parameters obtained from their (a) direct analysis, (b) integration in the time or in the frequency domain, and (c) the structural (elastic and anelastic) response are investigated. As an example of application of our analysis we consider the Catania (Sicily) area where a pilot project of GNDT (Gruppo Nazionale per la Difesa dai Terremoti) is in progress for the reduction of the seismic hazard at a sub-regional and urban scale. In such an urban area more than 500,000 people are living and the application of advanced seismological methods for the definition of earthquakes

1 Introduction

The typical seismic hazard problem mainly consists in the study of the effects associated to earthquakes, both on regional and on local scale, for a successive engineering analysis. The result of such an analysis, that has to be used for the seismic risk definition, can be expressed in various ways, e.g. with a description of the groundshaking intensity due to an earthquake of a given magnitude ("groundshaking scenario"), or with probabilistic maps of relevant parameters.

Historically, the most used parameter in the engineering analysis for the characterization of the seismic hazard is the PGA (Peak Ground Acceleration), a single-value indicator relatively easy to determine but that leads often to wrong seismic risk estimates. Actually, the peak values alone can not describe adequately all the effects associated to the ground shaking, since the frequency content and the duration of a seismic wavetrain play a fundamental role. A more complete analysis includes the calculation of the response spectra: the response of a given structure to the seismic ground motion can be studied analysing the behaviour of a simple damped oscillator. While the Fourier spectra shows the fine tuning of the energy contained in a wavetrain, the response spectra gives the maximum response of a oscillator to the whole seismic motion.

Although it has been recognized that the characteristics of ground motion such as its intensity, frequency content and duration are relevant to estimate its damage potential, some of these characteristics are usually ignored for the sake of simplicity.

On the other hand, the estimation of the damage potential of ground motion, by neglecting the mechanical characteristics of the earthquake-resisting structures will usually lead to unreliable and inconsistent results. This is due to the fact that the damage potential is not an absolute property of the ground motion, but it also depends on its interaction with the earthquake-resisting structure.

Thus, a rational methodology for the assessment of the earthquake destructiveness potential, particularly in case of inelastic behavior, should take into account simultaneously the relevant characteristics of the ground motion and of the earthquake-resisting structure.

Linear Elastic Response Spectra (LERS) do not represent a complete description of the ground motion damage potential in the case of inelastic behavior, in which most of the energy transmitted to the structure is dissipated through plastic deformations. The lessons learned from recent earthquakes and associate research indicate that the elastic spectra ordinates are not directly related to the structural damage. Extremely important factors such as the duration of the strong ground shaking and the sequence and duration of acceleration pulses are not taken into account adequately. The Inelastic Response Spectra (IRS), obtained directly from strong motion records, are necessary for the design at safety level, but they are not sufficient because they do not give a precise description of the quantity of the energy that will be dissipated through hysteretic behavior; they give only the value of the maximum ductility requirement. In several cases the observed behavior is not consistent with the usual seismic strength coefficients, but it can be explained by making use of energy concepts.

A large number of parameters have been proposed in literature to measure the capacity of an earthquake to damage built structures, but no one seems to be completely satisfactory. The adoption of inadequate parameters can lead to the definition of non realistic design earthquake and, consequently, to the unreliable evaluation of the seismic risk.

In this context, the damage potential of earthquake ground motion perhaps may be adequately characterized by means of energy parameters. In fact, energy-based methods could provide more insight into the seismic performance and could be considered as effective tools for a comprehensive interpretation of the behavior observed during destructive events.

The main problem associated with the study of seismic hazard is to determine the seismic ground motion at a given site, due to an earthquake, with a given intensity and epicentral distance from the site. A solution for the study of seismic hazard and associate seismic ground motion, at a given site and for a range of a given distance from the fault, could be to use a complete set of recorded strong motions and to group those accelerograms that have the same source, path and site effects. In practice however, such a database is not available, being the number of available recorded signals still relatively low. An alternative way is based on computer codes, developed from a detailed knowledge of the seismic source process and of the propagation of seismic waves, that can simulate the ground motion associated with the given earthquake scenario. In such a way, synthetic signals, to be used as seismic input in a subsequent engineering analysis, can be produced at a very low cost/benefit ratio. Anyway, the damage potential of such signals need to be evaluated on the basis of the parameters characterizing the earthquake destructiveness power derived from the available strong motion records.

The realistic definition of seismic input can be performed by means of advanced modelling codes based on the modal summation technique (e.g. Florsch et al.[1]). These codes and their extension to laterally heterogeneous structures (e.g. Romanelli et al.[2]) allow us to accurately calculate synthetic signals, complete of body waves and of surface waves, corresponding to different models of the source and of the medium, taking into account the effect of local site conditions.

As an example of application of our analysis we consider the Catania (Sicily) area where a pilot project of GNDT (Gruppo Nazionale per la Difesa dai Terremoti) is in progress for the reduction of the seismic hazard at a sub-regional and urban scale. In such an urban area more than 500,000 people are living and the application of advanced seismological methods for the definition of groundshaking scenarios can play a crucial role in the analysis of the seismic risk and in the reduction of possible losses.

2 Examples of ground motion synthesis in the Catania area

For the definition of the seismic source model to be used in the computations we choose to consider an earthquake similar to the destructive event that occurred on January 11, 1693. The focal mechanism parameters of the seismic source, located approximately in the center (latitude: 37.44°; longitude: 15.23°) of the

Northern Segment of the Hyblean fault, are: strike equal to 352°, dip equal to 80°, rake equal to 270°, focal depth equal to 10 km and seismic moment equal to $3.2 \cdot 10^{19}$ Nm.

The calculation of synthetic signals for a potential large earthquake is a task that has to face with the difficult problem of the generation and propagation of high frequency seismic waves, that are characterized by a big sensitivity to the small scale details of the rupture process and to the heterogenities present in the propagation medium. Therefore, such a problem should be solved taking into account the dynamics underlying the source physical process. However, in this work we want to focus mainly on the effects of the lateral heterogenities present in the medium of propagation since one of the final goals is to estimate the site effects. To minimize the number of free parameters we decide to account for source finiteness by properly weighting the source spectrum in the frequency domain using the scaling laws of Gusev[3], as reported in Aki[4]. The propagation of the seismic waves in the Catania area is modelled using the geotechnical informations collected within GNDT (GNDT[5]), that supplies a simplified geotechnical zonation map.

In Figure 1 the simplified geotechnical zonation map for the Catania area, together with the 13 simplified cross sections that were considered in the analysis of Romanelli et al.[6], are shown. Romanelli et al.[6] decided to employ the simplified map, in order to take into account the gross features of the geotechnical zonation and to produce a sort of map of the ground motion. The 2-D models associated with each cross section are built up putting in welded contact (from 2 to 4) different 1-D models: the regional model is chosen as bedrock model and the geotechnical information related with the selected boreholes are used for the local 1-D models. The map shown in Figure 1 is used to define the borders between the local models, i.e. the distances between the vertical interfaces separating the different 1-D models. We decide here to study in more detail, for the successive engineering analysis, the initial part of section S4 of Romanelli et al.[6], that the combination of the radiation pattern and of the path effect makes one of the sections with the highest peak ground motion parameters. The model of section S4 that we consider in this work corresponds to the part between the coastline and the soft soils; the model is formed by three 1-D models in welded contact, separated by vertical interfaces; the three laterally homogeneous models correspond to the bedrock model (M0) and to the two local models constructed using the data coming from the selected boreholes (see Figure 2).

Using the model of Figure 2 we calculate the synthetic signals, for the transverse component of motion (SH problem), at a series of equally spaced sites. The distance between each site is 200 m and the total number of computed signals is 20: 15 are calculated on the local model M1 (lavas) and 5 on M2 (sands and clays). The synthetic signals are calculated with the modal summation technique for laterally heterogeneous models (Romanelli et al.[2]), with a cut-off frequency of 10 Hz. The angle between the fault strike and the direction of the section (strike-section angle) is measured counterclockwise from the strike direction; the strike-receiver anlgle for all of the sites is 50 degrees.

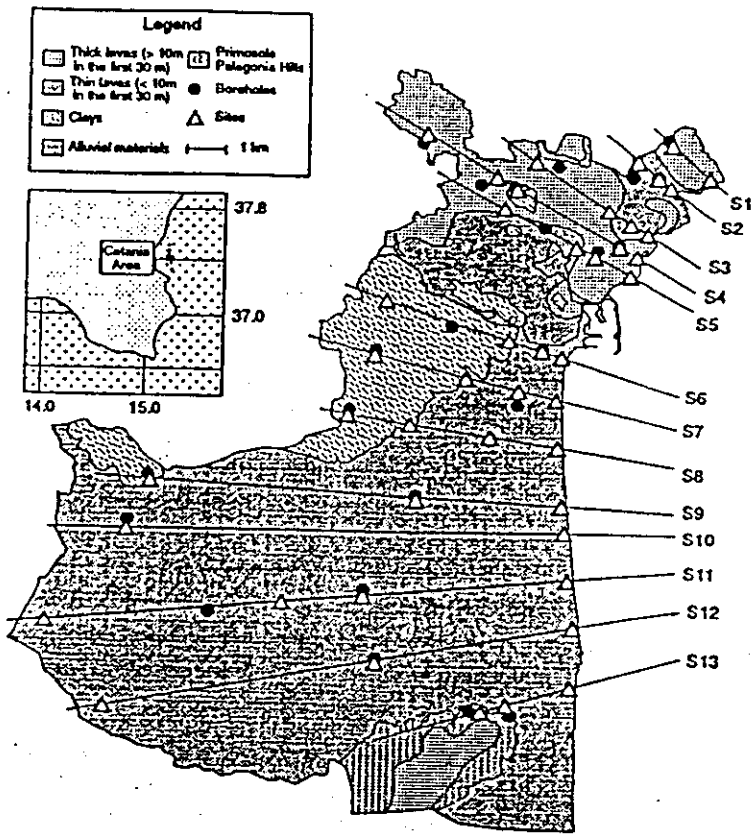

Figure 1: Simplified geotechnical zonation map of the Catania area and the laterally heterogeneous cross-sections considered by Romanelli et al.[6].

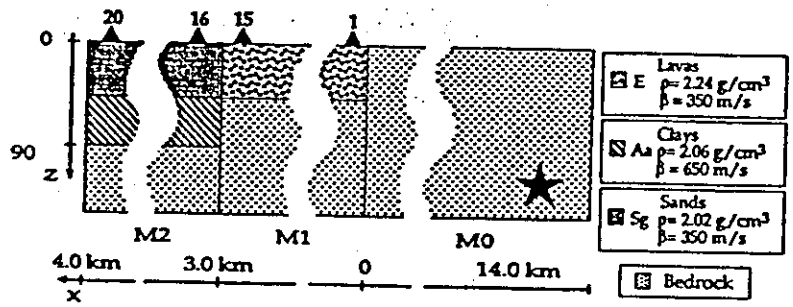

Figure 2: Model adopted for the initial part of section S4.

In Figure 3 the acceleration time series for the twenty sites along S4 are shown, together with the 1-D signals (left column) calculated with the modal summation technique for laterally homogeneous structures (Florsch et al.[1]) using the model M0 and with a cut-off frequency of 10 Hz. From the comparison of the 1-D and the 2-D time series it can be seen that the shape of the main peak of the wavetrain is similar. However the 2-D time series show greater amplitudes along all the section and the duration of the signal is highly increased. This can be explained by the fact that the sharp horizontal gradient present at the beginning of the local model represents a strong impedence contrast for the incoming wavefield. Such a contrast produces a strong scattered wavefield that propagates in the low-velocity layers at the surface of the local models.

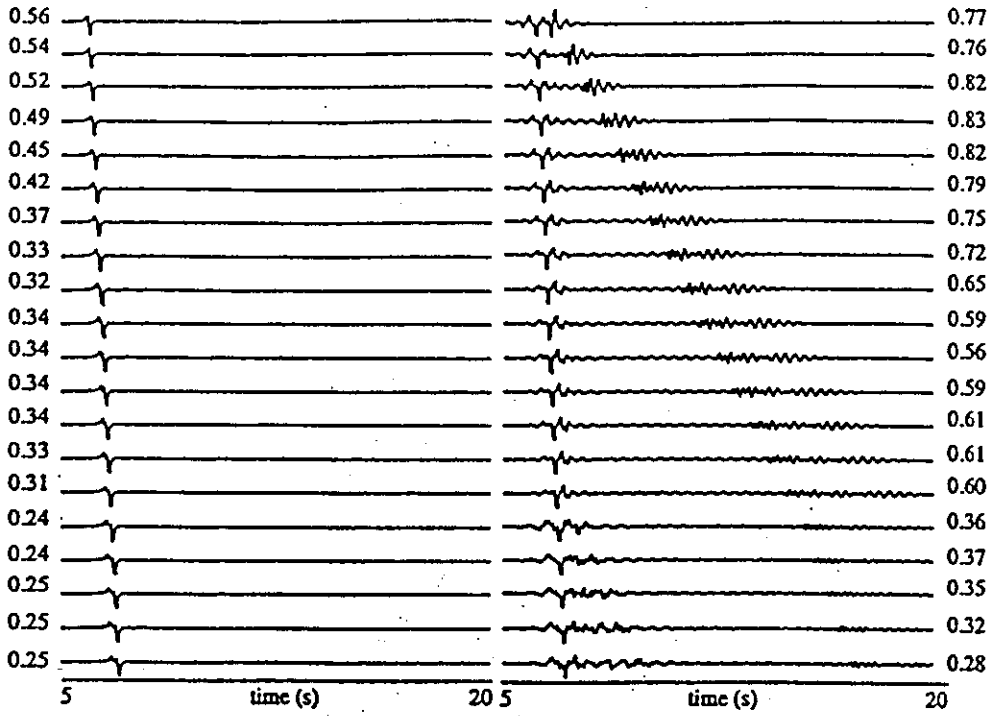

Figure 3: Synthetic accelerograms (transverse component) computed along S4: bedrock model (left column) and laterally heterogeneous model (right column). On each side the peak amplitudes (g) of the signals are shown

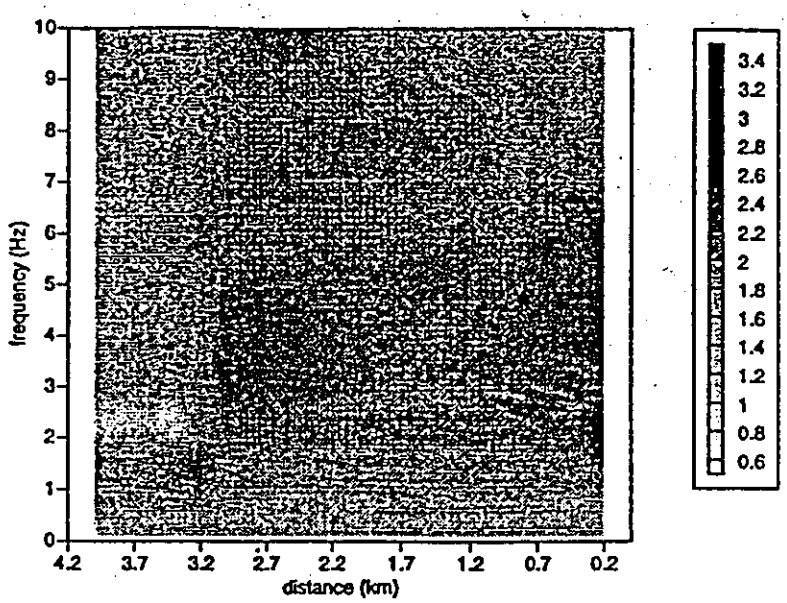

Figure 4: 2D/1D response spectra ratios versus frequency and distance along S4.

Moreover, the PGA/PGV mean ratio, equal to 20.5, is quite well correlated to the PGA/PGV mean ratio correspondent to accelerograms recorded on firm soil, at distances from the causative fault ranging from 12 to 30 Km, and for magnitude ranging from 6.5 to 7.1 (Decanini and Mollaioli[7]).

To estimate the site response we evaluate the ratio between the response spectra (RSR) calculated, at a given site, for the 2-D and the 1-D signals in order

to reveal the resonant frequencies and the corresponding level of amplification for the twenty sites of S4. In Figure 4 the RSR ratios are plotted versus frequency and versus the distance from the beginning of the local model (see also Figure 2 for the reference system). The effect of the sharp lateral heterogeneities is to create a higly energetic component of scattered waves that are dominant within the first 500 m after the vertical interfaces. The propagation in the last part of M1 seems to be responsible of the shifting of the resonant frequencies in the RSR at sites 12-15. This fact indicates that the site effect depends not only on the layering of the local geological structure, but that the relative position of the site with respect to the lateral heterogeneities is playing an important role for the local response.

3 Evaluation of the damage potential of the synthetic signals

Even though a number of parameters have been proposed in the literature for measuring the capacity of earthquake ground motion to damage structures, most of them are not consistent with building damage observed during earthquakes (Uang and Bertero[8]).

Among all the different parameters proposed for defining the damage potential, perhaps one of the most promising is the Earthquake Input Energy (E_I) and associate parameters (the damping energy E_ξ and the plastic hysteretic energy E_H) that has been studied by Uang and Bertero[9]. This parameter considers the actual behavior of a structural system and depends on the dynamic characteristics of both the ground motion and the structure. The input energy is a reliable parameter in selecting the most demanding earthquake and in the evaluation of the destructiveness of synthetic signals. Therefore, at a given site the input energy permits the selection of the possible critical motions for the response of the structure. However, in order to perform a reliable design, sizing and detailing when the damage can be tolerated, the input energy alone is not sufficient.

The fundamental concept in applying energy methods is the transformation of the equation of motion of a viscous damped single-degree-of-freedom (SDOF) system into an energy balance equation in which the input energy to the structure, due to the seismic shaking at the base is balanced by energy absorbed in the structure and by energy dissipated from the structure. Then, according to the procedures described by Uang and Bertero[9], the energy balance equation is given by,

$$E_I = E_k + E_\xi + E_a = E_k + E_\xi + E_s + E_H \qquad (1)$$

Where E_k represents the absolute kinetic energy, E_ξ is the damping energy, and E_a is the absorbed energy that is composed of the recoverable elastic strain energy, E_s, and of the irrecoverable plastic hysteretic energy E_H.

In previous work (Decanini and Mollaioli[7,10]) the absolute energy equation is used, since this criterion has the advantage that the physical input energy is reflected, in that E_I represents the work done by the total base shear at the foundation displacement, and it is suitable for the estimation of the energy terms

in the range of periods of interest for the majority of the structures. E_I can be expressed by:

$$\frac{E_I}{m} = \int \frac{d^2u_t}{dt^2}\, du_g = \int \frac{d^2u_t}{dt^2}\, u_g dt \qquad (2)$$

where m is the mass, $u_t = u + u_g$ is the absolute displacement of the mass, and u_g is the earthquake ground displacement. In the following the input energy per unit mass, i.e. E_I/m, will be denoted as E_I.

Figure 5 shows a comparison between the elastic input energy of three synthetic signals (synth_1, synth_3 and synth_5), evaluated for a damping ratio equal to 5%, and two accelerograms (Santa Cruz UCSC/Lick Obs. Elect. Lab., Ucsc0; and Gilroy # 1, Gavilan College, Water Tower, Gav. Tower 90) recorded during the Loma Prieta earthquake (1989; M=7.1) on firm soil (S1) and at distances from the surface projection of the causative fault (D_f) equal to 15 and 16 km, respectively. It can be observed that the frequency content is almost the same in both cases, and the maximum values of E_I are concentrated within the range of periods $0.3 \le T \le 0.5$ s. Therefore, distances from the causative fault being equal, the synthetic signals provide an elastic energy comparable to that obtained from records taken on firm soil for a magnitude approximately equal to 7.1. In confirmation of the previous assertion, Figure 6 illustrates a comparison between the synthetic signals, represented by the first signal, the mean and the mean plus one standard deviation (SD) of all the signals, and the design input energy spectrum proposed by Decanini and Mollaioli[7] for a soil S1, for a distance $12 \le D_f \le 30$ km, and a magnitude $6.5 \le M \le 7.1$.It should be recalled that lavas with Vs=350 m/s lie at the boundary of the distinction between firm (S1) and intermediate (S2) soil. Both the spectral shapes and the maximum values of the input energy of the synthetic signals are consistent with the design spectrum, even though the spectra of the synthetic signals appear to be more concentrated around their maximum values.

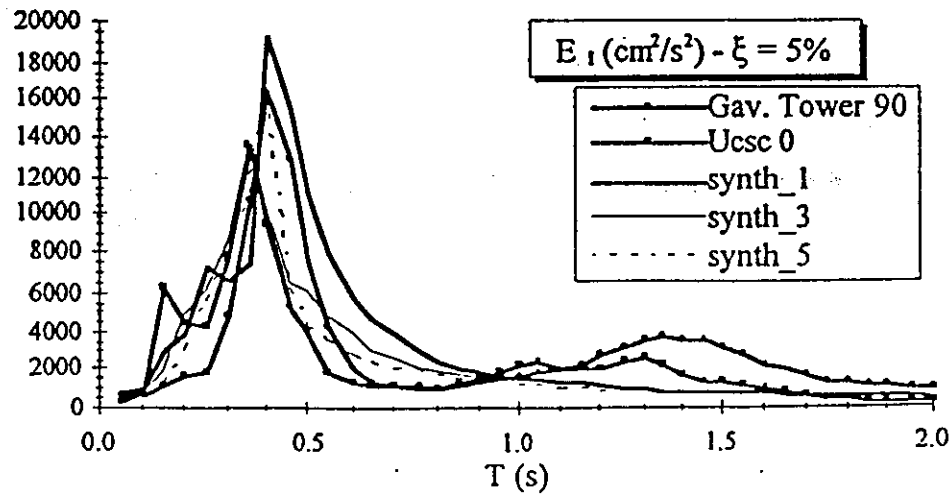

Figure 5: Elastic E_I (cm^2/s^2) spectra. Comparison between synthetic signals and strong motion records of Loma Prieta earthquake (1989), Soil S1.

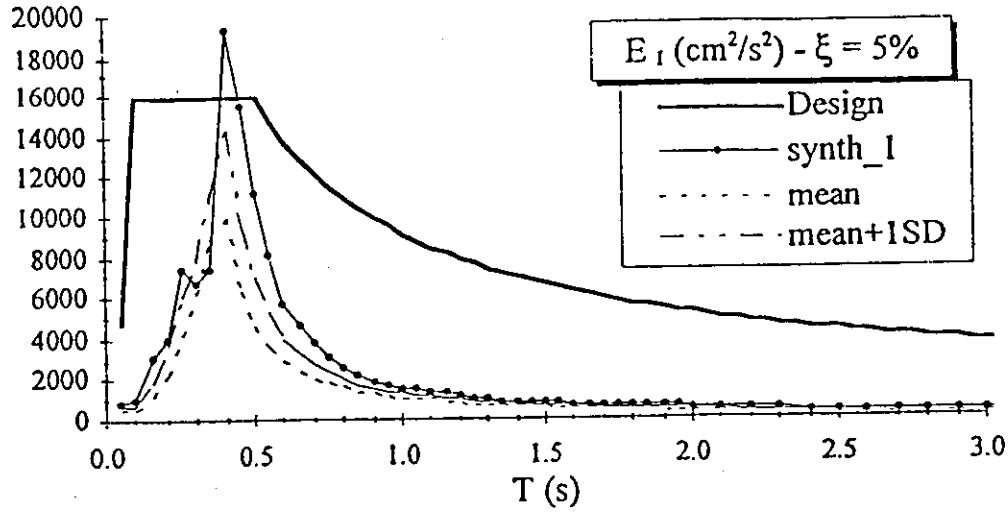

Figure 6: Elastic E_I (cm^2/s^2) spectra. Comparison between synthetic signals and design input energy spectrum (firm soil S1, $12 \leq D_f \leq 30$ km, $6.5 \leq M \leq 7.1$)

4 Conclusions

As a result of the study performed, it is possible to draw the following considerations:

a) The parameters PGA, PGV, t_D and PGA/PGV fall within the range of values normally found on firm soil, magnitude and distance to the causative fault being equal.

b) The synthetic signals provide an energy response which is typical of accelerograms recorded on firm soil; at a distance to the causative fault between 12 and 30 km, and a magnitude between 6.5 and 7.1.

c) The energy-based parameters is a powerful tool to evaluate the destructiveness of both synthetic signals and strong motion records.

Acknowledgements

We acknowledge financial support from GNDT, MURST (40% and 60% funds), EEC Contract ENV-CT94-0491, ENV-CT94-0513, ENV4-CT96-0491.

References

1. Florsch, N., Fäh, D., Suhadolc, P. & Panza, G.F., Complete Synthetic Seismograms for High-Frequency Multimode SH-Waves, *PAGEOPH*, 136, pp. 529-560, 1991

2. Romanelli, F., Bing, Z., Vaccari, F. & Panza, G.F., Analytical Computation of Reflection and Transmission Coupling Coefficients for Love Waves, *Geophys. J. Int.*, 125 , pp. 132-138, 1996.

3. Gusev, A. A., Descriptive statistical model of earthquake source radiation and its application to an estimation of short period strong motion, *Geophys. J. R. Astron. Soc.*, 74, pp. 787-800, 1983.

4. Aki, K, *Strong motion seismology*, Strong ground motion seismology, NATO ASI Series, Series C: Mathematical and Physical Sciences, Dordrecht, Vol. 204, pp. 3-39, 1987.

5. GNDT, Progetto Catania - Caratterizzazione geotecnica del territorio comunale di Catania a fini sismici, GNDT, Milano, 1997.

6. Romanelli, F., Vaccari, F. & Panza, G.F., Site response estiimation and ground motions scenario in the Catania area. Submitted to *Journal of seismology*.

7. Decanini, L.D. & Mollaioli, F., Formulation of Elastic Earthquake Input Energy Spectra, *Earthquake Engineering and Structural Dynamics*, 27, pp. 1503-1522, 1998.

8. Uang, C.M. & Bertero, V.V., Implications of Recorded Earthquake Ground Motions on Seismic Design of Buildings Structures. *Report No. UCB/EERC-88/13*, Earthquake Engineering Research Center, University of California at Berkeley, 1988.

9. Uang, C.M & Bertero, V.V., Evaluation of seismic energy in structures. *Earthquake Engineering and Structural Dynamics*, 19, pp. 77-90, 1990.

10. Decanini, L. & Mollaioli, F., Toward the definition of the relation between hysteretic and input energy, *6th U.S. National Conference on Earthquake Engineering*, Seattle, May 31-June 4, 1998.